2020

Development and Characterisation of an Immunocompetent Three-Dimensional Oral Mucosal Infection Model

Gould, Samantha

UNIVERSITY OF PLYMOUTH

DEVELOPMENT AND CHARACTERISATION OF AN IMMUNOCOMPETENT THREE-DIMENSIONAL ORAL MUCOSAL INFECTION MODEL

by

SAMANTHA GOULD BSc (Hons)

A thesis submitted to the University of Plymouth in partial fulfilment for the degree of

DOCTOR OF PHILOSOPHY

Peninsula Dental School

June 2020

Acknowledgements

Thank you to my friends, family, and their pets for the provision of food, pep talks, and company throughout. With special thanks to my Mum, for her countless phone calls of encouragement and support, and my Nan, for her wonderful conversations, and whose in depth knowledge of baking proves surprisingly translatable to the formation of collagen gels. Thank you to my Dad and brother George, for their optimism and pragmatism, respectively! With thanks to my supervisory team Vehid Salih, Louise Belfield, and Mathew Upton for their support and guidance, and the technical staff at the University of Plymouth, with special mention to Matt Emery, whose lab was a safe space and support was invaluable. With special thanks to Rachel Cole, who endured endless presentations on the *Staphylococcus*aurus 🦕, provided me with Sunday roasts, and whom without, my fridge would be full of expired food. I will be eternally grateful to Helene Stern, Barbara Durante and Andrew Foey for their advice, scientific enthusiasm, encouragement, and occasional shouting at me to just get on with it! With special thanks to Rabab Ahmad, who supported me through my hardest of times and whose kindness, sheer determination, and endurance is a true inspiration. With thanks to Toni Quinn, for her friendship, dog photos, proofreading, and patience! Finally, thank you to the NHS, for the wonderful underappreciated staff, for their hard work and mental health services, of which every PhD student will require at some point!

Author's Declaration

At no time during the registration for the degree of Doctor of Philosophy has the author been registered for any other University award without prior agreement of the Doctoral College Quality Sub-Committee. Work submitted for this research degree at the University of Plymouth has not formed part of any other degree either at the University of Plymouth or at another establishment.

Presentations at conferences:

- Oral presentation BSODR Leeds 2019
- Oral Presentation IADR Vancouver 2019
- Oral presentation: Plymouth university annual research event 2019
- Oral presentation: IADR London 2018
- Oral presentation: OMIG Gregynog 2018
- Poster presentation: Plymouth university annual research event 2018
- Oral presentation: Plymouth university annual research event 2017
- Poster presentation: Plymouth BSODR 2017
- Three-minute thesis competition: Plymouth University 2017
- Three-minute thesis competition: BSODR ECR day Sheffield 2017
- Poster presentation: Doctoral training alliance Nottingham 2016
- Poster presentation: Plymouth university annual research event 2016

Word count: 55,200

Signed: 

Date: 21/06/2020

Abstract

Development and Characterisation of an Immunocompetent Three-Dimensional Oral Mucosal Infection Model.

Samantha Gould

Oral mucosal models are valuable tools for studying oral infection. Existing models have been implemented to study pathogen tissue invasion and resultant damage. These models fail to incorporate an innate immune component such as macrophages, essential for study of host response to infection. Macrophages exist within a regulatory to inflammatory polarisation spectrum, whereby the local microenvironment determines their activity, contributing to the overall behaviour of a tissue.

Three-dimensional oral mucosal models were formed using primary (POK) or immortalized (HaCaT) keratinocytes seeded upon a human gingival fibroblast (HGF) embedded type-1 collagen matrix. Later, HaCaT based models (3DOMMs) were further developed to incorporate THP-1 pro-monocyte cells into the model matrix producing a novel immunocompetent oral mucosal model (IC3DOMM). Models were characterised using a variety of histological, biochemical, and molecular techniques to detail the model microenvironment and assess their capability to detect and respond to *Staphylococcus aureus* and/or *Candida albicans* infection.

The HaCaT based 3DOMM was selected to further develop into an IC3DOMM, due to its superior epithelial barrier, and ability to upregulate both IL-6 and IL-8 in response to infection, when compared to the to the POK based P3DOMM. Model-

incorporated THP-1 cells increased in size and altered morphology, suggesting differentiation into macrophages. The polarisation of THP-1-derived macrophages was not fully elucidated, as selected markers CD206 and CD163 did not sufficiently discriminate between THP-1 cells, PMA-derived, and VD3-derived macrophages.

Newly highlighted, was the inflammatory environment of the 3DOMM at early and late stage culture. High levels of IL-6 and IL-8 production strongly correlated with LDH release, hence cell death. However this did not detract from the models' ability to upregulate pro-inflammatory cytokine production in response to infection, and it is proposed that models are used at day 14 post production.

Individual model cell types modulated IL-6, IL-8, and/or TNFα production upon stimulation with supernatant, killed cells, collagen, and differentiation reagents (PMA/VD3), demonstrating the complexity of the tissue-engineered environment. Despite this, it is necessary to consider the model as a whole, not as a sum of individual interactions, as the collective local microenvironment may modulate all cell types contained within the model. Due to the 3DOMMs intact epithelial barrier, ability to upregulate pro-inflammatory cytokine production in response to infection, and confirmed potential to incorporate THP-1-derived macrophages, it is proposed that the novel IC3DOMM is a suitable model for the study of host response to infection.

Table of Contents

List of tables

List of Figures

List of abbreviations

3D	Three-dimensional
3DOMM	Three-dimensional oral mucosal model
ANOVA	Analysis of variance
AP-1	Activating protein-1
APS	Ammonium persulfate
ATP	Adenosine triphosphate
B	Both
BSA	Bovine serum albumen
CA	*Candida albicans*
CCR	Chemokine receptor
CD	Cluster of differentiation
CFU	Colony forming units
CLR	C-type lectin receptor
CTFR	Cell-trace far red
CXCL	Chemokine (C-X-C motif) ligand
CXCR	Chemokine (C-X-C motif) receptor
D10	Dulbecco's modified eagles medium supplemented with 10% foetal bovine serum
DAG	Diacylglycerol
DAMP	Damage associated molecular pattern
DF	Dilution factor
dH_20	Distilled water
DMEM	Dulbecco's modified eagles medium
DMSO	Dimethyl sulfoxide
DNA	Deoxyribonucleic acid
DPBS	Dulbecco's PBS
DS	Denture stomatitis
ECL	Enhanced cemiluminescence
ECM	Extracellular matrix
EDTA	Ethylenediaminetetraacetic acid
EGF	Epidermal growth factor
ELISA	Enzyme linked immunosorbent assay
ERK	Extracellular signal-regulated kinase
FBS	Foetal bovine serum
Fc	Fragment crystallizable
FITC	Fluorescein isothiocyanate
FTOM	Full-thickness oral mucosal models
gDNA	Genomic deoxyribonucleic acid
GF	Gingival fibroblast
GM-CSF	Granulocyte-macrophage colony-stimulating factor
gp	Glycoprotein
HaCaT	Human immortalised epidermal keratinocyte cell line
HGF	Human gingival fibroblast primary cells
HSV	Herpes simplex virus
IC	Immunocompetent
IC3DOMM	Immunocompetent three-dimensional oral mucosal model
IFNγ	Interferon gamma
IκBα	nuclear factor of kappa light polypeptide gene enhancer in B-cells inhibitor, alpha
Ικκε	(Ικκ)-related kinase epsilon
IL	Interleukin

IMS	Industrial methylated spirit
IRF	Interferon regulatory factor
IRAK	Interleukin-1 receptor-associated kinase
IRAS	Integrated research application system
JNK	c-Jun N-terminal kinase
K	Killed
KGM	Keratinocyte gold media
LBP	Lipopolysaccharide binding protein
LDH	Lactate dehydrogenase
LPS	Lipopolysaccharide
LTA	Lipoteichoic acid
M1	Pro-inflammatory macrophage
M2	Anti-inflammatory macrophage
MAPK	Mitogen-activated protein kinase
MCP-1	Monocyte chemoattractant protein 1
M-CSF	Macrophage colony stimulating factor
MD2	Lymphocyte antigen 96
MFI	Mean fluorescence intensity
MMP	Matrix-metalloproteinase
MOI	Multiplicity of infection
mRNA	Messenger ribonucleic acid
MSA	Mannitol salt agar
MyD88	Myeloid differentiation primary response 88
NET	Neutrophil extracellular trap
NFκB	nuclear factor kappa-light-chain-enhancer of activated B cells
NK	Natural killer
OCT	Optimal cutting temperature
OME	Oral mucosal equivalents
P3DOMM	Primary three-dimensional oral mucosal model
PAMP	Pathogen associated molecular pattern
PBMC	Peripheral blood mononuclear cell
PBS	Phosphate buffered saline
PBS-T	Phosphate buffered saline containing tween
PCR	Polymerase chain reaction
PerCP-Cy5.5	Peridinin-chlorophyll-protein Complex: CY5.5 Conjugate.
Pg	*Porphyromonas gingivalis*
PGN	Peptidoglycan
PLF	Periodontal ligament fibroblast
PMA	Phorbol-12-myristate acetate
PNUD	Palate not under denture
POK	Primary oral keratinocyte primary cells
POKM	Primary oral keratinocyte media
PRR	Pattern recognition receptor
PUD	Palate under denture
PVDF	Polyvinylidine (di)flouride
R	Receptor
RHOE	Reconstituted human oral epithelium
RIPA	Radioimmunoprecipitation assay
RNA	Ribonucleic acid
ROMT	Reconstituted oral mucosal tissue
RPMI	Roswell park memorial institute
SA	*Staphylococcus aureus*
SDA	Sabouraud dextrose agar
SDB	Sabouraud dextrose broth

SDS	Sodium dodecyl sulphate
SN	Supernatant
SPSS	Statistical Package for the Social Sciences
SR	Soluble receptor
TBK	Tank-binding kinase
TEM	Transmission electron microscopy
TEMED	Tetramethylethylenediamine
TGF	Transforming growth factor
THP-1	Human acute monocytic leukemia cell line
TIM	T-cell immunoglobulin and mucin-domain
TIRAP	Toll-interleukin 1 receptor domain-containing adapter protein
TLR	Toll like receptor
TMB	3,3′,5,5′-Tetramethylbenzidine
TNF	Tumour necrosis factor
TRAF	Tumor necrosis factor receptor-associated factors
TRAM	TRIF-related adaptor molucule
TRIF	TIR-domain-containing adapter-inducing interferon-β
Tris	Tris(Hydroxymethyl)aminomethane
TSA	Tryptic soy agar
TSB	Tryptic soy broth
VD3	1,25-(OH)2-Vitamin D3

1. Introduction

1.1. Oral mucosal modelling

The oral cavity is a complex environment. It contains a diverse microflora, which plays a role in health, homeostasis and disease (1). Oral hygiene regimes are widely practiced and involve the introduction of antimicrobial agents and mechanical disruption of biofilms (2). Both oral and systemic disease manifest in the oral cavity, including cancer, local and systemic infections, haematological disorders, gastrointestinal disorders, autoimmune disorders and dermatoses (3). Systemic disease therefore plays a role in oral health, as well as oral health influencing systemic disease (4). Studying these disease presentations provides an opportunity to further understand disease mechanisms and develop potential therapeutic options.

Historically, animal models were at the front line for studying oral disease, infection, cancer, wound healing, toxicology, and biocompatibility of orally administered agents (5–8). More recently *in vitro* monolayer cell cultures have provided an indication as to how healthy and diseased cells from the oral cavity will respond and function in the presence of intrinsic and extrinsic agents. Due to the isolated nature of monolayer studies, studying the response of such cultures focuses on the response of a singular cell type that does not sufficiently mimic the *in vivo* situation. The lack of both spatial interactions and cross-talk with surrounding cells and tissues renders it difficult to extrapolate these results to accurately predict the outcomes of an *in vivo* study (9).

The National Centre for the Replacement, Refinement and Reduction (NC3Rs) of Animals used within scientific research is an ethical initiative concerned with

animal welfare and ethics in medical and dental research (10). A wide range of projects have been supported for the purpose of developing non-animal ethical alternatives. An exciting new prospect within oral research is the development and optimisation of oral mucosal models that are able to accurately mimic the *in vivo* environment. As advances are made, the requirements for animal models are reducing. These novel *in vitro* models are more sophisticated than monolayer cell cultures and provide the opportunity to tailor each model to its desired application, allowing for the study of multiple cell types in an environment that spatially and morphologically mimics the native oral mucosa (11). These models are not without their challenges, and advances are still required in order to produce a suitable model for studying the complexity of oral disease (9).

1.2. Three-dimensional oral mucosal models

Tissue-engineered oral mucosa created for the purpose of modelling the oral cavity have been referred to by a variety of different names. Models incorporating both an epithelium and a lamina propria layer containing fibroblasts are termed full-thickness, or three-dimensional. Such models have been referred to as oral mucosal equivalents (OME), full-thickness oral mucosal models (FTOM), re-constituted oral mucosal tissue (ROMT), and, in the present study, will be described as three-dimensional oral mucosal models (3DOMMs) (12–14).

3DOMMs have been employed for a wide range of *in vitro* biocompatibility, toxicology, wound-healing, cancer, and infection studies. Such oral mucosal models are also being developed for tissue grafting purposes (11). A variety of cell types, scaffolds, and culture methodologies have been employed for this purpose, all with their own attributes and shortfalls. The overarching goal for the

field of oral mucosal modelling is to develop a full-thickness model that contains functional lamina propria and epithelial layers, with the formation of a basement membrane, in order to produce a structure that is analogous to the native oral mucosa. Within each individual application of the model there are likely to be additional objectives. For example, oral mucosal models created for grafting purposes are desired to be biodegradable; cancer models are required to contain cancer derived cells; and infection models are required to contain an intact epithelial barrier (15).

3DOMMs differ from oral epithelial models due to the presence of a fibroblast-containing lamina propria layer. Incorporating fibroblasts into a suitable matrix to create a lamina propria layer and overlaying this with keratinocytes to form an epithelium, has proven more informative than using epithelium only models, as these full-thickness models permit the study of the interaction between multiple cell types and the extra-cellular matrix (16). This is due to cross-talk between keratinocytes and fibroblasts, which occurs *in vivo*, and is reflected when these cell types are incorporated into a model together. Models that incorporated both fibroblasts and keratinocytes exhibited superior structural morphology and epithelial stratification, than models that incorporated either of the cell types in isolation (17). The 3DOMM environment also provides the ability to study cellular migration, matrix re-modelling, biochemical gradients, and the spatial interaction between a pathogen and the infected tissue (18–21). Overall, this allows a more informative overview when using such models for research purposes, when compared with monolayer epithelial models.

Not only are 3DOMMs a more suitable replacement for epithelium only models, they may also be preferable to non-human animal models, as disease manifests

differently within different species (21). Full-thickness oral mucosal and dermal models have been created with a variety of cell types, isolated from differing areas of the oral cavity and skin, including immortalized cell lines, commercially available primary cells, and primary cells from donor biopsies (22,23). Scaffolds range from de-cellularised dermis to a range of hydrogel mixes, including combinations of (or in isolation) collagen, fibrin, elastin, and agarose (24–26). Models have been created using a variety of methodologies, including the use of transwell inserts, electrospinning and 3D bio-printing techniques (21,27,28).

1.3. Oral infection

The oral immune system, along with the oral microbiota, collaborate to keep oral pathogens in check. The oral immune system consists of barrier mechanisms including: the tightly packed epithelial layer; presence of saliva; mucous; antimicrobial peptides; complement proteins; a cellular innate immune system, able to recognise and respond to conserved sites on pathogens; and the cellular adaptive immune system with its associated antibodies (29). Dysbiosis provides an opportunity for pathogens to prevail, disrupting the normal microbial balance and causing subsequent tissue damage. This shift in the composition of the microbiome may occur as a result of improper oral care regimes, the administration of antibiotic or antifungal agents, an impaired immune system, or due to systemic disease (1,30,31). Two of the most frequently discussed oral infections include periodontitis, mediated by pathogens such as *Porphyromonas gingivalis,* and denture stomatitis (DS), which is usually associated with the commensal organism and opportunistic pathogen *Candida albicans* (32,33). Periodontitis can cause inflammation of the gingiva, and subsequent periodontal tissue and alveolar bone loss, potentially resulting in tooth loss if left untreated

(32). DS is a condition experienced by denture wearers due to: improper cleansing of dentures; the disruption of normal salivary flow; denture colonisation of *Candida* species, most frequently *C. albicans;* and health and lifestyle risk factors such as diabetes mellitus and smoking (33–38). DS leads to erythema and oedema of the hard palate, although rarely causes a severe degree of discomfort, and is often diagnosed during routine examination (39). In severe cases of untreated DS, nodules may form on the hard palate due to inflammatory papillary hyperplasia, which may require surgical correction (40). It has also been proposed that DS infections may provide a portal of entry for blood stream pathogens (41). In recent years, a large focus of dental research has been placed upon these oral infections, aimed at gaining an understanding of disease pathogenesis and treatment options. Animal models have been frequently employed for periodontitis and DS research, however a recent paradigm shift has led to the development of *in vitro* models to study aspects of these diseases and obtain an understanding of the pathophysiology. These models have been somewhat informative when applied to study DS, however appear to be insufficient, at present, for the accurate study of periodontal disease (6,7,14,20,42,43). For both of these conditions, murine models often have disease artificially induced prior to their application as a disease model. This may lead to differences in the manifestation of disease, between these induced disease models, and naturally occurring disease within the human oral cavity (10,44). Furthermore, the murine and human immune system are not synonymous, meaning immune response to infection may differ, and hence the disease pathogenesis also (45).

1.4. Oral Infection models

Oral research is vital in order to gain an understanding of health and disease within the oral cavity. Such research provides an insight into the complex interactions between oral disease presentation and wider systemic disease (3,4,46,47). In contrast to medical research, dental disease research is relatively new, and emerging research models and techniques provide valuable insight into oral health and pathology, granting an opportunity for new treatment and prevention for oral disease. Oral disease models range from consenting live patients, live animal models, tissue explants, tissue-engineered oral tissue models, and monolayer cell cultures. *In vitro* models are advancing and are an informative means of studying cellular and tissue response to oral disease. At present, depending on the application, *in vitro* information may later need to be translated into animal models in order to confirm or expand upon *in vitro* findings, prior to progressing to clinical trials within humans. Additionally, *in vitro* models may be used as a prologue, to obtain data in order to justify a more considered and refined use of animal models(10).

Many research groups have implemented 3DOMMs to study pathogen-host interactions. Diverse methodologies have been employed for this purpose, including the use of different scaffolds and cell types, to study a range of bacterial, fungal and viral infections. **Table 1** summarises the methodologies and purposes for full-thickness skin, and oral infection models identified within recent literature.

Table 1: Summary of previously implemented 3DOMM methodology

Details are provided of infective agent, cell type, scaffold, and culture technique.

Infection	Scaffold	Keratinocyte	Fibroblast	Submerged	Air-liquid interface	Ref
Staphylococcus aureus & Pseudomonas aeruginosa	Decellularised dermis	Primary dermal	Primary dermal	1 Day	10-14 Days	(48)
HSV-1	Collagen	HaCaT	Primary dermal	5-7 Days	10-12 Days	(49)
HSV-1	Collagen	HaCaT	Primary dermal	5-7 Days	12-14 Days	(50)
Fusobacterium nucleatum	Collagen	Primary gingival	Primary gingival	3 Days	6 Days	(51)
Oral Microbiome	Collagen	TR146, HaCaT, or Primary dermal	NIH-3T3	5 Days	N/A	(52)
Candida albicans & Staphylococcus aureus	Collagen	NOK-si	Primary Gingival	Until epithelium reached confluence	14 days	(14)
Candida albicans	Collagen	FNB6 orTR146	Primary Buccal & Gingival	2 days	14 days	(42)
Staphylococcus aureus	Alvetex (polystyrene scaffold)	CCD1106-KERTr	Detroit 551	Fibroblasts only: 7 days Keratinocytes atop:3 days	21 days	(53)
Staphylococcus aureus	Collagen	Normal epidermal	Normal epidermal	Fibroblasts only: 8 days Keratinocytes atop: 2 days	10 days	(54)
Commensal *Streptococci & Staphylococci.*	Hydroxyapatite or Silicone	HOK	HGF	Fibroblasts only: 3 days Keratinocytes atop until confluent	Not disclosed	(55)
Porphyromonas gingivalis	None	TERT-2 OKF-6	Primary gingival	10 days	N/A	(56)
Candida albicans	Decellularised dermis	Primary	Primary	3 Days	14 Days	(20)
Candida albicans	Collagen	OKF-6 TERT-2	Primary gingival	Fibroblasts only: 2 days Keratinocytes atop: 6 days	14 days	(57)

As well as creating full-thickness models to study host response to oral infection, commercially available reconstituted human oral epithelium (RHOE) (epithelium only) and EpiOral (full-thickness) models were employed to either study tissue invasion of *Candida spp.,* or to compare the efficacy of full-thickness models with commercially available epithelium only models (20,35,42,58). The RHOE model by SkinEthic is created with a TR146 squamous cell carcinoma keratinocyte cell line, whereas EpiOral models by MatTek are created using primary oral cells; the MatTek models exhibit a stratified epithelium, unlike RHOE models (42). Full-thickness models have been shown to be more proliferative than epithelium only models, likely due to the interactions between the fibroblasts contained within the lamina propria layer and the epithelial keratinocytes (20). Furthermore, as with the native oral mucosa, proliferation was shown to be restricted to the basal layers of the epithelium, whereas within the epithelium only TR-146 model proliferation was seen throughout the epithelium (20). These commercially available models are expensive and are required to be used within a short period of time upon their receipt (57). Creating full-thickness oral infection models in the laboratory provides the opportunity to produce reproducible, cost effective models that are analogous to the native oral mucosa. Many research groups have successfully created oral mucosal models that appear structurally analogous to the native oral mucosa, displaying a multi-layered stratified epithelium that may be keratinised or non-keratinised depending on the area of the oral cavity the model is desired to represent. Models often differ from the native oral mucosa due to the lack of rete ridges, which are created *in vivo* through the mechanical pressures of mastication, although it has been indicated that it is possible to induce these within *in vitro* oral mucosal models (20,59).

There remains the question as to how representative these oral mucosal models are in terms of their responsivity to infection, due to the lack of an immune cell component. Some initial steps towards this have been achieved. Models have been shown to produce antimicrobial peptides and form a strong barrier against pathogenic invasion (20,60). Models have also been shown to produce pro-inflammatory cytokines in response to infective agents (13). It has even been possible to produce models that contain a microbiota (52). Several research groups have recently begun to incorporate innate immune cells into three-dimensional oral mucosal, or skin models, and a commercially available model from MatTek is currently marketed incorporating Langerhans cells (61–63).

Full-thickness models are a more informative oral model than monolayer studies, partially attributed to the incorporation of multiple cell types, hence the capability of epithelial-stromal cross-talk (11,18,64). This was the first step taken to represent the complexity of the oral cavity. Upon *in vivo* infection, multiple cell types will respond to an infective agent, all of which are able to influence the responses of others. Therefore, the incorporation of immune cells into such models is a positive step towards considering the true complexity of the oral environment. However, as of yet, these immune cell incorporated models have not been sufficiently implemented for studying host response to infection (61–63,65,66). Considering the host immune system is essential for the prevention and resolution of infection; it is necessary to incorporate innate immune cells into oral mucosal models in an informative manner, whereby they may be used for subsequent infection studies. Many models have incorporated different combinations of epithelial and stromal cells, with some introducing an immune cell component; however the interactions between these cells, and their

interactions with the model microenvironment, have not been examined in terms of pro-inflammatory cytokine production. It is the overall cytokine milieu that will determine the manner in which incorporated immune cells respond to pathogens. Therefore, to fully characterise the model's ability to represent *in vivo* infection, the interactions between cell types and their environment, and the resultant cytokine expression is of vital importance.

1.5. Hypothesis

It is possible, through the appropriate selection of keratinocyte and fibroblast cell types, and careful consideration of cellular interactions with a tissue-engineered environment to: i) produce a model that supports the incorporation, and permits the activity of macrophages; ii) and therefore develop an informative immunocompetent oral mucosal model that is suitable for the study of host response to infection.

1.6. Aims

This research is aimed at the development and characterisation of a three-dimensional oral mucosal model that is suitable for the study of host response to oral infection, and aims to consider and compare models created with immortalised (3DOMMs) and primary (P3DOMMs) keratinocytes. Specific attention will be paid to the ability of the models to respond to pathogenic agents, the interactions exhibited between the individual cell types, and the effects of the model environment. The models will be used to study tissue invasion and immune response to clinically relevant oral isolates of *Candida albicans* and *Staphylococcus aureus,* to determine their efficacy and potential applications as infection models. Finally, the 3DOMM environment will be assessed for its ability

to facilitate the incorporation, viability, and activity of innate immune cells, in order to develop an immunocompetent (IC) 3DOMM.

2. Methodology

2.1. General information

Cell culture and microbial culture were performed under aseptic conditions, using a laminar flow hood and Bunsen burner, respectively. Plasticware was obtained from Greiner. Tissue and cell culture plasticware was purchased sterile and endotoxin free. Powdered chemicals were obtained from Sigma Aldrich, dissolved into distilled H_2O, and filter sterilised prior to use.

2.2. Cell selection

HaCaT cells, a spontaneously immortalised keratinocyte cell line derived from histologically normal adult skin, were selected due to their longevity, reproducibility, and in the correct conditions, reported ability to form stratified, keratinised epithelia (67,68). Although HaCaT cells were initially derived from the skin, they have been employed to represent oral epithelia, and have been reported as suitable for studying keratinocyte inflammatory response (69,70). HaCaT also provide the added benefit of controlling differentiation, by means of calcium concentration, improving longevity, and permitting de-differentiation when desired (71).

HGF cells, are a commercially available human primary oral fibroblast cell type, obtained from the gingiva. HGFs were selected due to their anatomical location, as fibroblasts from different locations, even within the oral cavity, are physiologically diverse, and their activity is dependent on their origin (72,73).

POK cells are a commercially available human primary oral keratinocyte cell type. POK cells were selected over other primary oral keratinocytes due to their

availability, and reported growth in the absence of a fibroblast feeder layer, through the use of their proprietary media (indicated in their datasheet)(74).

THP-1 cells are a pro-monocytic cell line derived from a child with acute monocytic leukaemia (75). Unlike macrophages THP-1 cells are able to proliferate in culture, and due to their pro-monocytic nature THP-1 cells are non-adherent, unlike peripheral blood monocytes, making them an attractive choice due to their ease of application. THP-1 cells are well characterised, and are able to be differentiated into macrophages and subsequently polarised (76). Despite exhibiting some differing characteristics when compared to peripheral blood monocytes (due to their leukaemic origin), in the correct culture conditions, THP-1 cells are an informative and practical model for monocyte and subsequent macrophage studies(76,77).

Cells were purchased from ATCC, cell lot numbers and passage numbers are detailed in **Table 2**. THP-1 cells were kindly provided by Dr Andrew Foey of the University of Plymouth.

Table 2: Cell lines utilized within the present study.

Cell type	Product Number	Lot Number	Passage number
HaCaT	ATCC PCS-200-011	300493-3155F	39-48
HGF	ATCC PCS-201-018	305110-212	8-14
POK	ATCC PCS-200-104	80717999	3-6
THP-1	ATCC PCS-TIB-202	Unknown	10-20

2.3. Cell culture

2.3.1. General cell culture

HaCaT and HGF cells were maintained in DMEM containing glucose, L-glutamine, sodium pyruvate and phenol red, Gibco 11564446, and 10% FBS, Gibco 10500 batch #08Q1379K. POK cells were maintained in POK medium, which consisted of dermal cell basal medium, ATCC-PCS-200-030, supplemented with a keratinocyte growth kit, ATCC-PCS-200-040. THP-1 cells were maintained in RPMI 1640, containing 2 mM L-glutamine, Corning 10-040-CV, and 10% foetal bovine serum (FBS), Sigma Aldrich batch #BCBW3204. All adherent cells were cultured until approximately 70% confluence prior to passaging. HaCaT and HGF cells were detached using 0.25% Trypsin/EDTA, Fisher Scientific 25200072, and POK cells using primary cell trypsin solution, ATCC PCS-999-003, incubated at 37°C. Once the cells had detached the reaction was neutralised using equal volumes of complete medium for HaCaT and HGF cells and trypsin neutralisation solution, ATCC PCS-999-004, for POK cells. Once neutralised, the cells were transferred to a 15 ml falcon tube and centrifuged at 200 × g, so that the cells were pelleted. Supernatant was discarded and the pellet gently disrupted prior to resuspension in complete medium. Cells were then split into multiple flasks or applied for subsequent experimentation.

2.3.2. Freezing and resurrection of cell lines

Freezing medium for HaCaT and HGF cells consisted of DMEM + 10% FBS+ 10% dimethyl sulfoxide (DMSO). Freezing medium for THP-1 cells consisted of RPMI + 50% FBS + 10% DMSO. Freezing medium for POK cells consisted of POK medium +10% DMSO. Cells were frozen in 1 ml of freezing medium per

cryovial. Cryovials were placed in a room temperature Mr Frosty freezing container and frozen at -80°C for at least 24 hours, prior to being stored at liquid nitrogen vapour phase. Cells were defrosted rapidly using a 37°C water bath, placed in 9 ml of complete medium and centrifuged to remove excess DMSO. Cells were then resuspended in complete medium, placed in a pre-equilibrated flask of complete medium, and incubated in a humidified 37°C 5% CO_2 incubator.

2.4. Production of three-dimensional oral mucosal models (3DOMMs)

2.4.1. 3DOMM production

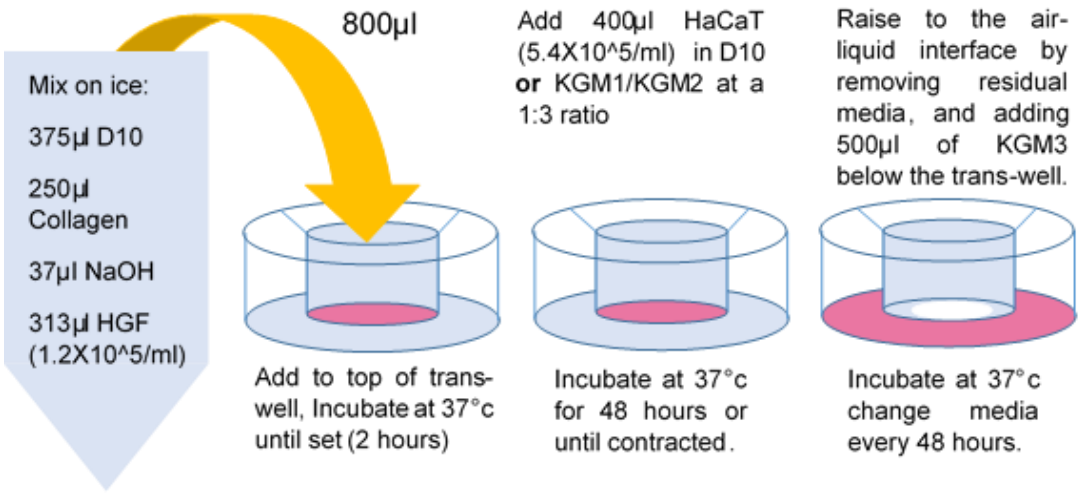

Figure 1: Standard methodology for the formation of a singular 3DOMM.
D10 refers to DMEM + 10%FBS

Three-dimensional oral mucosal models were formed in 0.4 µm polycarbonate mesh transwell inserts, Corning 3401, using rat-tail type-1 collagen, First link (UK) Ltd. 60-30-810, with a protein concentration of 2 mg/ml. Human Gingival Fibroblasts (HGF), ATCC PCS-201-018, were embedded into a collagen gel mix, containing: 25.6% collagen, 63.5% DMEM, 7% FBS and 3.8% 1M NaOH, as detailed in **Figure 1**. Once polymerised, a keratinocyte (HaCaT), ATCC PCS-200-011, overlay was added to the gel matrix. The models were left to mature for

between 12 and 23 days, experiment dependent, prior to use. Once the models had contracted (after approximately 48 hours), remaining media was removed. Subsequently 500 µl of KGM 3 (keratinocyte gold basal media, Lonza 00192151, supplemented with a bullet kit, Lonza 00192152, and 2.4 µM $CaCl_2$, **Table 3**) was added below the transwell insert, and changed every 48 hours thereafter. The production of a singular 3DOMM is detailed in **Figure 1**.

2.4.2. Keratinocyte gold media

Keratinocyte gold medium (KGM) was employed to introduce HaCaT cells to the model, KGM 1 and KGM 2 (at a ratio of 1:3), and once the models had been raised to the air-liquid interface KGM3. **Table 3** indicates the supplementation of KGM, Lonza 00192151, supplemented with a bullet kit, Lonza 00192152, and $CaCl_2$. Gentamycin/amphotericin was omitted from supplementation as the models were intended as infection models.

Table 3: KGM media formulations
Supplementation of KGM basal media to form KGM1, KGM2 and KGM3 to implement as culture media for 3DOMMs.

Supplement	KGM1	KGM2	KGM3
KGM basal medium	50 ml	50 ml	50 ml
Bovine pituitary extract	200 µl	200 µl	200 µl
Epidermal growth factor	50 µl	150 µl	50 µl
Hydrocortisone	50 µl	50 µl	50 µl
Insulin	50 µl	50 µl	50 µl
Transferrin	50 µl	50 µl	50 µl
Epinephrine	25 µl	25 µl	25 µl
Calcium Chloride (1M)	-	-	120 µl

2.4.3. Primary three-dimensional oral mucosal model (P3DOMM) production

P3DOMMs were created in the same manner as 3DOMMs, as per **Figure 1**, with the exception of medium for which D10/KGM was substituted with POK media. Instead of HaCaT cells, POK cells, ATCC PCS-201-018, were the epithelial cell type implemented in P3DOMM production. Once the models had contracted, remaining media was removed. Then 500 µl of POK medium was added below the transwell insert, and was changed every 48 hours thereafter, supernatants were subsequently stored for analysis by sandwich ELISA. P3DOMMs were then cultured for 14 days, due to the reported limited lifespan of primary oral keratinocytes, as directed by the manufacturer's instructions.

2.5. Histology

2.5.1. Sample preparation

Models were fixed in 4% paraformaldehyde for a minimum of 24 hours. After fixation, models were infiltrated with paraffin wax using a Leica TP1020 auto tissue processor. Models were passed through increasing concentrations of IMS (50%, 70% and 90%) for 1 hour periods, followed by three hours in 100% IMS whereby IMS was refreshed each hour. Once dehydrated, models were incubated in histolene (refreshed at each interval) for 0.5, 1.25, and 1.25 hours, prior to being infiltrated with wax for 1 hour followed by 2 hours in refreshed wax. Following this, wax infiltrated models were halved, and embedded in paraffin wax blocks aided by an embedding centre and cold plate, Leica EG1150H & EG1150C. Using a Leica RM2235 microtome, 5 µm sections were cut, placed in

a 50°C water-bath until flattened, and mounted upon glass slides. Once dry, slides were stained using a Haematoxylin and Eosin protocol.

2.5.2. Haematoxylin and Eosin staining

Slide mounted tissue sections were heated on a 60°C hot plate to remove paraffin wax. Slides were placed in a staining rack and agitated through 3 histolene changes, for a total time of 5 minutes. Histolene was drained by blotting the slide rack, and the samples were then taken through three changes of IMS, for a total time of 5 minutes. The rack of samples was then agitated in distilled water to observe whether the wax was sufficiently removed. Samples were then placed in Harris' haematoxylin for 10 minutes. Samples were then blued in tap water and the nuclear staining observed microscopically. If necessary, the nuclei were further blued in 1% lithium carbonate, and any residual background staining removed by dipping in acid alcohol. Samples were then placed in eosin for 5 minutes, and afterwards washed briefly in distilled water. Following this, the samples were agitated in two changes of IMS for a total of 2 minutes, followed by 2 changes of histolene for a total of 2 minutes. Samples were stored in histolene prior to mounting with DPX. Once dried, the slides were ready for observation and imaging.

2.6. Western blot

Prior to commencing the Western blot, RIPA buffer, Sigma Aldrich RO278, containing a 1% protease inhibitor cocktail, Cell Signalling Technology 5871, was added to samples, to extract the intracellular protein and protect against protease degradation. For 3DOMMs, samples were also briefly homogenised on ice, to aid protein extraction whilst preventing degradation due to temperature increase.

Samples were centrifuged briefly to remove cellular debris and supernatant was stored at -20°C prior to use. Upon defrosting total protein of each sample was quantified using a Pierce BSA protein quantification kit, Thermo Scientific 23227, measured against pre-quantified standards and determined colourimetrically. A quantity of sample equivalent to 30 µg of protein was diluted in PBS and mixed 4 parts to 1 part 5× Laemmli buffer, **Table 4.** The samples were mixed and boiled at 100°C for 8 minutes, and then centrifuged briefly. Then 10% acrylamide gels were created in house, **Table 5**. Gel electrophoresis equipment was obtained from BioRad, 165800FC**.** The hand cast stacking gel was formed first and set in 1.0 mm glass gel-electrophoresis cassettes, and levelled with 1 ml of ethanol. Once set, the loading gel was pipetted atop; immediately after, a 10 well spacer comb was pushed into the gel. Once the gel had polymerised, the spacer comb was removed to create the loading wells. Gels were loaded into an electrophoresis tank containing 1 part 5× electrophoresis buffer, to 4 parts dH_20, **Table 6**. Then, 5 µl of protein ladder, Geneflow S6-0024, was loaded to one well, and 20 µl of samples into test wells. The electrophoresis tank was set at 70 V and allowed to run until the protein ladder had passed the loading gel, and then raised to 100 V until the protein ladder spanned the length of the gel. Once complete the gel was washed in distilled water. Protein was transferred to pre-cut PVDF membranes, Invitrogen LC2005, activated in methanol and pre-soaked in transfer buffer. Proteins were transferred from the gel to the membrane with the aid of pre-cooled (4˚C) transfer buffer, **Table 6**, and a transfer tank, BioRad 17404070, and allowed to run for 12 hours at 25 V, at 4°C. After transfer, membranes were blocked in 5% milk in 0.05% PBS-Tween 20 at room temperature on a shaker plate for 1 hour. Primary antibodies were diluted in 2.5% milk in PBS-T, and incubated for 1.5 hours. Secondary antibodies were diluted in 2.5% milk, and

incubated for 45 minutes. Between each step membranes were washed 3 times in PBS-T. ECL chemiluminescent detection reagent, Bio Rad 1705060s**,** was mixed in equal parts (A and B) to a volume of 1 ml, and applied to the membrane. Membranes were read using an image-quant studio at 30 second intermittent exposures until strong bands could be observed.

Table 4: Production of 5× Laemmli buffer.

5X Laemmli buffer	
Reagent	**Volume**
0.5 M Tris-HCL pH6.8	1.75 ml
Glycerol	4.5 ml
0.5 g SDS in 2ml Tris-HCL	2 ml
0.25% Bromophenol blue in H_20	0.5 ml
β-mercaptoethanol	1.25 ml

Table 5: **Production of 10% acrylamide hand-cast gels for gel electrophoresis.**

Hand-cast Gels		
	Stacking Gel	**Volume**
Stacking buffer	2 M Tris pH 8.8 in dH_20	15 ml
	10% SDS in dH_20	0.8 ml
	dH_20	4.2 ml
	30% acrylamide	4.95 ml
	Stacking Buffer	3.75 ml
	dH_20	6.3 ml
	10% APS	100 µl
	TEMED	10 µl
	Loading Gel	**Volume**
Loading buffer	1 M Tris pH 6.8 in dH_20	10 ml
	10%SDS in dH_20	0.8 ml
	dH_20	9.2 ml
	30% acrylamide	1.005 ml
	Loading buffer	1.5 ml
	dH_20	2.3 ml
	10% APS	50 µl
	TEMED	5 µl

Table 6: Production of Western blot buffers.

5× Electrophoresis buffer pH 8.3		Transfer buffer	
Reagent	**Quantity**	**Reagent**	**Quantity**
Trizma base	12 g	Trizma base	28.8 g
Glycine	57.6 g	Glycine	6.06 g
SDS	4 g	dH_20	1600 ml
dH_20	800 ml – pH volume	Methanol	400 ml

2.7. Microscopy

2.7.1. Imaging

Live monolayer cultures were visualised and imaged using the Scopetek DCM-510 microscope camera, affixed to an inverted microscope. Tissue sections were visualised and imaged using a Leica DMD108 microscope/camera**.**

2.7.2. Confocal Microscopy

Models were either imaged live or cryostat sectioned prior to observation, as detailed in each experiment. A Leica SPE Confocal microscope was used to visualise and image the tissue. Lasers were selected to cover the recommended excitation and emission spectrum for cell-trace far red as detailed in the manufactures instructions (CTFR), FisherSci- 15531783.

2.7.3. Electron Microscopy

3DOMMs were fixed in glutaraldehyde (2.5% pH 7.2, 0.1 M) overnight. Tissues were transferred to PBS and then rinsed twice in sodium cacodylate (pH 7.2, 0.1 M) for a total time of 30 minutes. Tissues were then secondary fixed in osmium tetroxide (1% pH 7.2, 0.1 M) for 1 hour. Tissues were then rinsed twice in PBS and dehydrated through increasing concentrations of ethanol (30%, 50%, 70%, 90%) for 15 minute intervals. Then tissue was placed in 100% ethanol for three

15 minute intervals, where the ethanol was refreshed between each interval. Once dehydrated, tissue was infiltrated with increasing concentrations of agar low viscosity resin, diluted in 100% ethanol at a ratio of 30:70, 50:50, 70:30, and 100:0. Tissue remained in each concentration for 12 hours, with the exception of the 100% resin, which was repeated 3 times in refreshed resin, for a total of 72 hours, to ensure full infiltration. The resin-infiltrated tissues were placed in a coffin mould, encased in resin, and placed in a 60°C embedding oven for 12 hours, which permitted the polymerisation of the resin. Resulting blocks were sectioned using a Leica Ultracut E ultra-microtome, using a Diatome diamond knife. Sections were stained in uranyl acetate for 15 minutes, followed by Reynold's lead citrate for 15 minutes. Sections were observed and imaged using a JEOL 1400 transmission electron microscope. Sectioning was kindly performed by Glenn Harper of the University of Plymouth's electron microscopy suite.

2.8. Enzyme linked immunosorbent assay (ELISA)

Supernatants were analysed via Sandwich ELISA in order to identify the cytokines IL-6 (Capture BD Biosystems 554543, Detection BD Biosystems 554546), IL-8 (Capture BD Biosystems 553716 Detection BD Biosystems 554718), TNFα (DuoSet kit R&D Systems DY210-05), and IL-1β (DuoSet kit R&D systems DY201-05). ELISAs were performed in high bind flat 96 well ELISA plates, Greiner 665061. The details for each cytokine, including concentrations, volumes, incubation times, and temperatures can be found in **Table 7**. Capture antibodies were diluted in PBS to the desired concentration. Powdered BSA, Melford A30075-100, was weighed and made up into a 2% solution, in PBS, and used as a blocking buffer. Standards for IL-6 and IL-8 were obtained from the National Institute for Biological Standards and Control, TNFα and IL-1β standards

were included within each DuoSet ELISA kit. Three-fold serial dilutions were created of each standard between the ranges indicated in **Table 7**, a blank was also included. Secondary antibodies were diluted in 2% BSA PBS. Streptavidin HRP, R&D systems DY998, was diluted 1:200 in 2% BSA PBS. TMB, Biolegend 421101, was added at a ratio of 1:1 part A to part B. Stop solution, 1.8 M H_2SO_4 was added to the TMB reactive wells once the sample wells were visually within the range of the standard curve. Plates were read spectrophotometrically, at 450 nm in a VersaMax plate reader. In some instances supernatants were diluted to permit detection within the range of the ELISA standard curve; for all samples within a given experiment the same dilution was performed. A dilution factor was selected from preliminary analyses to reduce above-range data to a detectible level, whilst minimising the loss of low-range data. Any remaining above range values were taken to be the highest detectible value from the standard curve; any subsequent low range values were taken to be the minimum (above 0) detectible value from the standard curve.

Table 7: ELISA methodology.

ELISA reagent: concentration, volume, duration, temperature and diluent. Blue vertical lines indicate wash steps 3 times in 0.05% PBS-T. Standard values are indicated as the highest and lowest value of the standard curve, as well as the dilution factor (DF).

	Primary	**Blocking**	**Standards**	**Secondary**	**Streptavidin**	**TMB**	**Stop solution**
Timing (at 37°c)	2 hours	1 hour	2 hours	1 hour	0.5 hours	Variable	Instant
Volume per well	50 µl	150 µl	50 µl	50 µl	50 µl	100 µl	50 µl
IL-6	1 µg/ml in PBS	2% BSA in PBS	10,000 pg/ml DF 3 13.717 pg/ml	0.5 µg/ml in 2% BSA PBS	1:200 dilution in 2% BSA PBS	1:1 A:B	H_2SO_4
IL-8	2 µg/ml in PBS	2% BSA in PBS	10,000 pg/ml DF 3 13.717 pg/ml	0.5 µg/ml in 2% BSA PBS	1:200 dilution in 2% BSA PBS	1:1 A:B	H_2SO_4
TNFα	4 µg/ml in PBS	2% BSA in PBS	5000 pg/ml DF 3 6.56 pg/ml	50 ng/ml in 2% BSA PBS	1:200 dilution in 2% BSA PBS	1:1 A:B	H_2SO_4
IL-1β	4 µg/ml in PBS	2% BSA in PBS	1000 pg/ml DF 3 1.37 pg/ml	150 ng/ml in 2% BSA PBS	1:200 dilution in 2% BSA PBS	1:1 A:B	H_2SO_4

2.9. Flow cytometry

Cells were centrifuged at 200 × g and washed twice in Ca^{2+} and Mg^{2+} free PBS. Cells were resuspended at a density of 1-2.5 × 10^6 cells in 100 µl of PBS. Cell suspensions were divided between test groups and isotype controls and 5 µl of the desired antibody was added to the cell suspension, and mixed by pipetting. Antibodies are identified in individual experiments in subsequent chapters. Samples were incubated in the dark, on ice for 20 minutes to permit antibody binding. Cells were then washed three times in DPBS as above, and resuspended in 500 µl of DPBS. Flow cytometry was performed using a FACSCalibur flow cytometer for FITC channels (excitation: 488 nm; emission: 520 nm; Laser: blue), and PerCPCy5.5 channels (excitation: 482 nm; emission: 676 nm Laser: blue), acquiring 10,000 events per sample, in triplicate, wherever possible. Post-acquisition gating and analysis was performed using FCS Express.

2.10. Polymerase chain reaction (PCR)

DNA was extracted from suspected *C. albicans* strains using a DNeasy blood and tissue kit, Qiagen 69504, as per the manufactures instruction, supplemented with bead beating for 1 minute to ensure maximal extraction. DNA concentration was quantified using a nanodrop spectrophotometer, Thermofisher ND2000, and 50 ng of DNA was used per reaction. Forward and reverse primers for *C. albicans 5*‘ “TTT ATC AAC TTG TCA CAC CAG A” 3’ and 5‘ “ATC CCG CCT TAC CAC TAC CG” 3’ were applied for the detection of a positive *C. albicans* isolate, using *C. albicans* SC5314 gDNA as a positive control, and a no template control (78,79). DreamTaq Green PCR master mix (15 µl), Thermofisher K1081, was mixed with 50 ng of extracted DNA and 25 pM of each primer, giving a final reaction volume

of 30 µl. The PCR reaction was thermocycled using a Geneamp PCR system 9700. Samples were cycled as followed: initial denaturation at 94˚C for 10 minutes, followed by 30 cycles of (denaturation 94˚C for 30 seconds, annealing 55.3˚C for 30 seconds, and extension 72˚C for 30 seconds), and followed by a final extension at 72˚C for 30 minutes. Samples were then held at 4˚C upon completion. Upon completion of the amplification, 6 µl was loaded per well into a 1.5% agarose gel formed in a Tris Acetate EDTA buffer, containing CYBR safe dye, Invitrogen S33111. Samples were ran alongside 3.5 µl of 2 log quick load DNA ladder, NEB B7025, at 90 V until the ladder could be clearly resolved. Gels were viewed and imaged using a BioRad Gel Doc XR under UV light.

2.11. Data analysis

2.11.1. Statistical significance between groups

For all comparisons between groups, each individual group was tested for normality using a Shapiro-Wilk's normality test. If any group within the data set returned as non-parametric, all data groups involved in the comparison were analysed using a non-parametric Kruskal-Wallis test, followed by a Dunn's multiple comparisons test. If all individual data groups returned as parametric, a parametric one-way ANOVA test was performed followed by a Tukey's multiple comparisons test. Statistical *p*-values reported are those returned within the multiple comparisons tests.

2.11.2. Correlation analyses

In order to determine correlation between groups, a Spearman's rank test was applied. Spearman's rank provides a correlation coefficient that indicates how closely related the data of one group is to that of another group. Positive relationships between groups are indicated by a positive correlation coefficient (*r*), coefficients near to 1 indicate a strong correlation. Negative relationships between groups were indicated by a negative correlation coefficient, coefficients near to -1 indicated a strong correlation. A *p*-value is also provided, which informs the significance of the correlation between groups.

3. Development and characterisation of oral mucosal models

3.1. Introduction

3.1.1. Structure and function of the native oral mucosa

The oral mucosa acts as a barrier for the innate immune system, preventing pathogenic entry to the blood stream and tissues beneath. The epithelium undergoes constant challenge with a diversity of antigens, through food, microflora, and potential pathogens. The oral cavity also encounters strain due to mechanical, chemical, and temperature burdens as a result of mastication, food, beverages, and oral care regimes (80). The oral cavity's structure permits a protective barrier, whilst also providing the flexibility required for mastication and speech. Furthermore, due to the constant challenge by extrinsic factors it possesses stringent immunological mechanisms that work to promote health and homeostasis (81).

Various degrees of keratinisation are seen within the oral cavity, dependent upon the level of mechanical force the area will encounter (82). Areas of the hard palate and gingivae are keratinised, providing extra protection from mastication. The sublingual mucosa and buccal mucosa are non-keratinised. Within the oral mucosal epithelium, different keratins are expressed within the tissue layers. Keratins are differentially expressed dependant the overall extent of keratinisation exhibited within a given area, **Figure 2** (83). Keratins are intermediate filament proteins which promote mechanical stability and integrity of epithelia, as well as playing a regulatory role in terms of intracellular signalling including contributing to epithelial polarisation, and membrane trafficking (84).

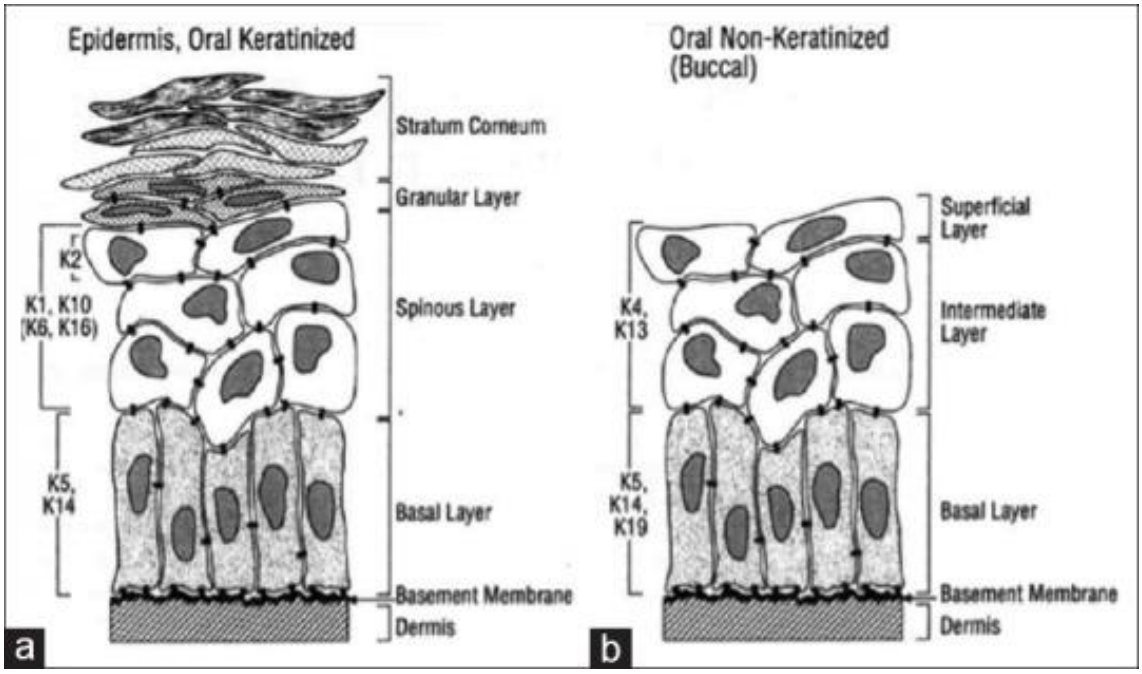

Figure 2: Structure and keratinisation of the a) keratinised and b) non-keratinised oral mucosa.

Figure by Nimish Deo, and Deshmuck. 2018 (83). Keratins are differentially expressed within epithelial layers and vary between keratinised and non-keratinised oral mucosa.

Keratins are expressed in a site dependent, and differentiation dependent manner. All stratified squamous epithelia express keratins 5 and 14 at the basal layers (85,86). Keratin 14 is involved in cellular proliferation; keratin 14 knockdown HaCaT cells displayed reduced proliferation and delayed cell cycle progression (86). Different keratins may withstand different levels of mechanical pressure. Typically, stronger epithelial tissues express a more diverse range of keratins; keratinised oral epithelia express keratins 5 and 14 in the basal epithelial layers, and keratins 1,10,6,16 and 2 in the spinous and granular epithelial layers; non-keratinised oral epithelia are reported to express keratins 5,14 and 19 in the basal epithelial layers, and keratins 4 and 13 in the intermediate and superficial layers (83). Keratins form obligate heterodimers whereby type-1 (acidic) keratins, form dimers with type 2 (basic) keratins. It is these dimers that form the basic

building blocks of keratin filaments, which consist of 32 individual α helical coils, twisted into a rope like filament, forming strong lateral hydrophobic interactions, enabling these filaments to promote structural integrity (87). Keratins 10,12,14,16 and 19 are examples of type-1 keratins, and 1,2,4,5 and 6 are examples of type-2 keratins (84).

The oral mucosal epithelium consists of a stratified squamous epithelium with proliferating cells at the basal layers. The number of epithelial layers varies depending on the anatomical region in which the keratinocytes reside. Differentiated cells migrate to the surface, undergo terminal differentiation, and replace shedding cells at the surface. The oral mucosal epithelium also contains anti-microbial factors, such as salivary peptides that aid in the defence against pathogens. These, alongside the tightly packed epithelial cells, constant epithelial shedding, and keratinisation, comprise the epithelial barrier, protecting the tissues beneath (80).

3.1.2. Skin vs oral keratinocytes

At a cellular level, oral and skin keratinocytes are morphologically similar (88). They both form organised stratified epithelia, which are highly proliferative at the basal layer, and as cells mature and differentiate they migrate towards the apical layers of the epithelium. Within the skin and keratinised areas of the oral mucosa, prior to sloughing (and subsequent replacement by newer cells), the squames of the apical epithelial keratinocyte layer offer extra protection against external pressures and microbial invasion (89).

At a tissue level, both exhibit a multi-layered epithelium, which is anchored to a basement membrane, atop a dense connective tissue layer termed the lamina propria, with the dermis being the skin equivalent. The lamina propria is responsible for the diffusion of vital nutrients and growth factors into the avascular epithelium. The lamina propria of skin and oral mucosa consists of fibroblasts, connective tissue, capillaries, macrophages, and extra-cellular matrix (ECM) material (88). Oral mucosa is considered more synonymous with skin than other anatomical regions of mucosa, however differences do still exist at a tissue level (88).

Skin contains appendages such as hair follicles, sebaceous glands, and sweat glands, which are not seen within the oral mucosa (90). The oral mucosa is more vascularised than skin (accounting for its colour), has increased permeability, and is moist. The oral cavity exhibits region-dependent keratinisation, however the skin is consistently keratinised throughout (88). Research involving skin or oral keratinocytes is often considered translational from one anatomical region to another. Studies have implemented oral and skin keratinocytes interchangeably as a means of *in vitro* modelling, and developing tissue for grafting purposes (70,91–93).

3.1.3. Fibroblasts

Fibroblasts are the most abundant cell type within connective tissue, and are responsible for producing extracellular matrix components including collagen. Fibroblasts also assist wound healing by facilitating contraction of the wound, and the formation and secretion of extracellular matrix material (94). The fibroblast population within an oral model has an overall effect on the tissue in which they

situate, and are able to affect epidermal morphogenesis, homeostasis, and differentiation (95).

Within the oral cavity, there is a large degree of fibroblast heterogeneity. Fibroblasts are the most abundant cell type within the periodontium and responsible for maintaining the connective tissues that support and anchor the teeth. Within the periodontium both gingival fibroblasts and periodontal ligament fibroblasts exist, exhibiting different roles in terms of morphology, secretion of proteins and growth factors, and proliferation rates (96). For creating an oral mucosal model, it is therefore necessary to ensure the fibroblast population is of the correct origin and therefore phenotype. Isolated gingival fibroblasts (GF) and periodontal ligament fibroblasts (PLF) have been used by Dabija-wolter *et al*., 2012, as a means of differentially creating junctional and sulcular epithelium. The fibroblast type employed, as well as the length of time in culture, was the defining factor as to how the tissue morphology reflected these two distinct epithelial phenotypes (97). This is an example of how fibroblasts isolated from different anatomical regions may lead to differing responses when cultured *in vitro*; fibroblasts are specialised to their tissue type, and fibroblasts isolated from different tissues are morphologically and functionally dynamic. Fibroblasts furthermore exhibit positional identity and memory (95). Therefore the population from which fibroblasts are isolated is crucial to their activity and subsequent activity of the model as a whole (73). For this reason, fibroblasts should be carefully considered to ensure a suitable physiological population is chosen for modelling purposes.

3.1.4. Immortalised vs Primary cells

Cells used for *in vitro* modelling purposes may be immortalised, either spontaneously or induced in the laboratory through the use of viral gene transfection (98). Immortalised cells continue to divide indefinitely, and unlike primary cells, do not reach senescence due to the lack of a Hayflick limit (99,100). For this reason, immortalised cells may always be considered as potentially cancerous, and can differ in phenotype from their progenitor cells. Immortalised cells are stable and may be used over a long period of time for *in vitro* study, as they undergo many population doublings without altering phenotype. Eventually even immortalised cells will undergo genetic drift, altering the cell line's genotype and phenotype. Furthermore, the serial passage of a singular cell line enhances the risk of the cell line acquiring mycoplasma contamination, which may significantly alter cellular response from its original phenotype (101). Despite these limitations, the reproducibility of experiments conducted with immortalised cell lines remains appealing; however immortalised cells may not always accurately reflect the native environment due to the changes that may occur, either as a result of the immortalisation process, or due to prolonged culture (102).

Primary cells are also employed for *in vitro* modelling purposes. They are often considered a closer representation of native tissue than immortalised cells, however they only hold their phenotype and viability for a limited number of passages, are more difficult to work with when compared to immortalised cells, and exhibit donor variability. Donor variability reflects the diversity seen between the individuals within the general population. For some purposes, this variability could be embraced; for example, if a novel therapeutic were to be tested on multiple individuals, preliminary data within cells obtained from multiple donors

may represent the general population better than *in vitro* repeats performed on cells obtained from one donor. Therefore, the outcome of the study may more accurately predict the variation that may be seen in a follow up *in vivo* study, conducted across multiple individuals. Obtaining primary cells often requires purchasing expensive cells from distribution companies or acquiring donor tissue. Obtaining multiple batches of donor cells at any one time would be expensive and unlikely to be feasible due to availability, or require ethical approval, which stipulates the applicant should minimise the amount of individuals required for a study to still be valid. Therefore obtaining enough cells from multiple donors, to accurately study donor variability and also provide a statistically powered sample size, would be complex, expensive, or unethical. Because of this, donor variability is rarely utilised to its potential, and often seen as a shortfall when using primary cells from multiple origins to conduct the same experiment. This is due to the lack of reproducibility exhibited, and the limited number of experiments that can be performed using primary cells obtained from one donor within the relatively low number of population doublings for which they maintain their initial characteristics and viability (103). As such, there are benefits and drawbacks to using immortalised and primary cells, and their application and use should be considered carefully. This thesis aims to consider both immortalised and primary keratinocytes for the application of developing an immunocompetent oral infection model.

3.1.5. Matrices

The choice of a matrix material requires careful consideration for its desired application. The most frequently used matrix used for *in vitro* infection modelling purposes is a collagen hydrogel, most frequently rat-tail type-1 collagen, **Table 1**.

Collagen, the most common extra-cellular matrix (ECM) protein, is manufactured by fibroblasts, and is therefore representative of a simple *in vivo* lamina propria (104). Type-1 collagen is the most abundant collagen within the dermis (104). Other more complex matrices have been employed for tissue grafting purposes, due to the highly contractile nature of collagen and its subsequent tendency to promote scar formation, interfering with the wound healing process (105). However, the use of type-1 collagen hydrogels permits a simple and reproducible technique, without the need for expensive specialised equipment for *in vitro* modelling purposes.

3.1.6. Basement membranes

Basement membranes are a thin specialised ECM connective tissue, consisting of mainly type IV collagen, situated between the lamina propria and epithelium, of the oral mucosa and skin (104,106). The basement membrane provides structural support by anchoring the epithelium to the lamina propria layer. It is involved in cellular functionality and communication between the epithelial layer and the underlying fibroblast-containing lamina propria layer (106). Basement membrane formation is a result of cellular secretion of proteins, such as laminin, occurring as a result of epithelial mesenchymal cross-talk (107).

3.1.7. Immunogenicity and the oral mucosal model

Cells that are not traditionally regarded as immune cells are able to evoke an immune response. This is achieved by recognition of a pathogen or tissue damage, which induce signalling pathways that call for immune cell activation and recruitment. It is also known that cells are able to respond to their local environment. The cellular messages (cytokines) within the local environment, in

combination with the recognition of a pathogen or damage, determines which downstream cytokines are released from the reacting cell, tailoring the way the cellular immune system responds. This chapter therefore focuses on characterising the interactions between model-incorporated cells and the 3DOMM environment, as well as exploring how these cells recognise and respond to pathogens.

3.1.8. Recognition of pathogens by pattern recognition receptors (PRRs)

The human innate immune system can recognise and respond to a wide variety of pathogens. Innate immune cells, and other cell types such as epithelial, and endothelial cells are capable of recognising pathogens via PRRs, which identify pathogens through conserved markers, termed pathogen associated molecular patterns (PAMPs). PAMPs allow the innate immune system to respond to pathogens they have never encountered before due to their ability to recognise these markers, which are associated with pathogenic challenge (108). PAMPs include cell wall components, secreted molecules, and nucleic acids; such recognisable PAMPs do not exist within host cells, which permits the innate immune system to discriminate between self and non-self. PRRs are often programmed to respond to specific PAMPs; the behaviour of the pathogen will also determine which PRR may respond, due to their localisation. Toll-like receptors (TLRs) may be membrane-bound and therefore expressed extracellularly (TLRs 1, 2, 4, 5 and 6) or expressed intracellularly, bound to endosomes (TLRs 7, 8 and 9) (109,110). Upon binding a PAMP, TLRs initiate a downstream signalling cascade that can instigate an immune response. Common TLR ligands are indicated in **Table 8**.

Table 8: Bacterial and Fungal PAMPS

PAMPs acting upon: TLR1/TLR2 heterodimer, TLR2, TLR2/TLR6 heterodimer, TLR3, TLR4, TLR5, TLR7/TLR8 heterodimer, TLR9 and TLR10. Black squares indicate confirmed TLR recognition of the PAMP. Question marks indicate proposed TLR recognition of the PAMP.

PAMP	Toll-like receptor													
	1	1/2	2	2/6	3	4	5	6	7	7/8	8	9	10	Ref
Bacterial														
Lipopolysaccharide						■								(111)
Diacyl lipopeptides				■										(112)
Triacyl lipopeptides		■												(112)
Peptidoglycan		?	■											(113) (114)
Lipotechoic acid			■			?								(115) (113)
Phenol solubule modulin			■	?										(116)
Glycolipids			■											(117)
Flagellin							■							(118)
CpG DNA												■		(119)
Fungal														
Zymosan				■										(120)
Mannan						■								(121)
Phospholipomannan			■											(122)
Glucurnoxylomannan						■								(123)

3.1.9. Toll-like receptor (TLR) signalling

Toll-like receptors form either homodimers or heterodimers to enable downstream signal transduction upon ligand binding. Some TLRs require additional adaptor molecules in order to form a TLR complex and therefore enable such a response. TLR2 forms heterodimers with TLR1 or TLR6; TLR2 may be reported alone in some studies regarding ligand recognition and signal

transduction, however depending on the ligand, TLR1 and TLR6 will have also been required in order to permit recognition and response to triacyl lipopeptides and diacyl lipopeptides, respectively (112). TLR4 forms a homodimer, and relies upon adaptor molecules such as CD14, LBP, and MD2 (124,125). Upon TLR activation, a downstream signalling cascade leads to the translocation of transcription factors to the nucleus, thus instigating cytokine production, **Figure 3** (126).

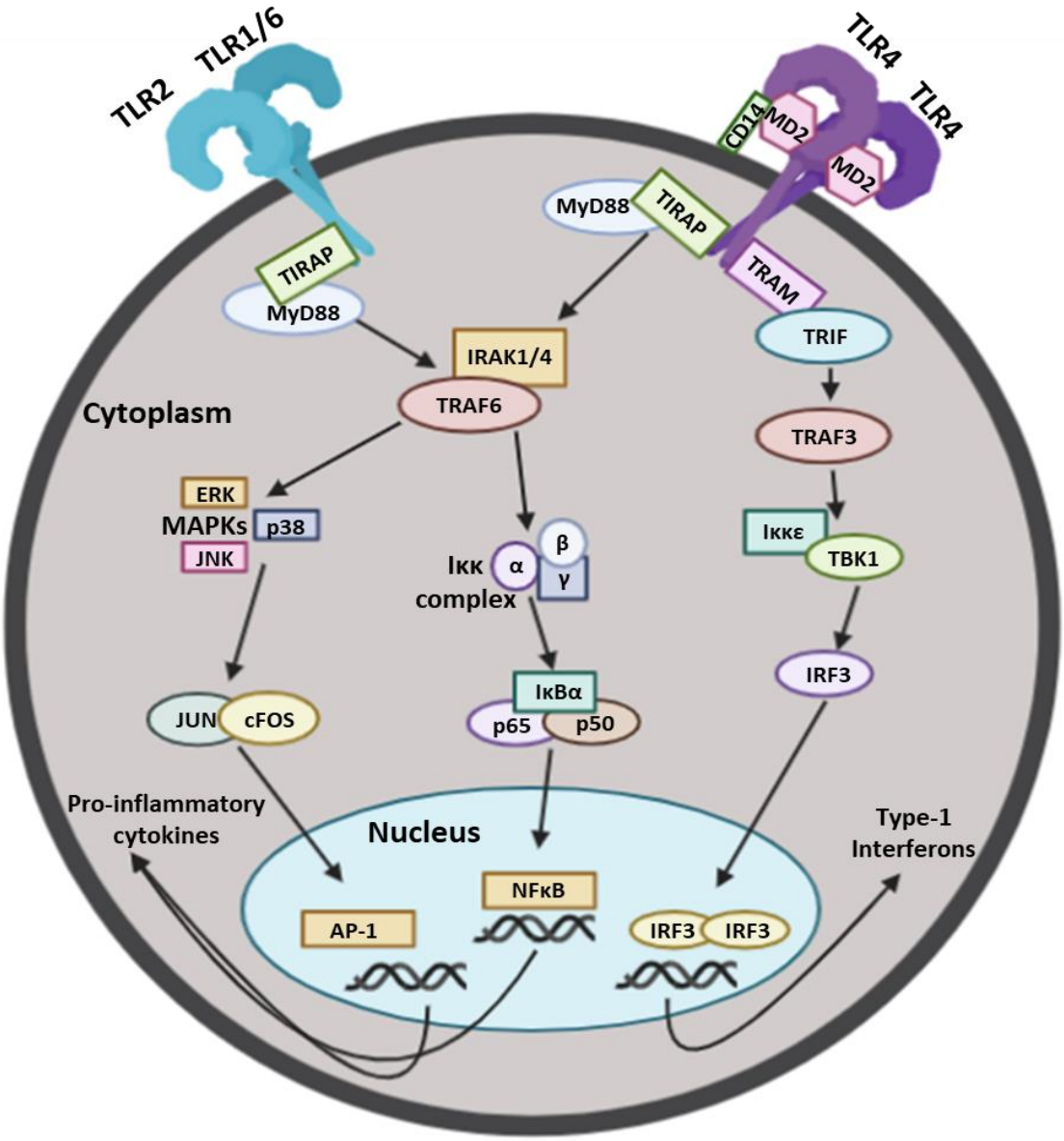

Figure 3: TLR2 and TLR4 signalling pathways.
From previous page: TLR2 forms heterodimers with TLR1 or TLR6 upon recognition of triacyl lipopeptides and diacyl lipopeptides respectively (112). TLR4 forms homodimers, in the presence of the adaptor protein MD2 which enables binding to LPS and signal transduction, in the presence of CD14 and LBP (124,125). TLR2 and TLR4 MyD88 dependent signalling pathway leads to the production of pro-inflammatory cytokines through translocation of the transcription factors NF-κB, and AP-1 to the nucleus (129). The TLR4 MyD88-independent pathway (TRIF-dependent) pathway, utilises a different signalling pathway, leading to the production of type-1 interferons through the translocation of transcription factor IRF to the nucleus (130). Figure informed by Goh *et al*., 2012 (126).

3.1.10. Pathogen associated molecular patterns (PAMPs)

Lipopolysaccharide (LPS) is isolated from the cell walls of gram-negative bacteria. LPS isolated from the oral bacterium, *Porphyromonas gingivalis* (PgLPS), as with LPS isolated from other gram-negative bacteria, is traditionally reported as a TLR4 agonist. Controversy exists over which TLRs are truly associated with PgLPS signal transduction. PgLPS has been shown to signal through both TLR2 and TLR4, and has been reported as a TLR2 agonist, with differential agonism/antagonism of TLR4, dependant on the local microenvironment (127). This phenomenon may be debunked with the explanation that LPS signalling through TLR2 is as a result of improper purification processes, resulting in other residual PAMPs existing alongside LPS, which may lead to TLR2 activation by different means (128).

LPS derived from the gram-negative bacterium *Escherichia coli* strain K12 (K12 LPS) is known to signal through TLR4. K12 LPS has been used as a TLR4 agonist within multiple studies, and has been shown to activate the TLR4 receptor

complex, and as a result trigger the downstream signalling cascade leading to subsequent cytokine production (131–133).

Lipoteichoic acid (LTA) is a ubiquitous cell wall component of gram-positive bacteria. It has been shown to produce a potent immune response. LTA is traditionally reported and implemented as a TLR2 agonist (134). The question has been raised as to whether TLR4 signalling is also required for LTA-mediated immune response (115).

Despite the fact there is controversy as to the exact receptors that recognise and respond to LPS and LTA, it is apparent that both TLR2 and TLR4 are highly involved. Many studies have supported the use of LTA as a TLR2 agonist and LPS as a TLR4 agonist. From this point onwards, downstream effects as a result of LPS signalling will cautiously be considered as a result of TLR4 activation, and LTA signalling as a result of TLR2 activation. However, ultimately it is the overall ability of the cells and subsequent 3DOMMs to respond to microbial challenge, not the exact mechanism in which they respond, that is of interest.

3.1.11. Pathogen recognition by 3DOMMs

The following sections focus on the expression of TLR2 and TLR4 within keratinocytes and fibroblast cells. TLR2 and TLR4 have been focused upon due to their ability to recognise gram-positive and gram-negative bacterial components, respectively, and fungal components, collectively, as indicated in **Table 8.** The purpose of this is to assess the ability of the 3DOMM cell types to recognise and respond to bacterial and fungal infection.

3.1.12. Immuno-responsivity of keratinocytes

TLR expression has been recently identified within epithelial cells, indicating they possess the ability to evoke an immune response to pathogens (135–138). In 2005, Kollisch *et al.* compared the relative expression of TLRs within primary keratinocytes and HaCaT cells (137). This was achieved by studying the mRNA expression of various TLR genes, as well as the adapter proteins MD-2 and CD14. Comparing the downstream pro-inflammatory cytokine expression when cells were stimulated with TLR ligands permitted the analysis of functional TLR activity. The ligands *S. aureus* peptidoglycan (PGN), and *E.coli* LPS, were used to stimulate TLR2 and TLR4, respectively. Primary keratinocytes and HaCaT cells were both shown to increase IL-8 expression in response to PGN compared to a negative media control, indicating that functional TLR2 is present at the cell surface. Interestingly, neither cell type displayed an increase in IL-8 protein production when stimulated with LPS. This may be explained by the lack of the MD-2 adapter protein, an essential component of the TLR4 signalling complex; although the relative expression of TLR4 and CD14 mRNA increased after LPS stimulation of HaCaT cells, the relative mRNA expression of MD-2 did not, accounting for the lack of IL-8 protein production in response to LPS (137).

TLR2 and TLR6 form a heterodimer that is capable of recognising the fungal cell wall component zymosan. The TLR2/6 complex is of interest within this thesis due to its ability to recognise and evoke a response to *C. albicans.* Olaru *et al*., 2010, showed the ability for HaCaT keratinocyte cells, as well as other immortalised and primary keratinocyte cells, to upregulate IL-8 production in response to zymosan. The suggested receptor for this upregulation is the TLR2/6 heterodimeric complex. This indicates that TLR6 is expressed within

keratinocytes, and most importantly the HaCaT cell line, as also demonstrated by their high level of TLR6 mRNA expression (139).

There is evidently considerable variation in the literature regarding TLR2 and TLR4 expression and functional ability within keratinocytes, therefore their capability to respond to gram-negative and gram-positive bacterial components remains uncertain (137,138,140,141). Such variation in detection, expression, and functionality of TLR2 and TLR4 warrant further exploration, and will be characterised for the HaCaT and POK keratinocyte cells employed within the present study.

3.1.13. Immuno-responsivity of fibroblasts

Fibroblasts have been recently identified to play an active role within the cellular immune response, due to their expression of TLRs. Upon activation via TLR recognition of a PAMP, fibroblasts mediate a downstream immune response through the secretion of cytokines and chemokines (142). Within periodontal ligament fibroblasts, TLR2 and TLR4 act as functional receptors upon bacterial invasion. Downstream production of pro-inflammatory cytokines of IL-6 and IL-8 were observed in response to stimulation with bacterial components, confirming receptor functionality (143). Constitutive expression of TLR2 and TLR4 has also been confirmed within dental pulp and gingival fibroblasts, indicating that fibroblasts capable of responding to a pathogen and instigating an immune response are prevalent throughout the oral cavity (142,144). The expression and confirmed functionality of TLR2 and TLR4 within human fibroblasts isolated from the gingivae have been reported on several occasions (142,145–148).

3.1.14. Immunogenicity of 3DOMMs

Three-dimensional oral mucosal models have been used as infection models. However, the majority of studies have focused upon tissue damage and invasion by a pathogen, as opposed to the tissue immune response upon recognition of a pathogen.

The commercially available, epithelium only, TR146 Skin-Ethic oral mucosal model by MatTek, and in-house tissue engineered models have been implemented to measure pro-inflammatory cytokine response (IL-1α, IL-1β, IL-6 and IL-8) to *C. albicans* stimulation (20,149). Such utilisation demonstrates one manner in which such models may be utilised to study host immune response to infection.

A variety of cell types and cell lines have been employed in the production of 3DOMMs. The capabilities of keratinocyte and fibroblast cells to respond to infection may differ depending on cell types used. Prior to the implementation of P/3DOMMs to study host response to infection, it was necessary to examine the individual cell types that will comprise these models, in terms of their abilities to recognise and respond to PAMPs.

Multiple techniques have been employed previously to study a cell line's ability to respond to pathogenic stimuli. This includes studying mRNA expression for genes associated with the immune response, looking for the presence of immune receptors using Western blot analyses, the identification of surface expression of PRRs through immune staining or flow cytometry, and looking for evidence of recognition by studying downstream markers of immune response. There are

shortfalls with any one of these techniques when used in isolation. For example, identification of mRNA expression does not guarantee a functional protein is synthesised downstream, nor consider potential post-translational modification of proteins. Observing protein presence through Western blot, does not ensure that the protein is localised correctly. Identifying surface expression through flow cytometry does not ensure that any adaptor proteins, or the downstream signalling cascade, is present. Finally, identifying downstream products such as cytokines, whilst perhaps one of the most robust ways of ensuring a functional signalling pathway is present, does not guarantee that the particular pathway/protein of interest is indeed the causative mechanism for cytokine release.

As one intended purpose of the present study was to determine whether the 3DOMMs are able to recognise and respond to microbial stimuli, the most suitable means of determining this was to identify changes in pro-inflammatory cytokine production, upon pathogenic stimulation. Prior to introducing pathogens to the model, studying the response of the individual cell types to PAMPs would provide an insight as to whether such models are likely to be suitable to study the immune response to infection. Furthermore, if the 3DOMM is able to produce pro-inflammatory cytokines that would elicit a downstream cellular immune response, the 3DOMM may be appropriate to further develop into an immunocompetent infection model.

3.1.15. Interleukin-6 (IL-6)

Traditionally IL-6 (also known as B-cell stimulatory factor 2 and interferon β2) was characterised as a cytokine capable of promoting the differentiation and immunoglobulin production of B cells, causing population expansion and activation of T-cells, and regulating the acute phase response through the production of acute phase proteins (150–157). It is now known that whilst inducing such responses, IL-6 is capable of orchestrating an even wider, more diverse range of immune responses, and may act in a regulatory manner depending on the local microenvironment (150,158). IL-6 is a truly multi-functional cytokine. It plays a vital role in normal physiogical activity, as detailed below in **Figure 4** (159).

In its role as a pro-inflammatory cytokine, IL-6 is implicated in many diseases involving chronic inflammation and autoimmunity, and is a favoured target for immunotherapy (160,161). IL-6 is a vital cytokine for normal immune functioning. Impaired IL-6 function has been linked with increased susceptibility to parasitic, bacterial, and fungal infection, of the skin, lungs, and gut (162–165). Such, infections carry high morbidity and mortality rates, demonstrating the necessity of IL-6 as protector against infectious disease. Further to this, IL-6 immunotherapy, which aims to inhibit all IL-6 activity, has a negative effect on general physiological function. This is due to the pleiotropic nature of IL-6 and its ability to affect a broad range of tissues beyond the immune system including regenerative processes, regulation of metabolism, maintenance of bone homeostasis, and cardioprotection (166). Blocking IL-6 function completely within disease may therefore adversely affect other beneficial regulatory functions (167).

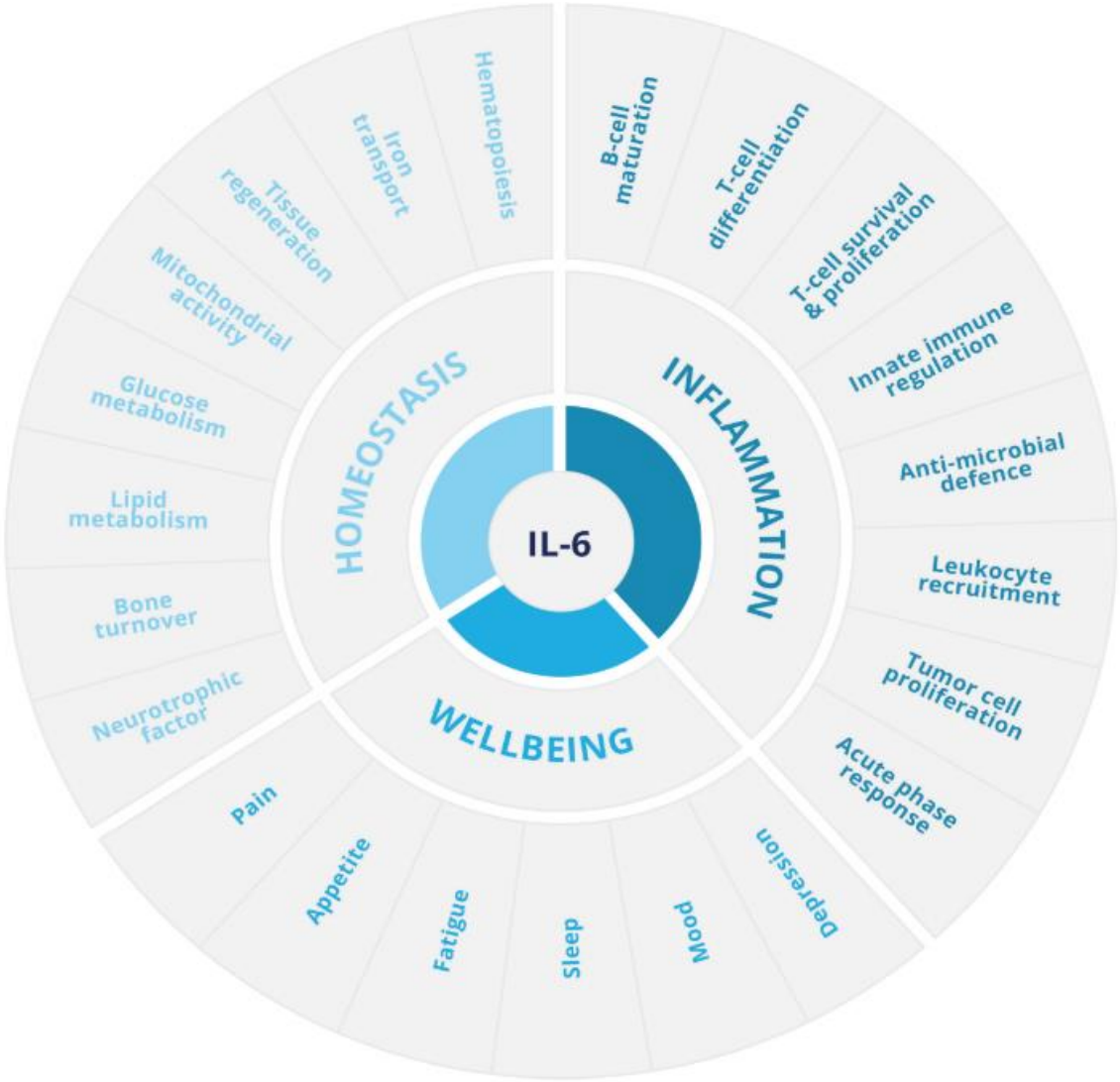

Figure 4: The many roles of IL-6.
IL-6 has roles in maintaining homeostasis, controlling inflammation, and regulating physiological functions, which affect general wellbeing; by Jones *et al.,* 2018.

Nearly all immune and stromal cells are able to produce IL-6. The cytokines IL-1β and TNFα, as well as TLRs, prostaglandins, adipokines, stress responses, and additional cytokines are all capable of inducing IL-6 synthesis (150). The IL-6 receptor (IL-6R) is present on the cell surface of hepatocytes, some leukocytes, monocytes, and neutrophils allowing direct response to IL-6 (168,169). IL-6 binds to IL-6R on the cell surface in the presence of membrane-bound gp130 to activate

the classic pathway in order to transduce signal; gp130 is expressed on the majority of cell types, most of which do not express IL-6R. IL-6R may also become cleaved by metalloprotease ADAM17, which is capable of releasing the membrane-bound IL-6R, generating the soluble receptor (IL-6SR). IL-6SR, in the presence of IL-6, may bind to a cell that expresses gp130 and induce signalling, despite the absence of membrane bound IL-6R. This non-classical pathway, known as trans-signalling, enables previously unresponsive tissues to become reactive to IL-6 (161). It is now considered that the classically activated IL-6 pathway is more tightly regulated, whereas the trans-signalling pathway is more likely to be implicated in chronic inflammation (158,161).

3.1.16. Interleukin-8 (IL-8)

IL-8, also known as CXCL8, is a chemokine (that was previously termed neutrophil-activating factor, monocyte-derived neutrophil-acting peptide, and monocyte-derived neutrophil chemotactic factor). IL-8 is most widely known for its role in neutrophil activation and recruitment. Cells that are capable of secreting IL-8 include: monocytes, CD8+ T-cells, macrophages, keratinocytes, fibroblasts, epithelial cells, hepatocytes, synovial cells, endothelial cells, tumour cells, and trophoblasts(170). Initial discovery and experimentation indicated that IL-8 could be produced upon the stimulation of monocytes with LPS, resulting in neutrophil migration (171–173). Since this discovery, it has been shown that IL-8 can also act upon other leukocytes such as CD8+ T-cells, NK T-cells, monocytes, macrophages, dendritic cells, mast cells, and basophils, due to their expression of IL-8 receptors CXCR1 and CXCR2 (174–178). Keratinocytes and fibroblasts have also been shown to express CXCR1 and CXCR2, indicating they may directly respond to IL-8 (179,180). Not all of the aforementioned cells

constitutively express IL-8 receptors as neutrophils do, however expression may be inducible due to the local cytokine environment (175).

Neutrophils constitute the first line of defence against invading bacteria, fungi and protozoa. IL-8 directly induces the migration of neutrophils to a site of infection and inflammation. A population of neutrophils exists in circulation prior to recruitment to an infective site. Upon recognition of IL-8, neutrophils will migrate against the chemotactic gradient, through the blood vessel wall, into the tissue, to attend the site of infection. Neutrophils are the most abundant innate immune cells within blood, and are the first responders to infection. Neutrophils aid pathogenic clearance through phagocytosis, degranulation, and the formation of neutrophil extracellular traps (NETs); and they promote recruitment of other innate immune cells such as macrophages in order to rid the body of infection. Phagocytosis is a process by which the neutrophil engulfs the invading pathogen. The pathogen is taken up into the cell's phagosome, which in turn fuses with endosomes and lysosomes, which releases contained proteases and other factors, forming highly acidic hydrolase-rich organelles that degrade the pathogen (181). Degranulation involves the release of the granules held within the neutrophil, which contain a potent mix of antimicrobial factors including antimicrobial peptides, reactive oxygen species, and proteases (182). Neutrophil extracellular traps are formed upon controlled neutrophil death, which occurs in a manner that promotes pathogenic entrapment and clearance through high concentrations of antimicrobial factors including histones, antimicrobial-peptides, and neutrophil granules (183).

3.1.17. Cell death

Cell death occurs for a variety of reasons. Cell death is a normal part of physiological function, whereby old cells die and are replaced by new cells; it is necessary for growth and survival. Cell death may also occur when the cell is exposed to an inhospitable environment, due to disease, inflammation, infection, and injury. There are several mechanisms of cell death. Apoptosis is a part of normal physiological function and may occur as a cell ages, or is no longer required. Apoptosis is an active and co-ordinated event. Apoptosis is characterised by blebbing, cell shrinkage, nuclear and DNA fragmentation, and chromosomal condensation. There is no leakage of intracellular content and the resulting apoptotic bodies are cleared by immune cells. Conversely, necrosis occurs when cells are exposed to extreme conditions, occurring from events such as infection, injury, and toxicity. Necrosis is a passive, uncoordinated event. Such conditions lead to a loss of membrane integrity, which in turn leads to a lack of cellular homeostatic mechanisms, resulting in swelling of the cell, disintegration of intracellular organelles, lysis, and subsequent death of the cell. Lactate dehydrogenase (LDH) is an indicator of cell death and is leaked through the permeabilised membranes of necrotic cells (184). The presence of LDH enables biochemical quantification of necrosis, as described in **Figure 5.**

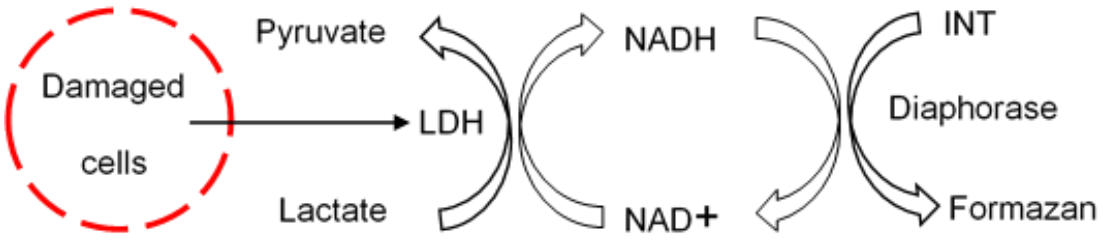

Figure 5: LDH Assay principal.
From previous page: damaged cells release lactate, which through a series of chemical reactions, leads to the formation of a red colour change, correlating with the proportion of cellular damage. LDH reduces NAD+ to NADH and H+ through the oxidation of lactate to pyruvate. The now free H+ ion in the presence of a diaphorase catalyst reduces the tetrazolium salt, to a formazan product leading to a red colour formation. Colour change is then measured at 490nm spectrophotometrically, and is proportional to the amount of LDH and hence damaged cells in culture.

Necrotic cell death may be recognised by the innate immune system. Damage associated molecular patterns (DAMPs) are intracellular contents, such as nucleotide sequences, which are leaked from cells upon necrosis (185,186). Such DAMPs are recognised by PRRs, and may instigate a downstream immune response. DAMP release may therefore correlate with pro-inflammatory cytokine release. This may occur in a bi-directional manner, whereby certain pro-inflammatory cytokines such as TNFα may lead to necrosis, and DAMPs released from necrotic cells may lead to pro-inflammatory cytokine production (187).

3.2. Aims

1. To compare the morphology of three-dimensional oral mucosal models created with immortalised and primary keratinocytes, with native oral mucosa.
2. To identify the baseline pro-inflammatory cytokine production of the P/3DOMMs, and determine the effect of the model environment on the incorporated cell types.
3. To determine the ability of HaCaT, HGF, and POK cells to respond to PAMPs.
4. To consider the optimum time-point to implement the newly developed 3DOMM as an infection model.

3.3. Methodology

3.3.1. Imaging

Live monolayer cultures were visualised and imaged using the Scopetek DCM-510 microscope camera, affixed to an inverted microscope. Tissue sections were visualised and imaged using a Leica DMD108. Transmission electron microscopy was performed as described in section 2.7.

3.3.2. Cell culture

Culture and maintenance of HaCaT, HGF and POK cells was performed as detailed in section 2.3.

3.3.3. 3DOMM production

In order to create the 3DOMMs 2.5 ml of 1.2 $\times 10^5$ HGF cells/ml in DMEM + 10% FBS, were mixed with 3 ml DMEM + 10% FBS, 2 ml collagen, and 300 µl NaOH. The gel combination was mixed by gentle inversion and 800 µl was added per 0.4 µm polycarbonate mesh transwell insert, and incubated at 37°C in a humidified 5% CO_2 incubator until polymerised (approximately 1-2 hours). Once polymerised, 0.4 ml 5.4 $\times 10^5$ HaCaT cells/ml in DMEM + 10% FBS were added to the top of a polymerised gel in KGM1 and KGM2 at a ratio of 1:3. Once contracted, models were raised to the air-liquid interface in KGM3. Further detail is provided in section 2.4.

3.3.4. P3DOMM production

P3DOMMs were created in the same manner as 3DOMMs. POK cells were used in replacement of the HaCaT cell line, at the same density. POK media was used

in substitution for DMEM and KGM. Models were cultured for a maximum of 14 days due to the limited life span of primary cells, as reported in the data sheet.

3.3.5. Pro-inflammatory cytokine production by 3DOMMs and P3DOMMs

Constitutive pro-inflammatory cytokine production by 3DOMMs and P3DOMMs was determined at 48 hour intervals. Models were created as indicated above. Day 0 was considered the day of model formation. Supernatant was collected on the day the model contracted, and the media refreshed with 500 µl of KGM3 for 3DOMMs and POK media for P3DOMMs. Media refreshment and subsequent storage of supernatants was repeated every 48 hours. Supernatants were stored at -20˚C prior to analysis for IL-6 and IL-8 production via sandwich ELISA, as detailed in section 2.8.

3.3.6. LDH assay

A Pierce-LDH cytotoxicity assay kit, Thermo-scientific 88953, was used to determine cell death, as per the manufactures instruction. 3DOMM LDH release was controlled against a maximum LDH release control by lysing 3DOMMs at each time point. Supernatant was also collected in order to look for correlation between IL-6 and IL-8 production by ELISA, and LDH release. In order to compare LDH release with IL-6 and IL-8 release, LDH release was considered as a percentage of the maximum LDH release control. Furthermore, LDH, IL-6, and IL-8 release were all normalised to a percentage of day 1 release, in order to follow the trend across the entire time-course.

3.3.7. Response to the P/3DOMM environment

Each cell type was stimulated with collagen, supernatant of the other cell type contained within the model, and (for P3DOMMs) killed cells of the other cell type. Initially, the effect of killed cells on HaCaT and HGF cells was not explored, however this is elucidated in chapter 5. All cells were studied at the same proportions they occur within the P/3DOMM. HGF cells were subsequently seeded at a density of 1.2×10^5 cells/ml and HaCaT/POK cells at 5.4×10^5 cells/ml.

Collagen was introduced to the cells as per the formation of the model matrix in the 3DOMM protocol; the desired cell type was subsequently embedded into the collagen matrix for 24 hours, prior to supernatant collection by aspiration after centrifugation at 200 × g. This was conducted to determine whether cellular the collagen matrix stimulated pro-inflammatory cytokine production by each individual cell type.

Supernatant was collected from cultured cell types set at the same seeding density as detailed above and used to stimulate the other cell type contained within the model. This was achieved in a pulse-chase manner, whereby the supernatant was added to the cell line at a 1:1 ratio with culture medium for 4 hours, and then removed. Cells were cultured for a further 18 hours in refreshed media, prior to supernatant collection and storage at -20˚C for subsequent analysis. This was to determine whether soluble factors secreted by one cell type stimulated pro-inflammatory cytokine production another cell type.

Killed cells were fixed using paraformaldehyde, through incubation at 4˚C for 30 minutes, killed cells were then washed 5× in PBS and examined microscopically

to ensure no viable cells were remaining, cells were then left for 24 hours to account for leaching, and washed again prior to use. Killed cells were added to the model at the same density as indicated above for each cell type. They were cultured with the live cells for 24 hours, prior to supernatant collection and subsequent storage at -20˚C, for later ELISA analysis. This was to determine whether contact with other cells stimulated pro-inflammatory cytokine production by model-incorporated cell types. **Figure 6** indicates the interactions studied for the 3DOMM- and P3DOMM-incorporated cell types. The effect of killed HGF and HaCaT cells on each other were not assessed on this occasion.

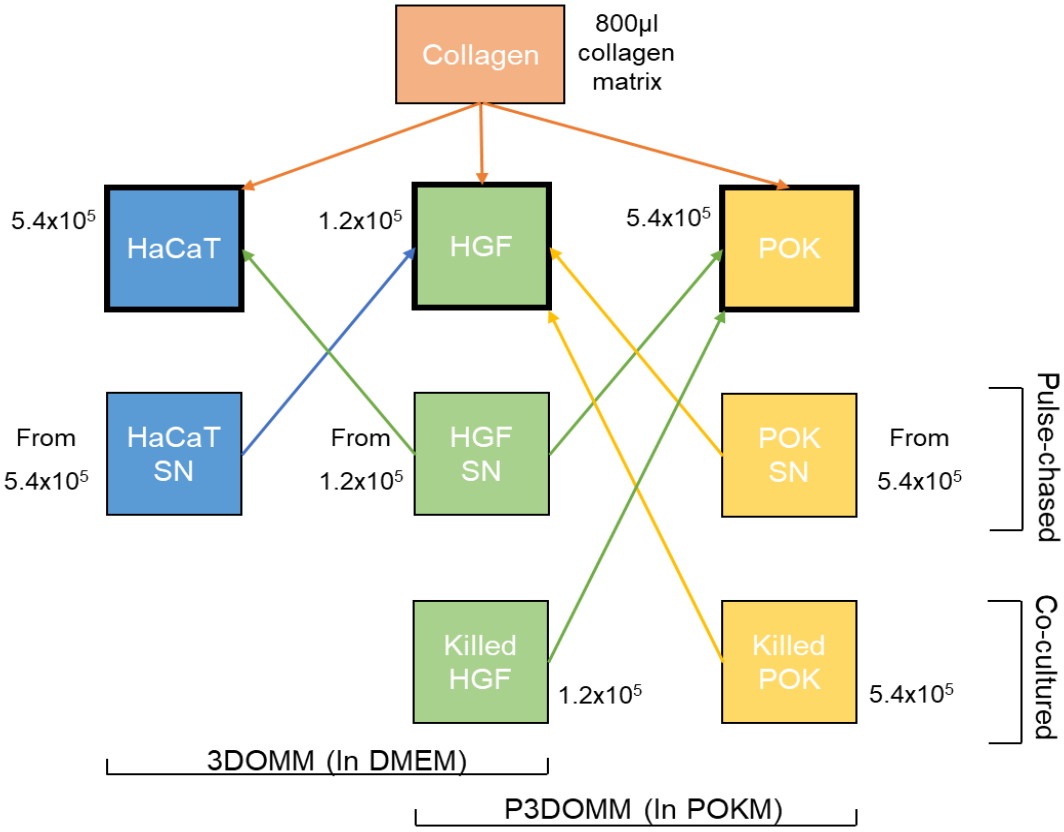

Figure 6: The individual interactions studied to determine the effect of the 3DOMM and P3DOMM environment on cellular pro-inflammatory cytokine production.
A diagram to demonstrate which model components (collagen, killed cells, and supernatant) were introduced to which model-incorporated cell types (HaCaT, POK and HGF), in order to assess whether the model environment was inherently stimulatory at day 1 of model production.

3.3.8. LPS/LTA stimulation of cell lines

HaCaT, HGF, and POK cells were seeded in 48 well plates and grown until confluence. HaCaT and HGF cells were stimulated with 0.001, 0.01, 0.1 and 1 µg/ml of K12 LPS, Invivogen tlrl-peklps, and 0.01, 0.1, 1 and 10 µg/ml of LTA, Invivogen tlrl-pslta. POK cells were stimulated with 0.01, 0.1 and 1 µg/ml of PgLPS, Invivogen tlrl-pglps, and 0.1, 1 and 10 µg/ml of LTA. Cells were stimulated for 18 hours, to permit enough time for cytokine production to be at an elevated level for multiple cytokines, prior to earlier peaking cytokines beginning being undetectable, this was to permit the recognition of a wide range of pro-inflammatory and anti-inflammatory cytokines within the same experiment (188,189). After this, supernatant was collected and stored at -20˚C for later analysis by ELISA. Data was normalised to a percentage of the control for each cell type, for each repeat.

3.3.9. TLR4 protein expression

Western blot was performed as per section 2.6, on confluent HaCaT cells and HGF cells, and 3DOMMs at day 19. 3DOMMs were homogenised to improve protein yield. Each sample was assessed for TLR2 and TLR4 using the primary antibodies (1 µg/ml) Santa Cruz 21759 and Santa Cruz 293072, respectively, and IgG binding protein m-IgGkBP-HRP, Santa Cruz 516102 (1/3000 dilution).

3.3.10. Cell surface expression of TLR2 and TLR4

HaCaT and HGF cells were grown until confluent, and gently detached using a cell-scraper. HaCaT and HGF cells were also stimulated with 10 µg/ml of LTA for an 18 hour period prior to detachment. Cell surface expression of TLR2 and TLR4 was assessed via flow cytometry, as detailed in section 2.9. FITC-labelled antibodies for TLR2, Invitrogen 11-9922-42, and TLR4, Santa Cruz 13593 FITC, as well as an isotype control, Invitrogen 11-4724-81, were used to stain live HaCaT and HGF cells and observed using a FACS-Calibur flow cytometer.

3.3.11. Data analysis and statistics

Statistical analyses are indicated in the figure legend for each experiment, including which statistical tests were performed, and the number of experimental repeats. For all ELISA data, as standard a minimum of three independent experimental repeats, containing three biological replicates were performed, unless stated otherwise. For each biological replicate, a minimum of 2 technical replicates were performed. Also indicated in the figure legend is which groups were compared, if this is not stated then a comparison was made between all groups in a given graph. To select the appropriate statistical test, using GraphPad software, a Shapiro-wilk test for normality was performed for all groups in a given comparison. Parametric data was assessed with the use of a one-way ANOVA, followed by a Tukey's multiple comparisons test. Non-parametric data was assessed using a Kruskal-Wallis test followed by a Dunn's multiple comparisons test. To assess correlation between LDH release and pro-inflammatory cytokine production a Spearman's rank test was performed, using SPSS software. For all, *p*-values lower than 0.05 were taken to indicate statistical significance.

3.4. Results

3.4.1. Culture of keratinocytes and fibroblasts

3DOMM production employed the use of the immortalized human skin keratinocyte cell line (HaCaT), and the human gingival fibroblast cell line (HGF). **Figure 7** displays the cell lines in active culture, prior to their incorporation into the 3DOMM. HaCaT cells form a cobblestone appearance. HGF cells appear elongated and aligned, growing alongside each other. Both cell types are strongly adherent.

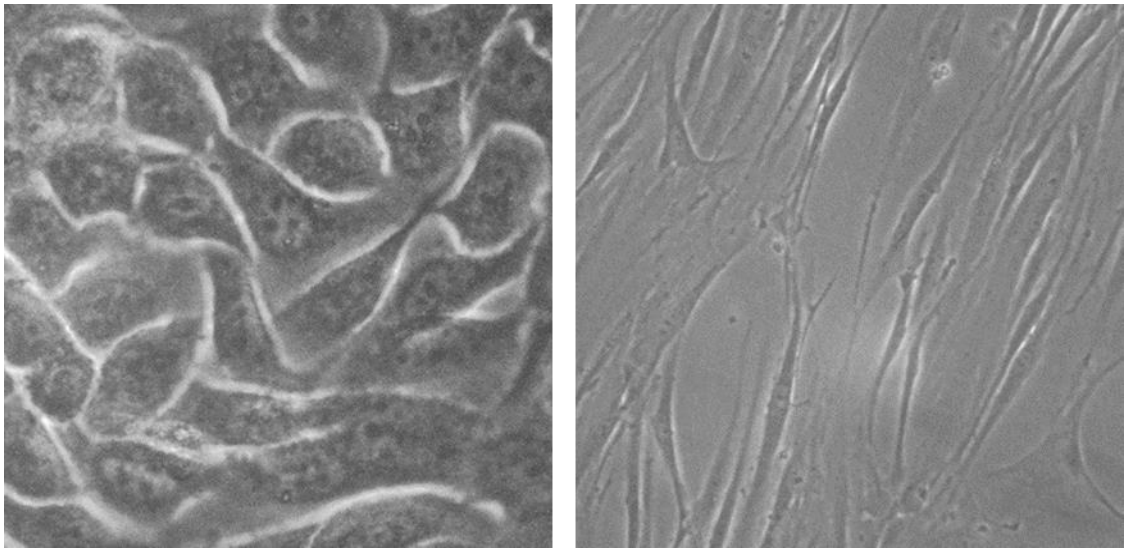

Figure 7: HaCaT and HGF cells in culture
HaCaT keratinocytes (left) and HGF fibroblast cells (right). Cells were imaged in active culture, grown in DMEM + 10% FBS at 400 X magnification .

3.4.2. Structure of the 3DOMM

The 3DOMM was created using the HGF and HaCaT cell types. Models were cultured for 19 days and assessed histologically in order to compare the tissue morphology with cross-sections of healthy native oral mucosa **Figure 8**. Both tissues exhibit an organised multi-layered epithelium. Epithelial layers are distinct

from the lamina propria layer within both the native oral mucosa, and 3DOMM. Notably, there is evidence of stratification of the epithelium within the native oral mucosa, however this is seen less within the 3DOMM. Image D of the 3DOMM does display a level of stratification that is less organised than that of both native oral mucosal images. A clear basement membrane is visible within the native oral mucosa, however not within the 3DOMM; there is a thinner, non-distinct eosin-stained layer in between the epithelium and lamina propria layer in image D, which may be indicative of basement membrane formation. Within the lamina propria layer, fibroblasts are identifiable by their haemotoxylin-stained nuclei. There are fewer visible nuclei within the lamina propria layer of the 3DOMM compared with the native tissue. At the apical layer of the epithelium, within both the native oral mucosa and the 3DOMM there are fewer nuclei present, and a flattened appearance indicative of squames. This may hint towards keratinisation. Image B indicates the lamina propria and epithelium have separated. There are rete ridges present within the native oral mucosa that are not present within the 3DOMMs.

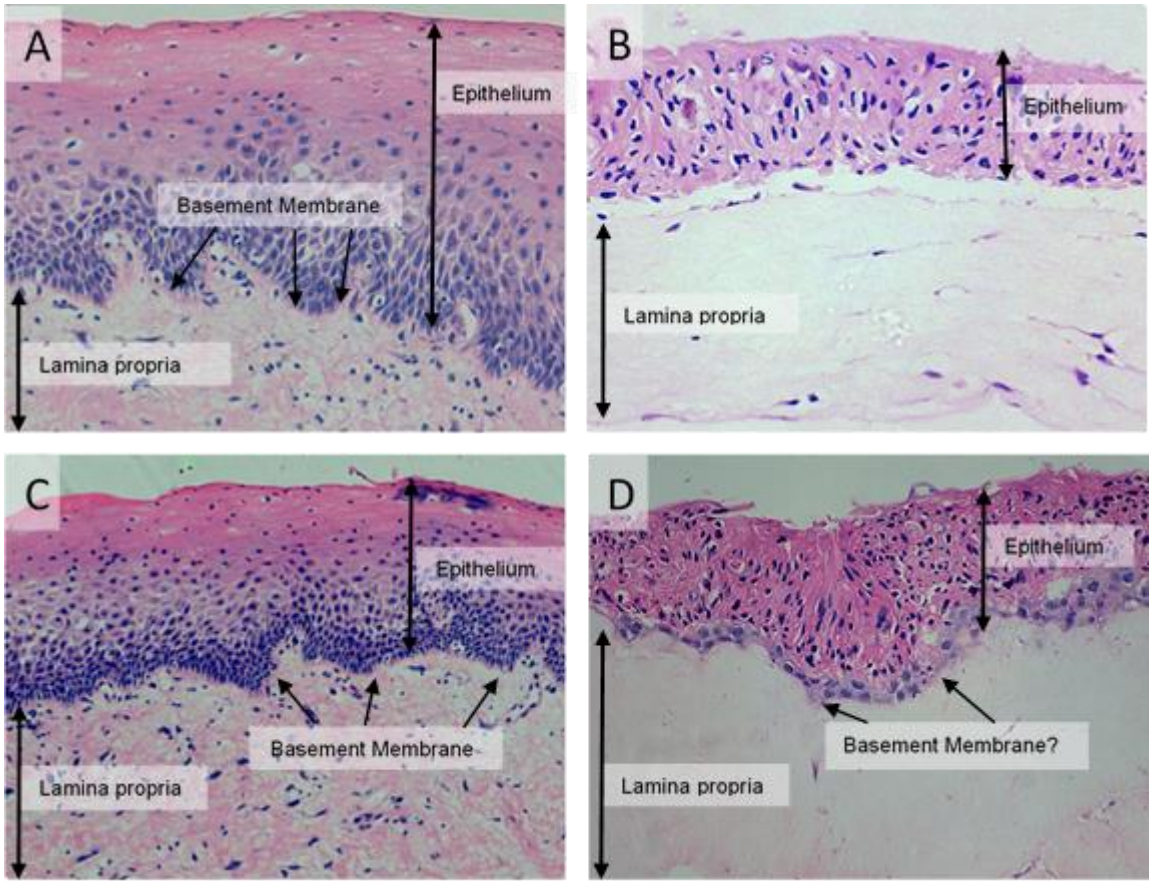

Figure 8: Histology of the 3DOMM compared with the native oral mucosa
A representative sample of paraffin embedded, 4 µm sectioned, haematoxylin and eosin stained, oral mucosal tissue (images A + C), and 3DOMMs (images B + D) at day 19 of growth (100 X magnification). Unstained sections of keratinised oral mucosal tissue were kindly provided by Dr P Laurance-Young, Dept. of Histopathology, Derriford Hospital, Plymouth, UK. Labels indicate the epithelial (keratinocyte-containing) and lamina propria (fibroblast-containing) layers of the tissue, and the basement membrane situated between.

To further assess the morphology of the 3DOMM, transmission electron microscopy (TEM) was applied. The models were cultured for 19 days prior to fixation, processing and imaging, **Figure 9**. Images indicate a cross-section of the 3DOMM where the epithelium meets the lamina propria layer. Image A indicates visible keratinocytes. Image B suggests the presence of a thin basement membrane, between the epithelial and lamina propria layers.

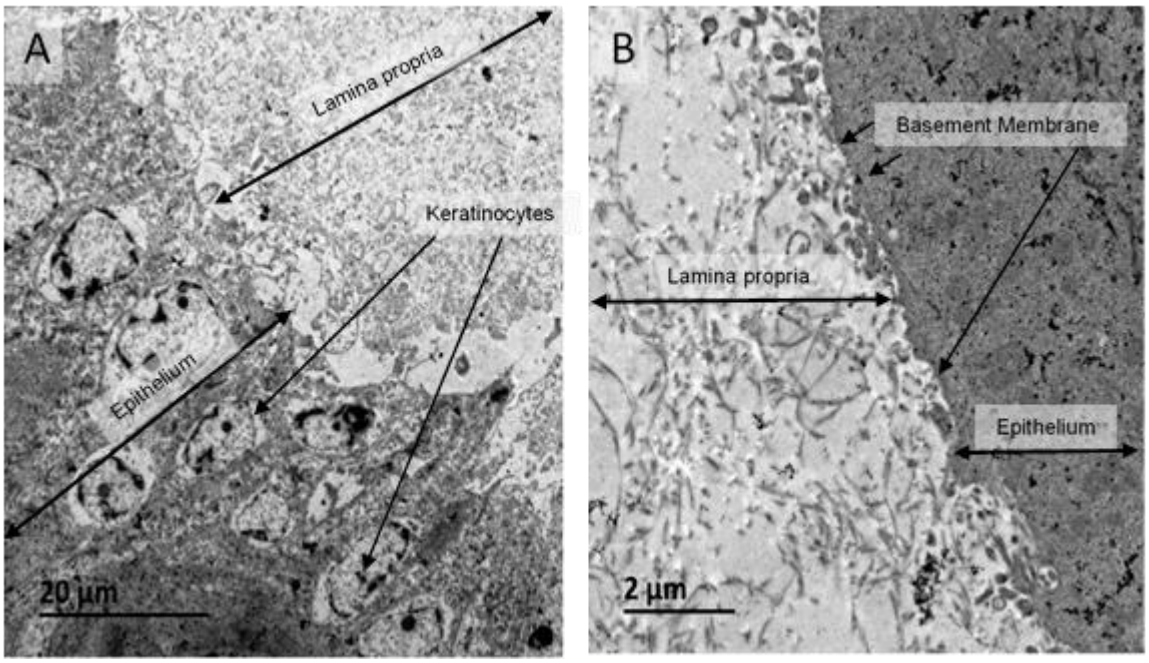

Figure 9: Transmission Electron Microscopy images of 3DOMMs at day 19. Labels indicate situation of the lamina propria, epithelium, basement membrane and HaCaT keratinocytes.

In order to determine whether the morphology of the 3DOMM varied upon different lengths of time in culture, 3DOMMs were cultured for a total of 16, 19 and 21 days, prior to fixation, sectioning, and staining for histological assessment, **Figure 10**. At day 16, models presented with a multi-layered epithelium, which was separated from the lamina propria layer of the model (A and D). At day 19, models appeared intact, and presented with an organised, but not stratified, epithelium (B and E), and signs of keratinisation (B). At day 21, the models indicated a multi-layered epithelium that contained gaps; epithelial cells could be seen to break away from the epithelium (C and F). Model F appeared to have areas of keratinisation. Statistical analysis revealed that there was no significant difference between the thicknesses of the epithelial layers at any of the time points ($p = 0.52$).

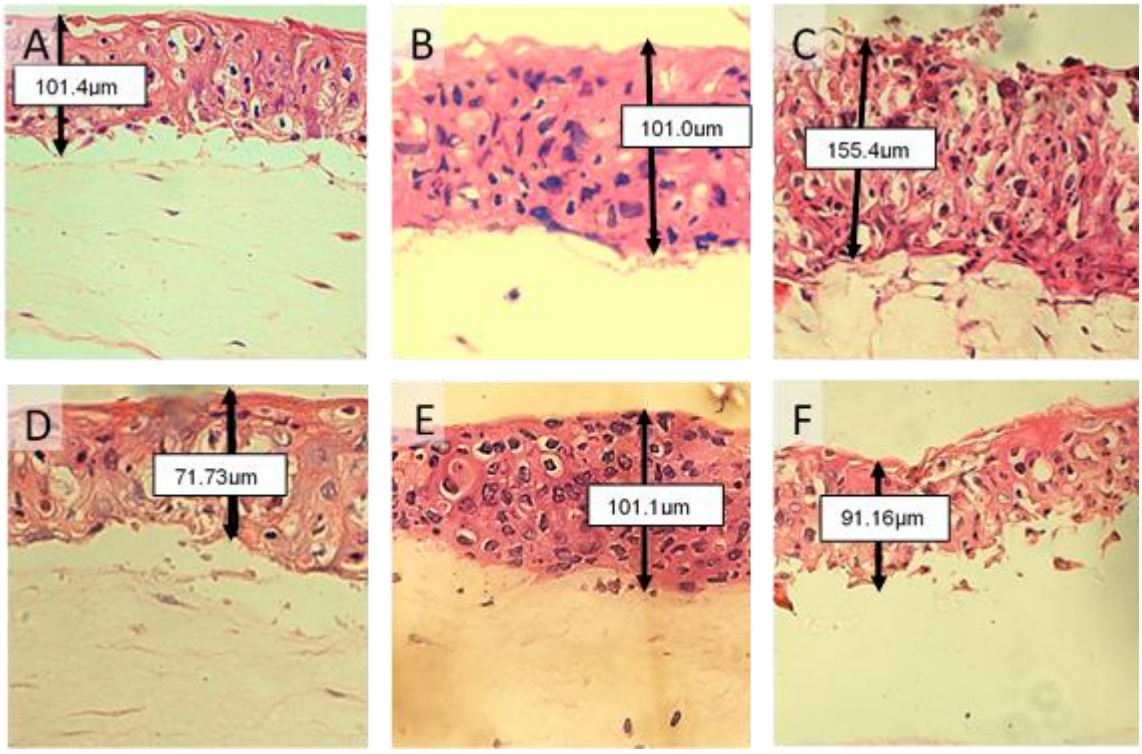

Figure 10: Histology of 3DOMMs cultured for 16, 19 and 21 days
A representative sample of paraffin embedded, 4µm sectioned, haematoxylin and eosin stained 3DOMMs. Models were grown for 16 days (Images A and D), 19 days (Images B and E) and 21 days (Images C and F). Images were taken at 200 X magnification. Indicated measurements display the thickness of the epithelium.

3.4.3. Structure of the P3DOMM

To determine whether the use of the primary oral keratinocyte cell type (POK) would permit the formation of tissue stratification, keratinisation, and a basement membrane, primary 3DOMMs (P3DOMMs) were created using POK cells and the HGF cell line.

Figure 11 depicts a comparison between 3DOMM and P3DOMM histology. The 3DOMM presented with a thinner epithelium than the P3DOMM, an average of 232.7 vs 459.3 µm. This did not correlate with the approximate number of average epithelial layers seen within the 3DOMM and the P3DOMM, which presented as 19 vs 10, respectively. The keratinocytes appeared larger and more disorganised

within the P3DOMM when compared with the 3DOMM. The P3DOMM epithelium did not appear intact, the cells were not tightly bound to each other, and the epithelium had separated from the lamina propria. Furthermore, there was no clear sign of stratification, basement membrane formation, or keratinisation within the P3DOMM. The 3DOMM displayed no clear sign of basement membrane formation; however the cells towards the apical layer of the epithelium appeared as flattened enucleated squames, indicative of keratinisation. Of the two tissues, the 3DOMM appeared most structurally similar to the native oral mucosa observed in **Figure 8**.

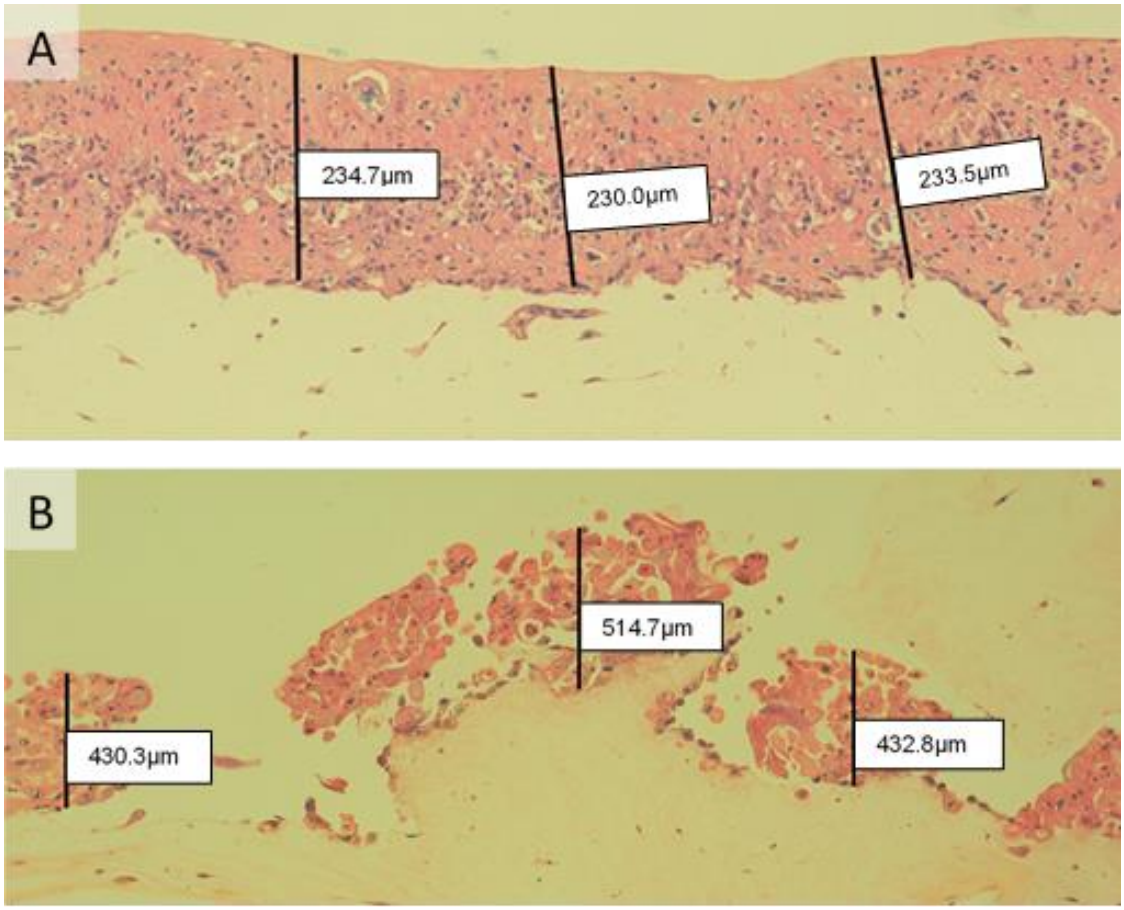

Figure 11: Histological comparison of 3DOMM and P3DOMM morphology
A representative sample of paraffin embedded, 4 µm sectioned, haematoxylin and eosin stained 3DOMM and P3DOMM (100 X magnification). Image A displays a 3DOMM (formed with HaCaT and HGF cells) at day 19 of culture. Image B displays a P3DOMM (Formed with POK and HGF cells) at day 14 of culture.

To determine whether the enlarged morphology of the primary keratinocytes was typical of these cell types, primary cells were cultured in monoculture and imaged, **Figure 12.** POK cells at passage 2 presented as islands of closely associated keratinocytes. Cells formed a cobblestone morphology. POK cells at passage 5 appeared irregular, with some larger cells. Some cells remained adherent, whereas other cells detached from the cell culture flask. The cobblestone appearance was less obvious, and cells were less tightly associated with one another, at the later passage.

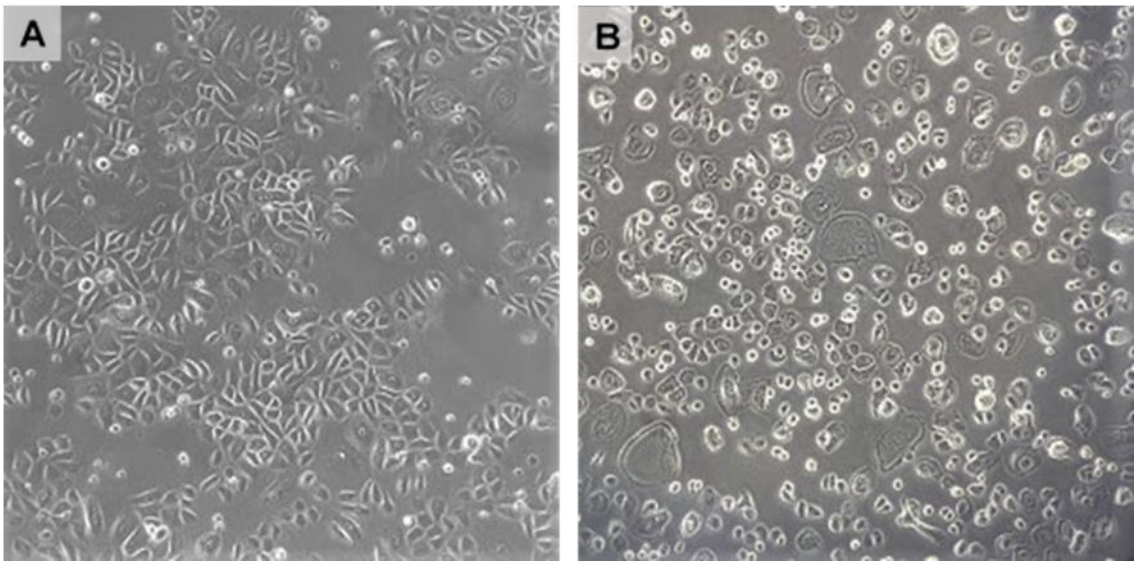

Figure 12: Primary oral keratinocytes in culture.
Images of primary oral keratinocytes (POK) in culture grown in POK medium (100 X magnification). POK cells at passage 2 (A) and POK cells at passage 5 (B).

3.4.4. 3DOMM pro-inflammatory cytokine production

Initially the 3DOMM was studied as a whole, in order to determine the pro-inflammatory cytokine output of the model prior to stimulation with any external factor. This was important to ascertain the local microenvironment, prior to the

use of the model to study cytokine production in response to infection. Knowledge of the local pro-inflammatory cytokine production was used as a means to predict the way any further cell types added to the model may respond to the current environment.

Firstly, the IL-6 and IL-8 pro-inflammatory cytokine production was measured during the course of 3DOMM development, **Figure 13**. IL-6 production was highest at day 1 of model production, with a value of < 30,000 pg/ml. A decrease in IL-6 production was observed from day 3 onwards, where IL-6 production plateaued and remained near this lower value of approximately 10,000 pg/ml for the rest of the culture period. As with IL-6, high levels of IL-8 were observed at day 1 after model production. A reduction in IL-8 was observed by day 3, and again at day 5. After day 13, IL-8 levels produced by the model began to increase.

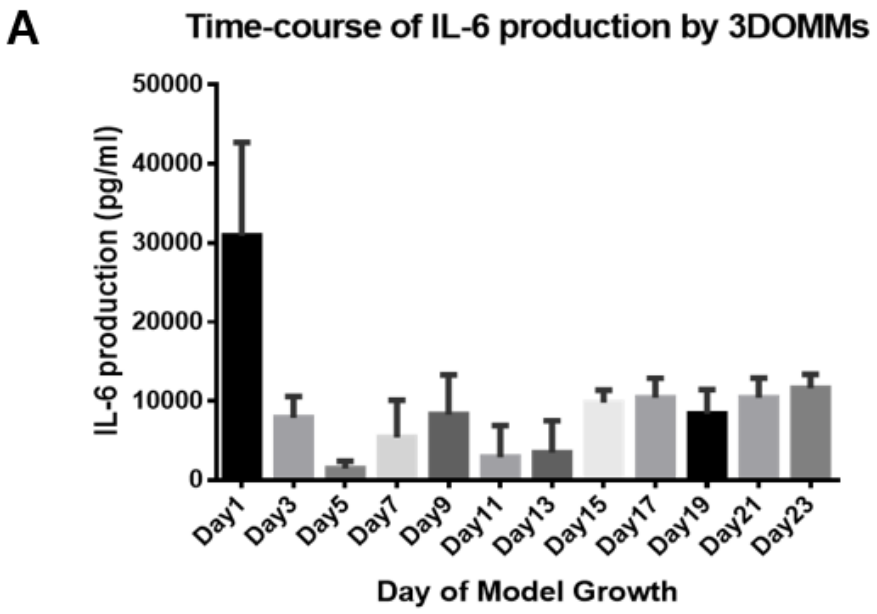

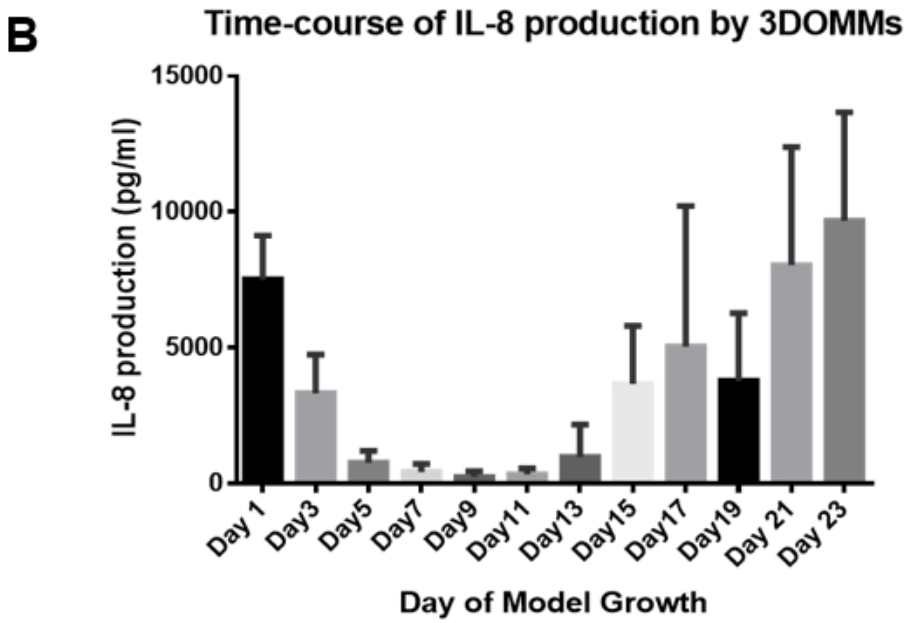

Figure 13: Time-course of constitutive pro-inflammatory cytokine expression (IL-6 and IL-8) by 3DOMMs

Models were created and grown for up to 23 days, supernatant was collected every 48 hours and stored prior to analysis by sandwich ELISA for IL-6 (A) and IL-8 (B) pro-inflammatory cytokine production. Data are from three independent experiments performed with four biological replicates. Day 1 is the first day that the models contracted. Error bars represent standard deviation.

After observing the high level of cytokine expression upon model production, the individual model components were used to stimulate the cell types of the model. This was to determine whether the soluble factors released by other cell types, or contact with the collagen matrix, led to stimulation of the cells and hence the initial high levels of pro-inflammatory cytokine release, **Figure 14**.

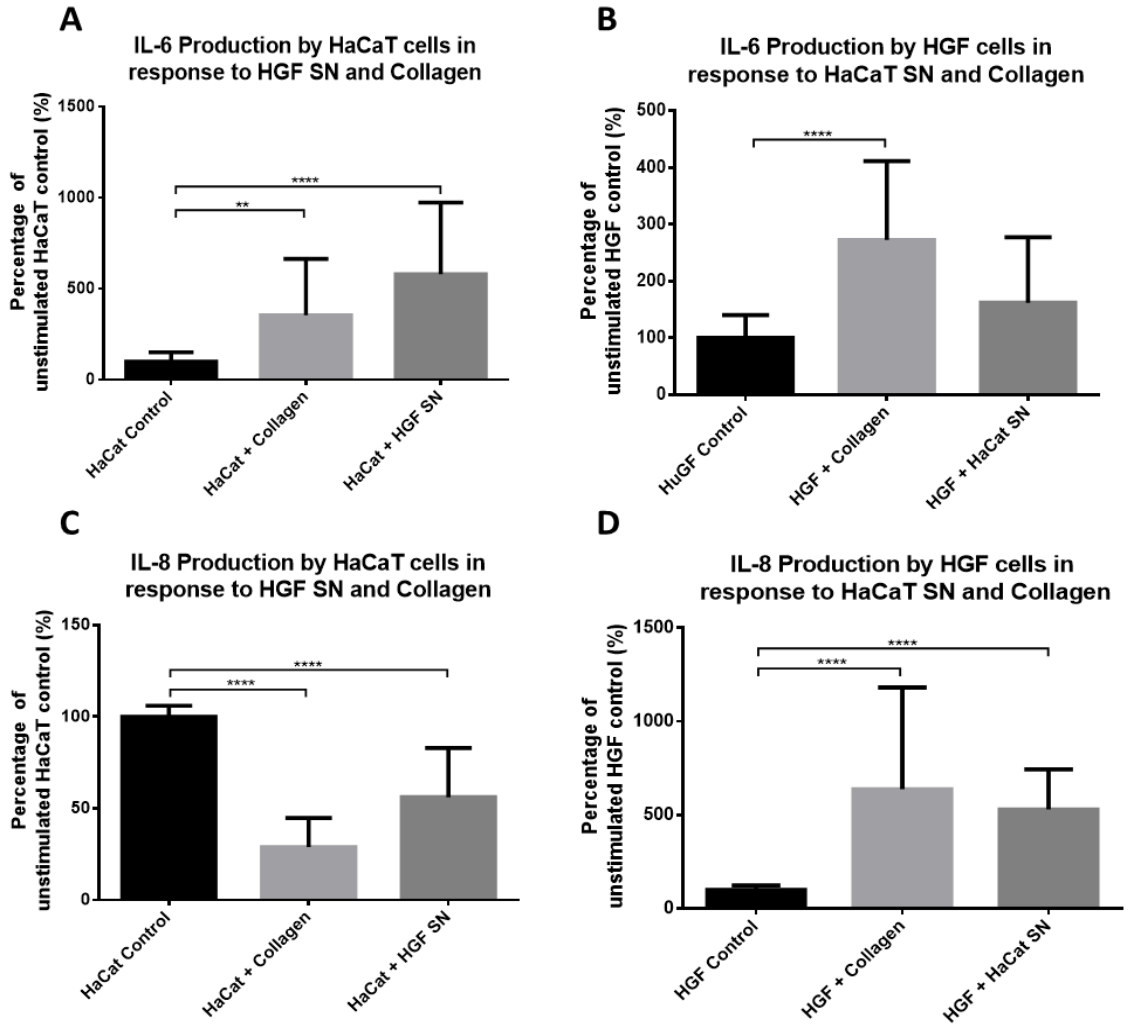

Figure 14: Pro-inflammatory cytokine production by HaCaT and HGF cells in response to 3DOMM components
IL-6 production by HaCaT (A), IL-6 production by HGF (B), IL-8 production by HaCaT (C), and IL-8 production by HGF (D), in response to collagen and supernatant (SN). Data are from three independent experiments performed in triplicate. Significant differences in cytokine production were compared between the unstimulated control and stimulated groups. Data normality was assessed using the Shapiro-Wilk test for normality. Statistical significance was determined using a Kruskal-Wallis test followed by a Dunn's multiple comparisons test. Statistical significance is indicated on the graph (* $p < 0.05$, ** $p < 0.01$, *** $p < 0.001$, **** $p < 0.0001$). Error bars represent standard deviation.

When HaCaT cells were stimulated with collagen or HGF supernatant, a significant increase was seen in IL-6 production when compared with the unstimulated control ($p = 0.0019$ and $p < 0.0001$, respectively). Conversely, IL-8 production by HaCaT cells was significantly less when cells were exposed to

collagen or when stimulated with HGF supernatant, compared to the unstimulated control ($p < 0.0001$ for both).

Within HGF cells, IL-6 production was significantly greater when stimulated with collagen, compared with the unstimulated control ($p < 0.0001$). There was also a significant increase in IL-8 production by HGF cells stimulated with collagen, and HGF cells stimulated with HaCaT supernatant, when compared with the unstimulated HGF control ($p < 0.0001$ for both).

As well as stimulation by model components, it was hypothesised that cell death may be partially accountable for the observed high levels of pro-inflammatory cytokine production. It is for this reason that LDH release was determined, in order to look for a correlation between LDH release and pro-inflammatory cytokine production. **Figure 15** indicates the relationship between IL-6 and IL-8 pro-inflammatory cytokine production, and LDH release. Spearman's rank correlation analysis indicates a strong positive correlation between LDH release and IL-6 production ($r = 0.936$), LDH release and IL-8 production ($r = 0.945$), and IL-6 and IL-8 production ($r = 0.891$) (reporting p values of $p = 0.00008$, $p = 0.00005$ and $p = 0.00052$, respectively). An overall trend is observed, indicating higher levels of release of all factors on day 1, with a gradual decline up until day 7. After this point the IL-6, IL-8, and LDH activity does not return to its original high level, however, there is an increase seen at day 15 and day 19 by all.

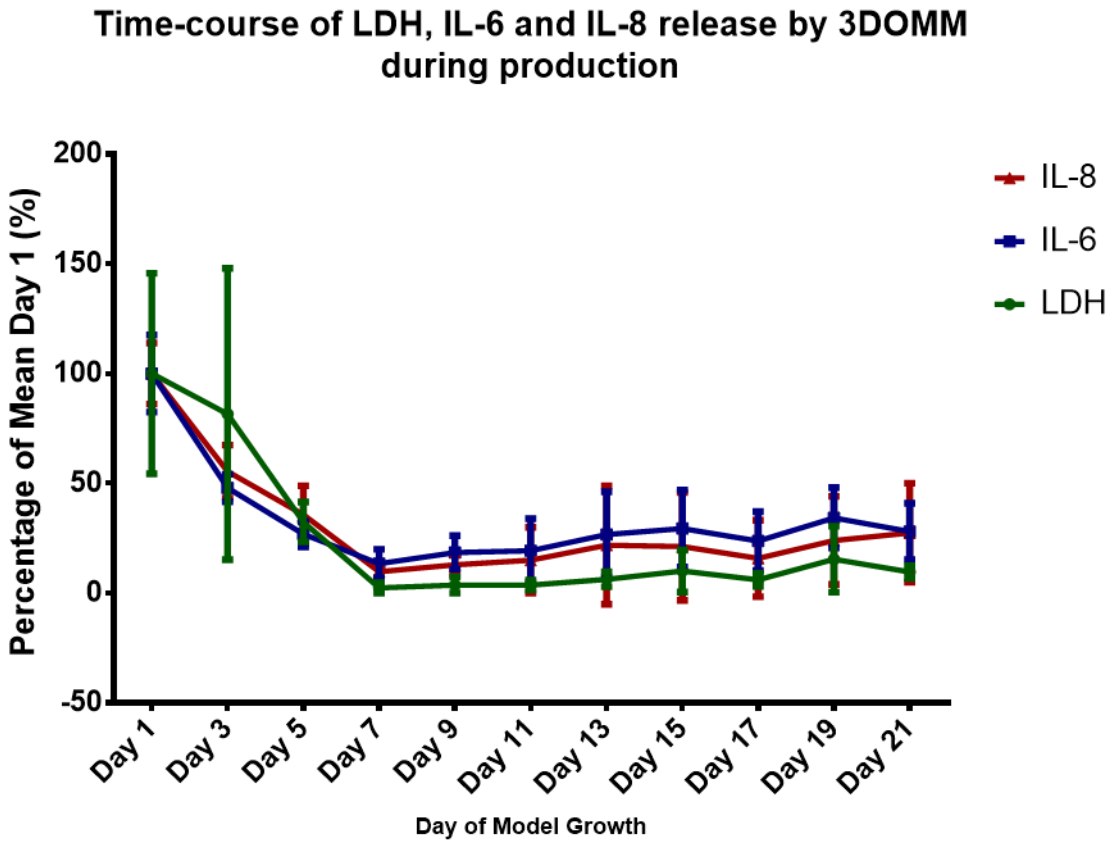

Figure 15: The relationship between 3DOMM LDH-release and pro-inflammatory cytokine production

LDH, IL-6 and IL-8 release over the course of 3DOMM production. Three experimental repeats with 4 biological replicates (performed in parallel). LDH activity was controlled using a maximum LDH control at each time point, by lysing models at the same day of growth. IL-6 and IL-8 production were measured via sandwich ELISA. LDH release was normalised to the maximum LDH control for the corresponding time point. LDH, IL-6 and IL-8 values for each time point are reported on this graph as a percentage of mean day 1 release. Data normality was assessed using a Shapiro-Wilk test. Correlation analysis was performed using the non-parametric Spearman's rank correlation test. Error bars represent standard deviation.

3.4.5. PAMP recognition by HaCaT and HGF cells

After gaining an insight into the constitutive pro-inflammatory cytokine production by the 3DOMMs, it was next necessary to determine if the models were capable of recognising and responding to infection. This was tested by studying the response of the individual HaCaT and HGF cells to the PAMPs LPS and LTA, in

order to ascertain whether the models as a whole are likely to be able to respond to pathogenic challenge, **Figure 16** and **Figure 17**.

When HaCaT cells were stimulated with increasing doses of LPS (0.001-1 µg/ml), **Figure 16,** there were no significant differences in IL-6 or IL-8 production between cells stimulated with LPS and the unstimulated control, nor between the different doses of LPS. When HaCaT cells were stimulated with increasing doses of LTA (0.01-10 µg/ml), there was no significant difference in IL-6 production upon stimulation, when compared with the HaCaT unstimulated control, nor between different doses of LTA. IL-8 production in HaCaT cells was significantly greater when stimulated with 10 µg/ml of LTA, when compared with HaCaT cells stimulated with 0, 0.01, 0,1 and 1 µg/ml of LTA ($p < 0.0001$, $p < 0.0001$, $p < 0.0001$, *and* $p = 0.0379$, respectively). A significant increase in IL-8 production by HaCaT cells was also observed when cells were stimulated with 1 µg/ml of LTA, when compared with the unstimulated control ($p = 0.0001$). There was no significant difference in IL-8 production between the unstimulated HaCaT control, and doses of LTA between 0.01 and 0.1 µg/ml.

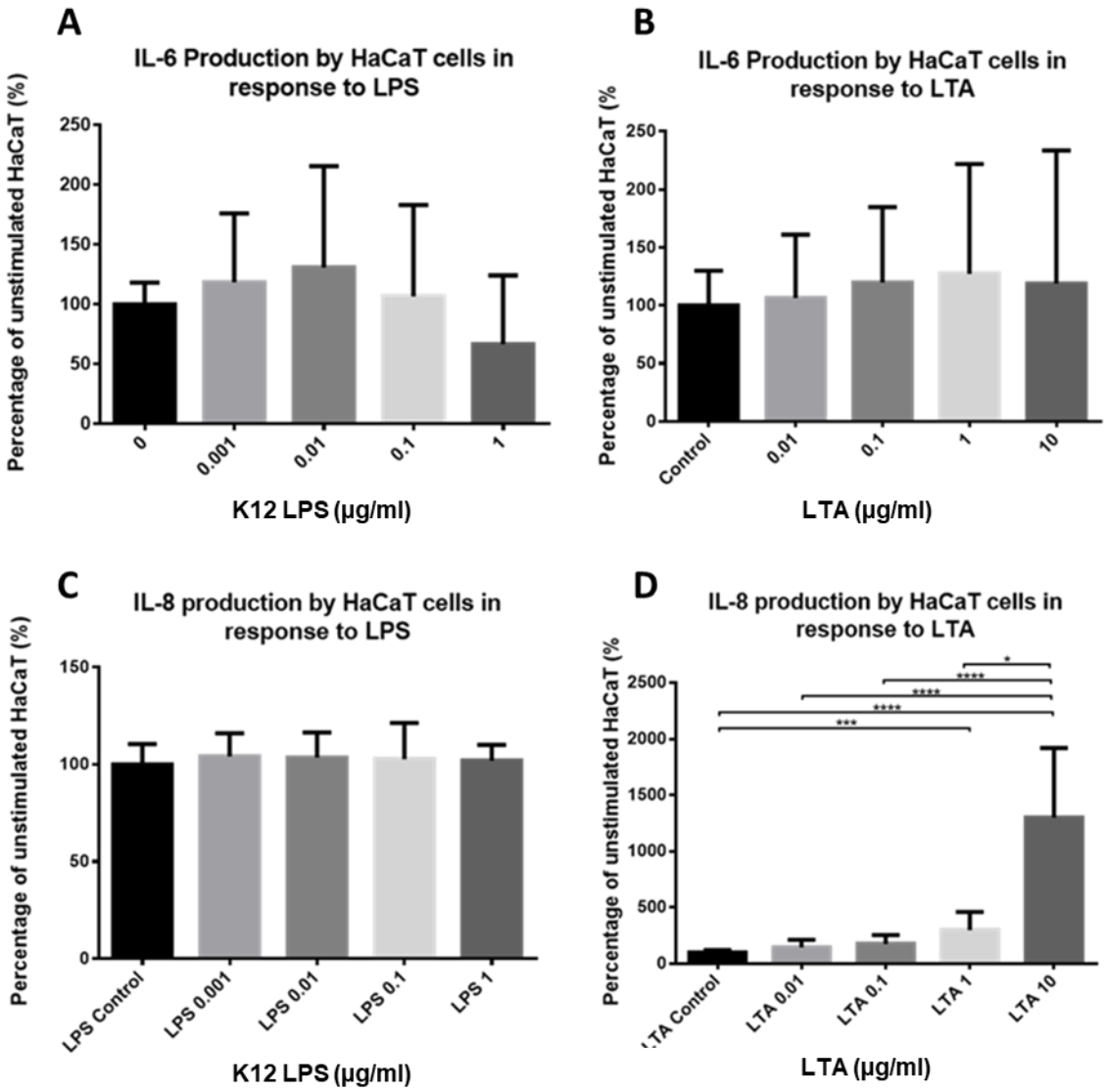

Figure 16: Dose response of LPS and LTA on HaCaT pro-inflammatory cytokine production

IL-6 and IL-8 production by HaCaT in response to K12 LPS (A and C respectively) and *Staphylococcus aureus* LTA (B and D respectively). Three experimental repeats, performed in triplicate (B,C,D), one experimental repeat performed in triplicate (A). Cytokine production was measured via sandwich ELISA after 18 hours of stimulation. Significant differences in cytokine production were compared to the every other group. Data normality was assessed using the Shapiro-Wilk test for normality. Data were transformed to a percentage of the control. Statistical significance for IL-8 production by HaCaT cells in response to LTA was determined using a Kruskal-Wallis test followed by a Dunn's multiple comparisons test. Statistical significance for IL-6 production by HaCaT cells in response to LTA, and IL-6 and IL-8 production by HaCaT cells in response to LPS was determined using a one-way ANOVA followed by a Tukey's multiple comparisons test. Statistical significance is indicated on the graph (* $p < 0.05$, ** $p < 0.01$, *** $p < 0.001$, **** $p < 0.0001$). Error bars represent standard deviation.

For HGF cells stimulated with increasing doses of LPS (0.001-1 µg/ml), **Figure 17**, a significant increase was seen in IL-6 production by HGF cells stimulated with 0.1 µg/ml of LPS, compared with the unstimulated control ($p = 0.0296$). There were significant differences observed between other groups, however none were significantly greater than the control. For HGF cells stimulated with increasing doses of LPS (0.001-1 µg/ml), there were no significant differences in IL-8 production between unstimulated HGF cells and stimulated groups, nor between differing doses of LPS.

HGF IL-6 production was significantly greater when stimulated with 10 µg/ml of LTA, than when unstimulated or stimulated with lower concentrations ($p < 0.0001$ for all). There was no significant difference between any other doses. For IL-8 production by HGF cells in response to increasing doses of LTA, IL-8 production by cells stimulated with 10 µg/ml of LTA was significantly greater than unstimulated cells, or cells stimulated with 0.01, 0.1 or 1 µg/ml of LTA ($p < 0.0001$, $p < 0.0001$, $p < 0.0001$, and $p = 0.0433$, respectively). There was also a significant increase in IL-8 production between HGF cells stimulated with 1 µg/ml of LTA compared with 0.01 µg/ml of LTA ($p = 0.0018$). There were no significant differences between other groups.

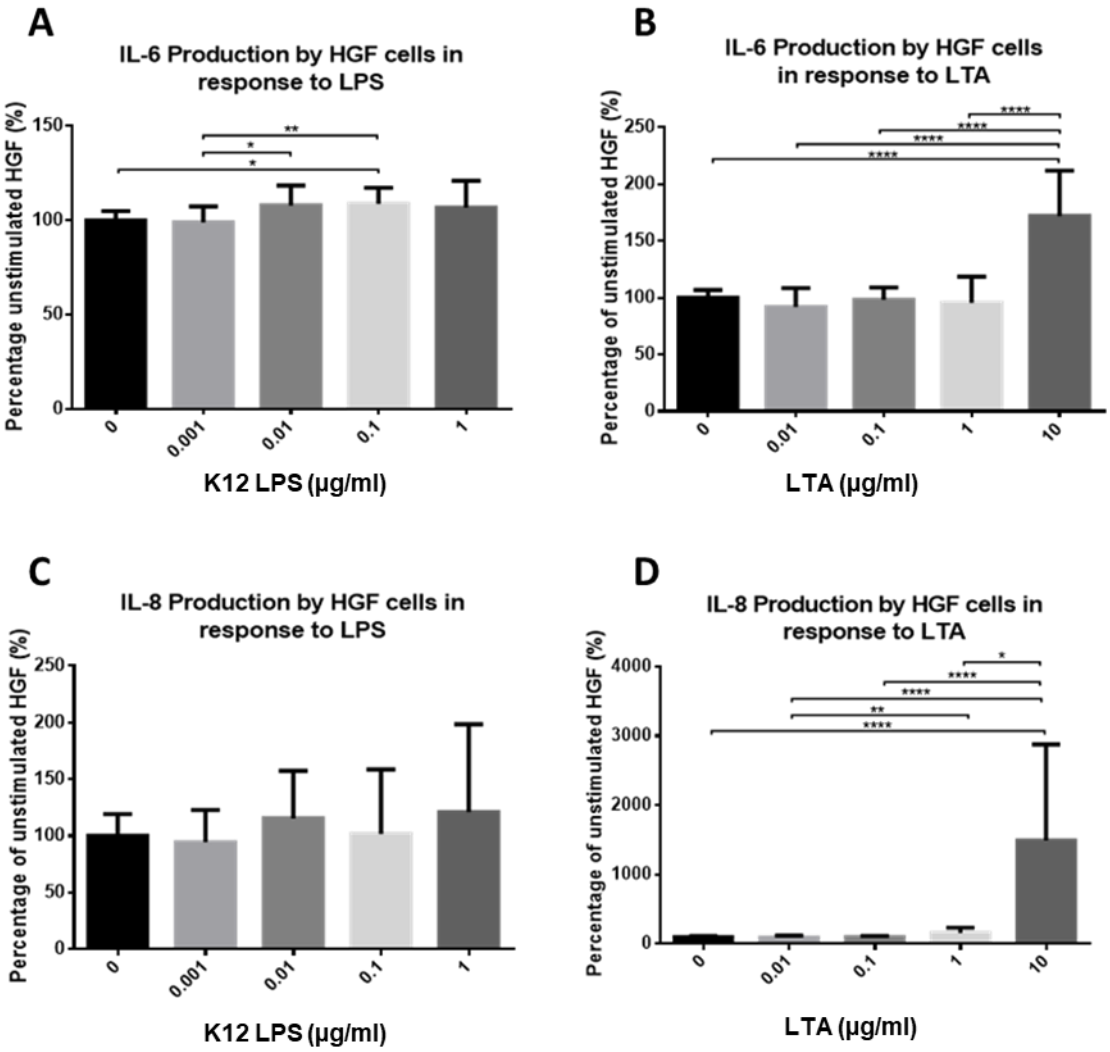

Figure 17: Dose response of LPS and LTA on HGF pro-inflammatory cytokine production

IL-6 and IL-8 production by HGF in response to K12 LPS (A and C respectively) and *Staphylococcus aureus* LTA (B and D respectively). Graphs indicate three experimental repeats performed in triplicate. Cytokine production was measured via sandwich ELISA after 18 hours of simulation. Significant differences in cytokine production were compared to the every other group. Data normality was assessed using the Shapiro-Wilk test for normality. Data were transformed to a percentage of the control. Statistical significance for IL-6 and IL-8 production by HGF cells in response to LPS was determined using a Kruskal-Wallis test followed by a Dunn's multiple comparisons test. Statistical significance IL-6 Production by HGF cells in response to LTA was determined using a one-way ANOVA followed by a Tukey's multiple comparisons test. Statistical significance is indicated on the graph (* $p < 0.05$, ** $p < 0.01$, *** $p < 0.001$, **** $p < 0.0001$). Error bars represent standard deviation.

Following this, TLR2 and TLR4 expression were explored within the HaCaT and HGF cell lines. Both Western blot and flow cytometry techniques were used to determine whether cells were producing the TLR2 and TLR4 proteins, and whether they were expressed on the cell surface. **Figure 18** indicates the presence of the TLR4 protein within HaCaT cells, HGF cells and 3DOMMs.

Figure 18: TLR4 expression of HaCaT, HGF and 3DOMMs.
A representative Western blot (performed in triplicate) of TLR4 protein expression by HaCaT, HGF and 3DOMMs. TLR4 presence was determined via Western blot of confluent HaCaT and HGF cells and models at day 19 of culture.

Data for TLR2 was not shown, as all antibodies tested appeared negative for the positive test-cell lysate control. Following the positive result of the TLR4 Western blot, but inconclusive result for TLR2 expression, flow cytometry was used to identify TLR2 and TLR4 localisation at the cell surface, **Figure 19**. Cells were unstimulated (control) and stimulated with 10 µg/ml of LTA for 18 hours, in order to compare TLR2 and TLR4 expression in unstimulated and stimulated HaCaT and HGF cells.

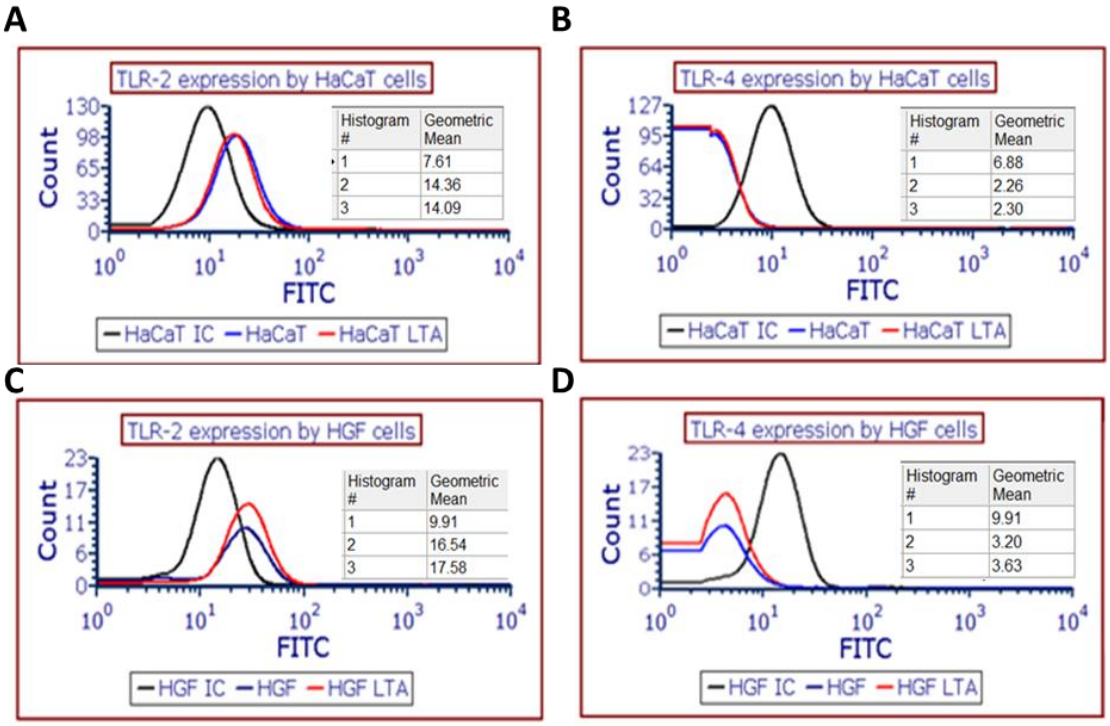

Figure 19: TLR2 and TLR4 expression by HaCaT and HGF cells at the cell surface
Cell surface expression of TLR2 and TLR4 by unstimulated and LTA stimulated HaCaT cells (A and B respectively) and HGF cells (C and D respectively). A representative sample of two experimental repeats, with three technical replicates of 10,000 events. Expression was assessed via flow cytometry. Cells were stimulated for 24 hours with 10 µg/ml of LTA. Black peaks depict the isotype controls (IC). Blue peaks depict the unstimulated cell type, and red peaks depict the cell types stimulated with LTA.

Both HaCaT and HGF cells were shown to express TLR2 at the cell surface in stimulated and unstimulated groups, as the mean fluorescence intensity value and hence geometric mean, produced a greater value than that of the isotype control. There appeared to be no distinct difference in TLR2 expression between stimulated and unstimulated groups. For both cell types, the values of mean fluorescence intensity for TLR4 were lower for test groups than that of the isotype control. For this reason, the TLR4 data could not be interpreted.

3.4.6. P3DOMM pro-inflammatory cytokine production

As with the 3DOMM, the P3DOMM was assessed for pro-inflammatory cytokine release during model production up until day 14, **Figure 20**. On day 4, the highest

level of IL-6 production was detected in the model supernatant. On day 8 the highest level of IL-8 was detected in the model supernatant.

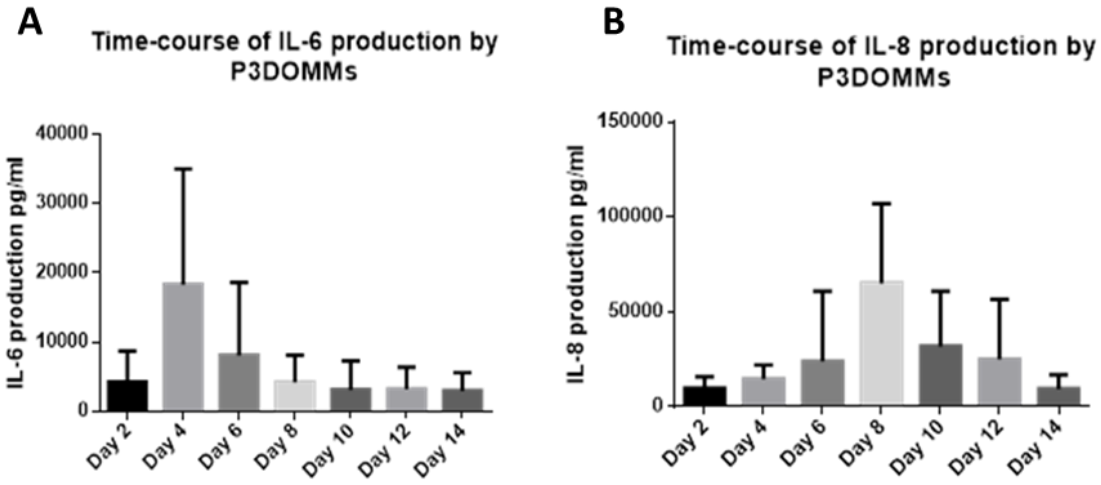

Figure 20: Pro-inflammatory cytokine production by P3DOMMs during culture
Constitutive pro-inflammatory cytokine expression IL-6 (A) and IL-8 (B) of P3DOMMs, during their production. Graphs indicate three experimental repeats with five biological replicates each. Models were created and grown for up to 14 days. Day 2 is the first day the models contracted. Media was changed and subsequently supernatant collected every 48 hours. Cytokine production was assessed via sandwich ELISA. Error bars represent standard deviation.

Next P3DOMMs were studied in a deconstructed manner to ascertain the effect of cell contact, soluble factors, and collagen, on each of the P3DOMM-incorporated cell types (POK and HGF), **Figure 21**.

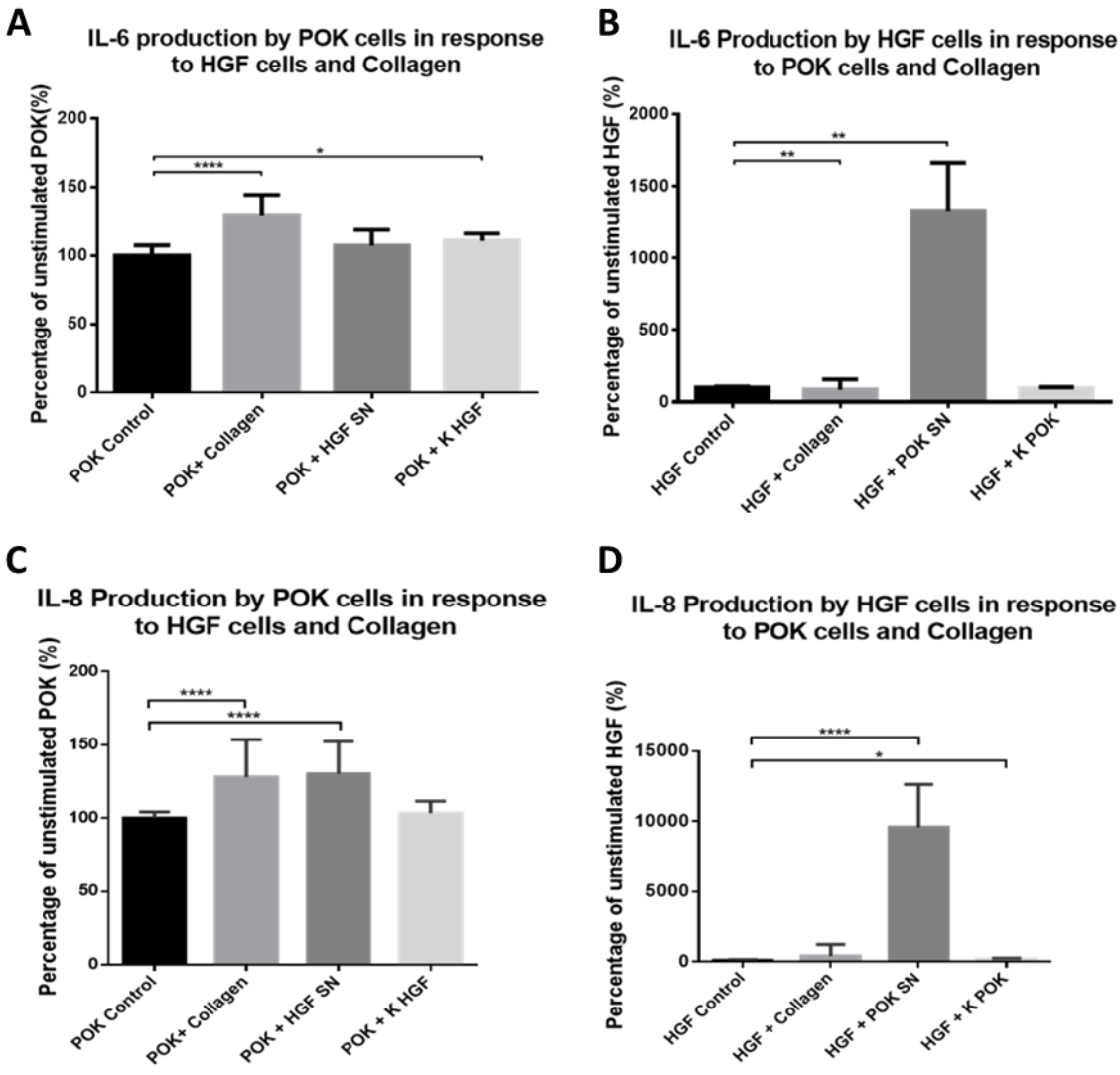

Figure 21: Pro-inflammatory cytokine production by POK and HGF cells in response to the P3DOMM environment

IL-6 production by POK (A), IL-6 production by HGF (B), IL-8 production by POK (C), and IL-8 production by HGF (D), in response to collagen, supernatant (SN), and killed cells (K). Data are from three independent experiments performed in triplicate. Cells were stimulated for 18 hours and the production of pro-inflammatory cytokines, IL-6 and IL-8, were measured via sandwich ELISA. Significant differences in cytokine production were compared between the control and each stimulated group. Data is standardised to a percentage of the unstimulated control. Data normality was assessed using the Shapiro-Wilk test for normality. Statistical significance for IL-6 POK response to HGF and collagen, and IL-6 and IL-8 HGF response to POK cells and collagen was determined using a Kruskal-Wallis test followed by a Dunn's multiple comparisons test. Statistical significance for IL-8 POK response to HGF and collagen was determined using a one-way ANOVA followed by a Tukey's multiple comparisons test. Statistical significance is indicated on the graph (* $p < 0.05$, ** $p < 0.01$, *** $p < 0.001$, **** $p < 0.0001$). Error bars represent standard deviation.

There was a significant increase in IL-6 production by POK cells, when stimulated with collagen or killed HGF cells, when compared with the unstimulated control ($p < 0.0001$ *and* $p = 0.0220$, respectively). Compared with unstimulated POK cells there was also a significant increase in IL-8 production when POK cells were stimulated with collagen and HGF supernatant ($p < 0.0001$ for both).

HGF cells stimulated with collagen or POK supernatant led to significantly more IL-6 production than when unstimulated ($p = 0.0011$ and $p = 0.0012$, respectively). Furthermore, HGF cells stimulated with POK supernatant or killed POK cells, led to significantly more IL-8 production than unstimulated POK cells ($p < 0.001$ and $p = 0.0219$, respectively). Collagen did not appear to stimulate IL-8 production in POK cells.

3.4.7. PAMP recognition by POK cells

After studying the response of primary cells to the P3DOMM components, POK cells were assessed for their ability to produce the pro-inflammatory cytokines IL-6 and IL-8, in response to the bacterial components LPS and LTA, **Figure 22**. POK cells stimulated with LPS and LTA showed no clear dose response to either PAMP in terms of IL-6 production. Moreover, no significant difference was observed between the unstimulated POK control and 0.01, 0.1 or 1 µg/ml of LPS or 0.1, 1 or 10 µg/ml of LTA; nor were there any significant differences between doses of either LPS and LTA.

POK cells stimulated with the highest dose of LPS, 1 µg/ml, produced significantly more IL-8 than the control ($p = 0.0155$). There was no significant difference between lower doses of LPS and the unstimulated control, nor between different

doses of LPS. There was an increase in IL-8 production by POK cells stimulated with 0.1, 1 and 10 µg/ml of LTA compared with the unstimulated control (p = 0.0220, p < 0.0001, and p <0.0001, respectively). There was no significant difference in IL-8 production by POK cells between different doses of LTA.

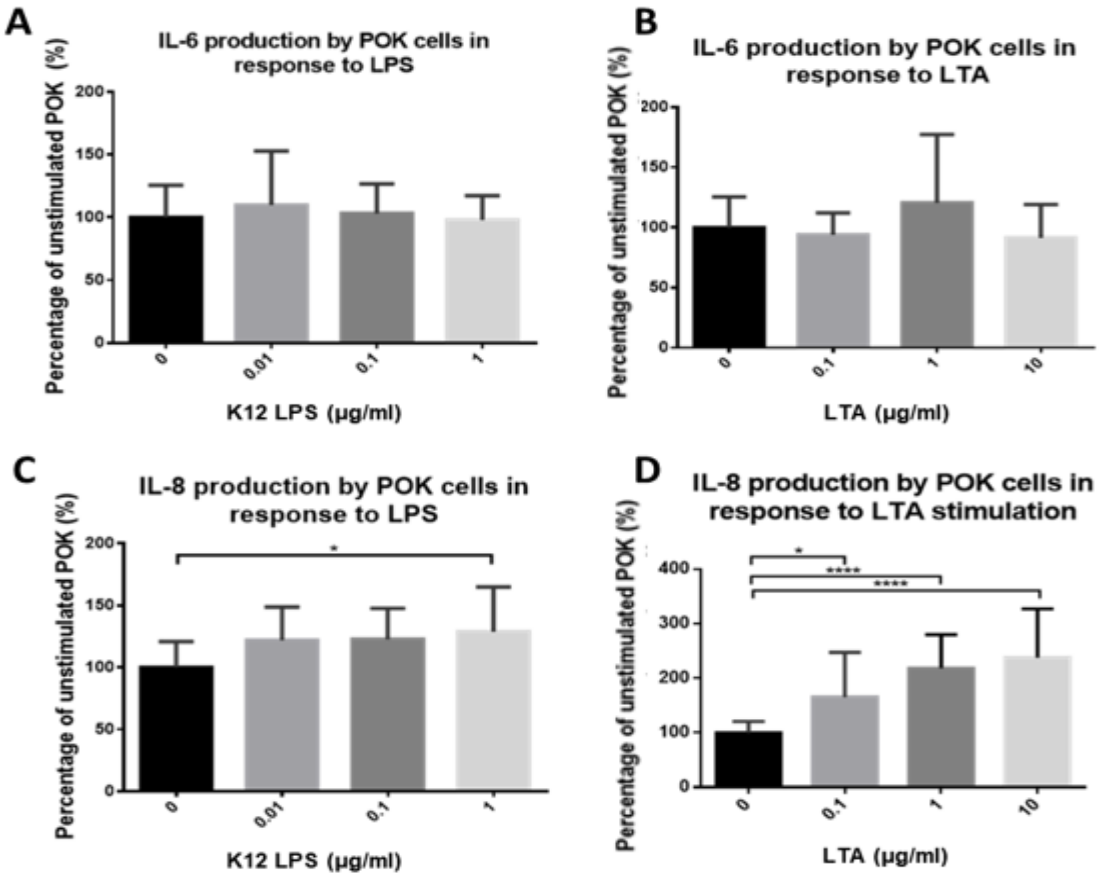

Figure 22: Dose response of LPS and LTA on POK pro-inflammatory cytokine production

IL-6 and IL-8 production by POK in response to K12 LPS (A and C respectively) and *Staphylococcus aureus* LTA (B and D respectively). Graphs indicate three experimental repeats performed in triplicate. Cytokine production was measured via sandwich ELISA after 18 hours of stimulation. Significant differences in cytokine production were compared to the every other group. Data normality was assessed using the Shapiro-Wilk test for normality. Data is standardised to a percentage of the unstimulated POK cell control. Statistical significance for IL-8 Production by POK cells in response to LTA, IL-6 Production by POK cells in response to LPS, and IL-6 production by POK cells in response to LTA, was determined by a Kruskal-Wallis test followed by a Dunn's multiple comparisons test. Statistical significance for IL-8 production by POK cells in response to LPS was determined using a one-way ANOVA followed by a Tukey's multiple comparisons test. Statistical significance is indicated on the graph (* p < 0.05, ** p < 0.01, *** p < 0.001, **** p < 0.0001). Error bars represent standard deviation.

3.5. Discussion

3.5.1. Considerations for oral infection models

This chapter explored the structure of the newly developed 3DOMMs to assess the morphology of their epithelial barrier at different stages of model growth, for both HaCaT- and POK-based models. Furthermore, this chapter considered the optimum time point in which to use the models to study infection, through balancing optimum model histology, whilst minimising baseline pro-inflammatory cytokine production. This chapter also characterised the ability of the HaCaT, HGF cells and POK cells to respond to PAMPs, and studied the interaction of the individual cell types with the 3DOMM environment.

3.5.2. Structure of the oral mucosal model

3DOMMs are structurally similar to the native oral mucosa. Models were reproducible in terms of structure, presenting with distinct epithelial and lamina propria layers. There was variability in terms of epithelial thickness between models, however for the most part epithelial thickness was consistent across an individual model, any variation was most likely to present as a thinner epithelium towards the model circumference, with a thicker centre. Models displayed varied attachment of the epithelium to the lamina propria, which may have resulted from model manipulation prior to embedding and sectioning. All models formed an intact multi-layered epithelial barrier consisting of tightly packed keratinocytes.

There was a lower degree of organisation within the 3DOMM epithelium than the native oral mucosa, due to the lack of stratification. Cells were often denser towards the basal layers of the epithelium, which may indicate a partially stratified

epithelium. Epithelial stratification and differentiation are dependent on the keratinocyte cell type and culture methodology used. The lack of stratification within HaCaT-based models has been identified elsewhere, and is attributed to deficient HaCaT-stromal cross-talk resulting from impaired IL-1 release by HaCaT cells, and may be resolved through the addition of either epidermal growth factor (EGF) or transforming growth factor alpha (TGFα)(68). The upper epithelial layers of the 3DOMM indicated a low degree of keratinisation, exhibiting only one to two layers of enucleated flattened squames. Keratinisation of the epithelium requires the terminal differentiation of stratified keratinocytes. It is ultimately determined by the local microenvironment and hence cell types, however it may be promoted by raising the models to the air-liquid interface, encouraging stratification of the epithelium, and by local growth factors (42,83). The most notable difference between the 3DOMM and the native oral mucosa was the lack of rete ridges within the 3DOMM. Rete ridges do not occur spontaneously within *in vitro* models as they are formed by mechanical pressures, and are seen within most keratinised oral epithelia. They help to anchor the epithelium to the lamina propria layer. It is theoretically possible to induce rete ridges *in vitro*, however these are often only considered to be required in order to create tissue robust enough for grafting purposes (59).

Fibroblasts appear less numerous in the lamina propria of the 3DOMM than within the native oral mucosa. Furthermore, fibroblast density appeared to vary between models. It is possible that numerically, there are the same number of fibroblasts per model, however their distribution may vary, depending on the thickness of the lamina propria, and how quickly the model polymerised after adding fibroblasts, therefore depending on the area sectioned, fibroblasts may alter in abundance.

Another possibility is that fibroblasts are not distributed evenly between models derived within the same batch. Therefore, some models may contain more fibroblasts than others. This could be resolved by ensuring the fibroblast containing gel is adequately mixed prior to introducing to each transwell insert. Although there was a relatively low abundance of fibroblasts across all models, when compared to the native oral mucosa, fibroblast seeding density was not increased. Fibroblasts are in stasis from the point they are embedded into the gel matrix. Incorporation of more fibroblasts was found to increase contraction of the 3DOMM, as indicated in preliminary study (data not shown), so that resulting tissue was smaller, stiffer, and hence more difficult to manipulate due to its size; therefore, the number of fibroblasts incorporated into the matrix was not increased. In future, alternative fibroblast batches should be taken into consideration, as fibroblasts from different donors often exhibit different levels of contractility, and variation has been indicated between donors of a different age (190,191). By selecting a less contractile batch, it may be possible to incorporate a higher density of fibroblasts, whilst not compromising the size of the resultant tissue.

A weak basement membrane appears to have formed within some of the 3DOMMs, but to a lesser extent than the distinct basement membrane seen within native tissue. Occurrence of a continuous, yet fragmented, basement membrane has been reported previously, with continuous basement membrane formation not being observed until the models were taken past 3 weeks of culture, longer than that of the models used within in the present study (107). Due to the separation of the lamina propria layer and the epithelium, it is difficult to tell within some models whether a basement membrane had begun to form and was

disrupted during the processing of the 3DOMM for histology. However, basement membranes are considered to provide structural support, maintaining the attachment of the epithelium to the lamina propria layers, therefore the lack of a defined basement membrane in the first place may have permitted this detachment (106). As basement membranes result from epithelial mesenchymal cross-talk, the lack of a basement membrane may indicate a deficiency in this area between the HaCaT and HGF cells.

The thickness of the 3DOMM epithelium did not consistently differ between day 16 and day 21. Models at day 19 presented with the best morphology, whereby the lamina propria was anchored to the epithelium most frequently, and the epithelium remained uniform and intact. Younger models indicated a separated epithelium, and older models contained cells breaking away from the epithelium, which may compromise the integrity of the epithelial barrier.

P3DOMMs were cultured for a shorter period than 3DOMMs due to the limited lifespan of primary cells within culture. The manufacturer's certificate of analysis provided with the primary oral keratinocytes indicated that the cells were only guaranteed to hold their phenotype for 15.87 population doublings. With this in mind, subsequent models were cultured for as short a time period as possible. In order to expand the cell population enough to permit for multiple repeats during experimentation, POK cells were available from passage 3.

P3DOMMs were less similar to the native oral mucosa that 3DOMMs. The disorganisation exhibited within the POK epithelium means the barrier integrity would be compromised, and suggests the model may be unsuitable for studying infection in its current form. POK cells at passage 5 in monoculture were

displaying a loss in keratinocyte phenotype, as indicated by their enlarged and dysmorphic appearance and lack of cell-to-cell contact, leading to randomly distributed cells that did not appear as discrete islands. It is most likely that the resulting enlarged dysregulated epithelium within the P3DOMM occurred due to the limited lifespan of the POK cells, which raises the question as to how appropriate they are for the production of oral mucosal models. Either the POK cells would need to be incorporated at an even lower passage, inhibiting the number of repeats in which experimentation may be performed on a single vial of cells, or the models may need to be cultured for less time, meaning that the thickness of the epithelium is likely to be compromised. Another factor, which may alter the epithelial development and organisation is the culture technique. Unlike the 3DOMMs which were grown in KGM 3 (a cell culture media previously described as suitable for use at the air-liquid interface), P3DOMMs were grown in the less well defined proprietary POK media (14). POK cells were found to be non-viable when cultured in other media, including DMEM, RPMI, and KGM. They failed to proliferate and many cells underwent apoptosis, therefore the implementation of other media in an attempt to improve epithelial integrity was not possible.

Morphologically the immortalized HaCaT cell line is more appropriate for creating an oral mucosal infection model than primary POK cells, due to the intact epithelial barrier formation observed within HaCaT containing models, but not POK containing models. The lack of epithelial stratification and consistent basement membrane prevents the models being described as analogous to the native oral mucosa. Despite this, these models appear to contain the necessary

structural components to act as a basic infection model, namely an intact multi-layered epithelium atop a lamina propria layer containing fibroblasts.

Due to the uncertain nature of model variability between batches, in terms of epithelial thickness, it may be necessary to determine a standardised “acceptable” range of epithelial thickness, when implementing the models to study host response to infection. As such models may be implemented for studying microbial invasion, the number of epithelial layers present will impact upon the pathophysiology of infection. By selecting a standardised range, and quantifying the epithelial thickness by sacrificing one model per batch, prior to their use for infection studies, the models may be applied in a more informative and reproducible manner. However this will not account for inter-batch variation. At present, it is not clear whether the epithelial variation will impact upon the models ability to recognise and respond to infection, if so, it may be necessary to further optimise methodology in order to ensure the models are more consistent.

3.5.3. Baseline pro-inflammatory cytokine production of the oral mucosal model

Characterising the ability of 3DOMMS and P3DOMMs to respond to infection required multiple considerations. Firstly, it was important to consider how the cells within the model were responding to their environment, to determine whether it would be possible to study upregulation of pro-inflammatory cytokines in response to infection, and to predict how incorporated immune cells may respond to the local environment due to the existing cytokine milieu

Not previously acknowledged is that 3DOMMs are inherently inflammatory, producing high levels of pro-inflammatory cytokines. Therefore, oral mucosal models at baseline are not modelling a healthy oral mucosa, in terms of the pro-inflammatory cytokine output they are constitutively expressing. Such pro-inflammatory cytokine production is unlikely to affect the models ability to study colonisation or invasion of infective agents; however the ability of the models to produce further pro-inflammatory cytokines in response to pathogen recognition may be altered due to the already inflammatory environment. This required further elucidation. Furthermore, should the models be further developed to contain innate immune cells, these cytokines may alter the activity of these cells, tailoring their response. This means using these models to study infection may not be representative of the healthy oral mucosa, which should not be inherently inflammatory prior to the introduction of a pathogen. This inflammatory environment was further investigated in order to determine whether it is possible to reduce these high levels of pro-inflammatory cytokines, and therefore create a healthy model.

As the models were initially studied as a whole, it was not possible to speculate which of the incorporated cell types were leading to such a pro-inflammatory environment; nor was it possible to determine what was leading to the high levels of pro-inflammatory cytokine production during the initial and latter stages of 3DOMM culture. This therefore required further investigation. As the highest levels of pro-inflammatory cytokine production were seen upon the formation of the model, it was considered that the model components might be stimulatory to the individual cell types. For this reason, the model was assessed in a deconstructed manner. Individual cell types were stimulated with the collagen

matrix, and supernatants of the other cell types incorporated into the model, in order to gain an insight into the cause of the observed inflammatory environment at day 1 of model production. Preliminary data (not shown) indicated that the pro-inflammatory cytokine production could be reduced by reducing the serum content of the model upon formation. It is this reduced serum model that is discussed.

The high level of pro-inflammatory cytokine production by the 3DOMM may be at least partially attributed to collagen matrix stimulation of HaCaT and HGF cells. The type-1 collagen used in the present study is dissolved in acetic acid, and therefore sodium hydroxide was used to neutralise the pH prior to the addition of cells. As the models are formed in DMEM, a bicarbonate-based medium, the pH of the model will be different outside of a 5% CO_2 incubator. Once incubated, the gel matrices would polymerise and prevent the assessment of pH levels using a traditional pH probe. Thus, pH was subjectively observed by eye, by way of the phenol red indicator within DMEM. It is possible that pH imbalance may contribute to the initial inflammatory environment through the promotion of DAMPs due to cellular damage, resultant from a pH that is too acidic or too alkaline. This in turn may lead to pro-inflammatory cytokine release (192,193). The model pH appeared to neutralise upon introduction to the CO_2 incubator. This effect may be minimised in future by equilibrating media in 5% CO_2 prior to induction to the model. IL-6 production was elevated in both cell types upon the introduction of the cells to a collagen matrix. A differential effect was present between both cell types in terms of collagen-induced IL-8 production; in HGF cells IL-8 increased, whereas in HaCaT cells IL-8 decreased. This increase in IL-6, yet decrease in IL-8 within HaCaT cells, was unexpected. This pattern of cytokine release by

epithelial cells may be a result of TGF-β1 production, which was not screened for in the present study. In bronchial epithelial cells, TGF-β1 has been shown to induce IL-6 production whilst inhibiting IL-8 release (194).

The HaCaT and HGF supernatant increased the overall pro-inflammatory cytokine production of the target cells. This indicates another mechanism that may induce pro-inflammatory cytokine production within the 3DOMM. Cells respond to their local microenvironment, including the physical, biological, and chemical factors surrounding them (195). The cytokine expression profile by an individual cell type is therefore likely to contribute to and modify the cytokine expression of another cell type resident in the same environment. It is difficult to fully deduce the complex interactions between the model components by studying any one potential stimulus at a time; however, these data provide an insight as to how the model's methodology may be modified in future to reduce the initial inflammatory state.

With regards to the current methodology for model production, many epithelial cells are added atop the lamina propria layer at one time. In fact, to promote rapid epithelial layer formation, more cells than the recommended seeding density are seeded atop the matrix. It is reasonable to assume that not all cells adhere to the matrix, some of which will subsequently undergo cell death. Furthermore, the increase in IL-8 production seen within the later stage of 3DOMM culture (from day 13 onwards), raised the question as to what was causing the sudden increase after this point. It was possible that this increase in pro-inflammatory cytokine production may again be a result of cell death. Cell death resultant from lack of oxygen and growth factors available to the cells within the model may rise as the

model thickness increases. The static culture of the 3DOMM is reliant upon passive diffusion to permit the passing of vital nutrients from below the transwell insert all the way to the apical epithelial layers. The lack of a vasculature and hence direct delivery of oxygen and growth factors means this model may be limited in its capabilities of diffusion, as cell numbers increase leading to necrosis from lack of oxygen and growth factors distributed into the more distal areas of the tissue (196).

For this reason, following on from the 3DOMM time-course a LDH assay was performed to determine whether pro-inflammatory cytokine production at day 1, and after day 13, was partially attributed to cell death. DAMPs mostly consist of intracellular components which are released upon cell death, such as DNA, RNA, histones, ATP, and uric acid (186). DAMPs, much like PAMPs, are recognisable by cellular PRRs such as TLRs, and lead to downstream pro-inflammatory cytokine release. The present study revealed a strong correlation between LDH release, IL-6, and IL-8 production. This indicates that higher level of pro-inflammatory cytokines are associated with higher levels of cell death. The highest level of cell death was seen at day 1 post-model production. The high levels of pro-inflammatory cytokine production may be explained by a number of mechanisms, firstly due to intracellular cytokine release upon cell death, and secondly due to stimulation of PRRs by DAMPs resulting from cell death.

The identification of model components and cell death as a cause for the high levels of model pro-inflammatory cytokine release, most likely does not encompass all causalities. If deemed necessary for future refinement, pro-inflammatory cytokine production may be minimised based upon these

indications. At present, these data suggest that culturing the model for a shorter period helps to overcome later occurrence of cell death. Should the model be required for longer-term culture, perfusion systems have been designed to increase the distribution of nutrients amongst tissue-engineered constructs (197).

As with the 3DOMMs, P3DOMM-incorporated cell types, namely POK cells and HGF cells, were studied individually for their response to the model environment, including the other cells incorporated into the 3DOMM, and collagen. An additional category was included in this experiment in order to assess how the cell-to-cell contact of POK cells and HGF cells was affecting the pro-inflammatory cytokine output.

P3DOMM pro-inflammatory cytokine production was followed for a shorter period than 3DOMMs due to the limited lifespan of primary cells within culture. Interestingly within P3DOMMs the highest level of pro-inflammatory cytokine production was not indicated upon model formation. This may be partially attributed to the use of a serum-free medium that contains hydrocortisone. It is already known that serum was found to increase pro-inflammatory cytokine production; furthermore hydrocortisone is known to have an immunomodulatory effect *in vivo* (198). The reason for the highest levels of pro-inflammatory cytokine production occurring at the mid-culture phase is less certain. At this point, no new stimulants were added to the model. Considering the histology results, it is possible that this may be the phase in which the epithelium begins to break down and therefore higher levels of cell death may be occurring leading to the increased levels of pro-inflammatory cytokine production through cell lysis and DAMP release. Levels may reduce after this point as there are a lower number

of cells remaining to release cytokines overall. This was not followed up for the P3DOMMs, due to inferior tissue morphology when compared to the 3DOMMs. Should the cell death theory be required to be confirmed, an LDH assay could provide further insight.

As with HGF cells, collagen matrix-stimulated POK cells led to an overall increase in pro-inflammatory cytokine release. The soluble factors in HGF and POK supernatant were able to stimulate the target cell types, which may contribute to the overall inflammatory environment of the model. The increase in IL-8 production observed from HGF cells upon stimulation with killed POK cells indicates that cell contact may also contribute to the P3DOMM inflammatory environment, however it is unlikely that POK and HGF cells come into contact due to their separation by the collagen matrix. Interestingly, the stimulation of HGF cells by collagen differed between this experiment and the previous 3DOMM experiment. This could be explained by the differing media used between these two experiments.

Not to be ignored, yet not explored in the present study, is the role of matrix metalloproteinases (MMPs) in the 3DOMM environment. MMPs are another possible cause of the later increase in pro-inflammatory cytokine production of 3DOMMs, due to their role in ECM remodelling and ability to evoke an immune response (199,200). Miller *et al*., 2002, indicated that MMP activity altered during different stages of culture of gingival fibroblasts embedded in a collagen gel between days 1 and 21 post seeding. MMP-1 activity was highest between days 10 to 21, gradually increasing from day 3 onwards. MMP-2 activity was highest between days 7 and 15 (201). This increase in MMP activity is likely to be

occurring within the 3DOMMs so it is possible that high MMP activity may correlate with the later stages of pro-inflammatory cytokine production, and contribute to this later inflammatory environment along with the already identified increase in cell death.

As well as creating a pro-inflammatory environment, and holding the potential to influence subsequently incorporated immune cells, high levels of the cytokines IL-6 and IL-8 are likely to modify the activity of the oral mucosal model itself. Keratinocytes may express IL-6R, whereas fibroblasts do not constitutively express IL-6R, although IL-6 is able to act on fibroblasts through trans-signalling, mediated by soluble IL-6R (161,202–204). Keratinocytes and fibroblasts have been shown to express CXCR1 and CXCR2, meaning the cells may respond directly to IL-8 secretion (179,180). Despite the pro-inflammatory nature of these cytokines, their resultant activity on both keratinocyte and fibroblast cell types may also promote tissue regeneration. IL-6 is known to modulate keratinocyte differentiation and increase proliferation within keratinocytes, and can therefore aid epithelial regeneration during wound healing (203,204). IL-8 enhances keratinocyte migration, increasing the rate of epithelial wound healing; low levels of IL-8R expression are attributed to slow healing wounds (205). IL-6 is recognised by fibroblasts, when in the presence of IL-6SR, which leads to expression of the monocyte chemoattractant MCP-1 (206). IL-8 can instigate a migratory phenotype within fibroblasts, which is associated with wound healing (207). Considering this, the high levels of IL-6 and IL-8 identified during model formation could be attributed to proliferation or tissue re-organisation occurring during model maturation.

In order to study pro-inflammatory cytokine release in response to infection, models should be utilised at a time point of lower pro-inflammatory cytokine production, enabling a measurable upregulatory response compared to baseline. Cells often have an upper limit of pro-inflammatory cytokine production, and ELISA assays certainly have an upper limit of detection. Considering this, it was decided that the 3DOMMs should be used during a period of lower pro-inflammatory cytokine production, where it is known that levels above this are able to be produced by the cells and detected by ELISA. Results have indicated that between day 3 and day 15, IL-8 expression was lower than 5000 pg/ml meaning an upregulation would be detectable. Although there was some increase seen between days 11 and day 15 in terms of IL-8 production, it was decided that day 14 was the optimum time point to attempt to study pro-inflammatory cytokine expression in response to pathogenic challenge. This was in order to balance the model histology, providing enough time for a multi-layered epithelium to develop, and minimal cytokine production.

3.5.4. Immunogenicity of the 3DOMM

An appropriate infection model should be able to recognise and respond to pathogenic challenge. For this reason, individual model-incorporated cell types were assessed for their ability to respond to PAMPs. As known TLR ligands, the PAMPs LTA and LPS are most commonly known for signalling through TLR2 and TLR4, respectively. The upregulation in pro-inflammatory cytokine production by HaCaT, HGF, and POK cells in response to LTA suggests a functioning TLR2 signalling pathway, and confirms that the cells incorporated into the 3DOMM are able to recognise and respond to this gram-positive bacterial component. This also indicates that the models may be able to respond to fungi through TLR2

recognition of phospholipomannan (122). This finding is supported within the literature, indicating that gingival fibroblasts express functional TLR2 (146,208). Furthermore, epithelial keratinocytes including oral and HaCaT cells have been shown to express functional TLR2 (137,139,209). Typically, lower levels of LPS are capable of elucidating a response within host cells (in the ng/ml range) than LTA, whereby higher doses are required to produce a downstream effect (between 1 and 10 µg/ml) (210).

The lack of response to K12 LPS by HaCaT cells disagreed with the finding by Olaru *et al*., 2010, which indicated an upregulation in IL-8 secretion upon HaCaT stimulation with LPS, but was supported by a study conducted by Kollisch *et al*., 2005 which indicated no upregulation in IL-8 expression upon HaCaT cell stimulation with LPS (137,139). It is not clear as to exactly why this differential effect is seen within HaCaT cells; however, it may be dependent upon the type of LPS employed as a stimulus. The present study used *E.coli* K12 LPS, the responsive study did not state their LPS source, and the unresponsive study used *E.coli* K235 LPS (137,139). It may be the case that the unstated LPS was an un-purified form of PgLPS, which has been reported to signal through both TLR2 and TLR4, this would lead to the observed downstream IL-8 production upon stimulation of HaCaT cells (128,208). Unlike the HaCaT cell line, POK cells responded to K12 LPS, indicated by an increase in IL-8 production. Primary oral keratinocytes have been shown to be responsive to LPS stimulation previously (211). Interestingly neither keratinocyte cell type upregulated IL-6 production in response to PAMPs.

Within the present study, an unusual effect was exhibited when HGF cells were stimulated with K12 LPS. Although a weak statistical significance was shown in IL-6 production by HGF cells, between unstimulated cells and cells stimulated with an intermediary dose of 0.1 μg/ml of K12 LPS, this did not occur at higher doses, nor was there a significant increase in IL-8 production for any doses. Other HGF stimulants such as LTA and the collagen matrix led to IL-6 and IL-8 production rising simultaneously. This differential effect cannot be explained at this point, however it should be noted that other studies have indicated functional TLR4 within human gingival fibroblast cells, therefore it is unlikely that the perceived response to K12 LPS by HGF cells is a statistical anomaly, and may be dose dependent (142,146).

To further characterise the PAMP responsivity of HaCaT and HGF cells, TLR2 and TLR4 protein expression and localisation was assessed within the 3DOMM-incorporated cell types. Western blotting for TLR2 and TLR4 revealed that TLR4 is expressed within HaCaT cells, HGF cells, and the 3DOMM. It was not possible to assess the presence of TLR2 due to issues with identifying functional antibodies; multiple antibodies were attempted, and revealed either no binding or binding at the incorrect molecular weight. These inconclusive results were mirrored in assays of positive test cell lysate provided by the manufacturer. The presence of TLR4 within the Western blot and the lack of LPS responsiveness from the cells warranted further exploration. It is possible that, as reported in the literature, there are a lack of adaptor proteins within the keratinocytes; however this was unlikely the case within the fibroblasts, which also displayed very limited response to LPS stimulation (137,145,212).

In order to determine why there was little response in the HaCaT and HGF cell lines to LPS, the cell surface expression of TLR4 was studied in unstimulated, and stimulated, HaCaT and HGF cells; TLR2 expression was also characterised. TLR2 expression occurred within HaCaT and HGF cells, as expected (due to their responsivity to LTA). TLR4 expression was less than that of the isotype control, which was deemed to be due to an issue with the antibody or isotype control utilised, as LPS-responsive macrophages used as a control, also followed this trend. It was therefore not fully possible to characterise the TLR expression by HaCaT and HGF cells, however it would appear that functional TLR2 receptors were expressed at the cell surface of both HaCaT and HGF cells due to their responsivity to LTA and the identification of TLR2 at the cell surface.

HaCaT cells do not appear to possess a functional TLR4 receptor complex, as they do not respond to LPS, despite possessing the TLR4 protein as indicated by Western blot. The expression of functional TLR4 is less certain within HGF cells. The literature indicates that a range of fibroblasts do express functional TLR4 (142,145–148). However only a limited response to the concentration of 0.1 µg/ml LPS was observed within HGF cells. Western blot confirmed the presence of TLR4 within HGF cells, however as with HaCaT cells, expression of TLR4 at the cell surface could not be confirmed. Considering the available information, it would appear that HGF cells do express TLR4 at the cell surface, however in this case, only displayed a limited response to LPS.

Differences are often exhibited between primary and immortalised cells (at baseline and when stimulated) (13,20,213). Donor variability has also been shown in cytokine production and was also evident between primary

keratinocytes obtained from biopsy (13). Despite the fact donor variability may hinder reproducibility, and the limited access to primary cells, it still may be possible that primary cells are a more suitable alternative, or a worthy opponent of the immortalised 3DOMM should the issue of the disorganised epithelium be resolvable. Primary cells have been used for creating full-thickness oral mucosal models, and may be a closer representation of the healthy oral mucosa (20). It is for these reasons that despite the epithelial morphology, a comparison was made between the HaCaT and primary cell types.

The effect that the high levels of pro-inflammatory cytokines within the 3DOMM environment will have on the 3DOMMs ability to model host response to infection is so far unknown. It is predicted that an inflammatory environment may also affect the response of any further incorporated immune cells. The local cytokine milieu is likely to have an effect on any innate immune cells subsequently incorporated. The present study later intends to develop a three-dimensional oral mucosal model that incorporates macrophages into the matrix, an immunocompetent 3DOMM (IC3DOMM). In order to minimise the pro-inflammatory environment, serum content should be kept to a minimum, the pH should be ensured to be physiologically correct, and models may need to be used for subsequent study by day 14. It would appear that the 3DOMM is likely to be more suitable for development as an immune competent model compared to the P3DOMM, as generally, lower levels of pro-inflammatory cytokines were produced during the time-course. Later incorporated immune cells will most likely be responsive to the pro-inflammatory cytokine milieu, which will not be limited to the IL-6 and IL-8 identified within the present study. For example, MCP-1, a chemokine responsible for the taxis of monocytes and macrophages, was also

identified within the 3DOMM environment, however unreported in the present study (214). IL-6 receptors are expressed on monocytes, and to a lesser extent, in subsequent macrophages. IL-6 contributes to the differentiation of monocytes into macrophages as opposed to dendritic cells, and influences the polarisation of macrophages (168,215,216). IL-8 receptors are also expressed upon monocytes and macrophages, meaning they may respond to IL-8 (175). However, as the anti-inflammatory cytokine milieu was not assessed, it is not possible to predict the overall effect the 3DOMM environment will have on any incorporated macrophages. Additionally, it is not the levels of cytokines alone that determine responsivity. Many regulatory mechanisms exist to prevent the overstimulation of cells and tissues by cytokines, including: regulation of receptor expression, receptor antagonists, decoy receptors, contact dependant negative regulators, disruption of downstream signalling pathways, and contrasting anti-inflammatory cytokines (217–222). For these reasons, the effect of the overall model environment on subsequently incorporated macrophages should be taken into account, and their incorporation should not be ruled out based on the identification of high levels of pro-inflammatory cytokines alone.

3.6. “Bridge”

As 3DOMMs and P3DOMMs were shown to be responsive to PAMPs, with the confirmation that all cell types could recognise and hence respond to the TLR2 ligand LTA, it is inferred that they may appropriate for the study of gram-positive-bacterial and fungal infections. Prior to any further model development, P/3DOMMs should be characterised for their suitability for modelling live infection; in terms of tissue colonisation and invasion, and pro-inflammatory cytokine response to infective agents. Only once the suitability of the current P3DOMMs and 3DOMMs have been compared, can the most promising model be selected to take forward to further develop into an immunocompetent oral mucosal infection model.

4. Infection modelling

4.1. Introduction

4.1.1. Candida albicans as a pathogen

Candida albicans is a eukaryotic dimorphic yeast. *Candida spp.* are the most common human fungal pathogens. *C. albicans* is typically classified as a commensal organism; however, in times of weakened host defence, or disrupted microbial balance, the organism can shift into a pathogenic role (223). *Candida* most frequently colonises the oral and vaginal mucous membranes. Of all *Candida spp.*, *C. albicans* is the most frequent cause of mycosis (224). The relationship between *C. albicans* and the human innate immune system is complex. *C. albicans* is capable of switching between its yeast and hyphal isoforms with ease. Depending on environmental factors, it possesses a myriad of virulence factors which aid its invasion, colonisation and persistence, making it an effective commensal and opportunistic pathogen. This switching ability between its yeast and hyphal form is an important virulence factor, and appears necessary for *C. albicans* to change from being a commensal to a pathogenic organism (41,225). The yeast to hyphal transition of *C. albicans* is often indicative of its pathogenic status, with the hyphal form being most frequently associated with tissue invasion, and may determine the necessity of the host to respond (226).

4.1.2. Recognition of *Candida albicans* by PRRs

C. albicans contains multiple cell wall components that possess conserved structural motifs including chitin, glucans, and mannans, which are exposed to

the extracellular environment, as well as internal nucleic acid sequences, all of which act as PAMPs and hence are able to be detected by PRRs (121,227–229).

TLRs are associated with the recognition of *C. albicans* PAMPs. Cell membrane associated TLR2, TLR6, and TLR4 have been shown to recognise *C. albicans* phospholipomannan and O-linked mannan cell wall components (122). Whereas the intracellular TLR7 and TLR9 have been shown to recognise *C. albicans* RNA and DNA, respectively (230,231). TLR2/6 as well as the C-type lectin receptor (CLR) dectin-1 recognise *C. albicans* β-glucan cell wall components such as zymosan (229,232). There are further PRRs which are capable of recognising components from *C. albicans* (110,233,234), however the focus of this research, in keeping with the rest of this thesis, will focus upon TLR-mediated recognition.

4.1.3. Staphylococcus aureus as a pathogen

S. aureus is a gram-negative bacterium. It is a commensal within approximately 30% of the general population, most commonly residing in the nasal cavity; it is also a frequent human pathogen (235,236). *S. aureus* is the causative agent of localised and systemic infections as diversely ranging as impetigo, pneumonia, and sepsis (235). Both the ability of *S. aureus* to cause such a wide range of infections, and its high level of antimicrobial resistance, means *S. aureus* is of significant research interest (237). *S. aureus* has also more recently been recognised as a coloniser of the oral cavity (36,37,236,238,239).

4.1.4. Recognition of *Staphylococcus aureus* by PRRs

S. aureus bacteria contain multiple PAMPs such as lipotechoic acid (LTA) and peptidoglycan (PGN), which are capable of being recognised by TLRs (210).

TLR2 mediates the host response to *S. aureus* and can form heterodimers with TLR1 and TLR6 to mediate response to pathogenic challenge (112,120).

4.1.5. Denture stomatitis

Denture stomatitis (DS) (also known as denture sore mouth, denture related stomatitis, and chronic atrophic candidiasis), is a disease specific to denture wearers that can cause erythema, oedema, and discomfort of the areas of the oral cavity in contact with the denture. The Newton classification defines DS in three stages ranging from localised inflammation and pinpoint erythema (Type 1), to inflammatory nodular or papillary hyperplasia (Type 3). Type 2 DS is the most common form identified, and is characterised by erythema and oedema, often spanning the entire area under a maxillary denture (240). Often patients are asymptomatic, particularly with the earlier stages. DS is believed to be triggered by a combination of factors, however *Candida spp.* colonisation, in conjunction with epithelial damage, is likely to be enough to induce stomatitis, particularly as the host defence is compromised due to denture wear (38,240). The ability of *C. albicans* to cause DS is thought to be attributed to lack of shedding of the acrylic denture surface, permitting colonisation and biofilm formation on the denture and lack of salivary flow. Absence of salivary flow leads to reduced sloughing of cells, and lack of anti-microbial factors between the denture surface and the hard palate (35). This effect is enhanced in the case of a poor denture cleansing routine (34).

The DS associated biofilms, which reside on both the oral mucosa and the denture prosthesis, are thought to be potential reservoirs for disseminated infection. Therefore all DS cases are of importance irrespective of pain (33,241–243). Multiple risk factors are known to influence the likelihood of DS

development including improper cleaning, immunosuppression, antibiotic use, salivary flow, diabetes mellitus, high carbohydrate diet, *C. albicans* carriage, microflora composition, age, gender, denture material, and denture age (33,34,36–38). The focus of the present study centres on the carriage of the yeast *C. albicans,* and the bacterium *S. aureus,* which has been isolated in conjunction with *C. albicans* in the oral cavity (36,37,236). It has been shown that their viability, virulence and antimicrobial resistance is altered in dual infections, in comparison to single infections (41,244,245).

4.1.6. *C. albicans* and *S. aureus* synergy in oral and systemic disease

C albicans and *S. aureus* infection in the oral cavity is of key interest in the present study for two reasons. Firstly, because of their potential role in DS; secondly, due to their synergistic relationship which may lead to highly virulent, difficult to resolve, systemic infections (41). In murine studies, dual infection of *C. albicans* and *S. aureus* results in 100% mortality when both organisms are injected intraperitoneally, compared with no mortality when treated with the same dose of either organism alone. This occurred within different strains of *S. aureus* regardless of its attributed virulence (246,247). Subsequent studies of the localisation of the organisms within co-infection indicated that *C. albicans* was somewhat protective of *S. aureus*, which after intraperitoneal injection were exclusively located within the fungal growth (245). Subsequently, confocal microscopy was used to identify that *in vitro S. aureus* was commonly found amongst the hyphal elements of *C. albicans* (238). Conversely when co-cultured in a higher serum content media, *S. aureus* appeared as distinct micro-colonies on the biofilm surface (244).

The dimorphic nature of *C. albicans* and subsequent hyphal invasion of tissue means in an environment where other microorganisms are associated with *C. albicans*, it may also provide a route of invasion for the associated organisms, such as *S. aureus* (41,248). *C. albicans* and *S. aureus* have been co-isolated from blood. Approximately 27% of all *Candida* blood stream infections are poly-microbial, and *S. aureus* is the third most common organism isolated in conjunction with *C. albicans.* This equates to approximately 11% of all poly-microbial blood stream infections (249). A breach in barrier integrity is required for *S. aureus* to gain entry beyond the epithelium, into lower layers of soft tissue, and the blood stream (41,241). However a number of patients with staphylococcal bloodstream infections have no documented obvious portal of entry such as a wound (250). This led Peters *et al*., 2012, to study the mechanisms by which *S. aureus* may gain *C. albicans*-mediated entry to the tissue. *C. albicans* cell wall adhesion molecule Als3p was shown to bind with staphylococcal adhesins (41,248). This details the mechanism of binding and suggests that upon hyphal tissue invasion, *S. aureus* may access the tissue by proxy, providing a route of entry for further dissemination. In addition, recent murine studies have implicated *C. albicans* in the induction of bacterial dysbiosis within the oral cavity, which leads to the promotion of invasive infection by disrupting oral epithelial tight junctions (251).

Aside from increased virulence, and aiding the entry of *S. aureus* into the tissue, another form of synergy that occurs between *S. aureus* and *C. albicans* is an increased antimicrobial resistance during co-infection. *S. aureus* displayed an increased resistance to vancomycin when co-cultured compared to single culture (244). In fact it has been shown that 27 proteins were differentially expressed

upon co-culture with *C. albicans* and *S. aureus* than when either organism was cultured alone, some proteins of which aid the evasion of host defence (238).

4.1.7. *C. albicans* and *S. aureus* isolated from the oral cavity of patients

Candida spp. and *Staphylococcus spp.* have been identified as oral colonisers within a healthy, non-denture wearing population. Within a sample size of 68 individuals, *C. albicans* was identified as the most common *Candida* species, present in 30 (44.12%) of the patients. Of the same cohort 9 (13.23%) patients possessed *S. aureus* (252). Few studies have investigated the co-isolation of *C. albicans* and *S. aureus* within the oral cavity in the context of the disease DS. **Table 9** describes the outcomes of three fundamental studies, which have been undertaken to identify *C. albicans* and *S. aureus* within the oral cavity of denture wearers. Monroy *et al.,* 2005, Chopde *et al.,* 2012, and Pereira at al., 2013, conducted studies which compared the colonisation of *C. albicans* and *S. aureus* in DS patients with a healthy denture wearing control group. Swabs were taken from the denture surface and the underlying oral mucosa. The results displayed are of *C. albicans* and *S. aureus* colonisation of the groups studied. Selective patient health and lifestyle information was also recorded in order identify risk factors for DS manifestation. Data shows *C. albicans* and *S. aureus* were isolated from the oral mucosa more frequently in patients suffering with DS, compared to healthy denture wearing controls, **Table 9**. Furthermore, **Table 10,** which focuses upon Monroy's study, indicates that *C. albicans* and *S. aureus* were more frequently co-isolated from the oral mucosa compared the prosthesis within DS patients, however this was reversed within healthy control participants. Dual

isolation of *C. albicans* and *S. aureus* from the mucosa of DS participants was more frequent than that of healthy denture wearers (36).

Table 9: *C. albicans* and *S. aureus* identification from the prosthesis and mucosa within the existing literature.

The outcomes of three fundamental studies which determined *C. albicans* and *S. aureus* carriage within healthy denture wearers and DS patients on the prosthesis and mucosa. The displayed results were determined by swabbing the hard palate and prosthesis of the examined cohorts in the Monroy *et al.,* 2005, Chopde *et al.,* 2012 and Pereira *et al*., 2013 studies. The columns to the right are descriptive of their inclusion, exclusion, and sample criteria. Some data has been reconfigured for display, to aid comparison with other studies. * Article displayed a discrepancy with reported data for the prosthesis carriage of *C. albicans* within the healthy control group, it was therefore excluded.

Study	**Healthy control patients**		**DS sufferers**		**Inclusion criteria**	**Exclusion Criteria**	**Sample collection**
	***C. albicans* carriage**	***S. aureus* carriage**	***C. albicans* carriage**	***S. aureus* carriage**			
Monroy 2005	Prosthesis *discrepancy Mucosa 20%	Prosthesis 62% Mucosa 24%	Prosthesis 26% Mucosa 86%	Prosthesis 36% Mucosa 84%	Edentulous Denture wearers	Recent antimicrobial therapy and oral hygiene procedures	Swabs Questionnaire Saliva samples
Chopde 2012	Prosthesis 68% Mucosa 51%	Prosthesis 52% Mucosa 53%	Prosthesis 28% Mucosa 86%	Prosthesis 40% Mucosa 84%	Denture wearers	Recent antimicrobial therapy	Swabs Questionnaire
Pereira 2013	Prosthesis 28% Mucosa 6%	Prosthesis 26% Mucosa 22%	Prosthesis 42% Mucosa 58%	Prosthesis 26% Mucosa 22%	Denture wearers	Recent antimicrobial therapy, diabetes and pregnancy	Swabs Oral rinse

Table 10: Single and dual isolation of *C. albicans* and *S. aureus* from the oral mucosa and denture prosthesis.

C. albicans and *S. aureus* isolated individually and co-isolated from the entire cohort's dentures and oral mucosa from Monroy *et al*., (2005). Both refers to *C. albicans* and *S. aureus*. Data was reconfigured to provide the percentage carriage for both denture stomatitis and the healthy control population.

	Denture-wearing control		**DS participants**	
Organism	**Oral mucosa**	**Prosthesis**	**Oral mucosa**	**Prosthesis**
C. albicans	7.3%	18.2%	8%	14%
S. aureus	12.7%	40%	6%	24%
Both	10.9%	23.6%	78%	12%
Neither	69.1%	18.2%	8%	50%

Pereira *et al.,* 2013, conducted a study, which examined the opportunistic microorganisms in 50 participants with DS, and 50 participants without. Samples were collected by means of oral rinses and swabs of the maxillary prosthesis and hard palate (239). Microbial counts were significantly higher in individuals who were suffering with DS. *C. albicans* was the most frequently discovered yeast across both sample populations. It was isolated in 94% of individuals with DS, and 34% of individuals in the healthy control group. Interestingly *S. aureus* alongside *S. epidermidis* were the most frequent bacterial species identified in both groups. *S. aureus* was found in equal amounts with the prosthesis and hard palate of DS patients, whereas more *S. aureus* was found in the oral rinses of healthy patients. Overall *S. aureus* was found within 42% of individuals with DS and 62% of individuals in the control group. Data were provided regarding *Candida spp.* and *Staphylococcal spp.* co-isolation. They identified 40% of the individuals with DS presented with both *C. albicans* and *S. aureus*, whereas only 20% of the healthy control group presented with both at any one time. The study suggests that *C. albicans*, in the presence of *S. aureus*, may increase the

likelihood of DS development and persistence. Sampling method was found to alter the identification of the microbes. Oral rinses allow samples to be collected from the entire oral cavity, which may disrupt the sample population if the organisms of interest reside in the DS lesion and contacting prosthesis areas only (239).

The aforementioned studies excluded participants who had recently undergone any form of antimicrobial therapy. Excluding participants who have recently received antifungals is counterintuitive; DS is often treated by antifungal therapy, so by excluding those who have received the treatment is to exclude patients with recurrent DS, and therefore to potentially ignore the more antimicrobial resistant strains. These studies also fail to compare *C. albicans* and *S. aureus* carriage between healthy non-denture wearers, healthy denture wearers, and DS patients, in any one individual study (36,37,239,252). Investigating the frequency of *C. albicans* and *S. aureus* carriage in denture wearers and non-denture control participants will identify whether denture wear alone influences *C. albicans* and *S. aureus* colonisation within healthy individuals. Incorporating DS patients into the same cohort will permit further exploration of the association between these microbes and DS prevalence. Assessing whether carriage differs significantly between control participants, healthy denture wearers, and symptomatic denture wearers within a single standardised study, with the same inclusion and exclusion criteria and data collection methods is therefore of significant interest. The above studies did not further utilise any obtained *C. albicans* and *S. aureus* isolates, such isolates hold the potential to act as clinically relevant strains to further study oral infection. The present study therefore aims to build upon the aforementioned studies, with the novel aspects of: including participants that have recently

received antimicrobial therapy; incorporating a non-denture control group, a denture wearing control group, and a DS group within the same cohort; and utilising positive isolates of *C. albicans* and *S. aureus* to study oral infection.

4.1.8. *C. albicans* and *S. aureus* infection of 3DOMMs.

Full-thickness tissue engineered models, including 3DOMMs and three-dimensional skin models, have been implemented as infection models, to study single and dual infections of *C. albicans* and *S. aureus* (14,20,42,53,54,57). They have been utilised to study tissue colonisation and invasion, strain virulence, tissue damage, host inflammatory response, antimicrobial efficacy, infection of biofilm colonised acrylic discs, and microbial virulence factor gene expression (14,20,42,53,54,57). The present study aims to use monolayer epithelial culture and 3DOMMs in a similar manner, with the novel addition focusing on the host inflammatory response to clinically relevant oral isolates. Furthermore, the present study aims to provide an insight into the proposed synergy of *C. albicans* and *S. aureus,* in an *in vitro* setting.

4.2. Aims

1. To obtain clinically relevant oral isolates of *C. albicans* and *S. aureus.*
2. To identify the frequency of colonisation of denture wearers, and factors associated with *C. albicans* and *S. aureus* carriage.
3. To assess the efficacy of P/3DOMMs to model single and dual infections of *C. albicans* and *S. aureus* in terms of studying tissue colonisation and invasion, and pro-inflammatory cytokine production in response to infection.
4. To explore the proposed synergistic relationship between *C. albicans* and *S. aureus.*

4.3. Methodology

4.3.1. Culture of *C. albicans*

C. albicans was maintained on Sabouraud-dextrose agar (SDA), Sigma Aldrich s3306 and Sigma Aldrich 05040, and subcultured monthly. Prior to use, an overnight culture was created by resuspending a single colony of *C. albicans* in Sabouraud-dextrose broth (SDB), and grown in a 37°C shaking incubator.

4.3.2. Culture of *S. aureus*

S. aureus was maintained on tryptic-soy agar, Sigma Aldrich 22092 and Sigma Aldrich 05040, and subcultured monthly. Prior to use, an overnight culture was created by resuspending a single colony of *S. aureus* in tryptic-soy broth (TSB), and grown in a 37°C shaking incubator.

4.3.3. Quantification of *C. albicans*

Prior to use, *C. albicans* was washed 3 times via centrifugation at 3000 x g for 5 minutes in PBS. Cultures were diluted 1 in 10 and counted using a haemocytometer. Cultures were then set to the desired density (experiment dependent) in cell culture media (experiment dependent). Cultures were stored at 4˚C to prevent growth prior to use.

4.3.4. Quantification of *S. aureus*

Prior to use, *S. aureus* was washed 3 times via centrifugation at 10,000 × g in PBS. *S. aureus* were quantified spectrophotometrically, and an OD of 0.2 at 595 nm was taken to equate to 2×10^7 cfu/ml, as revealed by preliminary experimentation. Cultures were then set to the desired density (experiment

dependent) in cell-culture media (experiment dependent). Cultures were stored at 4˚C to prevent growth prior to use.

4.3.5. Acquisition of patient samples

A statistician was consulted and power calculation was performed in order to predict the number of participants required in order to compare statistical significance of risk factors and microbial carriage between: denture wearing controls, non-denture wearing controls, and denture stomatitis participants. It was determined that a minimum of 20 participants should be recruited per group in order to make an accurate statistical comparison at 95% confidence limits. It was proposed that it would be feasible to collect 30 participant samples per group and therefore 90 participants in total, in order to increase statistical power and permit the possibility of performing a logistic regression analyses. For a smaller sample of data it was proposed that a Chi squared analyses should be used, which only requires at least one positive sample per category. For example, at least one participant from denture wearing controls, non-denture wearing controls, and denture stomatitis participants, would be required to carry *S. aureus* in order to compare the distribution of colonisation across each population. It was predicted that in a sample size of 30 at least one participant would carry each combination of organism, *S. aureus, C. albicans,* and both, due to their reported abundance in the general population and denture wearers (36,37,252). With thanks to Daniel Zahara from the University of Plymouth for statistical assistance.

Ethical approval was obtained from IRAS (ref. 208291) and the University of Plymouth prior to the commencement of the study. Participants were recruited using posters and patient information leaflets, and consent was obtained by

clinicians prior to participation, **appendices 1, 2, 3, 4, 5 and 6**. Participants and clinicians completed a questionnaire each, regarding the participants' oral health, denture wear, and health and lifestyle factors, **appendices 7 and 8**. Swabs, MWE Transwab-Amies MW170, were obtained from participants' hard palates and dentures. Three participants wearing a complete maxillary denture had a swab collected from denture surface and underlying hard palate. Seven participants wearing a partial denture had one swab collected from the denture surface, one swab taken from an area of the hard palate underlying the denture, and one swab taken from an area of the hard palate that does not underlie the denture. Twenty two non-denture wearers had one swab taken from their hard palate, as indicated in **appendix 9**. Exclusion criteria included those under 50 years of age, and those known to be immunosuppressed. Swabs were streaked across the desired area of the oral cavity for 10 seconds and rotated to ensure full coverage of the swab. Swabs were returned to their transport media and processed within 24 hours of collection.

4.3.6. Identification of *C. albicans* from patient samples

Streak plates were performed, using one side of the patient swab, on SDA containing 100 µg/ml chloramphenicol, in order to reduce isolation of undesired organisms. Plates were incubated at 37˚C for 48 hours. Colonies were assessed morphologically, and those indicative of *Candida spp.* were counted and their abundance recorded. Positive isolates were then struck onto chromogenic agar, OXOID CM1002, for further identification. Chromogenic agar plates were incubated for 48 hours at 37˚C and examined by eye. Green colonies were indicative of *C. albicans* or *C.dubliniensis*. *C. albicans* is the most likely organism due to its higher prevalence in the oral cavity, however in order to confirm,

samples were further identified through PCR using forward 5' "TTT ATC AAC TTG TCA CAC CAG A" 3' and reverse 5' "ATC CCG CCT TAC CAC TAC CG" 3' primers as detailed in section 2.10.

4.3.7. Identification of *S. aureus* from patient samples

Streak plates were performed using the reverse side of the swab used in section 4.3.6 on mannitol salt agar (MSA), OXOID CM0085, which is selective for bacteria that can grow within high salt concentrations. Subsequent plates were incubated at 37˚C for 24 hours. Visual identification of colonies was used to determine potential *S. aureus* isolates, and were counted and their abundance recorded. Colony morphology was observed; a golden appearance, and the fermentation of the MSA revealing a yellow colour, were taken to be indicative of an *S. aureus* isolate. Suspected isolates were confirmed to be *S. aureus* through subsequent coagulase and catalase biochemical tests.

4.3.8. Sample recording and data analysis

Patients were anonymised with a participant identification number. Upon receipt of samples and patient questionnaires, all data from the same participant was ensured to be catalogued by their participant information number, for further data analysis. Of interest was the frequency of single and dual isolation of *C. albicans* and *S. aureus* from the entire cohort, denture wearers, control patients, and DS sufferers. Of the entire cohort, only one diagnosed DS sufferer was encountered, therefore data were separated into either denture wearing or non-denture wearing control groups. Subsequent patient samples were used for infection of HaCaT monolayers and P/3DOMMs.

4.3.9. Single and dual infections of HaCaT monolayers with *C. albicans* and *S. aureus*

HaCaT cells were seeded in a T25 flask and grown until confluent. Overnight cultures of the type strains *C. albicans* SC5314, and *S. aureus* SA5025 were washed 3 times in PBS and set at an MOI of 0.1. Flasks were then incubated at 37°C in a humidified 5% CO_2 incubator. The co-cultures and uninfected control wells were imaged at 0, 1, 2, 4, 7, 12, 18 and 24 hours.

4.3.10. HaCaT cell dose response of single and dual infections of *C. albicans* and *S. aureus*

HaCaT cells were seeded at a density of 2.5×10^5 and grown until confluent at 37°C in a humidified 5% CO_2 incubator. *C. albicans* CASC5314 and *S. aureus* 116 were cultured in SDB, and TSB, respectively. Prior to use, *C. albicans* and *S. aureus* were washed 3 times via centrifugation in PBS. *C. albicans* was quantified using a haemocytometer. *S. aureus* was quantified spectrophotometrically. Both organisms were then set to a count of 5×10^5 CFU/ml (MOI 1), and 5×10^4 CFU/ml (MOI 0.1) in DMEM + 10% FBS. Control wells contained media only, 1 ml of each organism in DMEM + 10% FBS was added to each single infection well, for dual infection 0.5 ml of each organism was added to the same well, at the desired MOI. Organisms were co-cultured with HaCaT cells for 24 hours, and supernatant collected for subsequent ELISA analyses.

4.3.11. Infection of 3DOMMs and P3DOMMs

3DOMMs were grown until day 19, and P3DOMMs until day 14 (as previously described), and then infected with *C. albicans* SC5314 MOI 0.1 (1×10^5 CFU/ml), *S. aureus* P116 MOI 1 (1×10^6 CFU/ml), and both *C. albicans* and *S. aureus* MOI 0.05 and MOI 0.5, respectively. For 3DOMMs organisms were introduced in DMEM + 10%FBS, whereas for P3DOMMs organisms were introduced in POKM. Models were co-cultured with the infective agents for 24 hours prior to fixation. Models were fixed in 2.5% glutaraldehyde, and cut into quarters, two of which were processed for histology, and two of which were processed for electron microscopy. Histology and electron microscopy methodology are detailed in section 2.5 and section 2.7.3, respectively. Supernatants were also collected for analysis of pro-inflammatory cytokine production by ELISA and stored at -20˚C until required. Data were standardised to a percentage of the control for each repeat.

4.3.12. Histology time-course of *S. aureus* infection

3DOMMs were grown for 19 days and infected with MOI 1 (1×10^6 CFU/ml) of *S. aureus* 116 in DMEM + 10%FBS. Models were fixed at 24, 48, and 72 hours and processed for histology and subsequent imaging.

4.3.13. Single and dual infections of HaCaT monolayers with clinical isolates

Different combinations of patient samples, and type strains, were added to HaCaT cells to compare isolates obtained from patients with single and dual colonisation of *S. aureus* and *C. albicans*. *S. aureus* was added at an MOI of 1,

whereas *C. albicans* was added at an MOI of 0.1. Microbes were cultured atop a confluent HaCaT monolayer for 24 hours and supernatant analysed by ELISA. Data were standardised to a percentage of the control for each repeat.

4.3.14. Data analysis and statistics

Statistical analyses are indicated in the results section, in the figure legend for each experiment, including which statistical tests were performed, and the number of experimental repeats. For all ELISA data, as standard a minimum of three independent experimental repeats, containing three biological replicates were performed, unless stated otherwise. For each biological replicate, a minimum of 2 technical replicates were performed. Also indicated in the figure legend is which groups were compared, if this is not stated then a comparison was made between all groups in a given graph. To select the appropriate statistical test, using GraphPad, a Shapiro-wilk test for normality was performed to determine data normality of all groups intended to be statistically compared. Parametric data was assessed with the use of a one-way ANOVA, followed by a Tukey's multiple comparisons test. Non-parametric data was assessed using a Kruskal-Wallis test followed by a Dunn's multiple comparisons test. For all, *p*-values lower than 0.05 were taken to indicate statistical significance.

4.4. Results

4.4.1. Confirmation of *C. albicans* and *S. aureus* within patient samples

A total of 32 participants were recruited, with a mean age of 67, 47% were female, and 53% male. Ten participants wore maxillary dentures, 7 of which wore a partial prosthesis and 3 of which wore a complete prosthesis. The remaining 22 participants were non-denture wearing controls. Acrylic dentures were the most common, 2 patients wore chrome-cobalt-containing dentures. As the cohort was small, the data collected was insufficient to statistically identify potential risk factors associated with DS, and *C. albicans* and *S. aureus* carriage.

Participant swabs were screened for *C. albicans* and *S. aureus,* through the use of selective media and visual identification of phenotypic traits that are characteristic of the colonies for each species. Following this, suspected *C. albicans* isolates were confirmed using chromogenic agar, and subsequent PCR, **Figure 23**. *S. aureus* isolates were confirmed by their ability to ferment mannitol, forming yellow colonies on MSA, as well as coagulase positive and catalase positive biochemical tests.

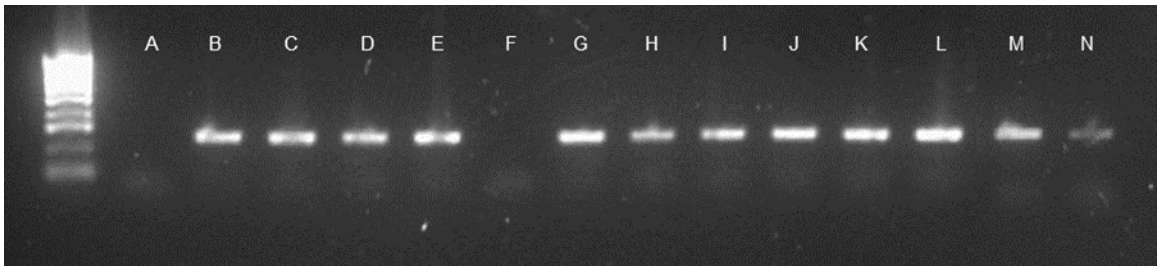

Figure 23: PCR confirmation of *C. albicans* isolation from patient samples
Confirmation of patient samples of *C. albicans* through PCR. D = denture, PUD = palate under denture, PNUD = palate not under denture, C = control patient. A: No template control, B: Positive control (SC5314), C: 120PUD, D: 301D, E: 5018, F: 301PUD, G: 116D, H: 217C, I: 202C, J: 120D, K: 216C, L: 204C, M: 120PNUD, N: 301PNUD.

All patient samples that indicated green colonies on chromogenic agar were confirmed to be *C. albicans* by PCR, with the exception of 301PUD. Therefore, 10 isolates of *C. albicans* were obtained from patient samples, 7 of which were from different participants. Of all suspected *Staphylococcus* isolates, only one was confirmed to be *S. aureus,* 116 PUD, the remaining 7 were found to be coagulase negative *Staphylococci.*

Table 11: Single *C. albicans* and *S. aureus* carriage, and dual carriage of both organisms within non-denture wearers and denture wearers.
Swabs were taken from the palate of control participants (n = 22*)* and both the palate and denture surface of denture wearers (n = 10). For participants with a partial denture, swabs were taken from the prosthesis, an area of the hard palate under the denture (PUD), and an area of the hard palate not covered by the denture (PNUD). Percentage (%) and number (#) refers to the carriage of each individual group.

Organism		**Non-denture wearers n = 22**	**Denture-wearers n = 10**			
		Oral mucosa	**Oral mucosa**	**PUD n=10**	**PNUD n=7**	**Prosthesis**
C. albicans	#	4	2	1	2	3
	%	18.2%	20%	10%	28.6	30%
S. aureus	#	0	1	1	0	0
	%	0%	10%	10%	0%	0%
Both	#	0	0	0	0	0
	%	0%	0%	0%	0%	0%
Neither	#	18	7	8	5	7
	%	81.8%	70%	80%	71.4%	70%

Of the entire cohort, only 1 participant was found to be carrying *S. aureus*, of which the same participant was also found to be carrying *C. albicans* (isolated from different sites, the palate and denture, respectively). This accounts for 3.13% of the total cohort, and 10% of the denture-wearing cohort. Seven participants in total were found to be carrying *C. albicans,* accounting for 21.88% of the total cohort. The percentage of single and dual carriage within non-denture

wearing and denture wearing participants is indicated in **Table 11**. Some participants indicated carriage of *C. albicans* in more than one area, for example on the denture, hard palate under the denture, and on an area of their hard palate that was not covered by a partial denture plate. The isolation of *C. albicans* and *S. aureus* from each area is also indicated in **Table 11**. As well as identifying the proportion of carriage within denture wearing and non-denture wearing participants, the isolation of oral samples of *C. albicans* and *S. aureus* provided clinically relevant patient samples, for which to implement in further study.

4.4.2. The effect of single and dual infections of *C. albicans* and *S. aureus* on an epithelial monolayer

Initially, *C. albicans* and *S. aureus* were added to monolayers of HaCaT cells, in order to study the morphology of the microbes and the response of underlying cells, during single and dual infections, **Figure 24**. The control cells experienced no change in morphology of the monolayer over the 24 hour time course. *C. albicans* alone presented at 0 hours as few singular yeast cells. By 1 hour, small islands of *C. albicans* hyphae had formed. These hyphal elements continued to multiply, and covered the majority of the field of view from 12 hours onwards; up until the 24-hour time point an intact epithelium could be observed below the hyphal structures. *S. aureus* initially could not be observed due to its relatively small size in relation to the HaCaT monolayer. At 4 hours, clusters of *S. aureus* could be observed, and from 7 hours onwards, the monolayer displayed signs of damage through lifting of the HaCaT cells. At 12 hours, the cellular boundaries became unclear. From 18 hours onwards, the HaCaT monolayer had lifted from the surface of the culture flask and cells were no longer intact. Dual infection with *C. albicans* and *S. aureus* began with only a few singular yeast cells visible. At

the 2 and 4 hour time-points, *C. albicans* appeared as clusters of both its yeast and hyphal forms, with *S. aureus* appearing amongst this. From this point onwards *C. albicans* presence was less obvious. At 18 hours, few elongated hyphae were observable over a hazy monolayer of epithelial cells with unclear boundaries. At 24 hours the HaCaT monolayer had lifted, and appeared entwined with *C. albicans* hyphae and *S. aureus.*

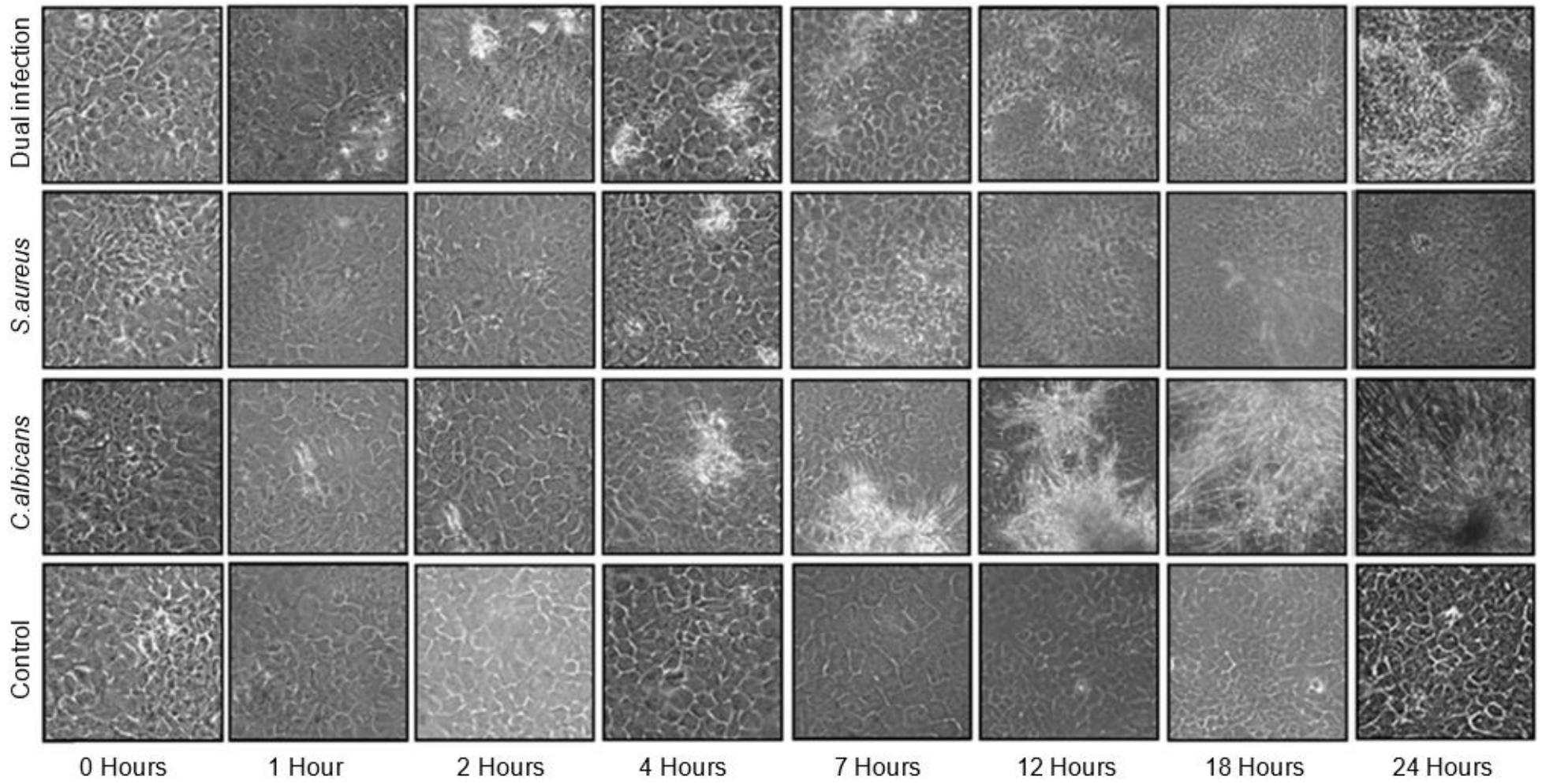
Dual infection
S.aureus
C.albicans
Control
0 Hours
1 Hour
2 Hours
4 Hours
7 Hours
12 Hours
18 Hours
24 Hours

Figure 24: HaCaT monolayer time-course with single and dual infections of *C. albicans* and *S. aureus.*
From previous page: a representative sample of an infection time-course (0-24 hours) of a HaCaT monolayer cultured with single and dual infections *C. albicans* SC5314 and *S. aureus* 116*,* as well as a non-infected control. Images were taken at 200× magnification over a 24 hour period.

4.4.3. The effect of single and dual infections of *C. albicans* and *S. aureus* on P/3DOMM morphology

After studying the effect of single and dual infections on a HaCaT monolayer, 3DOMMs were employed for the same purpose. The same models were used to produce histology and electron microscopy sections; subsequently, tissue morphology and microbial invasion were observed, **Figure 25** and **Figure 26** . A control model was produced that displayed a multi-layered intact epithelium, which upon visualisation did not appear keratinised. Fibroblasts appeared abundant within the lamina propria, and the epithelium and lamina propria were anchored together, with no observed separation. Models infected with *C. albicans* alone presented as a layer of hyphae atop the epithelial layer, **Figure 25**. There was no clear evidence of *C. albicans* hyphal invasion into the epithelium as a result of single *C. albicans* infection, in this case. *S. aureus* was present within the lamina propria layer, and appeared to line the cavities present within the tissue structure. For dual infections, *C. albicans* and *S. aureus* were present atop the epithelium and within the lamina propria layer. *C. albicans* formed a layer at the upper most of the section, above the epithelium. *S. aureus* appeared throughout the *Candida* layer, in clusters. Upon dual infection, *C. albicans* hyphae was observed within the epithelium. Electron-micrograph images, **Figure 26**, indicated *S. aureus* within the lamina propria area of the tissue. *C. albicans*

hyphae were shown to be penetrating the tissue of a disorganised epithelium. *C. albicans* was present in both its yeast and hyphal forms. **Figure 27** displays a length of 3DOMM infected with both *C. albicans* and *S. aureus. C. albicans* appeared to span the entire epithelium, with *S. aureus* entrapped underneath. *S. aureus* is only visible when in clusters due to its size. The layer of *C. albicans* hyphae varied in thickness. *C. albicans* hyphae appeared to penetrate the epithelium, as indicated.

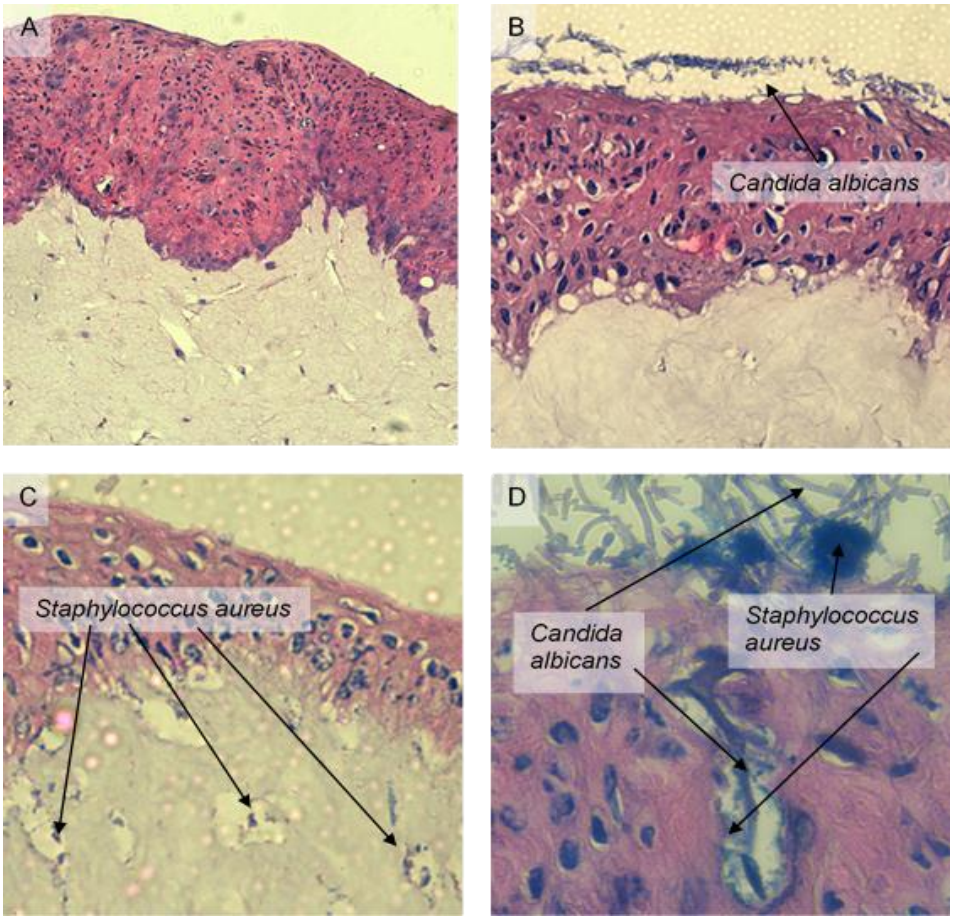

Figure 25: **Histology of 3DOMMs single and dual infections with *C. albicans* and *S. aureus***

A representative sample of paraffin embedded, 4 µm sectioned, haematoxylin and eosin stained 3DOMMs infected with *C. albicans* (MOI 0.1), *S. aureus* (MOI 1) and both (MOI 0.05 and 0.5, respectively). Models imaged are the same models as used for TEM. Image A displays a control model (100 X magnification), in absence of any infection. Image B displays a model infected with *C. albicans* (200 X magnification). Image C displays a model infected with *S. aureus* (200 X magnification). Image D displays a model infected with both *C. albicans* and *S. aureus* (400 X magnification). Magnifications between A, B, C and D vary in order to display the microbial interactions with the tissue.

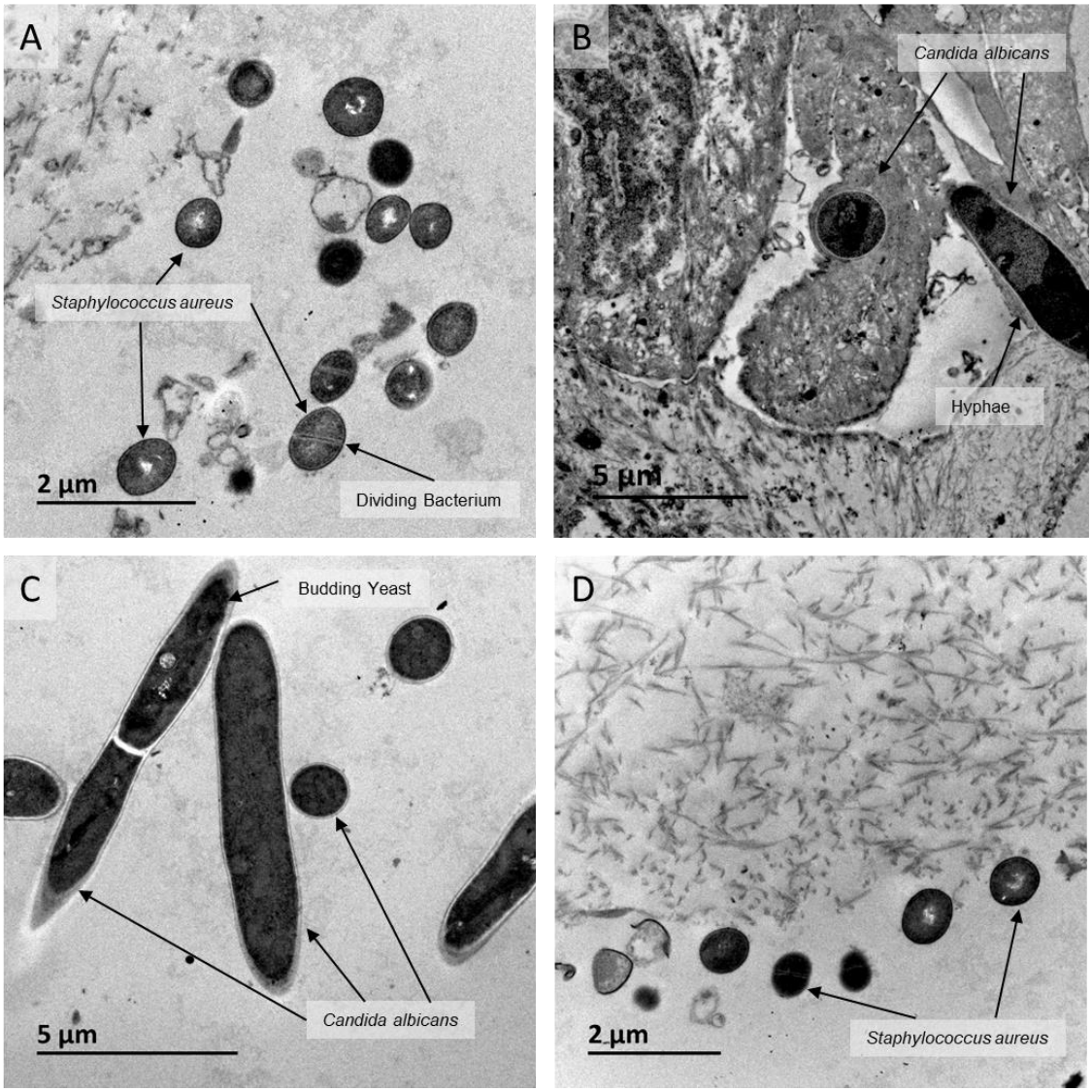

Figure 26: Transmission electron microscopy images of *C. albicans* and *S. aureus*. Both were directly seeded onto the 3DOMM at day 19 of culture and co-cultured for 24 hours prior to fixation and processing for TEM. Image A displays a collection of *S. aureus* bacteria including a dividing bacterium. Image B displays both the yeast and hyphal form of *C. albicans* situated within the 3DOMM towards the epithelial surface. Image C displays *C. albicans* in yeast and hyphal form, including a budding cell, situated above the epithelium (not in field of view). Image D displays *S. aureus* bacteria situated above the lamina propria layer of the 3DOMM. With thanks to Glenn Harper of the University of Plymouth's electron microscopy suite for his technical support in retrieving these images.

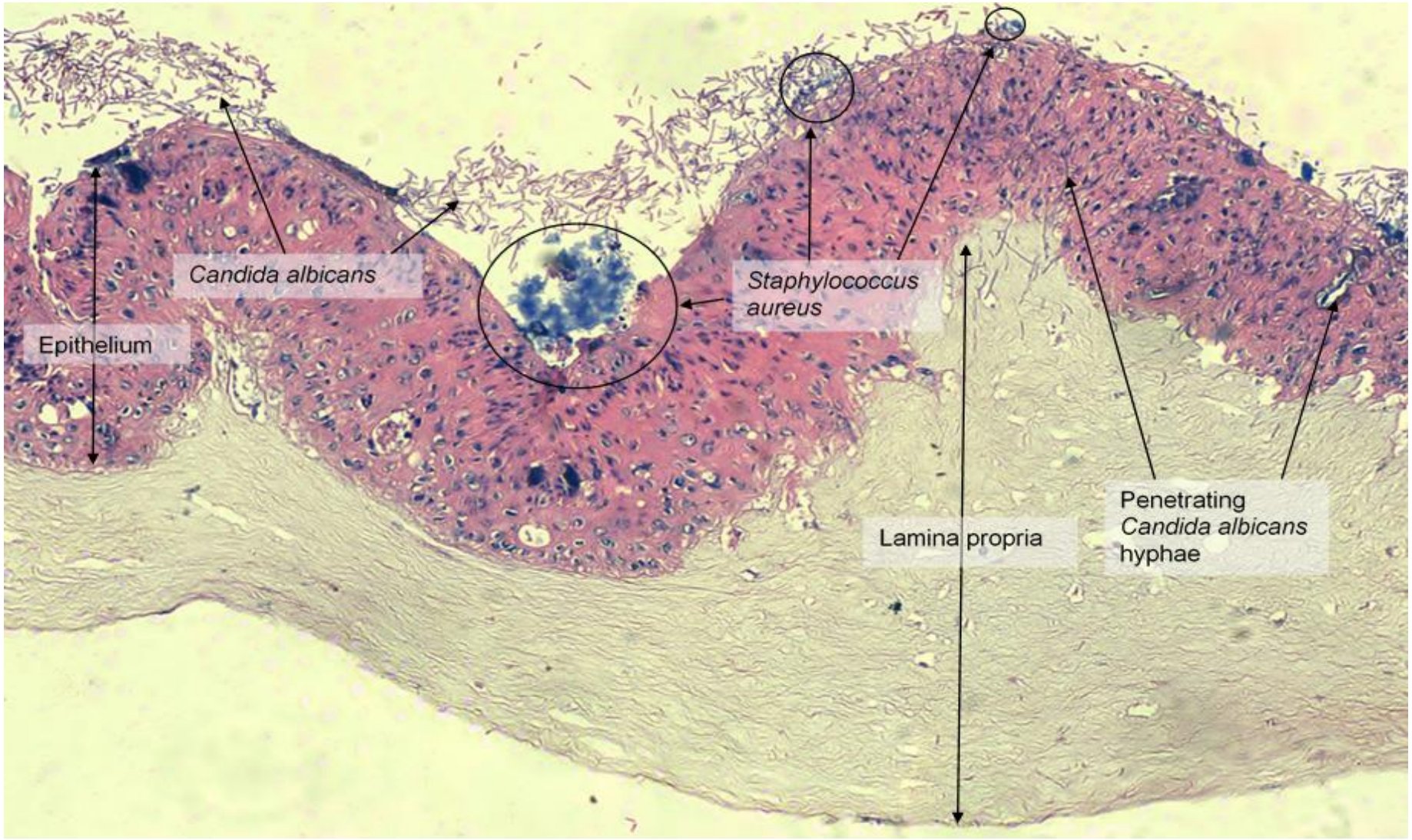
Candida albicans
Staphylococcus aureus
Epithelium
Lamina propria
Penetrating Candida albicans hyphae

Figure 27: Histology of 3DOMM dual species infection with *C. albicans* and *S. aureus*

From previous page: a haematoxylin and eosin stained, paraffin embedded, 4 µm sectioned, 3DOMM infected with *C. albicans* (MOI 0.05) and *S. aureus* (MOI 0.5) (100 X magnification). The model was infected at day 19 for a duration of 24 hours.

There was no apparent epithelial damage caused to any of the infected 3DOMMs observed so far. These models were co-cultured with the corresponding microbes for 24 hours. Considering the destruction of the monolayer of epithelial cells by *S. aureus* observed within **Figure 24**, it was proposed that upon longer co-culture with *S. aureus,* epithelial damage was likely to occur. **Figure 28** indicates the effect of culturing *S. aureus* with 3DOMMs for 24, 28 and 72 hours. The 3DOMMs created for this n = 1 study did not appear to have an intact epithelium in any of the models (wherever possible, a representative sample of the epithelium was selected for display in **Figure 28**). For this reason, it is not possible to deduce whether the lack of an epithelium within the 48 and 72 hour time points are due to *S.aureus* invasion and destruction, or due to the tissue morphology itself prior to introducing the infective agent. Nevertheless, at 72 hours there appears to be evidence of large globules of nuclear material that may be indicative of cell death.

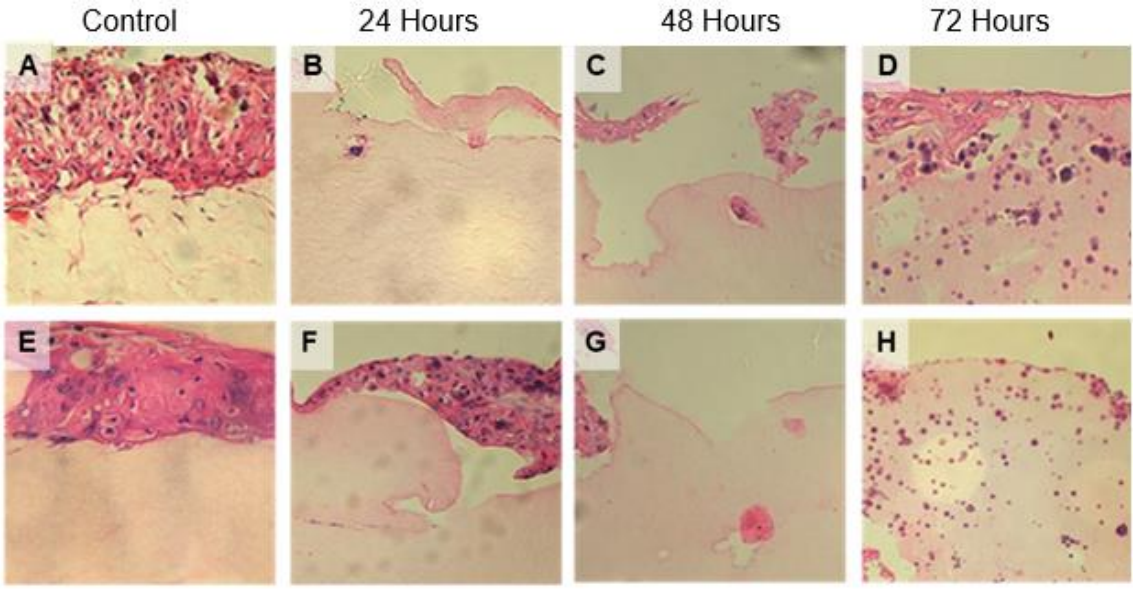

Figure 28: Histology of 3DOMMs infected with *S. aureus* for 24, 48 and 72 hours
Haematoxylin and eosin stained, paraffin embedded, 4 µm sectioned, 3DOMM infected with *S. aureus* (MOI 1) (200 X magnification). Bacteria were added to the models at day 19 of model growth and co-cultured for 24, 48, or 72 hours prior to fixation. Images displayed are representative samples of one experimental repeat performed in duplicate, Control (A and E), 24 hours of infection (B and F), 48 hours of infection (C and G) and 72 hours of infection (D and H).

Finally, to compare the HaCaT-based 3DOMMs with the use of primary oral keratinocytes for modelling infection, P3DOMMs were infected with single and dual infections of *C. albicans* and *S. aureus* **Figure 29**. As observed within Chapter 3, **Figure 29** indicated the presence of a broken epithelium, presenting within enlarged epithelial cells, with gaps between. Fibroblasts appeared throughout the lamina propria layer. *C. albicans* alone appeared to form a hyphal layer above an intact epithelium. Infection with *S. aureus* alone indicated a broken epithelium containing clusters of *S. aureus*, and fragments of epithelial cells amongst intact yet dysmorphic cells. Amongst the disjointed epithelial cells of the dual-species infected P3DOMM, a mix of *C. albicans* and *S. aureus* were abundant. *S. aureus* appeared in clusters alone, and associated with *C. albicans*

hyphae. Both organisms appeared closely associated with each other and the epithelial cells.

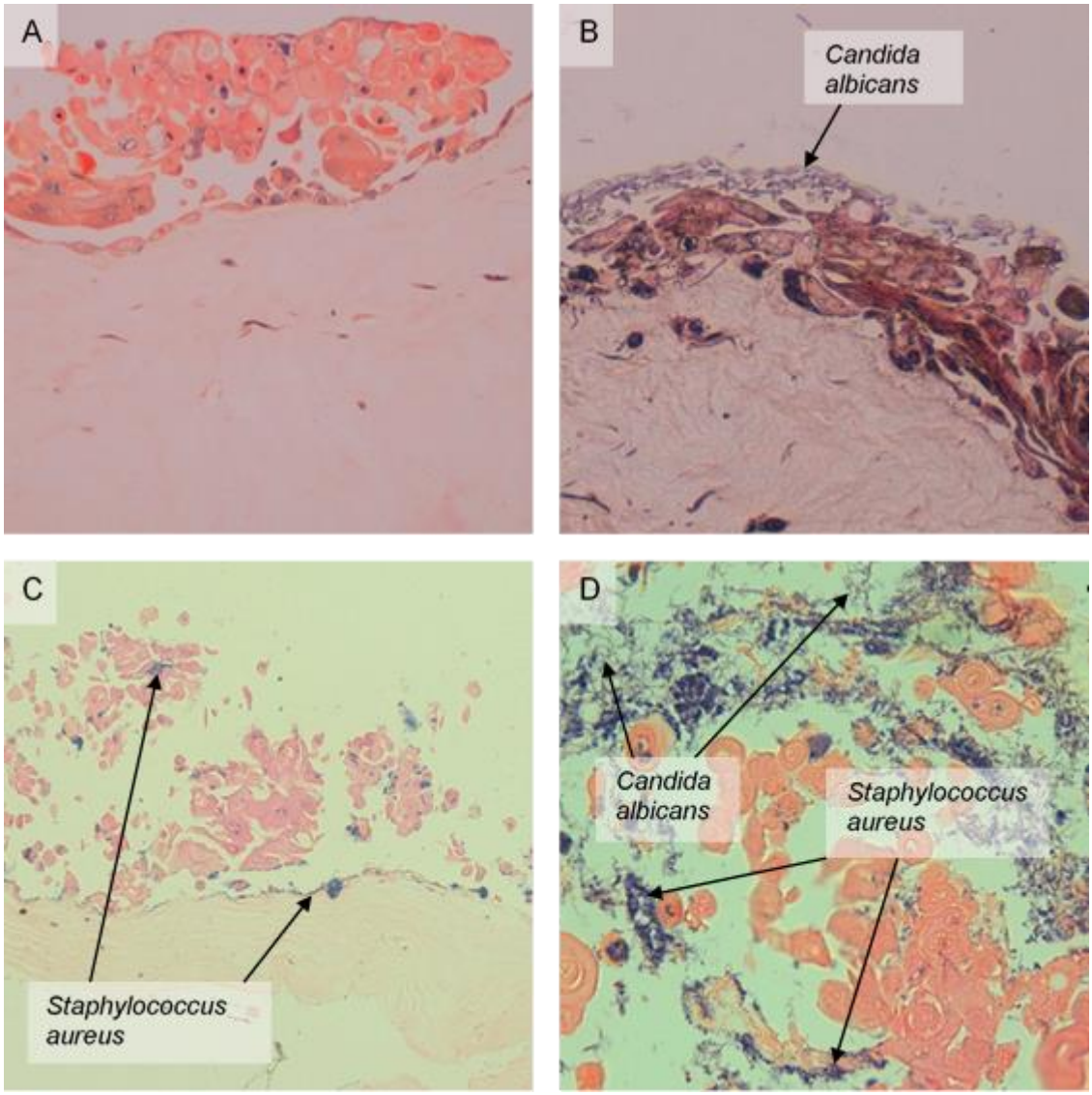

Figure 29: Histology of P3DOMM infection with single and dual species infection with *C. albicans* and *S. aureus*

A representative sample of paraffin embedded, 4 µm sectioned, Haematoxylin and eosin stained P3DOMMs infected at day 14 of model culture for 24 hours with *C. albicans* (MOI 0.1), *S. aureus* (MOI 1) and both (MOI 0.05 and 0.5, respectively). Image A displays a control model, in absence of any infection (200 X magnification). Image B displays a model infected with *C. albicans* (200 X magnification). Image C displays a model infected with *S. aureus* (100 X magnification). Image D displays a model infected with both *C. albicans* and *S. aureus* (400 X magnification).

4.4.4. Pro-inflammatory cytokine production by HaCaT monolayers in response to single and dual species infection

The capability of *C. albicans* and *S. aureus* to induce the production of pro-inflammatory cytokines IL-6 and IL-8 within HaCaT cells and P/3DOMMs were assessed. Firstly, a dose response was performed to determine an appropriate infective dose of *C. albicans* and *S. aureus* to introduce to HaCaT monolayers, in terms of MOI, **Figure 30**.

S. aureus at an MOI of 1 and 0.1 led to significantly more IL-6 production in HaCaT cells when compared to the unstimulated control, ($p = 0.0021$ and $p < 0.0001$, respectively for each MOI). *C. albicans* at an MOI of 1 and 0.01 also led to significantly more IL-6 production than the unstimulated control ($p < 0.0001$ for both MOIs). Dual infections of *C. albicans* and *S. aureus* at an MOI of 1 and 0.1 also led to an increase in IL-6 production when compared with the control ($p < 0.0001$ and $p = 0.0249$, respectively for each MOI).

S. aureus at an MOI of 1 and 0.1 led to a significant increase in IL-8 secretion by HaCaT cells, when compared to the unstimulated control ($p < 0.0001$ for both MOIs). *C. albicans* at an MOI of 1 and 0.1 also led to a significant increase in IL-8 production when compared to the unstimulated control ($p < 0.0001$ and $p = 0.0010$, respectively for each MOI). Furthermore, a significant increase in IL-8 production was observed when cells were stimulated with dual infections of both organisms, at either MOI, when compared to the unstimulated control ($p < 0.0001$ for both).

Statistical significance was also assessed between HaCaT cells introduced to *S. aureus* at an MOI of 0.1 and 1, *C. albicans* of an MOI of 0.1 and 1, and each individual organism with dual infections of both organisms at all concentrations. *S. aureus* at an MOI of 0.1 led to significantly more IL-8 production by HaCaT cells than when cells were stimulated with both organisms at an MOI of 1 or 0.1 ($p = 0.0002$ and $p < 0.0001$, respectively).

These data revealed the potential for a highly significant upregulation in both IL-6 and IL-8 pro-inflammatory cytokine production, upon infection of HaCaT cells with single and dual infections of *C. albicans* and *S. aureus* at either MOI. The lower dose of MOI 0.1 was carried forward for subsequent monolayer interaction studies.

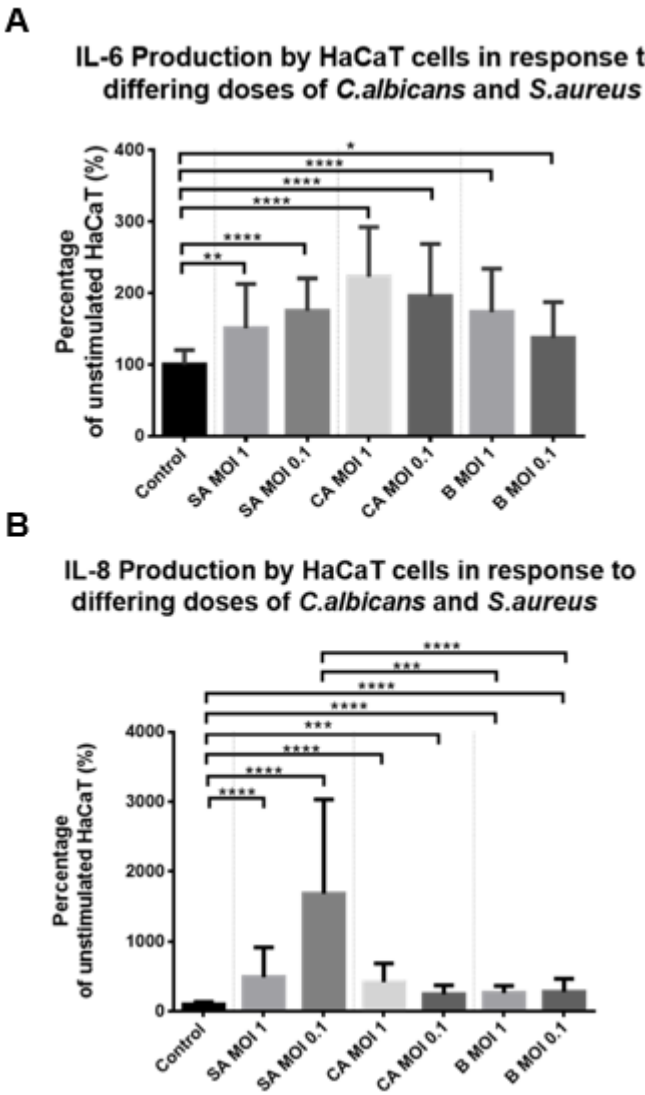

Figure 30: Pro-inflammatory cytokine production by HaCaT cells in response to different doses of *C. albicans* and *S. aureus*

IL-6 (A) and IL-8 (B) pro-inflammatory cytokine production by HaCaT cells infected with *C. albicans* (CA), *S. aureus* (SA), and both *C. albicans* and *S. aureus* (B). Graphs indicate three experimental repeats performed in triplicate. HaCaT cells were co-cultured with the infective organism for 24 hours, and cytokine production assessed via Sandwich ELISA. X-axis labels indicate the infective organism/s followed by the infective dose. Significant differences in cytokine production were compared between the control group and all test groups, between differing doses of the same organism, and between each individual organism and dual infections of both organisms. Data normality was assessed using the Shapiro-Wilk test for normality. Data is standardised to a percentage of the control. Statistical significance was determined using a Kruskal-Wallis test followed by a Dunn's multiple comparisons test. Statistical significance is indicated on the graph (* $p < 0.05$, ** $p < 0.01$, *** $p < 0.001$, **** $p < 0.0001$). Error bars represent standard deviation.

Next, HaCaT cells were infected with single and dual infections of *C. albicans* and *S. aureus* at an MOI of 0.1, **Figure 31**. IL-6 data is not displayed as all data

were below the ELISA detection range. There was a significant increase in IL-8 production by HaCaT cells stimulated with *C. albicans*, *S. aureus,* and both when compared to the unstimulated control ($p < 0.0001$ for all). However, there was no significant difference in IL-8 production between the different infective agents.

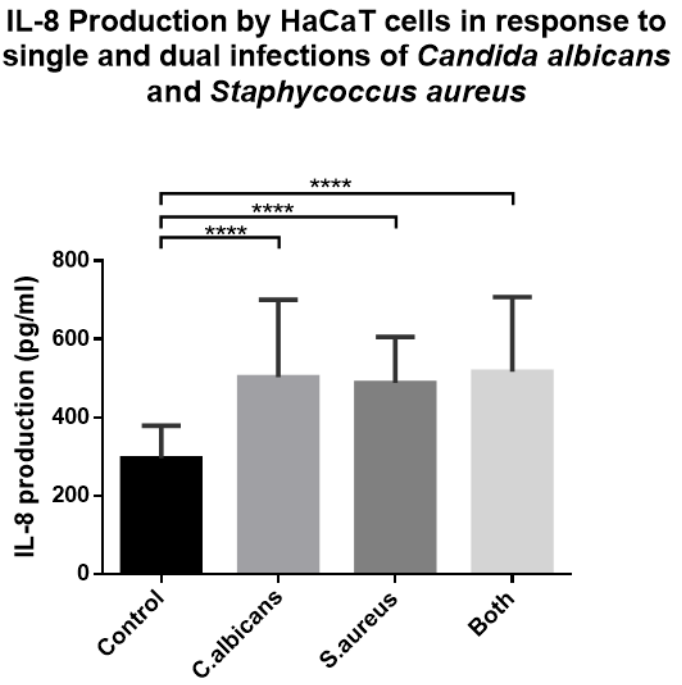

Figure 31: HaCaT response to single and dual infections of *C. albicans* and *S. aureus*

HaCaT IL-8 pro-inflammatory cytokine production infected with single and dual infections of *C. albicans* SC5314 and *S. aureus* 116. Graphs indicate seven experimental repeats, performed in triplicate. HaCaT cells were co-cultured with the infective organisms for 24 hours, and cytokine production assessed via Sandwich ELISA. Significant differences in cytokine production were compared to every other group. Data normality was assessed using the Shapiro-Wilk test for normality. Statistical significance was determined using a one-way ANOVA followed by a Tukey's multiple comparison's test. Statistical significance is indicated on the graph (* $p < 0.05$, ** $p < 0.01$, *** $p < 0.001$, **** $p < 0.0001$). Error bars represent standard deviation. IL-6 data was omitted as all data were found to be below range of the ELISA standard curve. Error bars represent standard deviation.

4.4.5. Pro-inflammatory cytokine production by P/3DOMMs in response single and dual species infection

As HaCaT cells were proven able to produce pro-inflammatory cytokines in response to live infective agents, it was hypothesised that 3DOMMs would also be responsive. Chapter 3 indicated the constitutively high level of pro-inflammatory cytokine production by the 3DOMM. This section therefore aimed to determine whether the 3DOMM was able to upregulate pro-inflammatory cytokine production in response to infective agents, or whether the high level of constitutive expression rendered the model ineffective to study upregulation of pro-inflammatory cytokine (IL-6 and IL-8) release.

For 3DOMMs, infection of *C. albicans* was performed at an MOI of 0.1, and *S. aureus* at an MOI of 1, to more accurately represent the proportion of organisms that would be identified in active infection *in vivo.* For infection with both organisms, half of each dose was added to the models.

Compared with the unstimulated control, 3DOMM infection with *C. albicans,* or *S. aureus,* or dual infections of both microbes led to a significant increase in IL-6 and IL-8 production ($p = 0.0013$, $p = 0.0071$ and $p = 0.0015$ for IL-6, and $p < 0.0001$, $p = 0.0001$ and $p = 0.0314$ for IL-8, respectively). There was no significant difference in 3DOMM IL-6 and IL-8 production, between single infections with *C. albicans,* or *S. aureus,* or dual infections with both organisms, **Figure 32.**

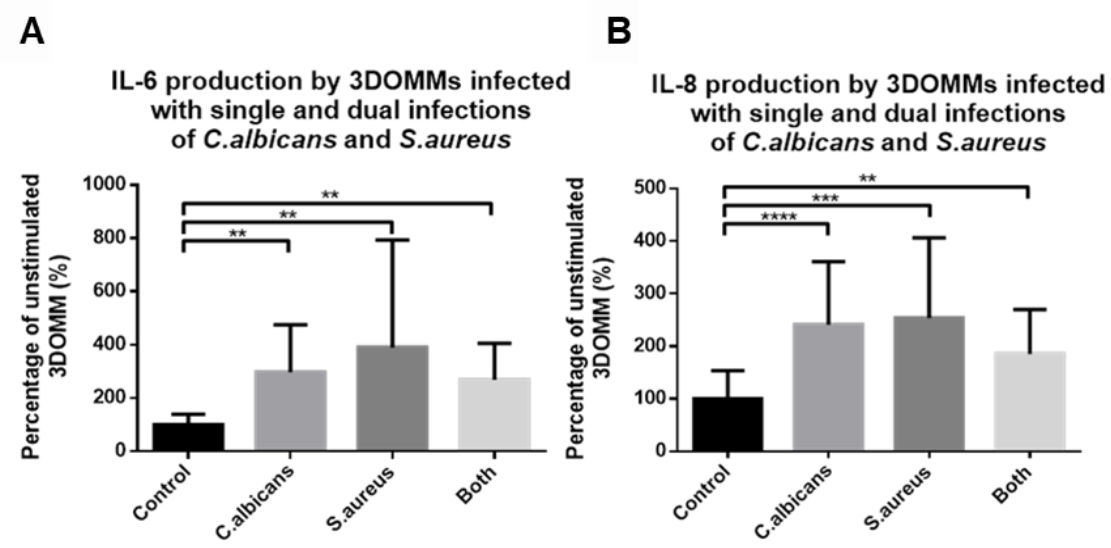

Figure 32: 3DOMM response to single and dual infections of *C. albicans* and *S. aureus*

IL-6 (A) and IL-8 (B) pro-inflammatory cytokine production by 3DOMMs infected with single and dual infections (Both) of *C. albicans* SC5314 MOI 0.1 and *S. aureus* P116 MOI 1. Graphs indicate three experimental repeats performed in triplicate. 3DOMMs were co-cultured with the infective organisms for 24 hours, and cytokine production assessed via Sandwich ELISA. Significant differences in cytokine production were compared to the every other group. Data normality was assessed using the Shapiro-Wilk test for normality. Statistical significance was determined using a Kruskal-Wallis test followed by a Dunn's multiple comparisons test. Statistical significance is indicated on the graph (* $p < 0.05$, ** $p < 0.01$, *** $p < 0.001$, **** $p < 0.0001$). Error bars represent standard deviation.

P3DOMMs were also infected with single and dual infections of *C. albicans* and *S. aureus* in the same manner as the 3DOMM. Infection of P3DOMMs with *C. albicans,* or *S. aureus,* or dual infections of both, led to significantly more IL-6 production by 3DOMMs than when unstimulated ($p < 0.0001$, $p = 0.0011$ and p = 0.452, respectively). P3DOMMs infected with *C. albicans,* or *S. aureus,* or both, indicated no significant difference in IL-8 production between the unstimulated control and P3DOMMs infected with any combination of microbes. Interestingly, despite the lack of significant difference in IL-8 production between the unstimulated control and infected groups, infection with *C. albicans* alone led to

significantly more IL-8 production by P3DOMMs than infection with *S. aureus* or both (p = 0.0002, and p = 0.0234, respectively), **Figure 33**.

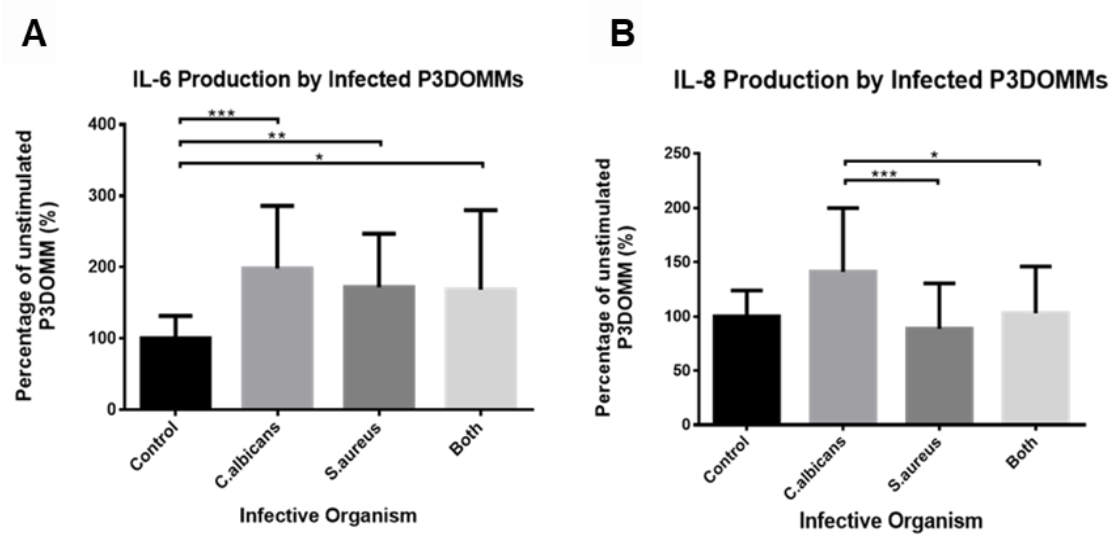

Figure 33: P3DOMM response to single and dual infections of C. albicans and S. aureus

Pro-inflammatory cytokine production, IL-6 (A) and IL-8 (B) , by P3DOMMs infected with single and dual infections (Both) of *C. albicans* SC5314 MOI 0.1 and *S. aureus* P116 MOI 1. Graphs indicate three experimental repeats performed in triplicate. P3DOMMs were co-cultured with the infective organisms for 24 hours, and cytokine production assessed via Sandwich ELISA. Significant differences in cytokine production were compared to the every other group. Data normality was assessed using the Shapiro-Wilk test for normality. Statistical significance was determined using a Kruskal-Wallis test, followed by a Dunn's multiple comparisons test. Statistical significance is indicated on the graph (* $p < 0.05$, ** $p < 0.01$, *** $p < 0.001$, **** $p < 0.0001$). Error bars represent standard deviation.

4.4.6. Single and dual species infection of HaCaT monolayers with *C. albicans* and *S. aureus* patient samples

Patient isolates of *C. albicans* and *S. aureus* were utilised by co-culture with HaCaT cells, in order to determine whether the lack of significant difference observed in pro-inflammatory cytokine production, between single and dual

infection of both organisms, was observed across multiple isolates. The type strains *C. albicans* SC5314 and *S. aureus* 1555 were used as control strains due to their well characterised virulence. Isolates obtained from patients were also utilised. Two isolates were selected because they were obtained from a patient with dual species colonisation (*C. albicans* 116 and *S. aureus* 116). Strains were co-cultured in isolation, and in combination with strains of the other species. This was to test the hypothesis that there would be a variation in pro-inflammatory cytokine production between single and dual species infection.

Single and dual infections of CASC5314 and SA1555, CASC5314 and SA116, CA116 and SA1555, and CA116 and SA116, indicated no significant difference in IL-6 production by HaCaT cells, between single and dual infections of any combination, nor between infection with any of the organisms and the unstimulated control, **Figure 34**.

Similarly, single and dual infections of CASC5314 and SA1555, CA116 and SA1555, and CA116 and SA116, caused no significant difference in IL-8 production by HaCaT cells, between single and dual infections of any combination, nor between infection with any of the organisms and the unstimulated control. However, there was a significant difference in IL-8 production between single infection of HaCaT cells with CASC5314, and dual infection with CASC5314 and SA116, whereby a significant decrease in IL-8 production was observed upon dual infection, compared with single infection of CASC5314. Despite this significance, there was still no significant difference in IL-8 production between the unstimulated control, and HaCaT cells infected with CASC5314 and/or SA116, **Figure 35**.

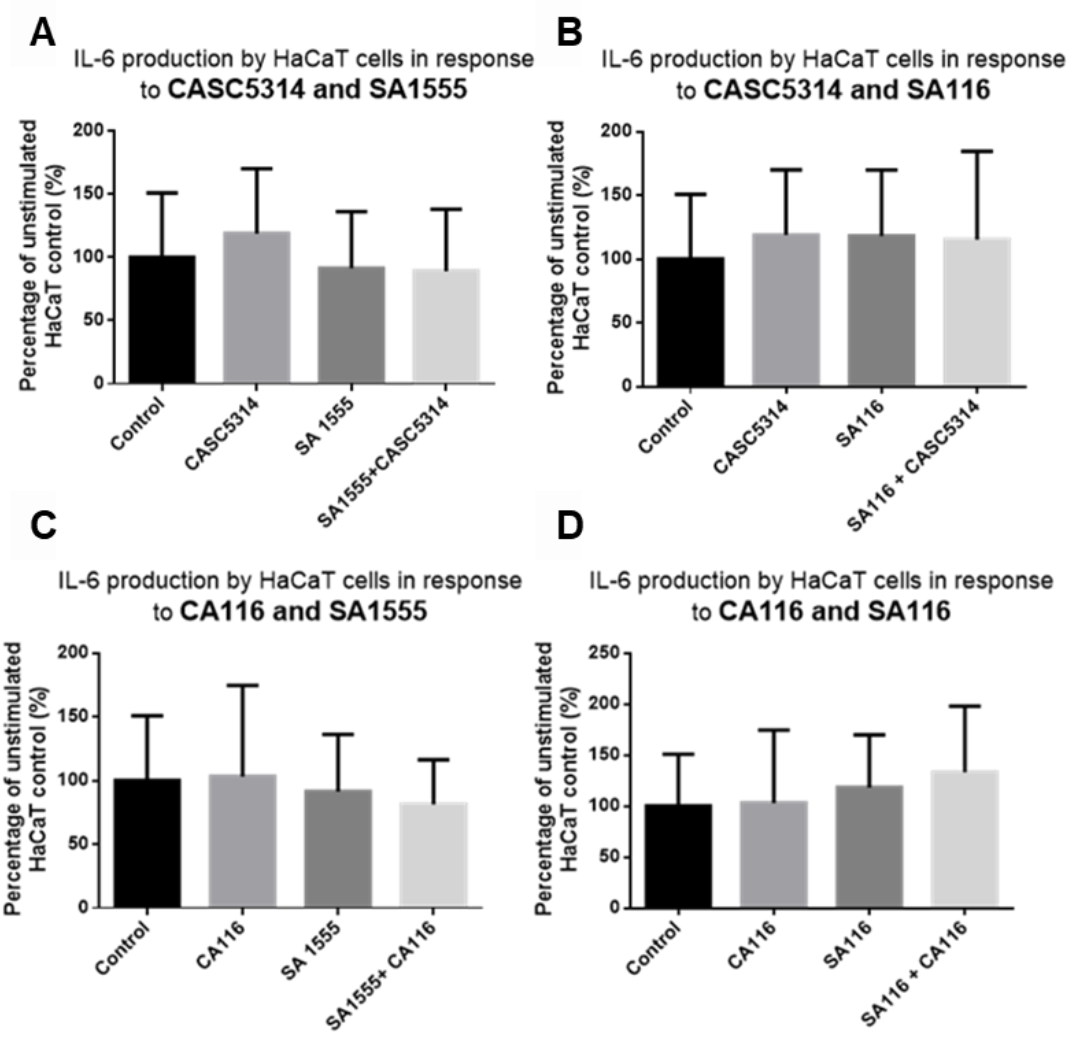

Figure 34: IL-6 production by HaCaT cells in response to single and dual infections of *C. albicans* and *S. aureus*

IL-6 pro-inflammatory cytokine production by HaCaT cells when stimulated with different isolates of *C. albicans* (CA) and *S. aureus* (SA), CASC5314 and SA1555 (A), CASC5314 and SA116 (B), CA116 and SA1555 (C), and CA116 and SA116 (D). Graphs indicate two experiments performed in triplicate. Data was standardised to a percentage of the control (unstimulated HaCaT) for each repeat. *C. albicans* SC5314 and *S. aureus* SA1555 strains are type strains. Strains dual isolated from the same patient are *C. albicans* 116 and *S. aureus* 116. *C. albicans* and *S. aureus* were co-cultured with a HaCaT monolayer for 24 hours at an MOI of 0.1 and 1, respectively. Cytokine production was measured via sandwich ELISA, and significant differences in cytokine production were compared between each individual graph. Data normality was assessed using the Shapiro-Wilk test for normality. All data was analysed using a one-way ANOVA followed by a Tukey's multiple comparisons test. Statistical significance is indicated on the graph (* $p < 0.05$, ** $p < 0.01$, *** $p < 0.001$, **** $p < 0.0001$). Error bars represent standard deviation.

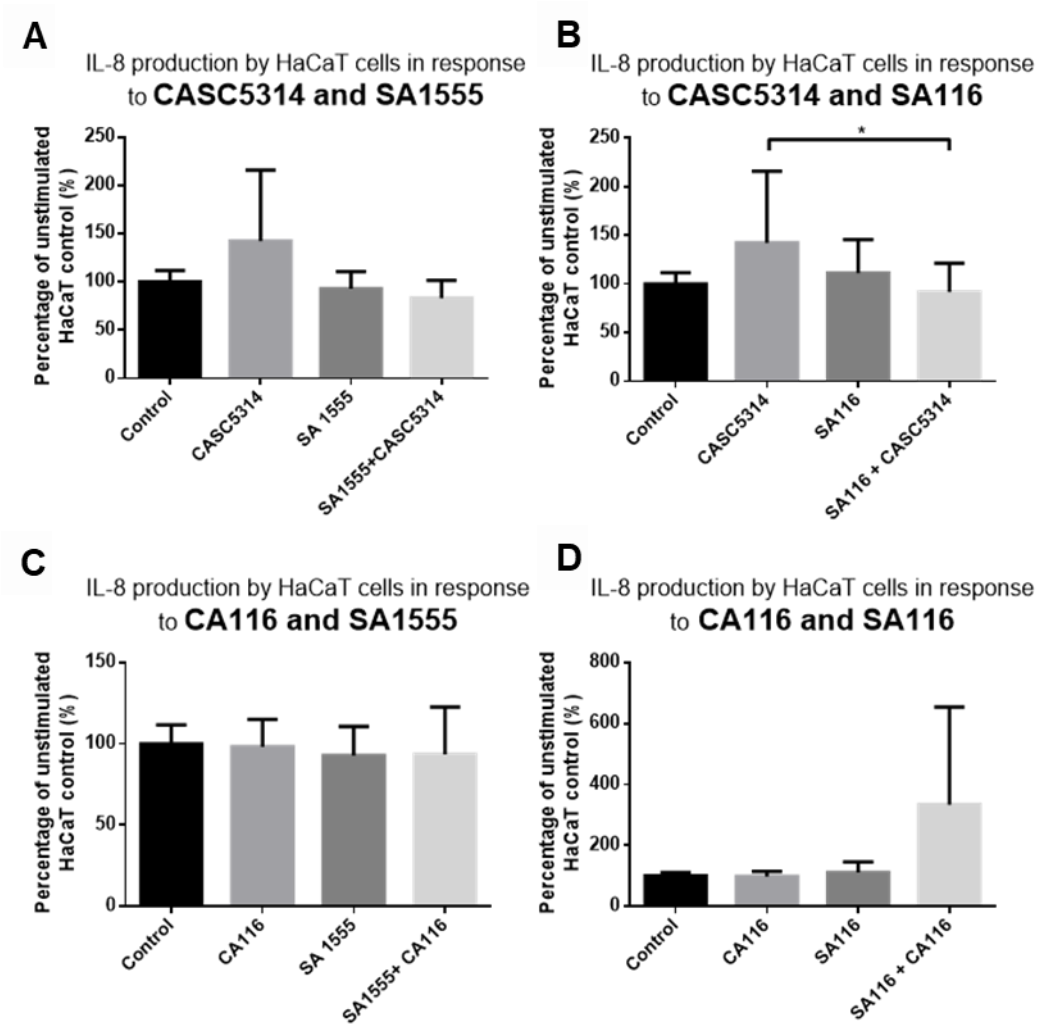

Figure 35: IL-8 production by HaCaT cells in response to single and dual infections of *C. albicans* and *S. aureus*

IL-6 pro-inflammatory cytokine production by HaCaT cells when stimulated with different isolates of *C. albicans* (CA) and *S. aureus* (SA), CASC5314 and SA1555 (A), CASC5314 and SA116 (B), CA116 and SA1555 (C), and CA116 and SA116 (D). Graphs indicate two experiments performed in triplicate. Data was standardised to a percentage of the control (unstimulated HaCaT) for each repeat. *C. albicans* SC5314 and *S. aureus* SA1555 strains are type strains. Strains dual isolated from the same patient are *C. albicans* 116 and *S. aureus* 116. *C. albicans* and *S. aureus* were co-cultured with a HaCaT monolayer for 24 hours at an MOI of 0.1 and 1, respectively. Cytokine production was measured via sandwich ELISA, and significant differences in cytokine production were compared between each individual graph. Data normality was assessed using the Shapiro-Wilk test for normality. All data was analysed using a Kruskal-Wallis test followed by a Dunn's multiple comparisons test. Statistical significance is indicated on the graph (* $p < 0.05$, ** $p < 0.01$, *** $p < 0.001$, **** $p < 0.0001$). Error bars represent standard deviation.

4.5. Discussion

4.5.1. Considerations for oral infection models

Oral isolates of *C. albicans* and *S. aureus* were obtained from participants, some of which were employed for subsequent monolayer and 3DOMM infection studies. The proportion of single and dual species colonisation within denture wearing and non-denture wearing participants, and the area of the oral cavity from which the organisms were isolated, were taken into consideration. This chapter explored the suitability of P/3DOMMs to study tissue colonisation and invasion upon live infection with single and dual species of *C. albicans* and *S. aureus*, whilst considering the ability of HaCaT monolayers and P/3DOMMs to produce pro-inflammatory cytokines in response to live infective agents. Further to this, this chapter employed the use of HaCaT monolayers and P/3DOMMs to explore the proposed synergistic relationship between *C. albicans* and *S. aureus*.

4.5.2. Oral isolates of C. albicans and S. aureus

There were several initial aims for the patient study; not all could be achieved due to the lower than desired number of participants recruited onto the study. Aims therefore were adapted based upon the number and proportion of participants. It was not possible to make a comparison between the isolation of *C. albicans* and *S. aureus,* between participants presenting with DS, healthy denture wearers, and non-denture wearing controls, as only one participant was found to present with DS. Furthermore, due to the low sample size it was not possible to determine associations between *C. albicans* and *S. aureus* carriage, and health and lifestyle factors of the participant, due to the lack of statistical power.

The acquisition of clinically relevant isolates of *C. albicans* and *S. aureus* from the oral cavity of patients was achieved, and these samples were later implemented for infection studies. Typically, type strains are employed in order to study oral infection, however type strains are rarely oral isolates, and therefore may exhibit different virulence factors than those typical of an oral resident. The novel isolation and implementation of oral strains provides the advantage of studying the oral mucosal response to microbes of the same biological niche. SA116, an oral mucosal isolate, was used frequently in the subsequent experimentation in order to test the efficacy of P/3DOMMs, and to study the interactions of P/3DOMMs and HaCaT monolayers, with single and dual infections of *S. aureus* and *C. albicans*. CA116 was also implemented for the study of dual infections alongside SA116.

Within the present study, it was also possible to indicate whether microbial carriage is more prevalent on the prosthesis or on the hard palate within the denture wearing population, with *C. albicans* being most frequently isolated on the denture, and *S. aureus* most frequently isolated on the palate under the denture. Uniquely, within the present study it was possible to compare the prevalence of *C. albicans* and *S. aureus* within denture wearers and non-denture wearers from the same demographic, whereas previous studies have focused upon DS denture-wearers compared with healthy denture-wearers (36,37,239). In the present study, 18.18% of participants in the non-denture wearing control group tested positive for *C. albicans* carriage, compared with 30% of the denture wearing population. No participants in the non-denture wearing control group presented with *S. aureus* carriage, compared to 10% of the denture wearing population.

Also unique to the present study is the swabbing of different areas of the hard palate for participants who wear a partial maxillary prosthesis, in order to explore the impact of denture wear upon the microbial composition within a single individual. Of the two participants who both tested positive for *C. albicans,* and wore partial maxillary denture, both exhibited denture and palate colonisation from an area not residing under the denture plate, whereas, unexpectedly, only one of the two participants exhibited colonisation of the area under the denture. This data cannot be extrapolated beyond the context of the present study, due to participation numbers, nor may it can be compared with existing literature, as other studies either only included patients with a complete maxillary prosthesis, or did not discriminate between the area of the hard palate sampled within their reported results (36,37).

Within the cohort of 32 patients, 3.13% carried both *C. albicans* and *S. aureus*, 21.88% carried *C. albicans,* and none carried *S. aureus* alone, however 21.88% were found to be carrying a species of coagulase negative staphylococci. In the general population it is commonly reported that anywhere between 30% and 50% of people are oral carriers of *C. albicans* (253). *S. aureus* is less frequently reported, and is thought to be present in the oral cavity of approximately 18% of people (236). Martins *et al*., 2002, identified oral *Candida* and *Staphylococcal* species using oral rinses on healthy participants who did not wear dentures. It was identified that 95.59% of participants carried *Staphylococcus spp.,*13.9% of which were *S. aureus,* which equates to 13.23% total *S. aureus* carriage of the entire cohort (252). Furthermore 61.66% of patients carried *Candida spp.,* of which 61.22% were *C. albicans,* which equates to 44.12% total *C. albicans* carriage of the entire cohort (252). These results are slightly higher, but at a

similar proportion, to those identified in the present study. Majima et al., 2014 studied *C. albicans* carriage within healthy control participants, and indicated that 14.7% of their cohort presented with *C. albicans* carriage, close to that of the 18.2% carriage observed within healthy control participants in the present study (254). The lower percentage of *C. albicans* carriage observed by Majima et al., may be attributed to the lower mean participant age, 34.67 years as opposed to 67 years in the present study, as *Candida* carriage is thought to increase with age; however, in the study performed by Martins et al., mean participant age was 34.45 years, lower than that of Majima's cohort, and *C. albicans* carriage was substantially higher (252,254,255).

Within denture wearers, the proportion of reported *C. albicans* and *S. aureus* carriage shifts. Monroy *et al*., 2005, identified the mucosal carriage of these microbes within denture wearers to be 51.4% and 52.4%, respectively (36). Chopde *et al*., 2012, indicated a similar proportion of carriage within denture wearers, 55.4% and 56.4%, respectively. These studies recruited larger cohorts of patients, 105 and 200 patients, respectively, compared with the 32 incorporated into the present study. Furthermore approximately half of the participants in both of these studies presented with DS, compared with 1 participant in the present study (36,37). It should be noted that as the aforementioned cohorts consisted of denture-wearers only, including both healthy participants and those with DS, and the reported percentages take into account both populations, it is not unexpected that the overall total proportion of *C. albicans* and *S. aureus* carriage differ from the present study, which also took into account non-denture wearing control participants. Monroy et al., 2005, and Pereira et al., 2013, demonstrated that dual carriage of *C. albicans* and *S. aureus*

in DS patients was greater than that of the healthy denture wearing population, due to the lack of DS participants recruited onto the present study, it is not possible to make this comparison (36,239).

The use of a single sampling methodology may explain the reduced isolation of *C. albicans* and *S. aureus* within the present study, compared to the overall reported prevalence in denture wearers. Pereira *et al*., 2013, implemented the use of oral and prosthesis swabs, as well as an oral rinse, to discover that within healthy denture wearing patients 34% carried *C. albicans*, 62% carried *S. aureus,* and 20% carried both, substantially more than indicated in the present study (239). Although, Chopde *et al*., 2012 used a similar sampling method to the present study, implementing the use of swabs, and a higher overall isolation of *C. albicans* and *S. aureus* was obtained (37). Lewis et al., 2015, studied denture wearer's by means of a denture swab, and found that of a total of 200 participants, an average of 30% of participants tested positive for *S. aureus* (239,256). Al-Dossary et al., 2018, identified that 61.5% of denture wearing participants carried *C. albicans,* as identified by an oral rinse (257). It is clear from the aforementioned studies that variation within sampling methodologies, cohort size, and study aims are present, meaning a direct comparison between each study and the present study is difficult. It is also apparent that even between similar studies, there is substantial variation in reported percentage carriage for *C. albicans* and *S. aureus*, as detailed in **Table 12**. Whether such differences are as a result of study design or the demographic of participants, is difficult to deduce, therefore it is not possible to confidently state the average percentage carriage of either organism within control participants, healthy denture wearers, nor participants with denture stomatitis.

With regards to the present study, the recruitment of more participants would have provided a more representative sample, with a higher statistical power, enabling more robust conclusions to be drawn. Also, the implementation of multiple sampling mechanisms would be likely increase the yield of *C. albicans* and *S. aureus* isolation due to the increased surface area sampled, and the inclusion of different biological niches within the oral cavity through the use of an oral rinse, however this should be used in combination with swab techniques, in order to not negate the ability to determine the localisation and association of microbial carriage within the oral cavity of denture wearers.

Table 12: Reported percentage carriage of *C. albicans* and *S. aureus* in the oral cavity

A comparison of the present study and relevant literature. Blank cells indicate that data was not reported in the associated study. C.a indicates *C. albicans,* S.a indicates *S. aureus,* and B indicates both. Some data has been reconfigured for display, to aid comparison with other studies.* Article displayed a discrepancy with reported data for the prosthesis carriage of *C. albicans* within the healthy control group, it was therefore excluded.

Study	Sample	Combination			Control			Denture control			Denture Stomatitis			Ref
		C.a	S.a	B	C.a	S.a	B	C.a	S.a	B	C.a	S.a	B	
Present study	Oral (all)	21.9%	3.1%	3.1%	18.2%	0.0%	0.0%	30.0%	10.0%	10.0%				
	Mucosa	18.8%	3.1%	0.0%	18.2%	0.0%	0.0%	20.0%	10.0%	0.0%				
	Prosthesis	9.4%	0.0%	0.0%				30.0%	0.0%	0.0%				
Alrayyes 2019	Oral rinse				24.0%									(258)
Al-Dossary 2018	Oral rinse				33.6%			61.5%						(257)
Lewis 2015	Prosthesis								30.0%					(256)
McCormack 2015	Oral (all)		18.0%											(236)
Majima 2014	Oral (all)				14.7%									(254)
Pereira 2013	Oral (all)							34.0%	62.0%	20.0%	94.0%	42.0%	40.0%	(239)
	Mucosa							6.0%	22.0%		58.0%	22.0%		
	Prosthesis							28.0%	26.0%		42.0%	26.0%		
	Oral rinse							20.0%	20.0%		52.0%	40.0%		
Chopde 2012	Mucosa	55.4%	56.4%					51.0%	53.0%		86.0%	84.0%		(37)
	Prosthesis	69.7%	45.3%					68.0%	52.0%		28.0%	40.0%		
Zomorodian 2011	Oral (all)	41.5%												(259)
Monroy 2005	Mucosa	51.4%	52.4%	42.9%				20.0%	23.6%	10.9%	86.0%	84.0%	78.0%	(36)
	Prosthesis	66.7%	49.5%	18.1%				*	61.8%	23.6%	26.0%	36.0%	12.0%	
Martins 2002	Oral rinse				44.1%	13.2%								(252)
Abu-Elteen 1998	Oral (all)				36.8%			78.3%						(260)

4.5.3. Tissue damage and invasion

HaCaT monolayers infected with *C. albicans* appeared to remain intact for the duration of 24 hours. *C. albicans* colonisation increased over time and transitioned from yeast to hyphal form. *S. aureus* disrupted the HaCaT monolayer by 12 hours, following this the epithelium began to lift and cells appeared non-viable due to the lack of cellular boundaries. It is well known that *S. aureus* can cause skin infections and disruption to the epithelium, which occurred rapidly in this case, most likely as it consisted of a single layer. *S. aureus* possesses virulence factors such as protein-A, alpha toxin, and exogenous proteases, that may cause disruption to the epithelial barrier, enabling it to pass into deeper tissues (261–263). Interestingly, dual infections with *C. albicans* and *S. aureus* presented with less damage to the HaCaT monolayer than *S. aureus* alone. This does not correlate with the reports of increased virulence indicated within the literature for dual infections, however the majority of these studies have focused on animal study mortality rates upon intraperitoneal injections (246,247,264). It is possible that the presence of *C. albicans* helped to protect the epithelium in this case, however it is more likely that incubating both organisms at any one time, even with half of the infective dose for each, may lead to a competition for nutrients, resulting in reduced numbers and inhibited growth of *Staphylococci*.

Control 3DOMMs had an intact epithelial barrier that adhered to the lamina propria. Models infected with *C. albicans* presented with a *Candida* biofilm atop the epithelium, irrespective of whether *S. aureus* was present. In some areas, *C. albicans* hyphae appeared to be penetrating the epithelium, however this was not a frequent occurrence, nor did it appear to damage the epithelial barrier. Other studies have reported *C. albicans* to cause disruption to the full-thickness oral

model epithelium, with frequent penetration of *Candida* hyphae (14,42,265). The present study used *C. albicans* SC5314, as did another study that contrastingly reported epithelial damage upon infection. Dongari-bagtzoglou *et al*., 2006, indicated that 24 hour infection with *C. albicans* SC5314 caused significant disruption to the tight junctions of the epithelium and subsequent invasion, however *C. albicans* was initially seeded at an MOI of 1, 10 times greater than that of the present study (265). Morse *et al*., 2018, demonstrated that *C. albicans* remained in yeast form, and caused less damage to the epithelial barrier within epithelium only RHOE models, compared to full-thickness Epi-Oral models. As *C. albicans* SC5314 has been demonstrated to cause epithelial damage within a 24 hour period previously, it is plausible to consider that the epithelia of the newly developed 3DOMMs, may be more robust than those discussed above; resulting in these lower levels of tissue invasion and visual damage, upon infection. Particularly, as preliminary data from the present study revealed no epithelial damage upon infection with higher doses of *C. albicans* SC5314, **Figure 36**.

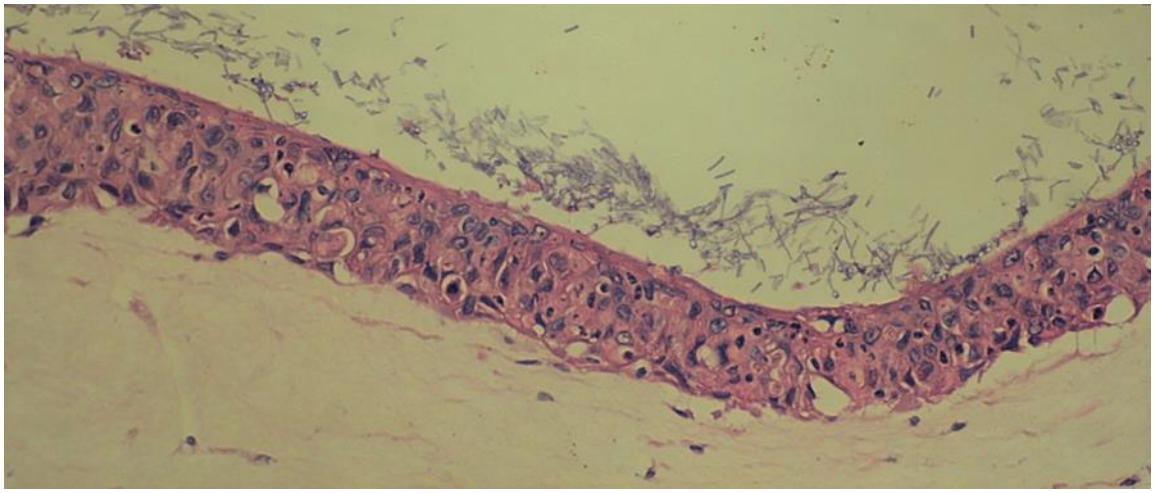

Figure 36: Infected 3DOMM with *C. albicans* at an MOI of 1
Histology of 3DOMMs infected at day 19 with *C. albicans* at 5×10^6 CFU/ml (MOI 1), for 24 hours (200 X magnification).

Histology and electron micrograph images revealed the presence of *S. aureus* within the lamina propria layer, despite the lack of an obvious route of entry. Infection with *S. aureus* alone did not cause disruption to the epithelial barrier of the 3DOMM, as supported by Carvalho Dias et al., 2018 (14). However it has been shown by Reddersen *et al.*, 2019, that upon infection with the higher dose of 1×10^9 CFU/ml, *S. aureus* may cause epithelial damage within a full-thickness epidermal model, as identified through histological analysis and LDH release (54).

Dual infection with *C. albicans* and *S. aureus* in the present study revealed no obvious epithelial damage, also absent with isolates alone. *S. aureus* appeared in clusters amongst the hyphal elements. *C. albicans* hyphae were demonstrated to be penetrating the epithelium, as confirmed through TEM, however this was an infrequent occurrence. From observing the histology, *C. albicans* single and dual infections appeared to present in the same manner, with some penetrating hyphae, but an overall intact epithelium. Carvalho Dias *et al*., 2018, reported the extent and depth of infection with dual species of *C. albicans* and *S. aureus,* were greater than when alone; this was not observed in the present study (14).

P3DOMMs infected with single or dual species of *C. albicans* and *S. aureus* exhibited infective agents throughout the epithelium. This was likely due to the fact the epithelium of the model was not intact upon infection, as opposed to a result of the microbes' ability to invade. This was supported by the disrupted control epithelium. Observations indicated more invasion of the P3DOMM within the dual species infection than infection with *S. aureus* alone, however for both, microbes were observed amongst the epithelial cells. The least invasion was observed within the *C. albicans* single infection, with few hyphae penetrating the

epithelium. Whilst the concept that dual species infection leads to increased virulence and invasion supports the observed literature, the already disrupted epithelium did not provide a sufficient epithelial barrier to comment on true tissue invasion. P3DOMMs were therefore deemed not suitable to be used to study the colonisation, invasion and virulence of live infective agents.

4.5.4. Pro-inflammatory cytokine production by P/3DOMMs in response to single and dual infections of *C. albicans* and *S. aureus*

HaCaT cells, 3DOMMs, and P3DOMMs have demonstrated their ability to produce pro-inflammatory cytokines in response to infection, supporting their use as infection models. For HaCaT cells, 3DOMMs, and P3DOMMs, a significant increase in pro-inflammatory cytokine production (IL-8; IL-6 and IL-8; and IL-6, respectively) was observed between the unstimulated control and cells/models stimulated with *C. albicans, S. aureus,* and dual infection of both organisms. 3DOMMs were the only models capable of increasing both IL-6 and IL-8 in response to live infective stimuli. This means that despite the high levels of constitutive pro-inflammatory cytokine production identified within chapter 3, it is still possible to measure upregulation in response to live infection. It was decided that due to variability seen within pro-inflammatory cytokine production between different batches of models, that data should be standardised to a percentage of the control for each repeat.

Within cells/models that displayed increased cytokine production upon infection, no significant differences in pro-inflammatory cytokine production were observed between single and dual infections of *C. albicans* and *S. aureus*. The effect of *C. albicans* and *S. aureus* single and dual infections on pro-inflammatory cytokine

production has not been frequently reported *in vitro.* In a murine intra-abdominal infection model, and a murine peritonitis model, it was identified that pro-inflammatory cytokine levels were elevated in co-infection compared with single infections of *C. albicans* and *S. aureus* (266,267). This does not agree with the results from the present study, however in a live murine model, other cytokine producing cells will be at play, such as macrophages and neutrophils. Within the present study, microbes were only exposed to epithelial and fibroblast cells. It may be the case that upon the further development of the 3DOMM into an immunocompetent model, the pro-inflammatory cytokine balance is shifted upon response to these different combinations of infective agents, due to the ability of multiple cell types to collectively respond. It may also be possible that this synergistic action is strain dependant, as for the studies discussed so far, only one strain of *C. albicans,* SC5314, and one patient isolate of *S. aureus,* P116, were implemented.

4.5.5. Immunogenicity of single and dual infections of *C. albicans* and *S. aureus*

To determine whether the lack of difference exhibited between single and dual infections of *C. albicans* and *S. aureus* was strain dependent, HaCaT cells were implemented to study different combinations of strains including the type strains *C. albicans* SC5314 and *S. aureus* 1555*,* and strains isolated from a participant with dual colonisation of *C. albicans* and *S. aureus,*116. To maintain proportions of *C. albicans* and *S. aureus* that would be isolated *in vivo,* and to seed with a low enough dose that the HaCaT monolayer will not be instantly destroyed, organisms were seeded at an MOI of 0.1 and 1, respectively. In this case, there

was no significant difference in pro-inflammatory cytokine production between the unstimulated HaCaT control, and any combination of patient samples.

Considering the fact that in other experiments, a significant increase in pro-inflammatory cytokine production between infected HaCaT and the unstimulated control was observed, the question was raised as to why an increase in pro-inflammatory cytokine production did not occur on this occasion. Experimental variation is common, however this should be accounted for through the implementation of multiple experimental repeats. The differences exhibited may possibly be a result of differing experimental repeats. For the initial study of pro-inflammatory cytokine production in HaCaT infected monolayers, the experiment was repeated 7 times providing additional statistical power to look for significant differences, compared with twice for the previously discussed experiment.

4.6. “Bridge”

This chapter demonstrated the ability of the 3DOMM to produce IL-6 and IL-8 pro-inflammatory cytokines in response to single and dual infections of *C. albicans* and *S. aureus*, as well as indicating its suitability to model microbial colonisation in a robust, reproducible, manner. For these reasons it was decided that the 3DOMM over the P3DOMM, was most suitable for further development into an immunocompetent three-dimensional oral mucosal infection model (IC3DOMM).

5. Development of an immunocompetent 3DOMM

5.1. Introduction

5.1.1. The oral immune system

The oral immune system is complex and specialised. It simultaneously works to prevent pathogenic invasion, whilst maintaining health and homeostasis, which is achieved by a careful balance between tolerance and response. The oral cavity encounters a diverse range of antigens on a daily basis, from the food that we eat, to the rich range of commensal microbes including bacteria, fungi, and archaea, which play a fundamental role within health (268). It is the innate immune system's role to prevent the entry and spread of pathogens to the tissues beneath, to recognise and respond to potential pathogens leading to pathogenic clearance, and to tailor the downstream response through the secretion of cytokines and presentation of subsequent antigens to the adaptive immune system (269). It is important that the immune system is able to differentiate between members of the microflora and pathogens. The oral immune system possesses stringent regulatory and tolerance processes that are able to differentiate between the safe resident microflora and food antigens, and pathogenic microbes. Compared with areas such as the gut, the understanding of the oral immune system is under-developed, however there appear to be parallels with the gut mucosal immune system (29,270–272).

5.1.2. Antigen-presenting cells of the oral mucosa

The two fundamental antigen-presenting cells of the oral mucosa are macrophages and dendritic cells. Oral tolerance relies upon the actions of dendritic cells, which sample antigens by extending their dendrites through the

epithelium, in order to present antigens to T-cells which reside in the associated lymphoid tissue (271,273). This process is vital to regulate homeostasis, maintain epithelial barrier function, respond to infection, and mediate adaptive immune responses, including the induction of inflammation and prevention of response, namely tolerance (274).

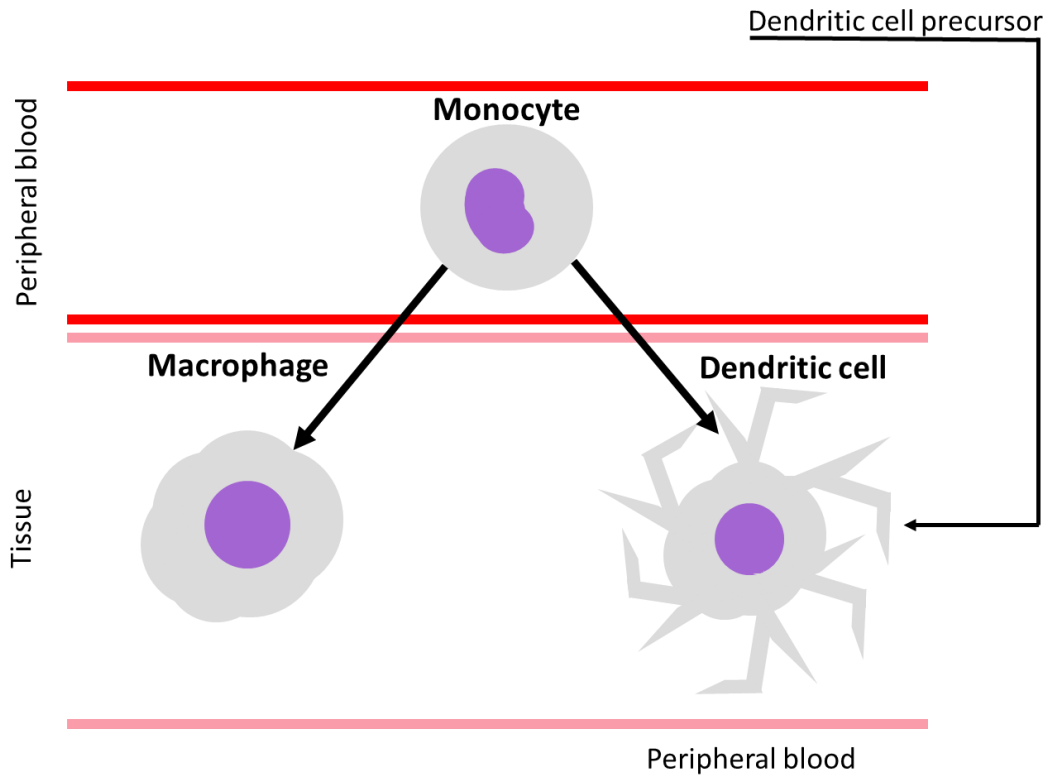

Figure 37: Monocyte-derived antigen-presenting cells.
Peripheral blood monocytes are precursors to macrophages and dendritic cells.

Tissue-resident macrophages reside within healthy oral mucosal tissue and play a role in the maintenance of tissue health and homeostasis. Peripheral blood monocytes may be differentiated into macrophages or dendritic cells, **Figure 37** (275). During disease, a substantial increase in the number of macrophages within the oral tissue is observed. Macrophages are phagocytes, and are

therefore able to engulf pathogens and present their antigens. They partake in a diverse range of activities as detailed in **Figure 38**, that are determined by the local microenvironment (276). Langerhans cells are specialised epidermal dendritic cells. Within epithelial tissues they sample exogenous antigens, once an antigen has been captured the Langerhans cells migrate to the local lymph and present to naive T-cells (277). Langerhans cells vary from dendritic cells in that they are considered a self-sustaining population within the tissue when in a homeostatic state, but may lead to the recruitment of monocyte-derived dendritic cells in the case of disease (278,279).

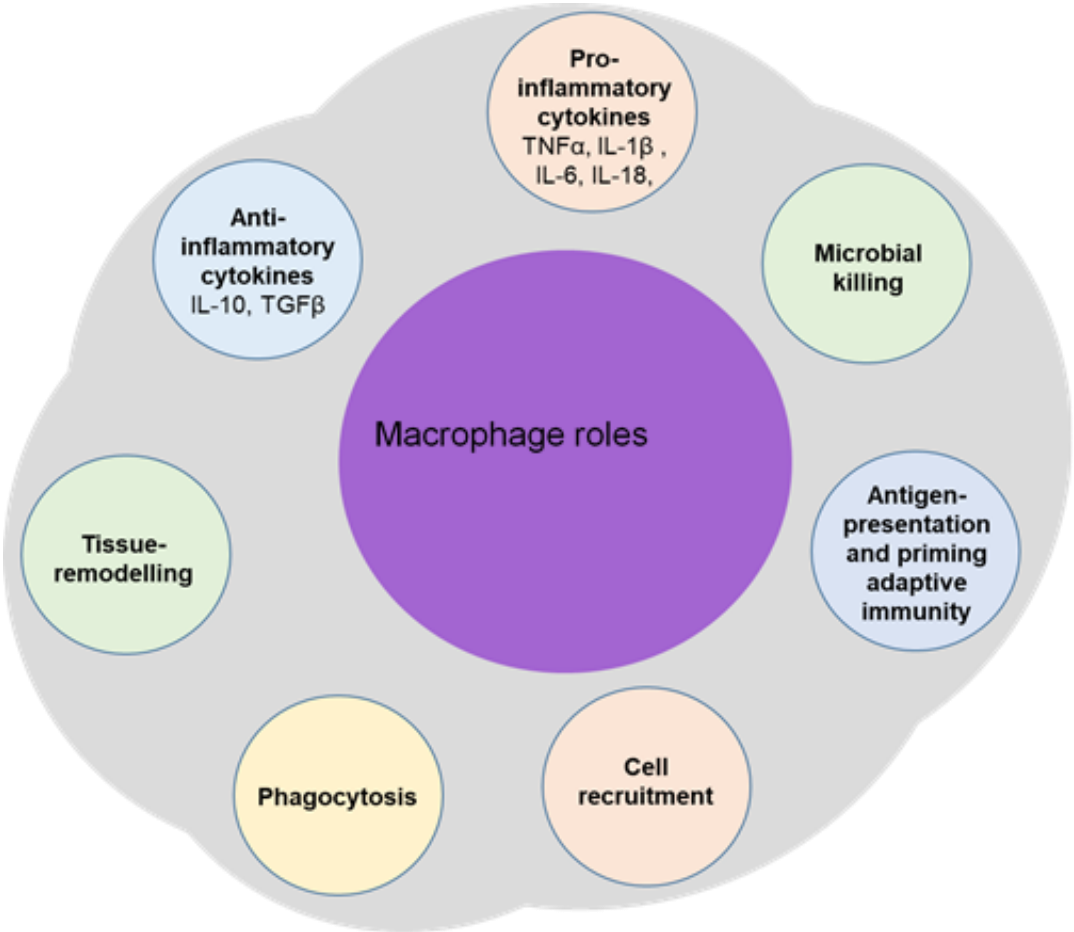

Figure 38: The diverse functions of macrophages.
Macrophages respond to their local microenvironment, bridge the gap between the innate and adaptive immune system through antigen presentation, and may act in an inflammatory or regulatory manner. Adapted from Merry *et al*., 2012

5.1.3. 3DOMMs incorporating Langerhans cells

To date, 3DOMMs have incorporated innate immune cells. A commercial 3DOMM containing Langerhans cells exists, however there are no significant resulting publications from implementing these models for infection research. Early research identified that it was difficult to work with mature Langerhans cells due to their lack of proliferative capacity. To overcome this, precursor Langerhans cells were implemented for the purpose of epidermal modelling, using $CD34^+$ progenitor cells isolated from either peripheral blood or human cord blood, and incorporated into the model in the presence of growth factors, leading to differentiation of the $CD34^+$ progenitor cells into Langerhans cells (65,66). In 2003, Sivard *et.al,* created a mucosal epithelial model that recruited these precursor Langerhans cells into the tissue structure consisting of a multi-layered epithelium cultured on a dermis, resulting in a full-thickness model. Langerhans precursor cells were cultured separately whilst the model epithelium developed, and then introduced after 6-8 days to the top of the epithelium. Models now containing Langerhans cells were cultured for a further week, allowing enough time for the Langerhans precursor cells to mature. After this, histology indicated that Langerhans cells had migrated towards the basal and suprabasal epithelial layers. The model appeared structurally analogous to the native oral mucosa, with the correct expression of cytokeratin markers to indicate differentiation of the tissue. This study used primary keratinocytes obtained from donor biopsies and Langerhans precursor cells from cord blood (61). The proposed application of these models was the study of immunological response to viral and bacterial infection.

5.1.4. 3DOMMs incorporating macrophages

Macrophages are entwined in the role of maintaining health and homeostasis, due to their multi-functional ability and responsivity to the local microenvironment. Depending on their activity, macrophages are often described as having either a pro-inflammatory (M1) or regulatory (M2) phenotype (280). In reality, the diversity of macrophage phenotypes is more complex than this, dependent upon a multitude of signals in which they encounter from their neighbours. However M1 and M2 phenotypes have been well characterised, and are a good indicator as to how a responding macrophage will orchestrate other surrounding cells, tailoring either an inflammatory or regulatory response (281). Macrophages have a large influence on the downstream response to a recognised pathogenic stimuli, they may induce pathogenic clearing, recruit further immune cells to respond to infection, activate T-cells through antigen presentation, remove apoptotic cells, and trigger wound healing and tissue repair, as per **Figure 38**, (282–284). Tissue-resident macrophages vary depending on the area in which they reside, they are ever present and are able to rapidly respond to infection. Macrophages can also be recruited from the blood stream in the case of active infection, in their precursor form of monocytes, this occurs when called upon by other immune cells or tissue-resident macrophages (285).

Because of their ability to switch the immune response between inflammation and regulation, and due to their ability to directly respond to pathogenic stimuli, the present study focused upon the incorporation of macrophages into the 3DOMM. Several independent research groups have managed to successfully incorporate macrophage cells into a three-dimensional tissue-engineered matrix, however their reported use since this initial development has been limited (62,63,286).

Linde *et al*., 2012, developed a tumour model, whereby peripheral blood mononuclear cell (PBMC)-derived macrophages were incorporated into a collagen gel matrix containing primary dermal fibroblasts, in order to study the matrix interactions with oral squamous carcinoma cell lines. Macrophages were polarised towards M1-like and M2-like macrophages using IFNγ and IL-4, respectively. The model was then employed to study tumour cell migration. Macrophages that were incorporated into the squamous cell carcinoma model, but not introduced to either IFNγ or IL-4, spontaneously polarised towards the M2-like macrophage phenotype after 2 weeks (62). Furthermore, the macrophages were indicated as viable, through immunostaining, three weeks after they were incorporated into the model environment, which surpasses the time point in which PBMC-derived macrophages are typically used in monoculture. It is, however, known that within native tissue macrophages can survive for months depending on the local tissue microenvironment (287–290).

Bechetoille *et al*., 2011, also produced an organotypic dermal model containing monocyte-derived macrophages and human dermal fibroblasts. Unlike Linde *et al*., 2012, this group used a solid, collagen, chitosan, and chondroitin 4-6 sulphate scaffold, as opposed to type-1 collagen alone (62,63). Dermal macrophages introduced into this environment, already containing dermal fibroblasts, and cultured for 8 days, maintained their anti-inflammatory phenotype. They took an active part in phagocytosis, expressed high levels of IL-10 and low levels of TNFα when stimulated with LPS, and maintained expression of M2-associated surface marker CD163. There was no evidence of reversion of the macrophages to a monocytic phenotype. There was no mention of an epithelial layer within this model (63).

5.1.5. THP-1 differentiation and polarisation

THP-1 cells are a frequently used macrophage model, which require differentiation and polarisation prior to their use. Within monoculture, THP-1 cells have been used as an alternative to PBMCs as a means of overcoming the expense and scarcity of primary cells. THP-1 cells were derived from a patient with monocytic leukaemia, and were shown to express Fc and C3b receptors, as well as undertake phagocytosis, and restore T-cell responses. They are mostly regarded as pro-monocytes due to their phenotypic differences when compared to primary monocytes, resulting from their leukaemic origin (291,292). Undifferentiated THP-1 cells are typically considered to be unresponsive to PAMP stimulation when cultured in the correct conditions. THP-1 pro-monocytes will only differentiate into subsequent macrophages upon introduction to appropriate cytokines and stimuli. *In vivo*, cytokines noted to lead to the differentiation of monocytes and further polarisation of macrophages into a pro-inflammatory M1 phenotype include GM-CSF and IFNγ (293,294). Cytokines noted to lead to an anti-inflammatory M2 phenotype include M-CSF, IL-4, and IL-13 (293,295,296). These results can be replicated *in vitro* with primary monocytes and monocytic cell lines.

THP-1 cells have been differentiated *in vitro*, and polarised into M1-like and M2-like macrophages with the aid of phorbol 12-myristate-13-acetate (PMA) and 1,25-dihydroxy-vitamin D_3 (VD3), respectively. PMA is a diacyl glycerol (DAG) analogue, hence protein kinase C activator, which leads to the differentiation of monocytes into macrophages. VD3 has been shown to alter the polarisation of macrophages through the upregulation of T-cell-IG-mucin-3 (TIM-3), which leads to inhibition of TNFα and IL-6 production and the upregulation of IL-10 and TGF-

β production (297). Research groups have implemented a variety of different concentrations and durations of exposure to differentiate and/or polarise THP-1 cells into such macrophages as detailed in **Table 13**. Both PMA and VD3 have been reported to differentiate THP-1 cells into macrophages, with PMA being reported as having a phenotype closer to a native macrophage in terms of morphology and adherence (298,299). Longer exposure to PMA, or higher concentrations, appear to further polarise the differentiated macrophages in to a pro-inflammatory M1-like phenotype (300,301). VD3 has been shown to polarise monocyte-derived macrophages away from an inflammatory phenotype, and increase the production of regulatory cytokines (299,302). The use of PMA, and to a lesser extent VD3, is accepted within the literature as a successful means of differentiating THP-1 cells into macrophages. Literature indicating their stand-alone use for further polarisation is less well reported. PMA and VD3 alone have been applied to differentiate and polarise THP-1 cells into M1-like and M2-like macrophages, to model the differing response of subsequent pro-inflammatory and regulatory macrophages, respectively (303,304).

There is controversy as to whether it is appropriate to refer to macrophages in such a simplistic manner as M1 and M2 phenotypes; as knowledge progresses, the description of macrophages in such a way is diminishing. Such description was derived as a result of the pro-inflammatory T-helper 1 cells, and the regulatory T-helper 2 cells, which are able to produce IFNγ and IL-4, respectively, both of which are able to lead to a different response in the macrophage (296). Traditionally, the M1 macrophage was reported to express high levels of the pro-inflammatory cytokines IL-6 and TNFα, whereas the M2 macrophage was described as producing IL-10 and TGFβ, both of which are regulatory cytokines,

promoting tissue repair and clearance of debris. Further study led to the description of additional subsets of macrophages, which expressed a different balance of pro- and anti-inflammatory cytokines, and cell surface markers, and were activated by different cytokines to those typically defined by the M1 and M2 subsets. These macrophages were termed M2a, M2b, M2c and M2d (280,305). In reality, it would appear that this approach to characterising macrophages is somewhat simplistic and reductive, and therefore redundant (306,307). Macrophages dynamically respond to their local environment. Although high levels of IFNγ are more likely to lead to an inflammatory macrophage phenotype, the true activity of the macrophage depends upon the collective cytokine environment. As a result of this, macrophages are not limited to either extreme of the polarisation spectrum (296). Although this is useful knowledge to have in regards to studying disease *in vivo*, due to the lack of other responsive tissue and immune cells when studying macrophages *in vitro*, it is still common to polarise the macrophages into a desired phenotype. The introduction of macrophages into a tissue-engineered construct may provide the unique ability to study macrophage response to infection *in vitro* in the absence of artificial polarisation, providing that the other cell types incorporated into the model are able to produce cytokines that lead to the activation and determination of macrophage activity.

The purpose of this chapter was to incorporate THP-1 pro-monocyte cells into the already developed 3DOMM, and to assess the ability of THP-1 cells to survive, differentiate, and polarise in the presence of the 3DOMM through either exogenous or endogenous stimuli. PMA and VD3 were used to differentiate THP-1 cells into macrophages, PMA-derived macrophages from this point onwards will be termed M1-like and VD3-derived macrophages M2-like. These terms are used

with caution, but as a result of careful consideration of the current literature, **Table 13**. This study aims to clarify whether the reported inflammatory and regulatory phenotypes of PMA and VD3 treated THP-1-derived macrophages are suitable for use within a 3DOMM environment. This methodology was chosen over the better characterised IFNγ- and IL-4-derived M1-like and M2-like macrophages, as a means of investigating the success of this practical and accessible protocol. Furthermore, this study poses the unique possibility that the other cell types incorporated into the model may negate the need for induced polarisation of differentiated macrophages *in vitro.*

Table 13: PMA and VD3 induction of differentiation and polarisation of THP-1 cells

Several studies took an all-in-one approach, and induced differentiation and polarisation within one step; others either differentiated and then polarised, or just differentiated. Note the variation in reported methodologies and certainty of outcomes. n.d. = no data available.

Methodology	**Differentiation**		**Polarisation**		**Reasoning and outcomes**	**Ref**
	Conc	Time	Conc	Time		
PMA **differentiation** of THP-1 cells into macrophages	5 ng/ml	48 h	n.d.	n.d.	PMA induced stable differentiation of THP-1 cells into macrophages responsive to weak stimuli.	(300)
PMA **differentiation** and **polarisation** of THP-1 cells into M1-like macrophages	100 ng/ml	48 h	100 ng/ml	48 h	Cells were washed after 48 hours, and then incubated for 48 hours further in PMA. THP-1 cells cultured were determined unresponsive to IL-10 and to express CCR7 and therefore M1-like.	(301)
PMA **differentiation** of THP-1 cells into macrophages	10 ng/ml 2.5 ng/ml	48 h 48 h	n.d.	n.d.	Using this concentration derived activated but not polarised macrophages.	(301)
PMA or VD3 **differentiation** of THP-1 cells into macrophages	100 nM Vd3 or 200nM PMA	72 h (VD3) or 72 h 120 h rest (PMA)	n.d.	n.d.	PMA and VD3 differentiated THP-1 cells into macrophages. PMA treatment increased adherence, 5 days rest further increased adherence and cytoplasmic volume. THP-1 cells stimulated with PMA and then rested displayed a higher degree of classical activation.	(298)
PMA **differentiation** of THP-1 cells into macrophages	25 nM PMA	48 h 24 h (rest)	n.d.	n.d.	A consistent phenotype of THP-1 differentiated macrophages was observed. An upregulation in TNFα was seen in response to LPS.	(308)
PMA or VD3 **differentiation** and **polarisation** of THP-1	n.d.	n.d.	25 ng/ml (PMA) OR 10nM (VD3)	72 h 168 h	THP-1 cells stimulated with PMA were considered M1-like macrophages and with VD3 M2-like macrophages.	(303,304)

cells into M1 or M2-like macrophages.						
PMA or VD3 **differentiation** of THP-1 cells into macrophages	10 nM (PMA) OR 100 nM (VD3)	72 h 72 h	n.d.	n.d.	THP-1 cells stimulated with PMA and VD3 increased phagocytosis, O_2-, CD14 and CD11b expression. PMA stimulated THP-1s became adherent, VD3 did not. PMA stimulated THP-1s halted proliferation, whereas VD3's proliferated at a reduced rate. VD3 induced a more monocytic cell type in terms of morphology and expression. Different signalling pathways are proposed to be involved in PMA and VD3 differentiation of THP-1 cells.	(299)
VD3 **polarisation**, of INF-Y differentiated THP-1 cells.	IFNγ 500 U/ml	n.d.	VD3 10 nM/ml	24H	VD3 was found to downregulate aromatase and IL-6, TNFα and IL-1β, within human macrophages. IFNγ-derived macrophages exhibited a significant reduction in their inflammatory phenotype when stimulated with VD3.	(302)
VD3 **Differentiation** and **polarisation** using RAW	n.d.	n.d.	10 nM and 100 nM	72H	Upregulation of the protein TIM-3, and a decrease in IL-6 and TNFα production, with an increase in IL-10 and TGF-β production.	(297)

5.1.6. TLR expression

Macrophages express PRRs, enabling them to respond to pathogenic challenge. Peripheral monocytes and tissue-resident macrophages have been shown to express a variety of TLRs including TLR2 and TLR4 (309–311). The degree of TLR expression may depend upon the local cytokine milieu, the presence of a stimulus, the activity and polarisation of the macrophage, and the location in which the macrophage resides (312,313).

5.1.7. Tumour necrosis factor alpha (TNFα)

TNFα is a pleiotropic cytokine that is capable of inducing apoptotic and necrotic cell death. It is secreted by a variety of cell types, but most predominantly by cells of the monocytic lineage, including macrophages. TNFα signals through two notable TNF receptors, TNFR1 and TNFR2. TNFR1 is expressed constitutively throughout mammalian tissue, and TNFR2 expression is restricted to particular cell types, including myeloid cells, T-regulatory cells (T-regs), glial cells, and endothelial cells. TNF receptor expression has also been shown to be inducible within epithelial cells, fibroblasts, T-cells, and B-cells (314). High levels of TNFα can lead to irreversible tissue damage due to its ability to induce apoptosis and necrosis. TNFα plays a crucial role within the immune system and is associated with a plethora of inflammatory diseases. TNFα can carry out a range of functions due to its ability to signal through multiple pathways (315). Within normal physiological function, TNFα conveys resistance to infection and immune stimulation, tumour resistance, sleep regulation, and embryonic development. It may also exacerbate the body’s response to infection, sometimes leading to subsequent tissue damage. TNFα is also capable of inducing the production of

other inflammatory cytokines, including: IL-1α, IL-6, IL-8, IFNβ, and more TNFα (316).

5.1.8. Interleukin 1 beta (IL-1β)

IL-1β is a pro-protein produced by monocytes and macrophages, and activated through proteolytic cleavage via caspase-1 (317,318). Keratinocytes can produce the inactive form of IL-1β, but do not possess the ability to cleave it into its active form (319). IL-1β plays an important role in host defence to infection. As with TNFα, IL-1β is also implicated in many inflammatory diseases (320). IL-1β is recognised by IL-1R and IL-1R2 both in conjunction with IL-1R3, these elicit pro- and anti-inflammatory responses, respectively (321). IL-1β leads to the further activation of macrophages and neutrophils to phagocytose and produce reactive oxygen and nitrogen species in response to an invading pathogen (318).

5.1.9. Macrophage cell surface marker expression

CD68, a marker of cells of monocytic lineage, is a valuable marker for the immunostaining of monocytes and macrophages. It is initially expressed intracellularly, and predominantly resides in endosomes and lysosomes, but is known to be shuttled to the cell surface. The murine CD68 orthologue, macrosalin, is present at the cell surface of macrophages (322). The role of CD68 has not been fully elucidated, however it has been proposed as a scavenger receptor, and possibly plays a role in antigen presentation (323). CD206, also known as C-type mannose receptor-1, is a cell surface marker commonly reported to be expressed on M2 macrophages (305). Furthermore, resident dermal macrophages are reported to constitutively express CD206 (324). CD163, also known as haemoglobin-haptoglobin scavenger receptor, is a cell surface marker

reported most frequently within M2-like macrophages, and is associated with high levels of IL-4, M-CSF, IL-6, and IL-10 (305,306). Macrophages co-expressing CD206 and CD163 express traits typical of the regulatory M2-like macrophage, including high levels of IL-10 and IL-1 receptor antagonist expression, and a high level of apoptotic cell uptake (325). CD163 alone has been reported insufficient as a M2-like macrophage marker, therefore in the present study it has been used in conjunction with CD206 (326).

5.2. Aims

1. To determine whether THP-1-derived M1-like and M2-like macrophages are suitable to be employed for the formation of an immunocompetent 3DOMM.
2. To determine the most suitable way to incorporate THP-1 cells into the model matrix.
3. To determine whether differentiation and polarisation of THP-1 cells is required in the 3DOMM environment.

5.3. Materials and Methods

5.3.1. Differentiation/polarisation of THP-1 cells

To form M1-like and M2-like macrophages, THP-1 cells were exposed to PMA, Sigma Aldrich P1585, or VD3, Sigma Aldrich D1530, at final concentrations of 25 ng/ml and 10 ng/ml, respectively. THP-1 cells (1×10^6 cells/ml) were cultured in the presence of 25 ng/ml of PMA for 72 hours, washed, and allowed to rest for a further 24 hours, prior to use for experimentation. THP-1 cells (1×10^6 cells/ml) were cultured in the presence of 10 ng/ml VD3 for 96 hours, then VD3 was refreshed at the same concentration and cultured for a further 96 hours. Prior to use, cells were washed in DPBS.

5.3.2. Production of IC3DOMMS

IC3DOMMs are three-dimensional oral mucosal models that incorporate THP-1 cells into the model matrix. All reagents were held on ice, for each model: 250 µl of collagen was mixed with 375 µl RPMI + 10% FBS, 156 µl of HGF-cells (2.4×10^5 cells/ml), 156 µl of THP-1 cells (2.4×10^5 cells/ml), and approximately 37 µl of 1 M NaOH. The model mixture was inverted to mix the reagents, and 800 µl was transferred to the well of a 12 well 0.4 µm polycarbonate mesh transwell insert. The model matrices were incubated at 37°C in a humidified 5% CO_2 incubator until polymerised. Once polymerised the gel matrix was overlaid with 0.4 ml of HaCaT cells (5.4×10^5 cells/ml) suspended in RPMI + 10% FBS. Models were raised to the air-liquid interface after 48 hours, thereafter the PMA/VD3 differentiation and polarisation protocol was followed, and the models were subsequently used for experimentation at day 12.

5.3.3. THP-1 differentiation and polarisation within IC3DOMMS

PMA and VD3 were added to the bottom of the transwell after IC3DOMMs were raised to the air-liquid interface, to form M1-like and M2-like macrophages, respectively. The average volume of the IC3DOMM after contraction was calculated by deducting the volume of any expelled media from the starting volume of 1200 µl, and was taken into account alongside the 500 µl of media added below the transwell. PMA and VD3 were added as per the THP-1 polarisation and differentiation protocol, and set to a final concentration of 25 nM and 10 nM, respectively, **Figure 39**. As it is necessary to maintain the concentration of PMA and VD3 during use, media was only changed upon the necessary wash steps indicated in the differentiation and polarisation protocol. Models were cultured for 12 days prior to use.

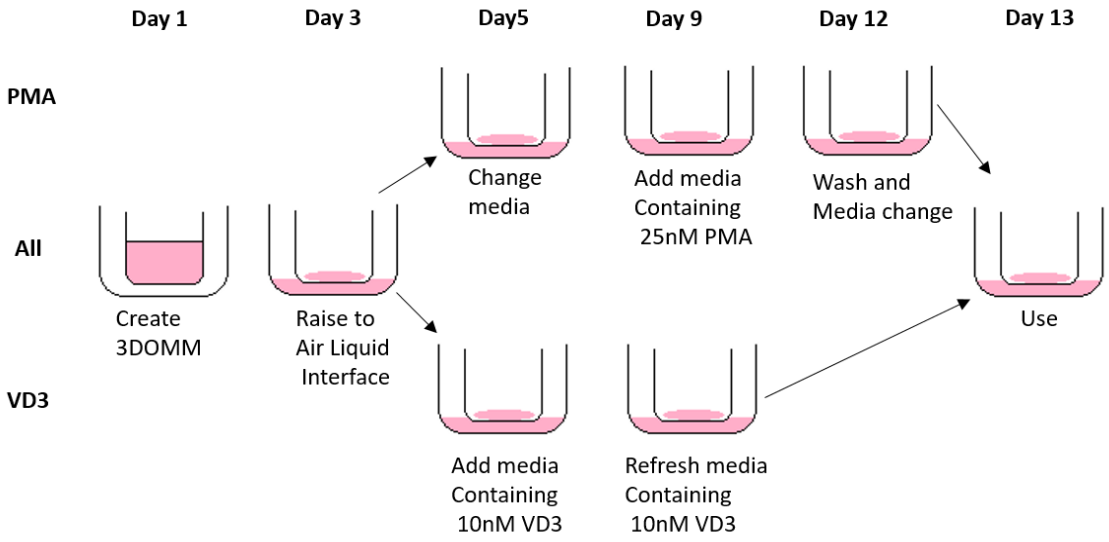

Figure 39: In situ differentiation and polarisation of THP-1 cells incorporated into IC3DOMMs using PMA and VD3.

5.3.4. Cell trace far red (CTFR) staining and imaging

For all CTFR-based experiments, THP-1 cells were washed in DPBS, counted and resuspended at a density of 2.5 × 10^5 cells/ml in 2 ml of PBS, along with 2 µl/ml of CTFR, FisherSci- 15531783, and gently resuspended. The cell suspension was incubated in the dark at 37°C for 20 minutes, and the reaction halted through the addition of serum containing medium. Cells were pelleted and resuspended at the desired seeding density. For THP-1 cells embedded into the model matrix, models were formed using CTFR-stained THP-1 cells as per the IC3DOMM protocol. Models were cryostat sectioned and viewed using confocal microscopy. For THP-1 cell recruitment, 1 × 10^5 THP-1 cells were added below a free-floating 3DOMM (formed as detailed in chapter 2), that was cultured until day 14, for either 24 or 72 hours in the presence or absence of stimuli (10,000 pg/ml MCP-1, R&D systems DY479, 20 ng/ml PMA, or 10 µg/ml LTA). Models were imaged intact, from the apical surface, using confocal microscopy, as detailed in section 2.7.2.

5.3.5. Cryostat sectioning

IC3DOMMs were cultured for 12 days and cryofixed in OCT mounting media, Agar Scientific AGR1180, using dry ice. Tissues were then mounted upon a sectioning chuck using OCT mounting media, and 4 µm sections cut using a Leica CM1100 cryostat, and mounted onto glass slides. Sections were cover-slipped and sealed to prevent drying. Cryostat sections were observed using confocal microscopy, as detailed in section 2.7.2.

5.3.6. ELISA

ELISAs were performed as detailed in section 2.8.

5.3.7. Response to the IC3DOMM environment

Each cell type (THP-1, HGF, and HaCaT) was stimulated with collagen, supernatant of the other cell types, and killed cells of the other cell types, **Figure 40**. Cells were studied at the same density they occur within the IC3DOMM. THP-1 and HGF cells were therefore seeded at a density of 3.07×10^4 cells/ml, and HaCaT cells at 2.16×10^5 cells/ml.

The 3DOMM protocol was followed, using RPMI in place of DMEM, in the absence of transwell inserts, and in the absence of a HaCaT overlay, in order to introduce the cells to the collagen matrix. After 24 hours, supernatant was collected by aspiration after centrifugation at 200 x g, and stored at -20˚C for subsequent analysis by sandwich ELISA. This was conducted to determine whether the collagen matrix stimulated pro-inflammatory cytokine production by each individual cell type.

To challenge cells with the supernatant of the other cell types contained within the IC3DOMM, supernatant was collected from the wells of cells set at the same seeding density they occur within a singular IC3DOMM, and used to stimulate the other cell types contained within the model. This was achieved in a pulse-chased manner, whereby the supernatant was added to the cell line for 4 hours, at a 1:1 ratio with RPMI + 10%FBS, and then removed via centrifugation (THP-1 cells), or aspiration (HGF and HaCaT cells). Cells were cultured for a further 18 hours prior to supernatant collection and storage at -20˚C for subsequent analysis by

sandwich ELISA. This was to determine whether soluble factors secreted by one cell type stimulated pro-inflammatory cytokine production another cell type.

Killed cells were fixed using 4% paraformaldehyde through incubation at 4˚C for 30 minutes, killed cells were then washed 5 times in PBS, and examined microscopically to ensure no viable cells were remaining. Killed cells were added to the model at the same density as indicated above for each cell type, cultured with the live cells for 24 hours prior to supernatant being collected and stored at -20˚C for ELISA. This was to determine whether contact with other cells stimulated pro-inflammatory cytokine production by model-incorporated cell types.

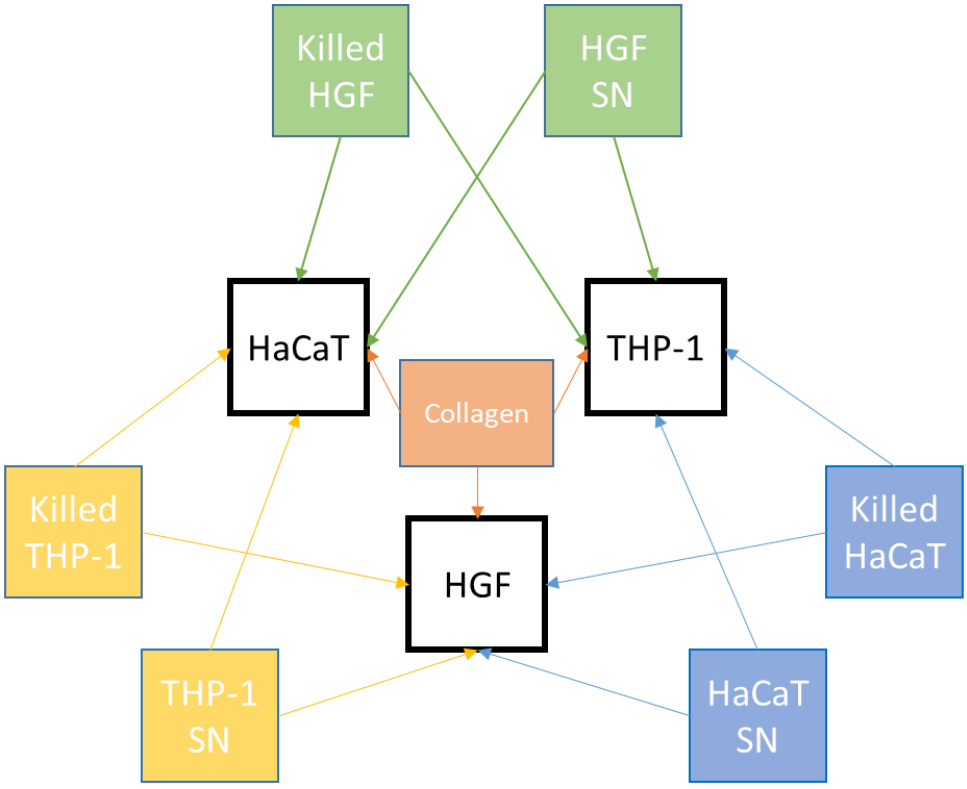

Figure 40: The effect of IC3DOMM components on HaCaT, HGF, and THP-1 cells
A diagram to demonstrate which model components (collagen, killed cells, and supernatant) were introduced to which model-incorporated cell types (HaCaT, HGF, and THP-1), in order to assess whether the model environment was inherently stimulatory at day 1 of model production.

5.3.8. LPS / LTA stimulation of cell lines

M1-like and M2-like macrophages were derived as per the differentiation and polarisation protocol, and seeded at a density of 1×10^6 cells/ml. Macrophages were then stimulated with 0.01, 0.1, and 1 µg/ml of PgLPS and K12 LPS; and 0.1,1, and 10 µg/ml of LTA. Supernatants were collected 18 hours post stimulation, stored at -20˚C, and subsequently analysed via sandwich ELISA, for the cytokines TNFα and IL-6.

5.3.9. HaCaT and HGF response to PMA and VD3

HaCaT and HGF were seeded at a density of 2.16×10^5 cells/ml and 3.07×10^4 cells/ml, respectively, equating to the quantity of cells seeded within a single 3DOMM, and allowed to adhere overnight. PMA and VD3 were added to HaCaT and HGF cells in the same manner as per the macrophage differentiation and polarisation protocol. Supernatants were collected 24 hours after the final wash step, and analysed for IL-6 and IL-8 cytokine production via sandwich ELISA.

5.3.10. Flow cytometry of macrophage polarisation markers

3DOMMs were created in transwell inserts using RPMI in place of DMEM, and THP-1 cells were seeded in the well below. Control wells, containing THP-1 cells only, were also seeded. The M1/M2 differentiation and polarisation protocols were followed, beginning on day 3 post-model production. At day 12, half of the test wells, including 3DOMM cultured and signally cultured THP-1s, were stimulated with 1 µg/ml of PgLPS, thereby creating 4 test groups: THP-1 control, THP-1 + LPS, THP-1 3DOMM, and THP-1 3DOMM + LPS. Eighteen hours post-stimulation cells were collected by gentle cell scraping (to maintain surface

antigens), and pooled for each test group, then washed 3 times in DPBS. Once washed each group of cells were divided into 3, and stained with PerCP-Cy5.5-labelled CD68, BioLegend 333814, and FITC-labelled CD206, BioLegend 321104, CD68 and FITC-labelled CD163, BioLegend 333618, and the respective isotype controls, BioLegend 400337 and BioLegend 400108. For each antibody, 5 µl was added to a maximum of 1×10^6 cells, and incubated on ice, in the dark for 20 minutes. Once stained, cells were washed 3 x in DPBS and their mean fluorescence intensity assessed flow cytometrically as detailed in section 2.9. All data were standardised to the mean isotype control value of the respective cell type.

5.3.11. Flow cytometry of macrophage TLR expression

THP-1 cells (control), M1-like, and M2-like macrophages were derived as per the macrophage differentiation and polarisation protocol. THP-1 cells, M1-like macrophages and M2-like macrophages were assessed unstimulated, and also assessed after pulse-chasing with 3DOMM supernatant. Supernatant from 3DOMMs at day 9 was used to stimulate 1×10^6 THP-1, M1-like and M2-like macrophages. 3DOMM supernatant was added to the macrophages at a 1:1 ratio with RMPI + 10% FBS, control wells contained RPMI + 10% FBS without stimulus. Model supernatant was cultured with the macrophages for 4 hours. Model supernatant was removed from the macrophages either via centrifugation (THP-1 and M2-like macrophages, due to their non-adherent nature) or direct aspiration (for the adherent M1-like macrophages), and replaced with RPMI + 10% FBS. Cells were cultured for a further 18 hours, prior to final supernatant collection. Supernatant was assessed via sandwich ELISA, for the pro-inflammatory cytokines TNFα, IL-6 and IL-1β. Post-stimulation, cells were collected, washed 3

times in DPBS, and stained with either TLR2 antibody, TLR4 antibody or the appropriate isotype control, and assessed flow cytometrically, as detailed in section 3.3.10.

5.3.12. Data analysis and statistics

Statistical analyses are indicated in the figure legend for each experiment, including which statistical tests were performed, and the number of experimental repeats. For all ELISA data, as standard a minimum of three independent experimental repeats, containing three biological replicates were performed, unless stated otherwise. For each biological replicate, a minimum of 2 technical replicates were performed. For flow cytometry data, experiments were performed at a minimum of two independent experimental replicates, with at least three biological replicates, which were pooled prior to analysis. Unless stated otherwise, three technical replicates of 10,000 events were analysed. Data was standardised to a percentage of the isotype control in order to make statistical comparisons, due to the well reported variation in flow cytometry data between each experimental repeat. Also indicated in the figure legend is which groups were compared, if unstated, a comparison was made between all groups. To select the appropriate statistical test, using GraphPad, a Shapiro-wilk test for normality was performed to determine data normality of all groups intended to be statistically compared. Parametric data was assessed with the use of a one-way ANOVA, followed by a Tukey's multiple comparisons test. Non-parametric data was determined using a Kruskal-Wallis test followed by a Dunn's multiple comparisons test. For all, *p*-values lower than 0.05 were taken to indicate statistical significance.

5.4. Results

5.4.1. Serum batch testing

Prior to the implementation of THP-1 cells within this study, a batch test was performed to identify a serum batch that did not lead to the stimulation of the cells. Five serum batches were tested and **Sigma Aldrich 3204** was selected as overall it led to the lowest levels of pro-inflammatory cytokine production within THP-1, M1-like, M2-like, HaCaT and HGF cells (data not shown).

5.4.2. THP-1 cell morphology

The morphology of THP-1 cells and both M1-like and M2-like macrophages was observed after following the differentiation and polarisation protocol, **Figure 41**. THP-1 cells appeared mostly rounded, with clear intact cell membranes, and few apoptotic cells within the field of view. M1-like macrophages appeared elongated, with some cells exhibiting numerous pseudopodia; in general M1-like macrophages had lost their rounded morphology. M2-like macrophages presented similar in morphology and size to the THP-1 cells, with three notable differences: semi-adherence, irregular borders, and increased granulation.

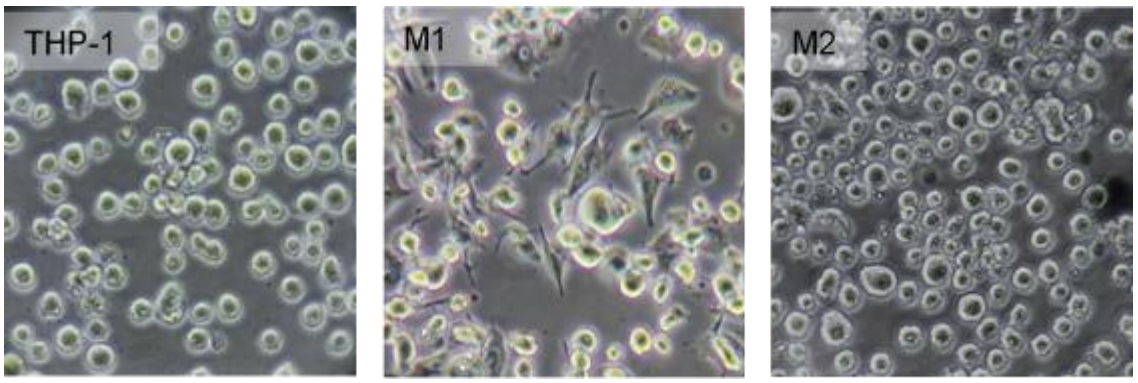

Figure 41: Images of THP-1, M1-like and M2-like macrophages in active culture.
From previous page: cells were cultured in RPMI + 10% FBS. M1-like and M2-like macrophages were differentiated and polarised using PMA and VD3, respectively. Images were taken at 200 X magnification.

5.4.3. Pro-inflammatory cytokine production in response to PAMPs

The overall purpose of developing an IC3DOMM was to produce a model that is representative of the *in vivo* response to pathogens, hence able to recognise and respond to pathogenic stimuli. Therefore, prior to commencing model development, M1-like and M2-like macrophages were stimulated with PgLPS, K12 LPS, and LTA in order to ensure they were able to respond to PAMPs and hence pathogens, **Figure 42**. Furthermore, a dose response was performed for each PAMP so that any subsequent experimentation could be performed at a responsive yet quantifiable dose.

TNFα production by M1-like and M2-like macrophages stimulated by 1 µg/ml of PgLPS was significantly greater than the unstimulated control and lower dosages of PgLPS. M1-like macrophages stimulated with all concentrations of K12 LPS produced significantly more TNFα than when unstimulated, however there were no significant differences between concentrations. The only K12 LPS concentration which produced a significantly different TNFα response in M2-like macrophages when compared to the unstimulated control was 1 µg/ml. For both M1-like and M2-like macrophages, stimulation with 10 µg/ml of LTA caused a significant increase in TNFα expression when compared with the unstimulated control, yet lower concentrations did not produce a significant response for either cell type. From these data, it was possible to see that THP-derived M1-like and

M2-like macrophages were responsive to PAMPs. Concentrations of 1 µg/ml of PgLPS and K12 LPS were selected as a suitable concentration for subsequent M1-like and M2-like macrophage experimentation, as well as 10 µg/ml of LTA. These concentrations were able to evoke a significantly different level of pro-inflammatory cytokine production within all cell types when compared to their respective unstimulated controls.

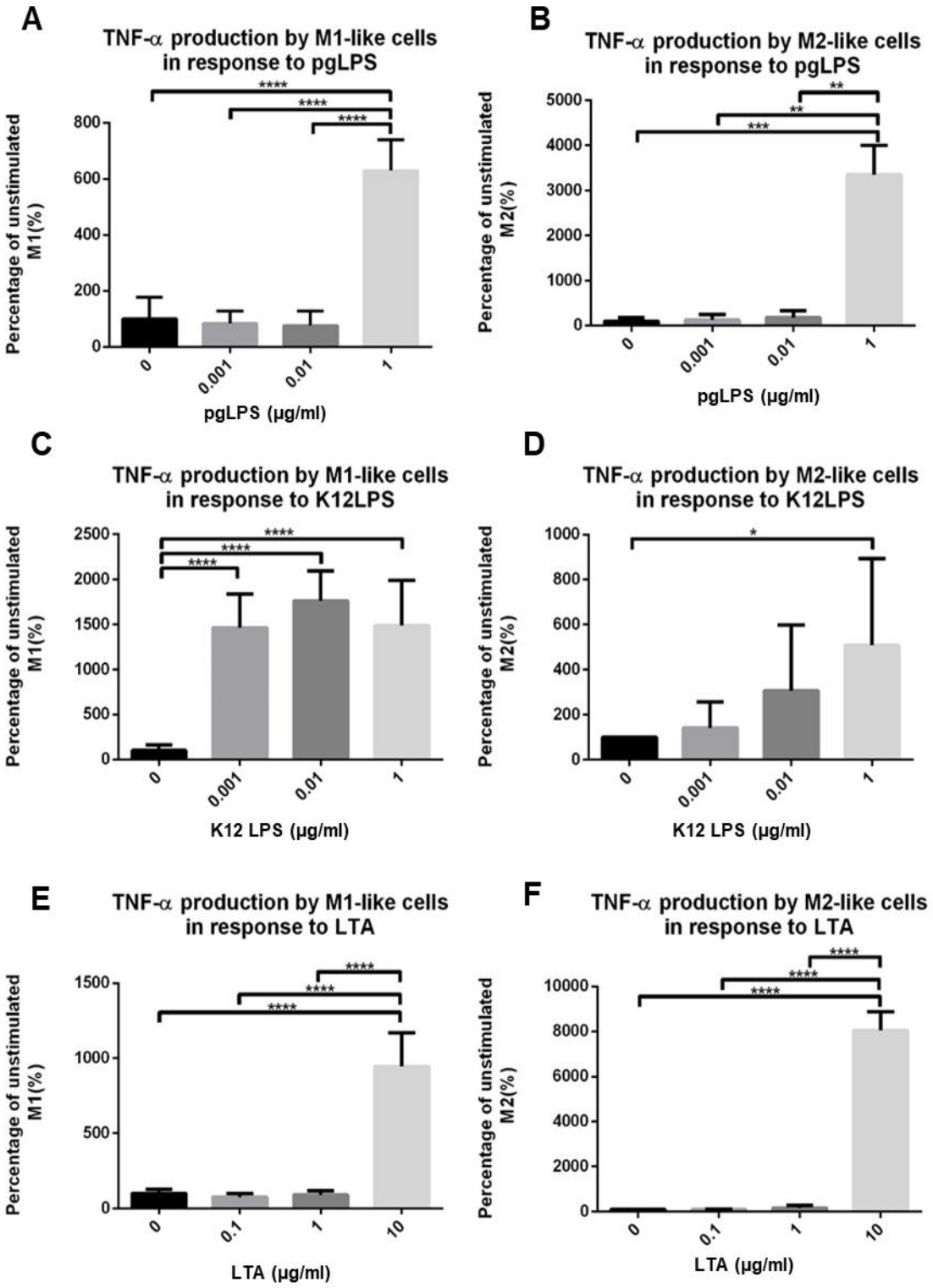

Figure 42: TNFα production by M1-like and M2-like macrophages in response to differing doses of PgLPS, K12 LPS and LTA.

M1-like and M2-like TNFα pro-inflammatory cytokine production in response to 18 hours of stimulation with increasing doses PgLPS (A and B respectively), K12 LPS (C and D respectively), and LTA (E and F respectively). Graphs indicate one experimental repeat, performed in triplicate, as a preliminary experiment to select dose and confirm response. Cytokine expression was determined via sandwich ELISA. Significant differences were

determined between all groups. Data normality was assessed using the Shapiro-Wilk test for normality. Statistical significance for M2-like production of TNFα in response to PgLPS and K12 LPS a Kruskal-Wallis test, followed by a Dunn's multiple comparisons test. Statistical significance for all other experiments was determined using a one-way ANOVA followed by a Tukey's multiple comparison's test. Statistical significance is indicated on the graph (* $p < 0.05$, ** $p < 0.01$, *** $p < 0.001$, **** $p < 0.0001$). Error bars represent standard deviation. This data was collected in collaboration with Hélène Stern.

5.4.4. Incorporation of THP-1 cells into the model

Following the confirmation that the THP-1-derived M1-like and M2-like macrophages were able to respond to pathogenic stimuli, IC3DOMM development was continued. In order to determine the best way to incorporate THP-1 cells, and subsequent M1-like and M2-like macrophages into the model, many considerations had to be made. Firstly the question was raised as to whether it is more appropriate to embed or to recruit THP-1 cells into the 3DOMM matrix.

THP-1 cells are immortalised and continue proliferating, observations within preliminary studies have indicated that M1-like macrophages have a limited lifespan once terminally differentiated, and the lifespan of M2-like macrophages is even shorter. It is unknown as to whether this limited lifespan is also seen when incorporating the M1-like and M2-like macrophages into the model. Furthermore, the viability and proliferation status of THP-1 cells in a collagen matrix is yet to be determined. Therefore, prior to commencing further research, a preliminary experiment was performed at n = 1; THP-1 cells and the short-lived M2-like macrophages were embedded into the matrix and followed for 4 days, **Figure 43**. It was shown that THP-1 cells appeared viable with clear illuminated boundaries, and when embedded alongside fibroblasts, appeared in relative stasis with no

obvious evidence of population doublings occurring once embedded into the matrix. After only four days, there were no remaining viable M2-like macrophages; they had no clear boundary, and appeared to have undergone lysis.

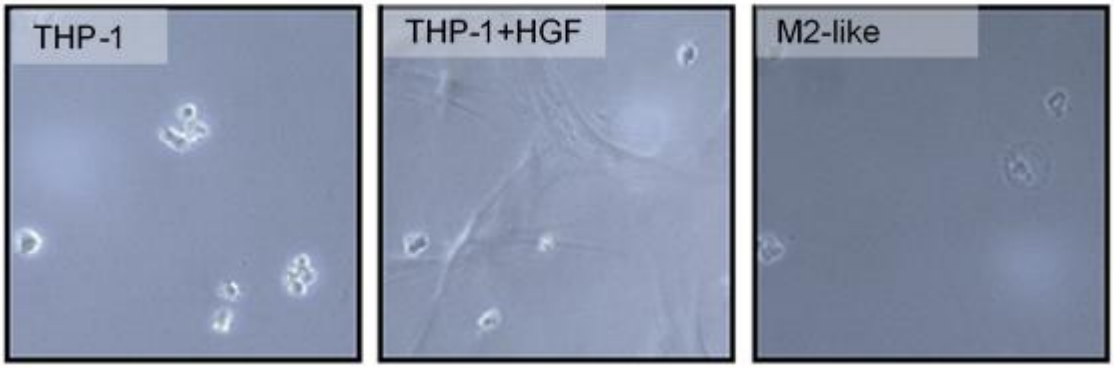

Figure 43: Images of THP-1, THP-1 and HGF, and M2-like macrophages embedded in a collagen matrix.
Cells were cultured in RPMI + 10% FBS. M2-like macrophages were differentiated and polarised using VD3. THP-1 cells and M2 like macrophages were embedded in a collagen matrix, formed as per the IC3DOMM protocol, in the absence of keratinocytes. Cells were cultured in the matrix for 4 days and then imaged at 200 X magnification.

With the knowledge that M2-like macrophages do not survive in the matrix for long, the incorporation of pre-differentiated macrophages at day 1 of 3DOMM production was ruled out. Next, it was determined whether it would be more suitable to recruit THP-1 cells into the model towards the end of the model growth period, or to embed THP-1 cells into the matrix upon model production.

First, THP-1 cells were embedded into the model matrix at day 1 of model production, and subsequently differentiated/polarised *in situ*. At day 14 of model production the morphology and viability of THP-1 and THP-1-derived cells were observed using confocal microscopy, **Figure 44**. THP-1 cells added to the model

matrix appeared viable, with distinct areas of fluorescence regardless of differentiation protocol. THP-1 cells from all groups appeared larger than usual, and a further enlarged image of THP-1 cells introduced to the PMA differentiation protocol displayed a non-rounded morphology suggestive of a macrophage.

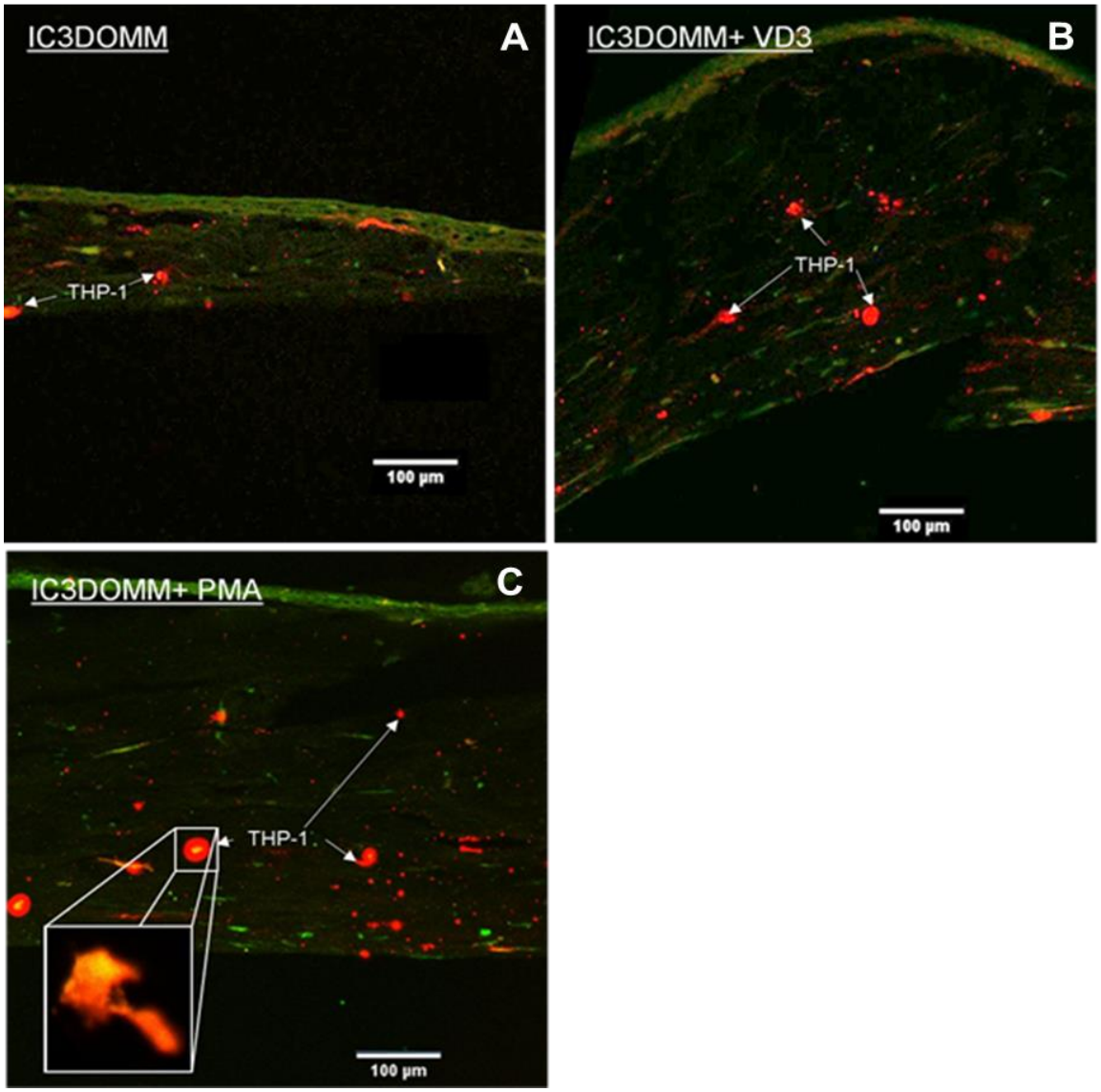

Figure 44. THP-1-derived macrophages differentiated *in situ*
Confocal microscopy images of a cryostat sectioned IC3DOMMs at day 14 of culture. THP-1 cells were stained with cell-trace far red (CTFR) and incorporated into the model matrix at day 1. IC3DOMMs were cultured in RPMI+10%FBS (A), with the addition of VD3 (B) or PMA (C), following the IC3DOMM differentiation and polarisation protocol. Tissue cross-sections are displayed with the epithelium at the top. Labels indicate THP-1 cells in the lamina propria layer. An enlarged area of a PMA stimulated THP-1 cell, contained within the IC3DOMM is indicated by the white box. Green = auto-fluorescence, red = CTFR staining of THP-1 cells. Images were taken at 50 X magnification.

In parallel to this THP-1 cells were introduced to the periphery of 3DOMMs in order to determine whether cells migrate into the model matrix unaided or with the aid of exogenous factors. The following were added to the epithelium of the 3DOMM: MCP-1 a chemoattractant for monocytes; PMA a differentiation promotor; and LTA a TLR2 agonist. Models were cultured for 24 and 72 hours with CTFR stained THP-1 cells, and viewed and imaged using a confocal microscope in the presence and absence of such stimuli.

Figure 45 indicates THP-1 cells associated with the periphery of the 3DOMM. The exact localisation of THP-1 cells was difficult to determine as the models were imaged live in their full-thickness state. However, with the aid of Z-stack technology it was possible to view the entirety of 3DOMMs layer by layer, which suggested that THP-1 cells were associated with the periphery and not necessarily distributed throughout the model epithelium or matrix. Images displayed are a representative sample of one plain of view.

THP-1 cells are present in all images, except for the negative control and 3DOMMs imaged after 72 hours of co-culture with THP-1 cells. THP-1 cells are indicated in red, and appeared to be circular, with clear boundaries. Cells incubated in the presence of LTA, MCP-1 and PMA stimuli appeared to be more numerous in models co-cultured with the stimulated THP-1 cells for 72 hours as opposed to 24 hours. For unstimulated THP-1 cells incubated with the 3DOMM, cells appeared more numerous at 24 hours and were absent at 72 hours. Due to the success of THP-1 cells embedded into the model, this study was not repeated, despite producing inconclusive results in terms of the localisation of THP-1 cells.

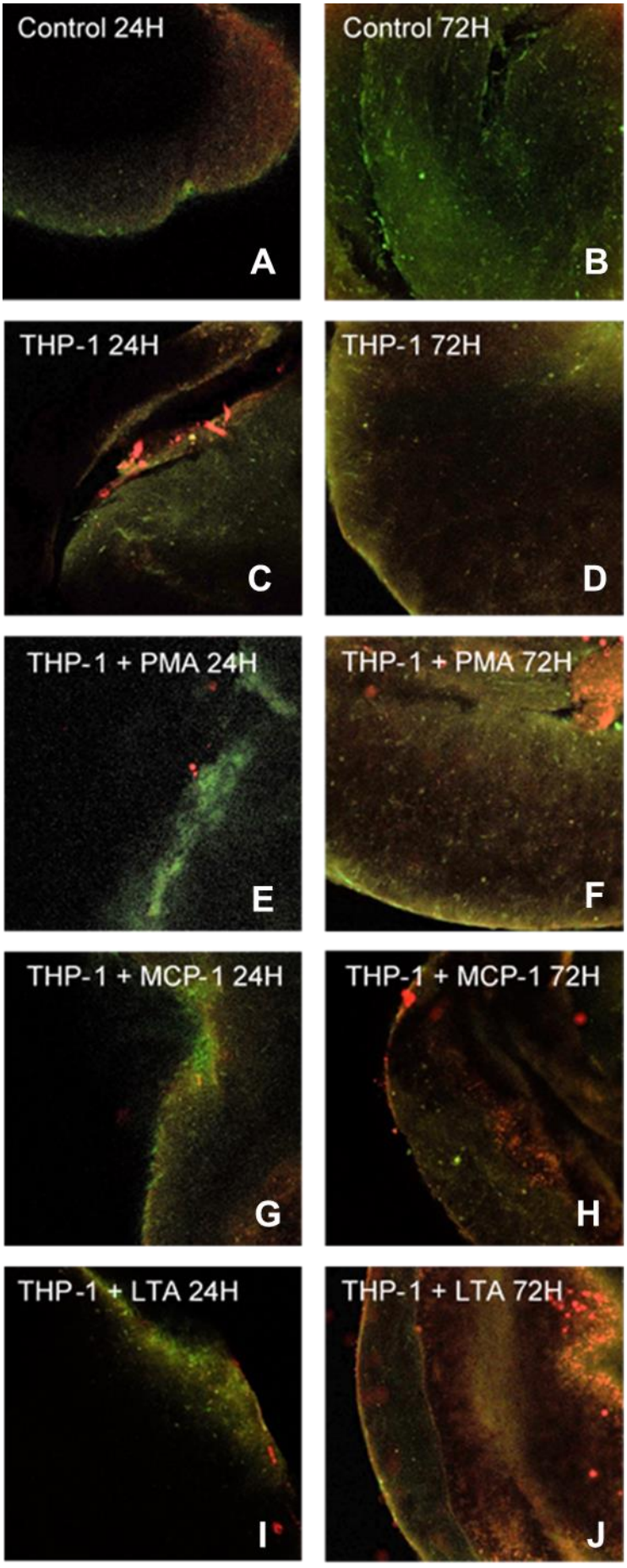
Control 24H
A
Control 72H
B
THP-1 24H
C
THP-1 72H
D
THP-1 + PMA 24H
E
THP-1 + PMA 72H
F
THP-1 + MCP-1 24H
G
THP-1 + MCP-1 72H
H
THP-1 + LTA 24H
I
THP-1 + LTA 72H
J

Figure 45: THP-1 cells added to the periphery of 3DOMMs
From previous page: confocal microscopy images of THP-1 cells added to the periphery of 3DOMMS at day 14 of culture. THP-1s were co-cultured with the 3DOMMs for either 72 or 24 hours. MCP-1 was added to the apical surface of the 3DOMMs. PMA and LTA were added to the supernatant alongside the THP-1 cells. 3DOMMs were oriented laterally for imaging. Images A and B represent control models which did not contain THP-1 cells for 24 and 72 hours respectively. Images C and D represent models introduced to THP-1 cells in the absence of stimulus for 24 hours and 72 hours respectively. Images E and F indicate models incubated with THP-1 cells with PMA for 24 and 72 hours respectively. Images G and H indicate models incubated with THP-1 cells and MCP-1 for 24 and 72 hours respectively. Images I and J indicate models incubated with THP-1 cells and LTA for 24 and 72 hours respectively. All images were taken at 50 X magnification.

5.4.5. The effect of the IC3DOMM environment on HaCaT, HGF and THP-1 cells

The most suitable means of incorporating THP-1 cells into the IC3DOMM was to embed the THP-1 cells into the model matrix upon model production and differentiate them *in situ*. It was decided to determine the effect of the IC3DOMM components on THP-1 cells, and the effect of the THP-1 cells on HaCaT and HGF cells, as all of these components make up the IC3DOMM environment and may affect the activity of the incorporated cell types. As within chapter 3, each cell type was stimulated with killed cells to determine the effect of cellular contact. Cells were also stimulated with cellular supernatant, to determine the effect of soluble factors secreted from the other cell types that constitute the IC3DOMM, and the collagen matrix itself. Cellular response to these 3DOMM components was determined by pro-inflammatory cytokine production, IL-6 and IL-8 for all cell types, with the addition of TNFα for THP-1 cells, **Figure 46**, **Figure 47** and **Figure 48**.

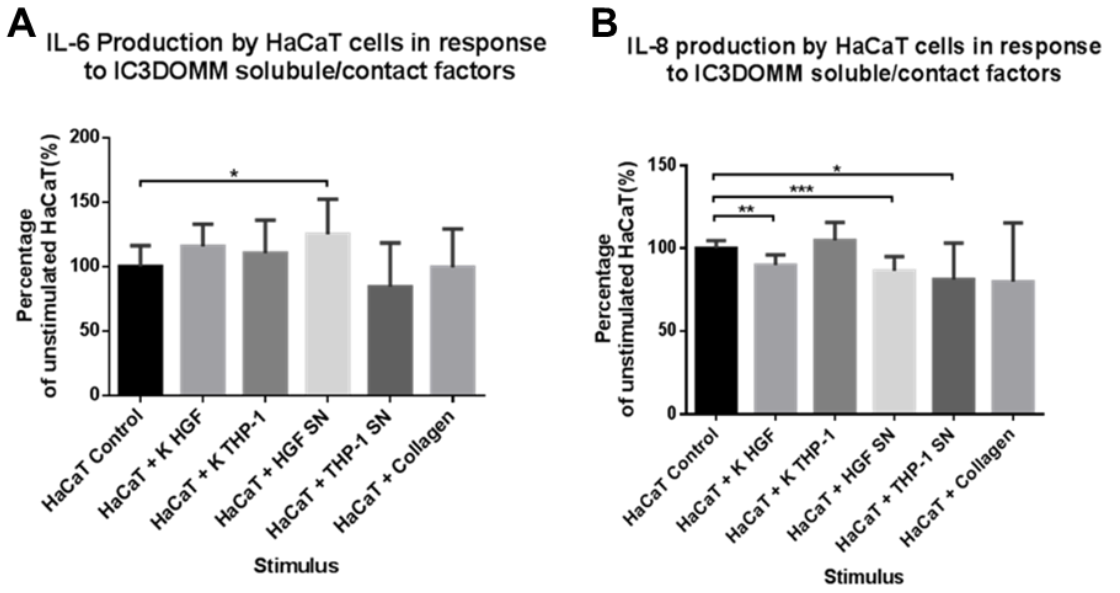

Figure 46: HaCaT pro-inflammatory cytokine production (IL-6 and IL-8) when stimulated with IC3DOMM components.

Pro-inflammatory cytokine production, IL-6 (A) and IL-8 (B), by HaCaT cells stimulated with: paraformaldehyde-killed cells (HaCaT + K HGF), (HaCaT + K THP-1), supernatant (HaCaT + HGF SN), (HaCaT + THP-1 SN), and collagen (HaCaT + collagen), was determined. Killed cells and collagen were added for 24 hours prior to supernatant collection. Supernatant was added to the cells for 4 hours and then removed; cells were incubated for a further 18 hours prior to supernatant collection. Cytokine expression was determined via sandwich ELISA. Graphs indicate three experiments, performed in triplicate. Significant differences were determined between the unstimulated HaCaT control and all test groups. Data normality was assessed using the Shapiro-Wilk test for normality. Statistical significance for IL-8 production by HaCaT cells in response to IC3DOMM soluble/contact factors was determined using a Kruskal-Wallis test, followed by a Dunn's multiple comparisons test. Statistical significance for IL-6 production by HaCaT cells in response to IC3DOMM soluble/contact factors was determined using a one-way ANOVA followed by a Tukey's multiple comparison's test. Statistical significance is indicated on the graph (* $p < 0.05$, ** $p < 0.01$, *** $p < 0.001$, **** $p < 0.0001$). Error bars represent standard deviation.

HaCaT cells stimulated with pulse-chased HGF supernatant produced significantly more IL-6 and IL-8 than when unstimulated ($p = 0.0174$ and $p = 0.0008$, respectively). A significant increase in IL-8 production was also observed when HaCaT cells were stimulated with killed fibroblasts or when pulse chased with THP-1 supernatant, when compared with the unstimulated control ($p = 0.093$ and $p = 0.00161$, respectively), **Figure 46**.

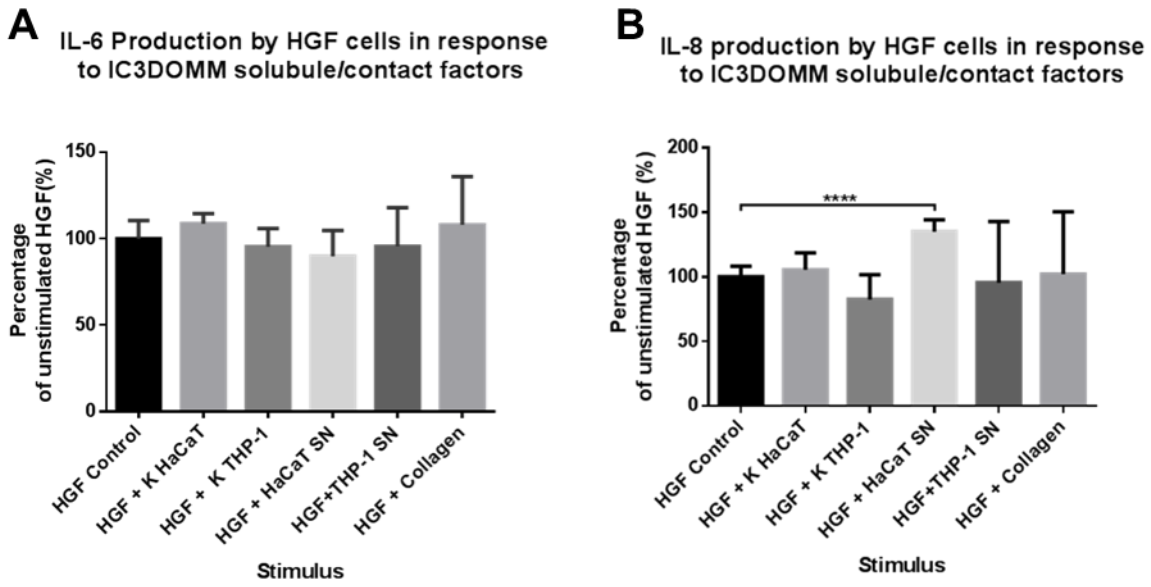

Figure 47: HGF pro-inflammatory cytokine production (IL-6 and IL-8) when stimulated with IC3DOMM components.

Pro-inflammatory cytokine production, IL-6 (A) and IL-8 (B), by HGF cells stimulated with: paraformaldehyde-killed cells (HGF + K HaCaT), (HGF + K THP-1), Supernatant (HGF + HaCaT SN), (HGF + THP-1 SN), and collagen (HGF + collagen). Killed cells and collagen were added for 24 hours prior to supernatant collection. Supernatant was added to the cells for 4 hours and then removed; cells were incubated for a further 18 hours prior to supernatant collection. Cytokine expression was determined via sandwich ELISA. Graphs indicate three experiments, performed in triplicate. Significant differences were determined between the unstimulated control and all test groups. Data normality was assessed using the Shapiro-Wilk test for normality. Statistical significance for all groups was determined using a Kruskal-Wallis test, followed by a Dunn's multiple comparisons test. Statistical significance is indicated on the graph (* $p < 0.05$, ** $p < 0.01$, *** $p < 0.001$, **** $p < 0.0001$). Error bars represent standard deviation.

IC3DOMM components did not cause a significant increase in IL-6 production by HGF cells, in comparison to the unstimulated control, **Figure 47**. However, HGF cells pulse-chased with HaCaT supernatant led to a significant increase in IL-8 production when compared to the unstimulated control ($p < 0.0001$).

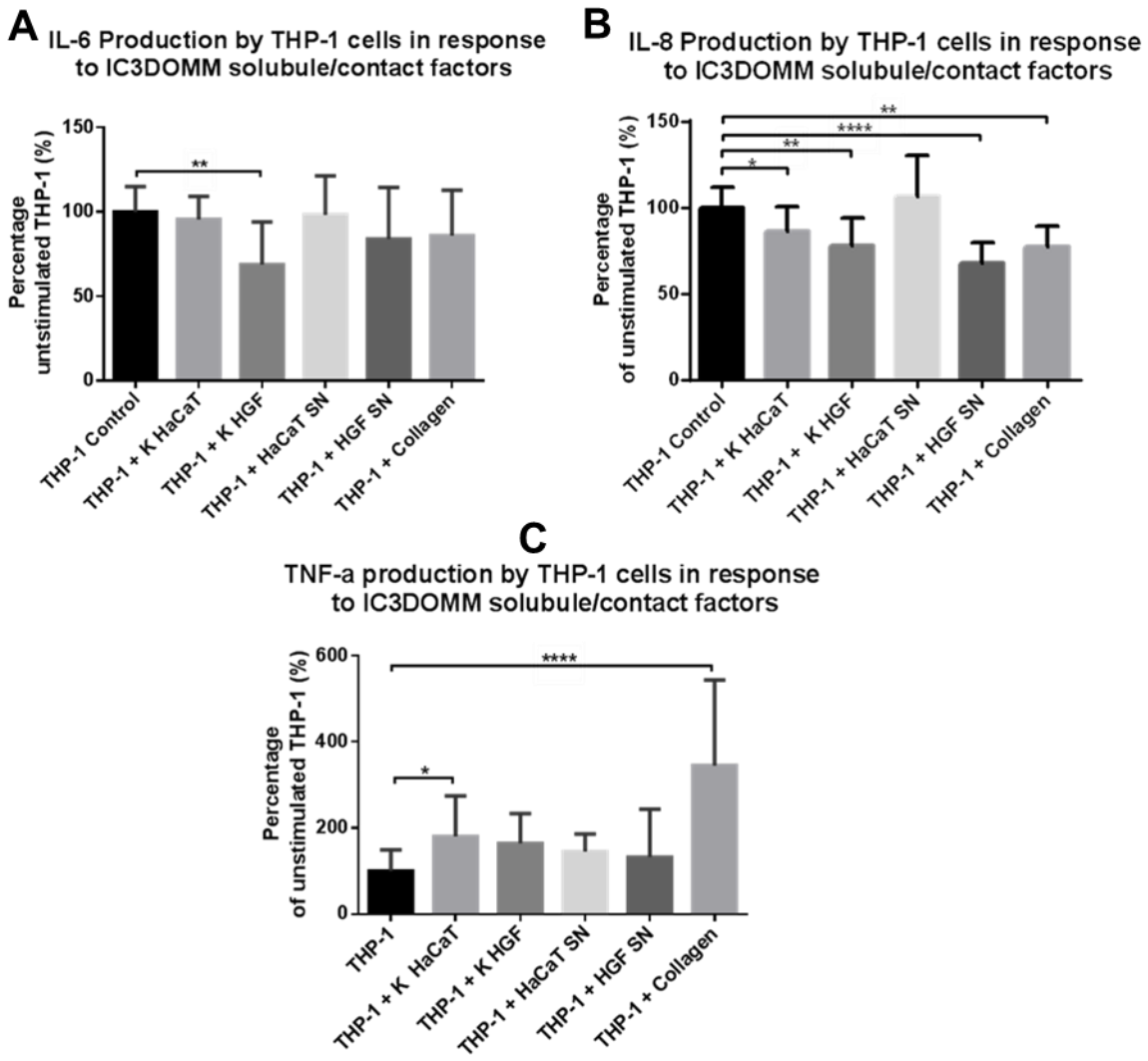

Figure 48: THP-1 pro-inflammatory cytokine production (IL-6, IL-8 and TNFα) when stimulated with IC3DOMM components.

Pro-inflammatory cytokine production, IL-6 (A), IL-8 (B), and TNFα (C) by THP-1 cells stimulated with: paraformaldehyde killed cells (THP-1 + K HaCaT), (THP-1 + K HGF), supernatant (THP-1 + HaCaT SN), (THP-1 + HGF SN), and collagen (THP-1 + collagen). Killed cells and collagen were added for 24 hours prior to supernatant collection. Supernatant was added to the cells for 4 hours and then removed; cells were incubated for a further 18 hours prior to supernatant collection. Cytokine expression was determined via sandwich ELISA. Graphs indicate three experiments, performed in triplicate. Significant differences were determined between the unstimulated control and all test groups. Data normality was assessed using the Shapiro-Wilk test for normality. Statistical significance for TNFα production was determined using a Kruskal-Wallis test, followed by a Dunn's multiple comparisons test. Statistical significance for IL-6 and IL-8 production was determined by one-way ANOVA followed by a Tukey's multiple comparisons test. Statistical significance is indicated on the graph (* $p < 0.05$, ** $p < 0.01$, *** $p < 0.001$, **** $p < 0.0001$). Error bars represent standard deviation.

THP-1 cells produced significantly less IL-6 when introduced to killed fibroblast cells than when unstimulated (p = 0.0042), **Figure 48**. Other IC3DOMM components did not lead to a significant alteration in IL-6 production by THP-1 cells when compared to the unstimulated control. THP-1 cells produced significantly more IL-8 when they were unstimulated compared to when they were introduced to killed HaCaT cells, killed HGF cells, collagen, and HGF supernatant (p = 0.0429, p = 0.0014, p < 0.0001 and p = 0.0012, respectively). Collagen caused a highly significant increase in TNFα production when compared to the unstimulated control (p < 0.0001). Killed HaCaT cells also led to a significant increase in TNFα production by THP-1 cells when compared to the unstimulated control (p = 0.0361).

From this point onwards, THP-1 cells were to be incorporated into the matrix at the point of IC3DOMM production, meaning it may have been necessary differentiate and polarise THP-1 cells into macrophages *in situ.* For this reason, it was essential to determine the effect of PMA and VD3 on HaCaT and HGF cells. **Figure 49** indicates the baseline pro-inflammatory cytokine production by HaCaT and HGF cells upon following the differentiation and polarisation protocol as applied to THP-1 cells.

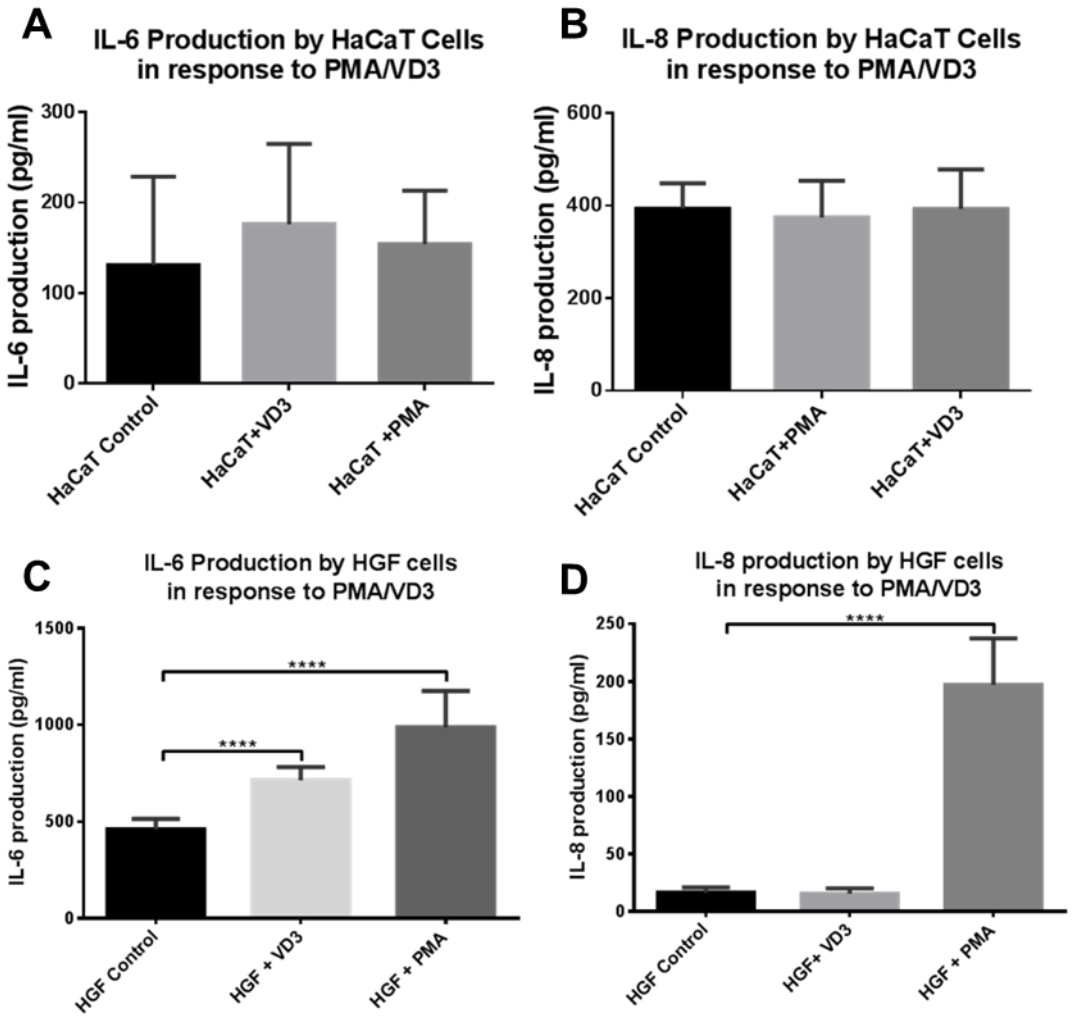

Figure 49: HaCaT and HGF cells pro-inflammatory cytokine production (IL-6 and IL-8) when grown in the presence of PMA and VD3.

IL-6 and IL-8 pro-inflammatory cytokine production was assessed after HaCaT (A and B, respectively) and HGF (C and D, respectively) cells were cultured in the presence of PMA and the VD3 for the duration of the THP-1 polarisation and differentiation protocol. Cytokine production was determined via sandwich ELISA. Graphs indicate three experiments performed in triplicate. Significant differences were determined between the test groups and respective control. Data normality was assessed using the Shapiro-Wilk test for normality. Statistical significance for HGF production of IL-8 in response to PMA and VD3 was determined using a Kruskal-Wallis test, followed by a Dunn's multiple comparisons test. Statistical significance for IL-6 production by HGF in response to PMA and VD3, and IL-6 and IL-8 production by HaCaT cells in response to PMA/VD3, was determined using a one-way ANOVA followed by a Tukey's multiple comparison's test. Statistical significance is indicated on the graph (* $p < 0.05$, ** $p < 0.01$, *** $p < 0.001$, **** $p < 0.0001$). Error bars represent standard deviation.

When HaCaT cells were treated with PMA or VD3, there was no significant increase in either IL-6 or IL-8 production when compared to the unstimulated HaCaT control. IL-6 production by HGF cells was significantly greater when treated with VD3, compared with when unstimulated ($p < 0.0001$). Both IL-6 and IL-8 production were significantly upregulated when PMA was introduced to the HGF cells ($p < 0.0001$ for both).

5.4.6. The effect of PMA and VD3 on model morphology

The effects of PMA and VD3 on 3DOMMs and IC3DOMMs were assessed via histology to determine how the differentiation and polarisation protocol affects model morphology. **Figure 50** indicates an intact epithelium atop a lamina propria layer for all models, with the exception of PMA stimulated IC3DOMMs.

Towards the basal layers, small condensed nuclei/nuclear fragments, which appear densely stained with haematoxylin, were present in 3DOMMs treated with PMA and VD3, and IC3DOMMs treated with PMA. This occurrence appeared more frequently within the THP-1 absent 3DOMMs, when treated with PMA.

Within models that contain THP-1 cells (IC3DOMMs), epithelial islands were observed within the lamina propria layer. An example of this can be seen within the PMA stimulated IC3DOMM, which displays a keratinocyte island, rather than the epithelium. This was coupled with a thinner overall epithelium. This phenomenon did not occur within the 3DOMMs.

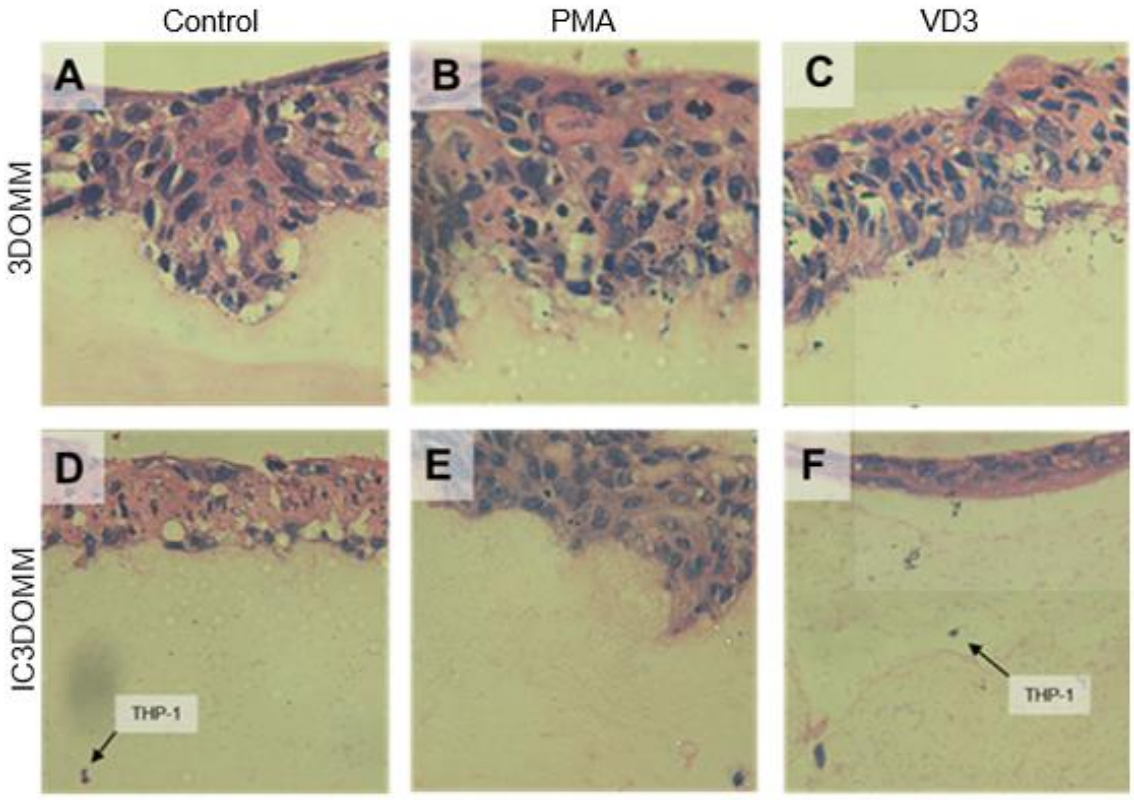

Figure 50: The effect of PMA and VD3 on 3DOMM and IC3DOMM morphology
A representative sample of haematoxylin and eosin stained, paraffin embedded, 4 µm sectioned, 3DOMMs and IC3DOMMs at day 14 (400 X magnification). Unstimulated 3DOMMs and IC3DOMMs (A and D respectively), 3DOMMs and IC3DOMMs cultured as per the PMA differentiation and polarisation protocol (B and E respectively), and 3DOMMs and IC3DOMMs cultured as per the VD3 differentiation and polarisation protocol (C and F respectively).

5.4.7. TLR expression by THP-1 derived macrophages

Seeing as M1-like macrophages and M2-like macrophages were shown to be responsive to PAMPs that are traditionally reported to signal through TLR2 and TLR4 (LTA and LPS), it was proposed that both of these receptors are expressed at the cell surface of the M1-like and M2-like macrophages. This was assessed flow cytometrically, with the additional aim of determining whether the 3DOMM environment alters the expression of such receptors.

THP-1, M1-like, and M2-like macrophages were assessed for the presence of TLR2 and TLR4 at the cell surface. Each cell type was also stimulated with supernatant from the 3DOMM in a pulse-chased manner, for 4 hours, and then cultured for a further 18 hours after the supernatant had been removed. This was performed in order to determine whether 3DOMM supernatant altered TLR expression at the cell surface, **Figure 51**. Data for TLR4 is not shown, as the mean fluorescence intensity value for all TLR4 groups was less than that of the isotype control, as also observed within Chapter 3.

THP-1 cells displayed two cell populations, identifiable by two peaks on the THP-1 histogram in **Figure 51**. Both unstimulated and 3DOMM stimulated THP-1 cells expressed TLR2, indicated by the higher mean value for TLR2 groups, than the value for the isotype control. This is represented in the histogram, due to the increase in mean fluorescence intensity (MFI) value for FITC by THP-1 cells stained with the TLR2 antibody, when compared to cells stained with the isotype control. Across the multi-population THP-1 cells, overall it would appear that unstimulated THP-1 cells expressed more TLR2 than cells treated with 3DOMM supernatant.

M1-like macrophages presented as a single cell population, with a clear distinct peak on the histogram. The MFI and hence histogram peak for TLR2 expression by unstimulated M1-like macrophages was greater than that of the isotype control, indicating TLR2 expression. Furthermore, the MFI and the histogram peak for 3DOMM-stimulated TLR2 expression by M1-like macrophages indicates that cells stimulated with 3DOMM supernatant appeared to express more TLR2 at the cell surface than unstimulated cells.

Two populations of M2-like macrophages are indicated in **Figure 51** with two peaks displayed on the histogram for both the isotype control and unstimulated TLR2 expression. 3DOMM stimulated M2-like macrophages presented with a more uniform cell population than their unstimulated counterparts, as indicated by only one peak on the histogram. For both unstimulated and 3DOMM stimulated M2-like macrophages, the mean fluorescence intensity value for TLR2 staining within both groups is less than that of the isotype control, suggesting that there is no TLR2 expression at the cell surface.

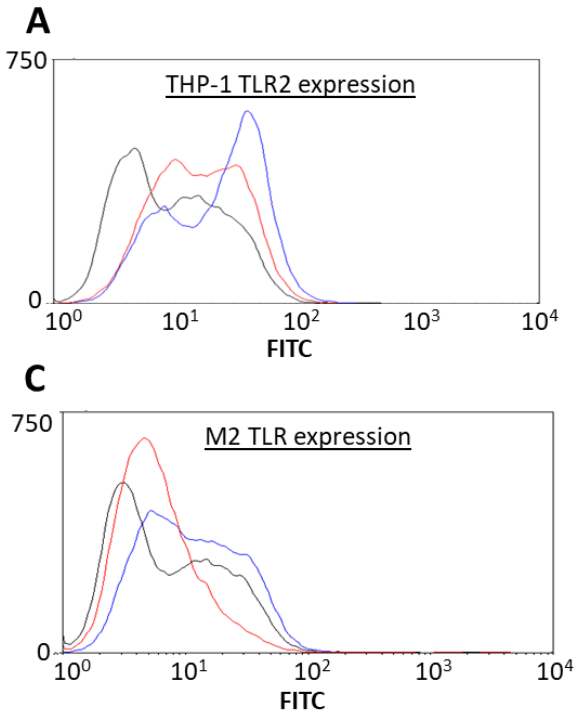

D

Mean	THP-1 (A)	M1 (B)	M2 (C)
Isotype control	17.4	28.0	21.9
Unstimulated	30.8	40.9	16.8
Stimulated with 3DOMM SN	22.2	50.7	17.2

Figure 51: Cell surface expression of Toll-like receptor 2 within THP-1, M1-like and M2-like macrophages

TLR2 expression was assessed by flow cytometry. Three experimental repeats, each with three biological replicates were pooled for each condition, data displayed is an average of three technical replicates at 10,000 events. Isotype control (black) is displayed for each cell type. TLR2 expression was assessed for unstimulated (blue) (THP-1 (A), M1-like (B) and M2-like (c)) cells, and cells stimulated with 3DOMM supernatant (red), obtained from 3DOMMs at day 9, and used to pulse chase THP-1, M1-like or M2-like cells. A table of the mean fluorescence intensity is included for each cell type under each condition (D).

5.4.8. Macrophage marker expression within THP-1-derived macrophages

Macrophage markers have been reported to differ from monocyte markers, and between macrophage subsets. The pan-monocyte marker CD68, and the M2 macrophage markers CD163 and CD206, were assessed via flow cytometry, in order to determine whether differentiation and polarisation could be determined by differential expression of cell surface markers **Figure 52**. It was found that for unstimulated THP-1 cells, M1-like, and M2-like macrophages, there was no significant difference between surface expression of CD68, CD163, or CD206.

Cell surface marker expression was further studied to determine whether expression of CD68, CD163, and CD206 by THP-1, M1-like, and M2-like macrophages, altered upon stimulation with LPS. Surface marker expression was compared between unstimulated cells and cells after 18 hours of stimulation with LPS, **Figure 53**.

No significant upregulation was found in surface marker expression, (CD68, CD163, or CD206) in response to stimulation with LPS, in any of the cell types, when compared to their respective unstimulated controls. Significant differences were assessed between all groups, including between differing unstimulated and LPS-stimulated cell types. There was significantly greater CD163 expression by THP-1 cells stimulated with LPS, compared with M2 cells stimulated with LPS ($p = 0.0324$). No significant differences were found between other groups, for all markers.

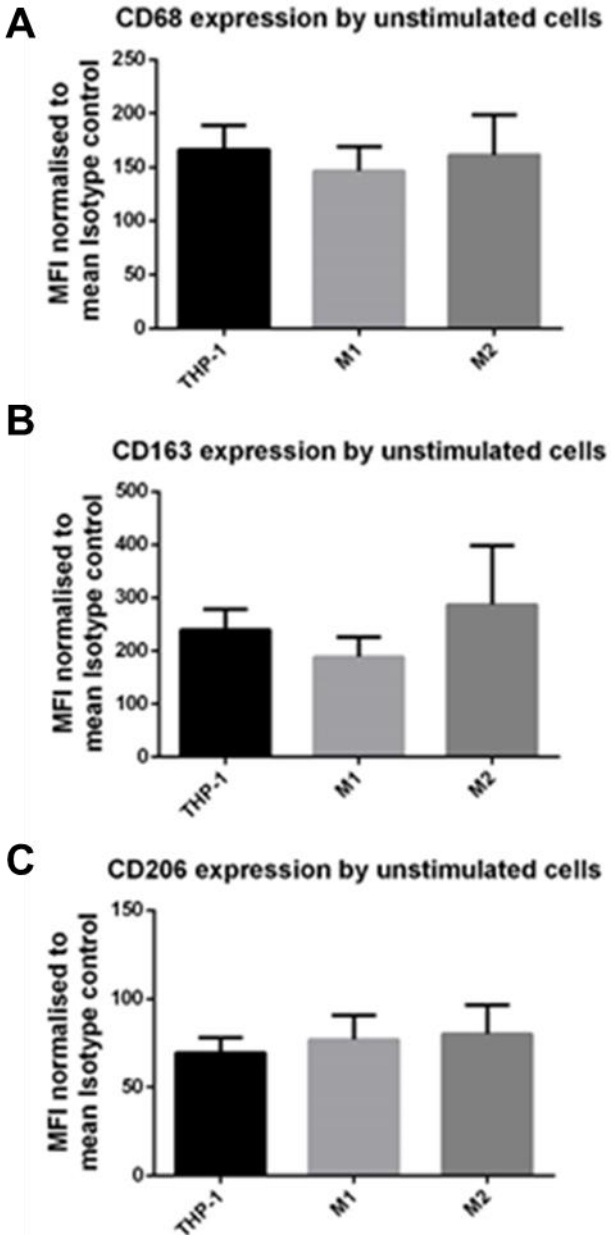

Figure 52: THP-1, M1-like and M2-like, cell surface expression of CD68, CD163 and CD206

Cell surface expression of macrophage markers CD68 (A), CD163 (B) and CD206 (C) on THP-1, M1-like and M2-like macrophages. For CD68 graphs indicate four experimental repeats, for which three biological repeats were pooled prior to analysis. For CD163 and CD206 graphs indicate two experimental repeats, for which three biological repeats were pooled prior to analysis. Three technical replicates of 10,000 events were performed for THP-1 and M2 cells and three technical replicates of at least 5,000 events were performed for M1 cells. Surface expression was determined using flow cytometry and read via mean fluorescence intensity (MFI). MFI for each group was standardised to the respective isotype control. Significance was assessed across each surface marker (CD68, CD163, and CD206) to look for significant difference between THP-1, M1 -like and M2-like macrophages. No significant difference was found between CD68, CD163 and CD206 groups. Normality was assessed using a Shapiro Wilk's test and significance assessed using a Kruskal-Wallis, followed with a Dunn's multiple comparisons test. Error bars represent standard deviation.

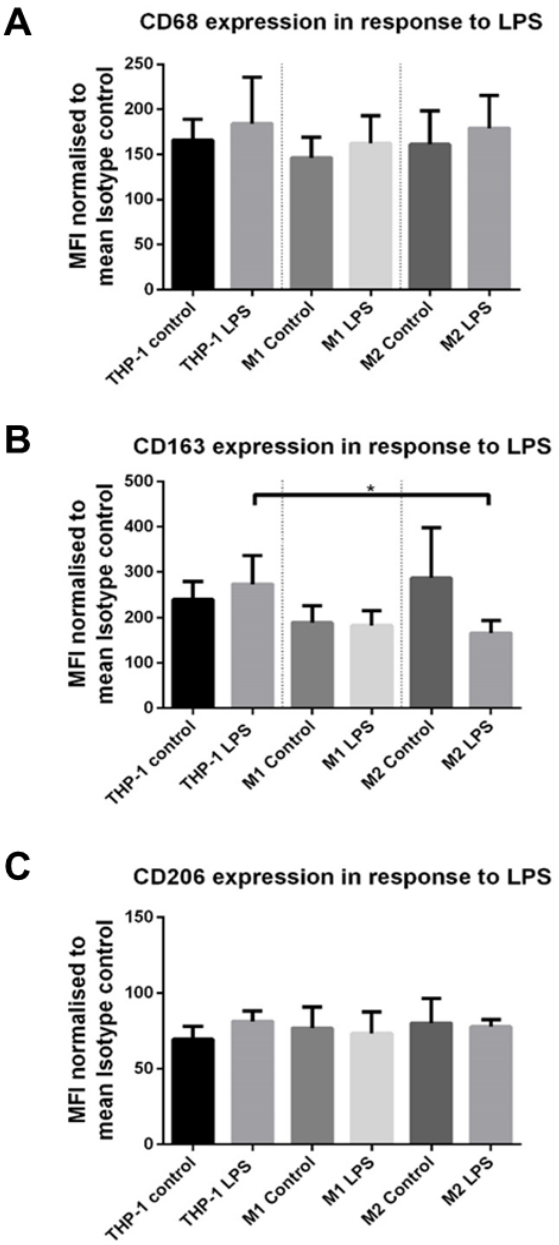

Figure 53: THP-1, M1-like and M2-like, cell surface expression of CD68, CD163 and CD206 in response to LPS

Cell surface expression of macrophage markers CD68 (A), CD163 (B) and CD206 (C) on THP-1, M1-like and M2-like macrophages in response to 1 µg/ml of PgLPS. For CD68 graphs indicate four experimental repeats, for which three biological repeats were pooled prior to analysis. For CD163 and CD206 graphs indicate two experimental repeats, for which three biological repeats were pooled prior to analysis. Three technical replicates of 10,000 events were performed for THP-1 and M2 cells and three technical replicates of at least 5,000 events were performed for M1 cells. Surface expression was determined using flow cytometry and read via mean fluorescence intensity (MFI). MFI for each group was standardised to the respective isotype control. Significance was assessed across each surface marker (CD68, CD163, or CD206) between all groups. Normality was assessed using a Shapiro Wilk's test and significance assessed using a Kruskal-Wallis, followed with a Dunn's multiple comparisons test. Error bars represent standard deviation.

Following this, the CD68, CD163 and CD206 surface marker expression was assessed for THP-1, M1-like, and M2-like macrophages grown in the presence of a 3DOMM **Figure 54**. THP-1 cells were cultured, and the differentiation and polarisation protocol followed in the presence of the 3DOMM, to determine whether macrophage surface marker expression differed between cells cultured alone, and those cultured in the 3DOMM environment. The pan-monocyte marker CD68 was significantly higher in THP-1 cells and M2-like macrophages grown in the presence of 3DOMMs, when compared with the M1-like control (p = 0.0032 and p = 0.0377, respectively). There was no significant difference in expression between each cell type (THP-1, M1-like, and M2-like) and their respective 3DOMM cultured counterparts. Furthermore, there was found to be no significant difference between CD163 or CD206 expression between all groups, including comparisons between control, and 3DOMM cultured macrophages.

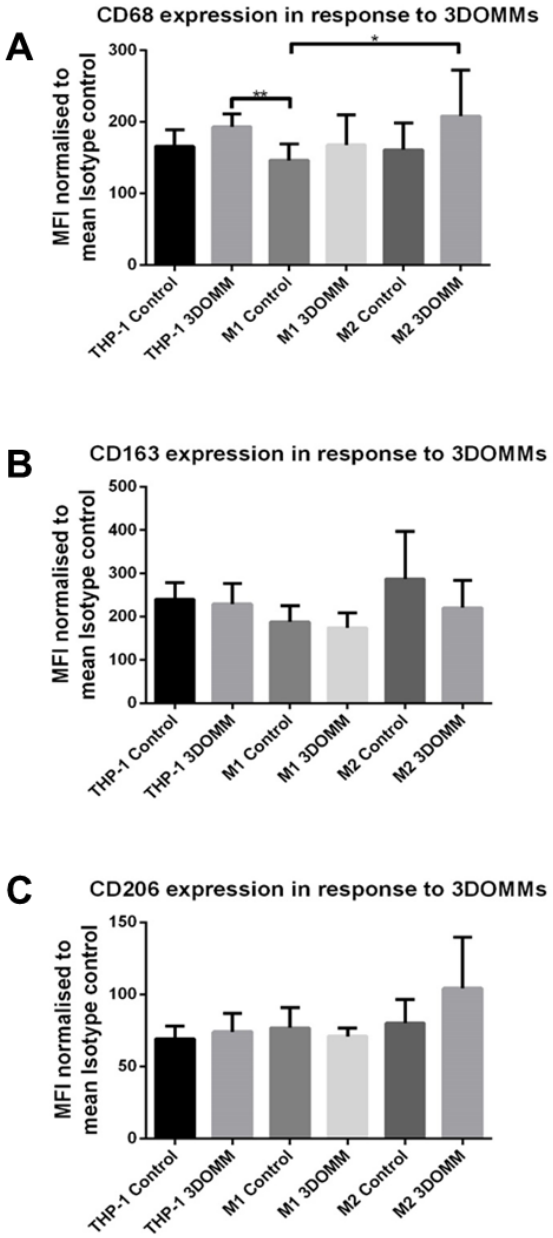

Figure 54: THP-1, M1-like and M2-like, cell surface expression of CD68, CD163 and CD206 in response to 3DOMM co-culture.

Cell surface expression of macrophage markers CD68 (A), CD163 (B) and CD206 (C) on THP-1, M1-like and M2-like macrophages when grown in the presence of a 3DOMM. For CD68 graphs indicate four experimental repeats, for which three biological repeats were pooled prior to analysis. For CD163 and CD206 graphs indicate two experimental repeats, for which three biological repeats were pooled prior to analysis. Three technical replicates of 10,000 events were performed for THP-1 and M2 cells and three technical replicates of at least 5,000 events were performed for M1 cells. Surface expression was determined using flow cytometry and read via mean fluorescence intensity (MFI). MFI for each group was standardised to the respective isotype control. Significance was assessed across each surface marker (CD68, CD163, or CD206) between all groups. Normality was assessed using a Shapiro Wilk's test and significance assessed using a Kruskal-Wallis, followed with a Dunn's multiple comparisons test. Significance is indicated on the graph (* $p < 0.05$, ** $p < 0.01$, *** $p < 0.001$, **** $p < 0.0001$). Error bars represent standard deviation.

5.4.9. Macrophage polarisation and response to the 3DOMM environment

Following the evaluation of the cell surface expression of macrophage markers on THP-1 cells, M1-like macrophages, and M2-like macrophages, the pro-inflammatory cytokine profile of each cell type was assessed when unstimulated, and stimulated with 3DOMM supernatant. Firstly, this was performed to gain an indication as to whether there was any difference perceived in pro-inflammatory cytokine production between the proposed pro-inflammatory M1-like, and anti-inflammatory M2-like macrophage cell types. Furthermore, this was aimed to further elucidate the effect, if any, of the 3DOMM on any macrophages incorporated into the model. THP-1 cells, M1-like macrophages, and M2-like macrophages were therefore pulse-chased with 3DOMM supernatant, and their subsequent production of TNFα and IL-1β was determined, **Figure 55**.

Statistical significance was first assessed between the unstimulated cell types. M1-like macrophages produced significantly more TNFα and IL-1β than THP-1 cells, when unstimulated ($p < 0.0001$ and $p = 0.0001$, respectively). M1-like macrophages at baseline also expressed significantly higher levels of TNFα than M2-like macrophages ($p < 0.0001$).

Following this, statistical significance was assessed between each unstimulated cell type, and their respective stimulation with 3DOMM supernatant. There were no significant difference seen between TNFα or IL-β production between stimulated and unstimulated THP-1 cells and M2-like macrophages, nor was there a significant difference in IL-1β production between stimulated and unstimulated M1-like macrophages. There was however a significant difference in TNFα production between stimulated and unstimulated M1-like macrophages

(p = 0.0333), whereby TNFα production was lower upon stimulation with 3DOMM supernatant.

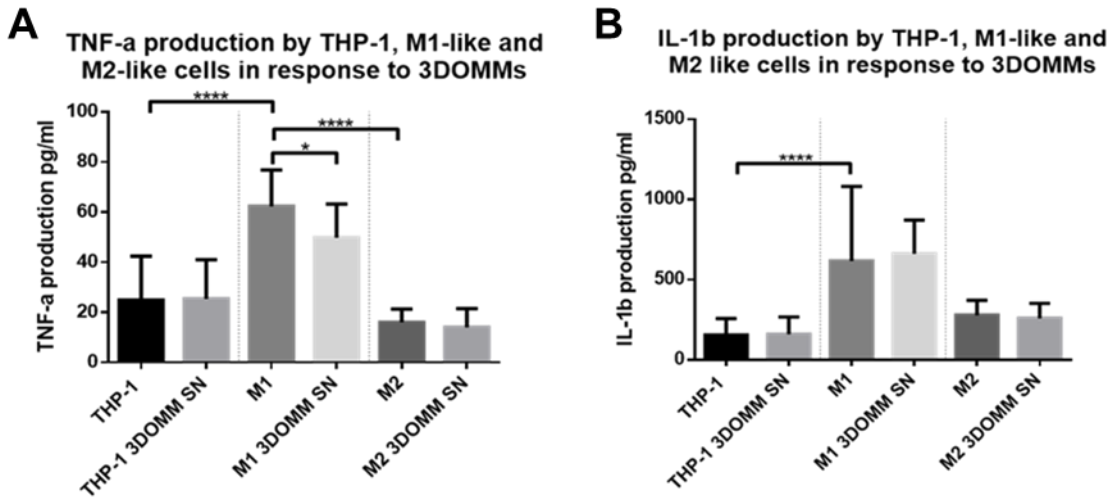

Figure 55: TNFα and IL-1β production by THP-1, M1-like and M2-like macrophages, constitutively and in response to 3DOMM supernatant.
Cells were pulse-chased with 3DOMM supernatant or a media control for 4 hours, and incubated for a further 18 hours before analysis by ELISA for TNFα (A) and IL-1β (B). Graphs indicate three experimental repeats performed in triplicate at minimum. Statistical significance was tested between THP-1, M1-like and M2-like unstimulated control. Statistical significance was also tested between each stimulated cell type and their respective negative control. Data normality was assessed using the Shapiro-Wilk test for normality. For TNFα, a one-way ANOVA was performed, followed by a Tukey's multiple comparisons test. For IL-1β a Kruskal-Wallis test was performed, followed by a Dunn's multiple comparisons test. Statistical significance is indicated on the graph (* p < 0.05, ** p < 0.01, *** p < 0.001, **** p < 0.0001). Error bars represent standard deviation.

5.5. Discussion

5.5.1. Considerations for immunocompetent oral mucosal models

Only a few previous studies have incorporated immune cells into 3DOMMs, none of which have incorporated the THP-1 pro-monocyte cell line. For this reason, firstly the suitability of THP-1 cells as a macrophage model was considered. It is necessary to derive a methodology of introducing immune cells to the 3DOMM matrix that promotes the viability of the THP-1 cells and that is reproducible. A novel consideration for the implementation of THP-1 cells into 3DOMMs is the possibility that the model environment itself may lead to the activation and polarisation of the cells, meaning this may negate the need for the *in vitro* artificial induction of macrophage polarisation. Throughout this chapter, these concepts were explored, with the special consideration as to how the newly developed IC3DOMM environment impacts upon the cell types incorporated within.

5.5.2. THP-1 cells as a macrophage model

The differential morphology observed between THP-1 cells and PMA-derived M1-like macrophages is a good indicator of the differentiation of monocytes into macrophages through their adherence, increased cytoplasmic volume, and formation of pseudopodia that aid mobility and phagocytosis (298,308,327). M1-like macrophages appeared as a single population within flow cytometry, indicated by the single peak on the histogram. These data support the notion that PMA derives macrophages from THP-1 cells. Despite the increasing confidence that PMA induces the differentiation of THP-1 cells into macrophages, it was shown that there was no significant increase in CD68 expression, the pan-monocyte marker, between THP-1 monocytes, and M1-like macrophages. It has

been shown that macrophages typically express higher levels of CD68 than their monocyte precursors (328). However, due to the flow cytometry methodology used, only CD68 at the cell surface would have been observable; as a predominantly intracellular protein, permeabilisation of the cells before future analysis may prove more informative (322).

VD3 differentiated M2-like macrophages, were closer in morphology to THP-1 pro-monocytes than they were to M1-like macrophages, and for the most part remained in suspension, with some adherent cells observed. VD3 cells contained multiple populations, as indicated by multiple peaks on the flow cytometry histogram. Some cells appeared more granular, supported by imaging. Granularity occurs more within macrophages than monocytes, suggesting that some level of differentiation had taken place (298,329). VD3 differentiated M2-like macrophages exhibited no pseudopodia, nor were they particularly adherent, which differs from reports of M2-like macrophages derived from PBMCs and THP-1 cells using IL-4, but supports previous findings regarding VD3 differentiation of THP-1 cells (299,330). The differences observed between the VD3 differentiated M2-like macrophages and traditionally reported macrophages may be indicative of an insufficient differentiation and polarisation protocol. It has been suggested previously that VD3 does alter THP-1 cells from their monocytic state, however does not appear to lead to the formation of a fully differentiated macrophage as PMA does, due to the resultant cells' lack of adherence, continued proliferation, and lower phagocytic activity (298,299). At the time of this discovery it had been suggested that VD3 leads to an alternative differentiated state than PMA induced macrophages, which were reported to be inflammatory (299). Over time, this interpretation of an alternative differentiated state took on

the description of an M2-macrophage. However, although evidence does support the idea that VD3 differentiated THP-1 cells are not inflammatory, and hence not M1-like macrophages, it does not support the idea that VD3 differentiated macrophages are mature anti-inflammatory macrophages either; rather, some form of intermediary monocyte/macrophage phenotype, that has not undergone the full differentiation process. The results from this study strongly support the idea that the VD3-derived M2-like macrophages differ from the PMA-derived M1-like macrophages, and also support the idea that VD3-derived cells are not phenotypically a macrophage, due to their lack of adherence, low cytoplasmic volume, and lack of distinct markers attributed to their reported phenotype (M2-macrophage markers CD163 and CD206). To back this up, in future the anti-inflammatory cytokine production by VD3-derived M2-like macrophages may be assessed. All things considered, future experimentation may require the implementation of alternative methodologies. Other groups have successfully used THP-1 cells and PBMCs to derive M2-like macrophages through the use of various combinations of M-CSF, IL-4, IL-13, and PMA (293,295,296,331–333). Therefore, should macrophage polarisation be required, there are other means to achieve this.

A final note: despite the differing morphology of the VD3-derived M2-like macrophage from the traditionally reported macrophage, this does not necessarily mean they are completely unsuitable for all applications within the *in vitro* situation. Nor does it mean that the more successfully derived PMA-derived M1-like macrophages are suitable for all applications. Although other methodologies are more suitable for the formation of M2-like macrophages, no one model is perfect. This is due to the complex environment *in vivo*, which

cannot accurately be replicated *in vitro* with the aid of few select cytokines/chemicals. Not explored in detail within the present study, but an exciting prospect for future work, is to discover the secretome of the 3DOMM, to determine whether the traditionally reported polarising cytokines are able to be produced. If they are, the task to artificially induce the most phenotypically relevant appropriately polarised macrophage may no longer be required.

5.5.3. Integration of macrophages into the 3DOMM

THP-1 cells differentiated into macrophages, have a relatively limited life span due to the reduction in proliferation capability observed within monocyte-derived macrophages. This terminal differentiation does not occur within all macrophages, with some tissue-resident macrophages acting as self-sustaining populations, maintaining their proliferative capacity (285). The THP-1-derived macrophage lifespan was not extended through the incorporation of the cells into the 3DOMM matrix and therefore the integration of mature macrophages into the matrix at the point of 3DOMM creation was ruled out, as by the time the epithelium would have begun to develop, the macrophages will have expired.

THP-1 cells alone embedded in the matrix continued to proliferate, indicated by clumping of the THP-1 cells. THP-1 cells in the presence of HGF cells did not proliferate as rapidly, perhaps a result of cross-talk between the HGF cells, which themselves are in stasis when embedded in a collagen matrix, as indicated in Chapter 3. This occurrence was consistent, and the clumping effect, characteristic of continued proliferation, was not observed within IC3DOMMs cultured for 12-14 days, indicated by subsequent histology and confocal microscopy.

A preliminary study indicated that 3DOMMs produce MCP-1 (data not shown). THP-1 cells express MCP-1 receptors and migrate towards high concentrations of MCP-1 (334). With this in mind, the THP-1 migration study was developed. The rationale behind using PMA was to determine the effect of THP-1 differentiation upon cellular migration. Conclusions could not be drawn from this study, however it has been shown previously that the longer THP-1 cells are incubated with PMA, the less responsive they are to MCP-1 induced migration (334). At this point, it was not yet known whether THP-1 cells are differentiated as a result of the 3DOMM environment. LTA was included to stimulate pro-inflammatory cytokine production by the 3DOMM in order to determine whether this enhanced migration. It is difficult to draw conclusions on the effect of the individual stimuli included upon THP-1 migration, as the results were not conclusive due to the nature of the imaging technique used. THP-1 cells were visible at the periphery of the 3DOMM, but it was not possible to tell if the cells had migrated into the matrix, and as the cells appeared to have a similar degree of luminescence, it is proposed that the majority of the 3DOMM-associated THP-1 cells were on the same plane. In future work, the location of the cells could be determined through the use of cryopreservation and cryostat sectioning of the models. However upon consideration, even should the cells migrate into the matrix, it would be difficult to accurately quantify how many cells had made this migration, and therefore would be likely to hinder the reproducibility of the model.

Embedding THP-1 cells into the model matrix at the point of formation and differentiating them *in situ* appears to be the most effective way to create an IC3DOMM. A similar methodology was applied by by Linde *et al*., 2012, for the incorporation of dermal fibroblasts and macrophages into a collagen matrix.

Whereby macrophages were successfully incorporated and subsequently differentiated *in situ*, with the use of IFNγ + LPS and IL-4, for M1-like and M2-like macrophages, respectively. Furthermore, the spontaneous immortalisation of naive macrophages to an M2-like phenotype, in the presence of a tumour environment, was observed. This supports the possibility of polarising macrophages *in situ,* and demonstrates the ability of a tissue engineered environment to tailor macrophage activity (62).

5.5.4. HaCaT and HGF response to the IC3DOMM environment

Killed THP-1 cells and THP-1 supernatants did not stimulate HGF cells, indicated by the lack of increase in pro-inflammatory cytokine production. However, soluble factors in THP-1 supernatant did stimulate HaCaT cells as represented by their increase in IL-8 production. As PMA and VD3 induced pro-inflammatory cytokine production within 3DOMM cell types there is concern as to whether this may inhibit their ability to respond to further stimuli. However, considering the overall pro-inflammatory environment exhibited within the 3DOMMs, it is unlikely that this will make a dent in the overall cytokine milieu. Despite this, PMA and VD3 may still affect the response of the model as a whole. PMA may alter the proliferation of keratinocytes, as well as induce terminal differentiation (335,336). With regards to fibroblasts PMA is able to induce apoptosis (337). VD3 may alter keratinocyte proliferation and increase resistance to apoptosis (338,339). VD3 may also affect the behaviour of fibroblasts, and it has been reported previously that it leads to a reduction in fibroblast mediated collagen gel contraction, as well as increasing collagen synthesis (340,341). Considering this, and the uncertainty with regards to VD3 induced polarisation, an alternative, polarisation and differentiation protocol may be required for subsequent models.

5.5.5. Macrophage response to the 3DOMM environment

Cell surface markers have been reported as an accurate way to classify macrophage phenotypes, and have been used alone and in conjunction with other techniques such as the identification of cytokine production and antimicrobial agents to differentiate between M1 and M2 populations in disease (324,326,342). A simple way to determine the effect of the 3DOMM on the polarisation of THP-1 cells could be to compare surface marker expression of cells cultured in the 3DOMM environment with cells of a known polarisation. M2-macrophage markers CD163 and CD206 are typically expressed at lower levels within M1 macrophages compared to M2 macrophages (305,343). Within the present study, the lack of significant difference in expression of all macrophage markers between the THP-1, M1-like, and M2-like macrophages, indicates that surface expression of these markers is not sufficient to determine macrophage polarisation in this model, and therefore cannot be used to study the effect of the 3DOMM on THP-1 polarisation. It was expected that surface marker expression may differ between the M1-like macrophages and M2-like macrophages, due to the reported higher levels of CD163 and CD206 within M2-like macrophages. This lack of difference may further support the idea that the THP-1 differentiation and polarisation protocol is ineffective at producing differentiated and polarised M2-like macrophages. CD163 expression by THP-1 cells and their derivatives, has previously been reported as lacking, which is thought to be a result of the cell line's leukaemic origin, however in the present study CD163 expression was not totally absent, as demonstrated by expression levels being greater than that of the isotype control for THP-1 cells, M1-like macrophages, and M2-like macrophages (76). It should be noted that for CD206, the observed MFI was less

than that of the isotype control, indicated by percentages lower than 100%. Therefore the CD206 antibody employed for studying cell surface marker expression may be ineffective, or perhaps use of an isotype control is not the most appropriate way to conduct flow cytometry experiments in high Fc receptor expressing cells (344,345).

The pro-inflammatory cytokine profile of M1-like and M2-like macrophages proves more promising a means of determining cellular polarisation and subsequently the effect of the 3DOMM environment on THP-1 cells in terms of differentiation and polarisation. Baseline TNFα, and IL-1β production by M1-like macrophages were significantly greater than that of THP-1 cells. This is indicative of the differentiation of M1-like macrophages away from the THP-1 phenotype. This is further supported by the ability of M1-like macrophages to respond to LPS and LTA, as indicated in the present study and within the literature (346). THP-1 cells are typically considered unresponsive to PAMPs due to their lower level of CD14 expression than traditional peripheral blood monocytes, and require differentiation in order to effectively respond to stimuli (77,347).

The baseline level of TNFα production by M2-like macrophages and THP-1 cells did not significantly differ. Baseline and stimulated TNFα pro-inflammatory cytokine production has been demonstrated to be absent and low, respectively, within VD3-derived M2-like macrophages (298,303). This information alone, neither supports nor denies the premise that M2-like macrophages used within this study were not fully differentiated. The fact that M2-like macrophages were responsive to LPS and LTA within the present study suggests that the M2-like macrophages at least partially differentiated away from the typically unresponsive

THP-1 phenotype. To fully characterise the M2-like macrophage population, and determine their functionality, their response to bacteria in terms of phagocytosis and anti-inflammatory cytokine production, such as IL-10 and TGF-β, would need to be determined (307).

The lack of an increase in pro-inflammatory cytokine production by THP-1, M1-like and M2-like macrophages when pulse-chased with 3DOMM supernatant indicates that the soluble factors being secreted from the 3DOMM at day 9 are not stimulatory towards the THP-1-derived macrophages. In fact, M1-like macrophages stimulated with 3DOMM supernatant led to a significant reduction in TNFα production, indicating an anti-inflammatory effect. The lack of stimulatory response does not necessarily mean that THP-1 cells will remain unaffected by the 3DOMM altogether. Considering the data explored in chapter 3 indicating that the 3DOMM is inherently inflammatory, and taking into account the fact that 3DOMM supernatant has been shown to modify pro-inflammatory cytokine production by M1-like macrophages, it is very possible that the overall model environment may modify the response of THP-1 derived macrophages. For example, if macrophages should encounter a pro-inflammatory stimuli, inadvertently, from their environment, cells may not respond to an induced experimental stimulus in the same way upon secondary stimulation. This is due to the initiation of tolerance upon prolonged or repeated exposure to stimuli such as LPS (348). This may lead to skewed results when studying infection. The impact the 3DOMM environment has on macrophage activity is of significant interest. An interesting observation was the effect that 3DOMM supernatant had on VD3-derived M2-like macrophages. Throughout the present study M2-like macrophages presented with multiple populations when assessed visually or by

flow cytometry. However, after being introduced to 3DOMM supernatant, only a single population of M2-like macrophages was indicated on the M2-like histogram when assessing TLR2 expression.

If the model environment is leading to the spontaneous polarisation of the THP-1 cells, as experienced within similar models, the response of the cells to any subsequent infection may be considerably altered to that of an induced polarised state(62). At present, it cannot be deduced whether the culture of the THP-1 cells within the collagen matrix for the full period of model growth has an effect on the THP-1 polarisation. Individual IC3DOMM components were shown to modify pro-inflammatory cytokine production by THP-1 cells in the present study, with collagen and killed fibroblasts leading to an increase in TNFα production, and multiple components, including collagen, leading to a reduction in IL-8 production. This cytokine skew indicates that whilst the IC3DOMM environment may not necessarily be inducing an overall pro-inflammatory state within THP-1 cells, the baseline environment is being modified, which may alter downstream response to infection. It was envisaged that the flow cytometry markers alone would provide an indication as to polarisation, but due to their inefficiency at determining between macrophage subsets, another approach has to be considered.

5.6. Conclusion

These data shed light onto the complex inter-workings of an immunocompetent oral infection model. Studying the individual components of the IC3DOMM has led to the identification that THP-1-derived macrophages alone, and incorporated into a model environment, may be acting in a manner dissimilar to their *in vivo* counterparts. This raises further questions within the quest to develop an IC3DOMM, whereby an alternative macrophage model may need to be considered. Next to be addressed should be the development of a methodology which may accurately identify the polarisation of macrophages *in situ* to determine the success of the differentiation and polarisation protocol, and to ascertain the effect of the 3DOMM environment upon the macrophage, in the absence of artificially induced differentiation and polarisation. Considering the multitude of interactions taking place within the model environment, it is now time to stop considering the model in a deconstructed manner, but to consider the model as a whole.

6. General discussion: considerations, limitations, and future work

Considering the results of the present study, it is proposed that the newly developed 3DOMM is suitable for the study of host response to infection, in terms of pro-inflammatory cytokine production, and tissue colonisation and invasion. The 3DOMM proved superior to the P3DOMM due to its intact epithelium, and ability to upregulate the pro-inflammatory cytokines IL-6 and IL-8 in response to single and dual infections of *C. albicans* and *S. aureus.* Clinically relevant oral isolates of *C. albicans* and *S. aureus* were obtained from denture wearing participants, and have been implemented in studying host response to infection with the newly developed 3DOMMs. Novel to the present study was the identification and subsequent report of an inherently pro-inflammatory 3DOMM environment, resulting from cell death and stimulation of the incorporated cell types by the 3DOMM environment itself. Also novel to the present study was the successful incorporation of THP-1 pro-monocyte cells into the model matrix, as a first step to form an immunocompetent model. So far it has been identified that the differentiation and polarisation protocol leads to pro-inflammatory cytokine production within the incorporated epithelial and stromal cell types, and also that collagen stimulates TNFα production by THP-1 cells, further demonstrating the complex interactions between incorporated cells and the model environment. Further consideration should be taken as to the effect of the model environment on the differentiation and polarisation of THP-1 cells, prior to their implementation to study host response to infection. **Table 14** indicates the individual aims addressed within the experimental chapters of this thesis, along with their associated outcomes, that led to the characterisation and development of the

3DOMM and subsequent IC3DOMM. A schematic figure is included to demonstrate where the 3DOMM and IC3DOMM currently fits into the field of tissue-engineered oral mucosal models **Figure 56**.

Table 14: **Summary of aims addressed within this thesis and their outcomes, as discussed within experimental chapters.**

Aim	Outcomes
To compare the morphology of three-dimensional oral mucosal models created with immortalised and primary keratinocytes, with native oral mucosa.	• 3DOMMs were structurally similar to the native oral mucosa with the exception of rete ridges and epithelial stratification. • 3DOMMs were highly reproducible in terms of morphology and structural integrity, with the except for the infrequent occurrence of a weakly occurring basement membrane and consistent variation of epithelial thickness. • 3DOMM morphology was superior to P3DOMM morphology due to the presence of a robust intact epithelium.
To identify the base-line pro-inflammatory cytokine production of the P/3DOMMs, and determine the effect of the model environment on the incorporated cell types.	• 3DOMMs and P3DOMMs were inherently inflammatory. • 3DOMMs produced the highest levels of IL-6 and IL-8 upon model formation, levels of IL-6 and IL-8 reduced after this point, but IL-8 levels rose again after day 13. • Cell death, determined by LDH release correlated with higher levels of pro-inflammatory cytokine production. • The effect of the 3DOMM environment on the incorporated cell types may at least partially contribute to this inflammatory environment, due to model components leading to the stimulation of cells.
To determine the ability of HaCaT, HGF and POK cells to respond to PAMPs.	• HaCaT, HGF and POK cells were all able to produce pro-inflammatory cytokines in response to 10 µg/ml of LTA. • HaCaT cells were not responsive to LPS, whereas HGF cells were responsive to mid-range concentrations (0.1 µg/ml), and POK cells were responsive to 1µg/ml.
To consider the optimum time-point to implement the newly developed 3DOMM as an infection model.	• Model epithelial thickness did not vary much between day 16 and 21, however the epithelium was most consistently anchored to the lamina propria layer at day 19. • Due to high levels of pro-inflammatory cytokine production at the former and later stage of model growth, it was proposed that the models would be more informative to study host

	pro-inflammatory cytokine production in response to infection at a lower period of baseline pro-inflammatory cytokine production (days 5-15). • It is proposed that the models are used at day 14 so that the epithelium has enough time to develop, whilst minimising pro-inflammatory cytokine production, so that an upregulation may be measured in response to infection.
To obtain clinically relevant oral isolates of *C. albicans* and *S. aureus.*	• One isolate of *S. aureus* and 10 isolates of *C. albicans,* 7 of which were obtained from different patients, were obtained from patient oral swabs of the hard palate and denture.
To identify the frequency of colonisation of denture wearers, and factors associated with *C. albicans* and *S. aureus* carriage	• Due to a lower than expected uptake onto the participant study it was not possible to determine risk factors associated with *C. albicans* and *S. aureus* carriage. • Of the total 32 participants, 21.88% carried *C. albicans* and 3.13% carried both *C. albicans* and *S. aureus.* • Of non-denture wearers, 18.18% carried *C. albicans* alone, compared with 30% within the denture-wearing group. • No participants carried *S. aureus* alone, whereas 10% of the denture wearing group carried both *C. albicans* and *S. aureus*.
To assess the efficacy of P/3DOMMs to model single and dual infections of *C. albicans* and *S. aureus* in terms of studying tissue colonisation and invasion, and pro-inflammatory cytokine production in response to infection.	• 3DOMMs were determined more suitable to study host response to infection than P3DOMMs due to their superior epithelium, which was intact and hence prevented immediate invasion of microbes, unlike P3DOMMs. • 3DOMMs were superior than P3DOMMs due to their ability to upregulate both IL-6 and IL-8 pro-inflammatory cytokines in response to all combinations of single and dual infections of *C. albicans* and *S. aureus.* • P3DOMMs did not upregulate IL-8 upon infection.
To explore the proposed synergistic relationship between *C. albicans* and *S. aureus.*	• This study observed *C. albicans* and *S. aureus* associated together and separately within dual infections, however there was no clear indication of synergy, particularly as within

	monolayer studies *S. aureus* was more detrimental to the epithelial monolayer alone, than when associated with dual infection with *C. albicans.* • There was no significant difference in pro-inflammatory cytokine production by infected HaCaT monolayers and 3DOMMs, between single and dual infections of *C. albicans* and *S. aureus.*
To determine whether the THP-1 derived M1-like and M2-like macrophages are suitable to be employed for the formation of an immunocompetent 3DOMM	• THP-1-derived M1-like and M2-like macrophages were responsive to LPS and LTA indicating they are able to produce pro-inflammatory cytokines in response to PAMPs. • At baseline, M1-like macrophages produced significantly more TNFα than THP-1 cells or M2-like macrophages, indicating their more inflammatory phenotype. • Questions were raised as to the suitability of VD3 to differentiate and polarise THP-1 cells into M2-like macrophages due to the lack of phenotypical macrophage morphology, and multiple populations observed within M2-like macrophages. • It is proposed that an alternative polarisation and differentiation protocol should be selected.
To determine the most suitable way to incorporate THP-1 cells into the model matrix	• Embedding THP-1 cells into the model matrix at day 1 of model production, followed by subsequent differentiation and polarisation *in situ* was the most suitable means of macrophage incorporation. • THP-1 cells, M1-like and M1-like macrophages were visible in the model matrix at day 14, and M1-like macrophages appeared to have an enlarged, elongated, appearance indicative of a macrophage.
To determine whether differentiation and polarisation of THP-1 cells is required in the 3DOMM environment	• It was not possible to differentiate between macrophage subsets due to insufficient polarisation markers; therefore, it was not determined whether the 3DOMM environment itself, lead to differentiation or polarisation of THP-1 cells into macrophages. • 3DOMM supernatant was not found to have a stimulatory effect on THP-1, M1-like or M2-like macrophages, demonstrated by the lack of increase in pro-inflammatory cytokines.

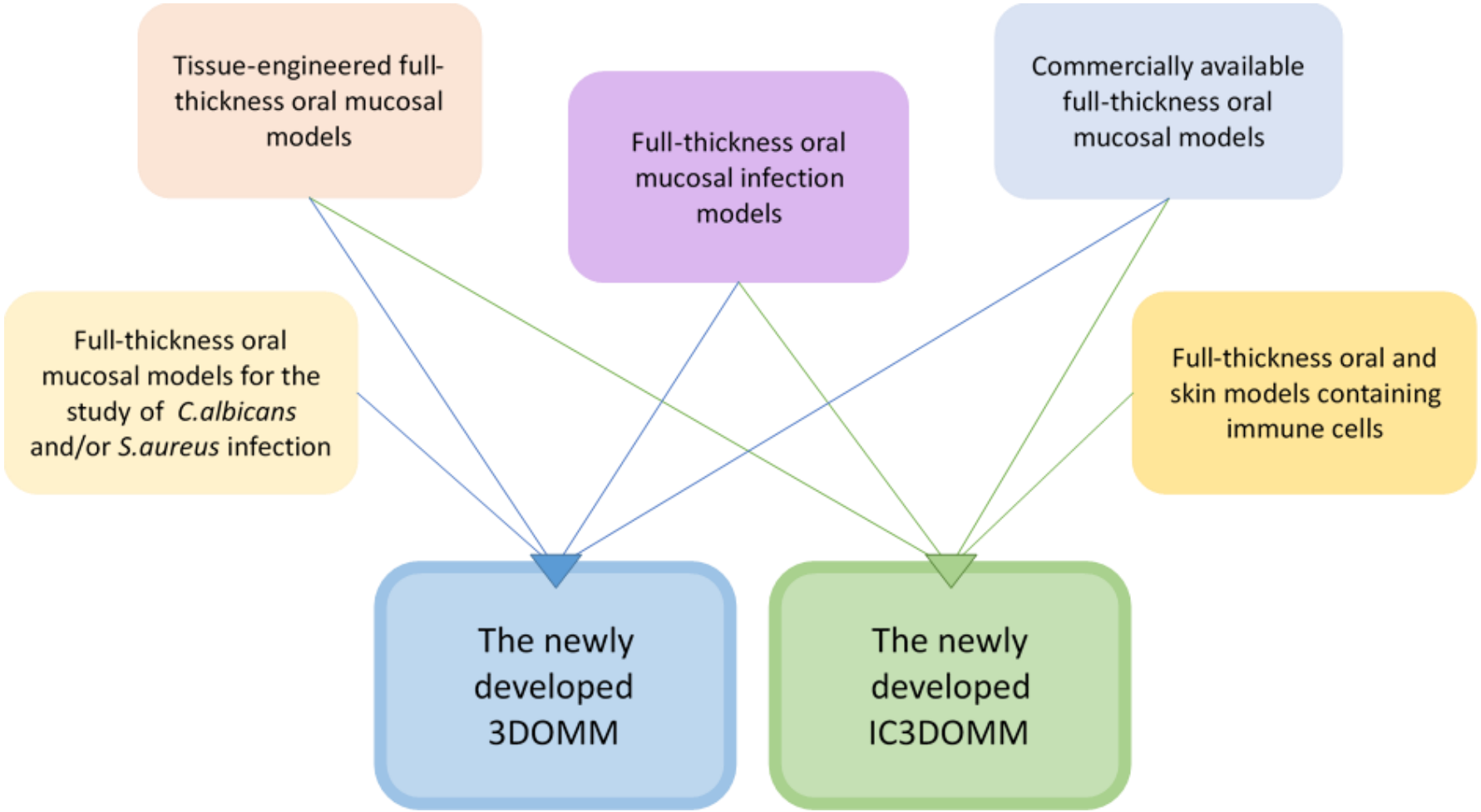

Figure 56: A schematic demonstration of the fields of literature leading to the development and application of the newly derived 3DOMM and IC3DOMM.

6.1. Challenges faced within model development

6.1.1. Studying the model as a whole

The overarching aim of the present study was to develop an IC3DOMM that was able to effectively and informatively model oral infection in a manner representative of *in vivo* oral mucosa. An early challenge faced within 3DOMM development was the identification of high levels of pro-inflammatory cytokines being produced at baseline. In order to gain an understanding of the causes, it was possible to study the models cellular components individually. **Figure 57** has been included to indicate the complexity of the interactions taking place within the IC3DOMM. It demonstrates interactions identified within the present study that contribute towards pro-inflammatory cytokine production by the IC3DOMM cell types, as well as the model as a whole; this is an area that for the most part has been overlooked within previous literature. However, due to cross-talk between the cell types within the model environment it is unlikely that the sum of the responses of the individual cell types equates to the model as a whole. The complexity of epithelial mesenchymal cross-talk extends to the structure morphology of the model, whereby cross-talk between the keratinocytes and fibroblast cells within a 3DOMM leads to differential protein expression, model contraction and basement membrane deposition in the presence of both cell types, but not in the absence of any one cell type (349,350). Therefore, whilst proving informative for some purposes, and valuable to initially predict the abilities of the individual cell types, studying the model in a deconstructed manner is only useful up to a point, and individual cellular interactions may not always accurately represent cellular behaviour and response within the model environment. The

model must therefore be considered as a whole when taken forward to study infection.

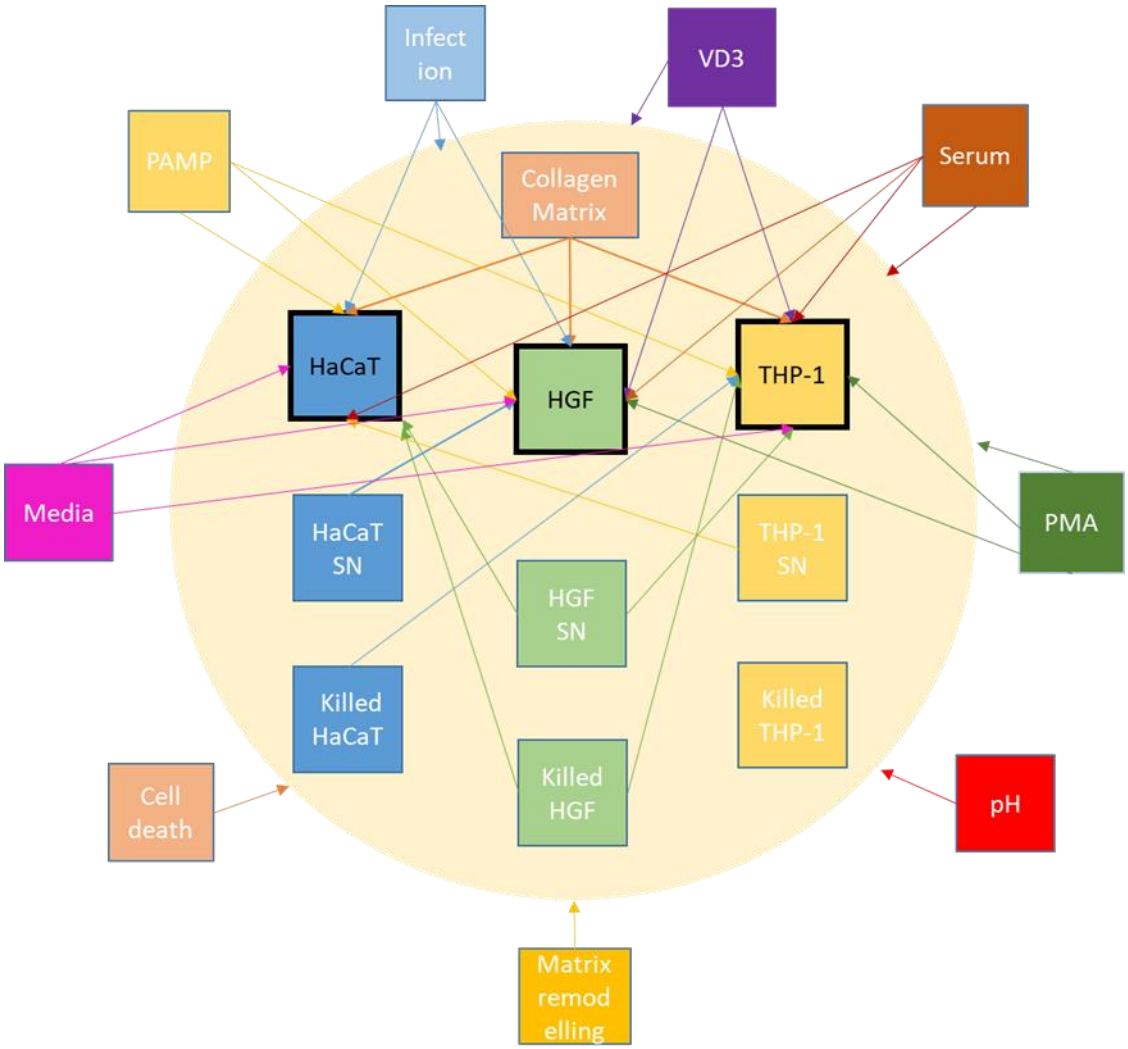

Figure 57: The complex interactions underpinning IC3DOMM pro-inflammatory cytokine production, as identified within the present study.
This figure is included as a demonstration of the complex environment, previously overlooked within the field of oral mucosal infection modelling. Arrows indicate stimuli that have led to the upregulation of pro-inflammatory cytokine production within: HaCaT cells, HGF cells and THP-1 cells, as well as the model as a whole (indicated by arrows leading to the periphery of the inner circle). It should be noted that the stimuli incorporated in this diagram are representative of those identified within the present study, and are not exhaustive.

Careful consideration was taken in order to determine the best way to study the surface expression of cells embedded within a gel-based matrix. It was at first thought important to develop a way of studying the individual cell types in a manner that did not require the models to be sacrificed, so that cells could be studied in a time-dependent manner should it be so desired. Furthermore, a relatively low cell number of THP-1 cells were added to the lamina propria layer; meaning that sacrificial techniques such as the digestion of the matrix, would most likely lead to too few cells for analysis by flow cytometry. It is for this reason that the THP-1 cells have been studied in a separate manner, external from the 3DOMM. The THP-1 cells were therefore cultured below a transwell insert containing the 3DOMM, so it was exposed to the full array of soluble factors that exist within the 3DOMM microenvironment. The only absent factor, which was previously identified to lead to stimulation of THP-1 cells, was the response of THP-1 cells to collagen. Whilst this methodology should have provided a strong indication as to the overall effect of the 3DOMM environment on the polarisation of THP-1 cells (had the markers chosen for indication of polarisation been successful), it was not possible to quantifiably determine the THP-1 cell pro-inflammatory cytokine production as a result of these culture conditions. This was due to the manner in which the THP-1 polarisation and differentiation protocol had to be carried out within the 3DOMM environment. This led to a variation in the resulting cell number per well and between M1-like, M2-like and THP-1 cells, meaning that any cytokine readouts would not have been directly comparable. The suspension cells could have been re-seeded, however for the adherent M1-like macrophages, detachment and re-seeding may have led to an altered response and lack of adherence. For this reason, in future, a methodology should be devised to study either the *in situ* polarisation or permit the removal of the cells

from the collagen matrix for further study. This would also account for the direct effect of collagen on THP-1 cells.

6.1.2. Choosing a suitable keratinocyte cell line

In the present study, HaCaT cells appeared more appropriate than POK cells to form a robust, reproducible epithelium. POK cells maintained their epithelial phenotype for few passages, and their morphology and monolayer integrity was unpredictable in nature; of the two cell types compared, in terms of model morphology HaCaT cells were the most suitable epithelial cell type. However, as introduced previously, HaCaT cells are skin keratinocytes. In terms of morphology there are no differences exhibited between skin keratinocytes and oral keratinocytes, in fact oral keratinocytes are more similar to skin than any other mucosal tissue (88). At the histological level, there are differences between dermal and oral tissue, however these structural differences result from the presence of other cell types, and appendages such as hair, which may be omitted from tissue-engineered models. Despite these similarities, the use of HaCaT cells instead of immortalised oral epithelial cells must be further discussed at a cellular level. Response to injury between oral and skin keratinocytes varies, oral mucosal wounds heal faster, and in a less inflammatory manner than dermal wounds, with oral wound healing resulting in minimal scar formation when compared with dermal wounds (351). Initially it was unknown whether this differing response was a result of the tissue as a whole, or whether keratinocytes at least partially contribute to the differences exhibited within wound healing of these two structurally similar tissues. It has now been indicated that the discrepancies in wound healing are not solely as a result of the local environment, such as salivary flow and the local microflora. Skin explants incorporated into the

oral mucosa have exhibited keloid scar formation at their new site of residence, indicative of their maintained skin phenotype. Furthermore, as a result of the proliferative and migratory capacity of oral keratinocytes, when compared to skin keratinocytes, differences are exhibited in the rate of wound healing (351). This may impact upon infection studies, particularly upon the case of pathogenic damage to the epithelium, whereby skin keratinocytes would not be representative of oral keratinocytes in their ability to rapidly regenerate the epithelium. Furthermore, if the oral mucosa is inherently less inflammatory than skin, the implementation of a skin keratinocyte may lead to a falsely high baseline and responsive cytokine level upon infection, leading to results that are not representative of the oral mucosa. It is also possible that the lack of differentiation exhibited within the 3DOMM epithelium may be a result of the HaCaT cell line employed. HaCaT cells have been reported to exhibit insufficient epithelial mesenchymal cross-talk, leading to a reduction in basement membrane deposition and lack of epithelial stratification (68). This, in turn, may also account for the limited keratinisation exhibited within these newly developed oral mucosal models.

The implementation of the immortalised oral keratinocyte cell line, FNB6, for the construction of 3DOMMs has been successful on multiple occasions (13,42). It is proposed that a comparison should be made between IC3DOMMs formed with the HaCaT and the FNB6 cell lines to determine if other benefits, besides the stratification of the epithelium and basement membrane deposition, are observed. For example, any further considered epithelial cells should have the models resultant pro-inflammatory cytokine production deliberated when incorporated into a 3DOMM. Macrophage response to any new cell types should

also be assessed. It should always be ensured that model morphology and response to infection is balanced, to ensure the newly developed IC3DOMM is as similar to the native oral mucosa as possible.

6.1.3. The THP-1 model

THP-1 cells are useful tools for *in vitro* immunological studies due to their continuous proliferative state, but as a leukaemic pro-monocyte cell line they inherently come with their own limitations, such as an alteration in traditional monocyte and subsequently derived macrophage markers (76). The present study shed light on the success of the commonly used PMA and VD3 differentiation and polarisation protocols employed to derive THP-1 cells into macrophages. THP-1 cells have however been successfully reported to be differentiated and polarised into macrophages using methodologies that more accurately represent the *in vivo* situation (293–296,331–333). Considering the benefit of the proliferative capacity, easy access, and reproducibility of THP-1 cells, the first step in the further development of this model would be to explore the use of a range of differentiation and polarisation protocols in order to characterise the possibilities of THP-1-derived macrophage functionality. Should this not be successful, PBMCs may be considered as an alternative cell source, for the incorporation of macrophages into the model matrix.

One phenomenon observed within the THP-1-incorporated IC3DOMMs, but not within the 3DOMMs, was the presence of keratinocyte islands within the model matrix, and a thinner epithelium than 3DOMMs. This has been observed by other research groups in the past for THP-1 cells (data not published) and should be

further explored. Should this occurrence be frequent, it may be necessary to alter the macrophage cell type incorporated into the model.

6.2. Future work

6.2.1. Short term goals

Several aims exist with regards to the study of macrophage polarisation within the IC3DOMM. Firstly, it is necessary to identify and implement macrophage polarisation markers, whereby the characterisation of confirmed polarised macrophage subsets may be used as a reference point, to compare THP-1 cells and THP-1-derived macrophages. Next, THP-1 cells incorporated into the IC3DOMM for the duration of the full length of model culture should be studied for spontaneous polarisation, to determine whether the 3DOMM is able to induce THP-1 differentiation and polarisation at resting, or upon infection. An alternative, yet interesting starting point would be to identify the full cytokine profile of 3DOMMs under different conditions, to determine whether the cell types are capable of producing cytokines that naturally lead to the differentiation and polarisation of monocytes into subsequent macrophages. Once sufficient polarisation markers are identified, it may be necessary to consider a methodology for the removal of macrophages embedded into the collagen matrix, so that their polarisation may be determined. Previously, research groups have reported having successfully digested tissues through the aid of collagenases, in order to study surface marker expression of immunological cell types through flow cytometry (352,353). This methodology may be useful for the characterisation of macrophage polarisation *in situ,* at a point where it is appropriate for the model to be sacrificed at the end of experimentation. Other methodologies include the

use of cryostat sectioning and immunostaining techniques, to study surface marker expression, along with the monitoring of secretable factors such as reactive oxygen species and arginase from the tissues (326). Dependent on these findings, a conclusion may be made as to whether the artificial induction of macrophage polarisation is required in the 3DOMM environment. Should the IC3DOMMs not be capable of spontaneous polarisation of THP-1 cells, as discussed previously, it will be necessary to employ a differentiation and polarisation protocol superior to that of the PMA and VD3 protocols explored within the present study.

Once fully characterised, the next apparent step would be to implement the IC3DOMM as an infection model and study the involvement of the THP-1-derived macrophages in host-response to infection. Studying cellular migration, phagocytosis, and downstream response to live agents would provide a more informative overview of this newly developed model's ability to accurately represent *in vivo* infection. It is also of interest to compare the study of host response to infection between 3DOMMs and IC3DOMMs, in order to determine how incorporated macrophages alter the overall tissue response.

6.2.2. Long term goals

Should the IC3DOMM be proven a successful model to study host-response to infection, the work does not stop there. It is proposed that the next step would be to attempt to incorporate multiple immune cells into the model matrix. It is also of interest as to whether a population of tissue-resident macrophages are able to lead to the recruitment of peripheral blood monocytes. THP-1 cells and their derivatives are known to express MCP-1 receptors and secrete MCP-1,

respectively; they are also able to secrete IL-8 in response to infective agents (334,354). Additionally, as demonstrated in the present study 3DOMMs are able to secrete both of these chemoattractants. It is of interest to explore the incorporation of THP-1 cells and neutrophils within the culture media of the model, and determine if this leads to the recruitment of such cells into the model matrix upon the induction of infection, due to the IC3DOMMs ability to secrete MCP-1 and IL-8.

Not to be ignored, and to be further characterised, are the roles of other host defence mechanisms, such as anti-microbial peptides, saliva, host microflora, and further innate immune cells. Models incorporating some of these aspects of host defence have been in development (23,52,60,61). However, as demonstrated within this thesis, interactions between cell types, the matrix material, and culture conditions may all lead to deviations of the oral mucosal model away from healthy tissue. In order to develop a model that responds to infection in the same manner as *in vivo* native oral mucosa would, it may be necessary to incorporate each of the aforementioned aspects. Considering the models available today, when compared with monolayer culture, great developments have been made within the field of oral tissue engineering. However when comparing the present oral mucosal models with the complex environment of an *in vivo* oral cavity, there is still a lot of progress to be made. Careful, considered steps should therefore be taken towards the incorporation of a variety of immunological aspects into the IC3DOMM, in order to develop a model that is fully representative of host response to infection. Each small development represents success in its own right, adding to the pre-existing tool kit of oral mucosal models, and permitting the study of the immune response to

infection from the angle of the oral mucosa, and any subsequently incorporated immune cells.

6.2.3. Future directions

As well as the provision of an informative tool for the study of host-response to infection, in terms of microbial invasion, cell damage, pro-inflammatory cytokine production, macrophage polarisation, and macrophage response, the IC3DOMM, or its subsequent derivatives, have the potential to determine wider immune response to infection through the incorporation of multiple immune-cell types. In addition to this, by substituting the epithelial cell type for squamous cell carcinoma cell lines, the model could be suitable for studying macrophage involvement in oral cancer progression, persistence, and invasion. Similar models have been applied for the study of biocompatibility, and wound healing; the IC3DOMM may provide a novel insight into the involvement of innate immune cells in such events. Furthermore, it would be interesting to determine whether such models may be able to act as microbiome models. The presence of innate immune cells in microbiome models may help to more accurately model mucosal-microbiome interactions *in vitro*. Macrophages and dendritic cells are involved in keeping the oral flora in check. Such models would not only be an informative step in terms of studying host-microbiome interactions, but also may form the basis of a more biologically relevant model when it comes to studying host response to infective agents, as the microflora its self protects against pathogenic insult (355).

6.3. Conclusions

An immunocompetent oral mucosal infection model would provide a valuable tool for the study of oral disease. This thesis has developed a methodology to incorporate innate immune cells into a reproducible three-dimensional oral mucosal model, with the intention to provide an informative tool for studying host response to infection. This thesis has demonstrated the complex interactions underpinning the oral mucosal model environment, as well as the inherently inflammatory state of the model. It is hoped that future work within the field takes into consideration how these interactions may drive the model's ability to accurately represent the native oral mucosa upon infection. This thesis has also demonstrated the ability of the HaCaT- and HGF-incorporated 3DOMM to model host response to infection, in terms of tissue colonisation and invasion, and pro-inflammatory cytokine production by the model in response to the pathogenic agents *C. albicans* and *S. aureus*. Prior to the implementation of the IC3DOMM to study host response to infection, the incorporated THP-1 cells should be fully characterised in terms of their differentiation and polarisation within the IC3DOMM environment. Once achieved, this model may be implemented in the study of pathogen-host interactions, as well as being taken forward to incorporate further aspects of the innate immune system, in the quest to develop an *in vitro* model that is truly representative of the *in vivo* oral mucosa.

Bibliography

1. Kilian M, Chapple ILC, Hannig M, Marsh PD, Meuric V, Pedersen AML, et al. The oral microbiome – an update for oral healthcare professionals. Bdj. 2016;221(10):657–66.

2. Choo A, Delac DM, Messer LB. Oral hygiene measures and promotion: Review and considerations. Aust Dent J. 2001;46(3):166–73.

3. Porter SR, Mercadante V, Fedele S. Oral manifestations of systemic disease. Nat Publ Gr. 2017;223(9):683–91.

4. Kane SF. The effects of oral health on systemic health. Gen Dent. 2017;65(6):30–4.

5. Stokes WS. Animals and the 3Rs in toxicology research and testing. Hum Exp Toxicol. 2015;34(12):1297–303.

6. Oz HS, Puleo DA. Animal models for periodontal disease. J Biomed Biotechnol. 2011;2011:1–8.

7. Samaranayake YH, Samaranayake LP. Experimental oral candidiasis in animal models. Clin Microbiol Rev. 2001;14(2):398–429.

8. Ishida K, Tomita H, Nakashima T, Hirata A, Tanaka T, Shibata T, et al. Current mouse models of oral squamous cell carcinoma: Genetic and chemically induced models. Oral Oncol. 2017;73:16–20.

9. Duval K, Grover H, Han LH, Mou Y, Pegoraro AF, Fredberg J, et al. Modeling physiological events in 2D vs. 3D cell culture. Physiology. 2017;32(4):266–77.

10. Colby LA, Quenee LE, Zitzow LA. Considerations for infectious disease research studies using animals. Comp Med. 2017;67(3):222–31.

11. Moharamzadeh K, Colley H, Murdoch C, Hearnden V, Chai WL, Brook IM, et al. Tissue-engineered oral mucosa. J Dent Res. 2012;91(7):642–50.

12. Kinikoglu B, Auxenfans C, Pierrillas P, Justin V, Breton P, Burillon C, et al. Reconstruction of a full-thickness collagen-based human oral mucosal equivalent. Biomaterials. 2009;30(32):6418–25.

13. Jennings LR, Colley HE, Ong J, Panagakos F, Masters JG, Trivedi HM, et al. Development and Characterization of In Vitro Human Oral Mucosal Equivalents Derived from Immortalized Oral Keratinocytes. Tissue Eng Part C Methods. 2016;22(12):1108–17.

14. de Carvalho Dias K, de Sousa DL, Barbugli PA, Cerri PS, Salih VM, Vergani CE. Development and characterization of a 3D oral mucosa model as a tool for host-pathogen interactions. J Microbiol Methods. 2018;152(May):52–60.

15. Abou Neel EA, Chrzanowski W, Salih VM, Kim H-W, Knowles JC. Tissue engineering in dentistry. J Dent. 2014;42(8):915–28.

16. Caddeo S, Boffito M, Sartori S. Tissue Engineering Approaches in the Design of Healthy and Pathological In Vitro Tissue Models. Front Bioeng Biotechnol. 2017;5(AUG):1–22.

17. Wojtowicz AM, Oliveira S, Carlson MW, Zawadzka A, Rousseau CF, Baksh D. The importance of both fibroblasts and keratinocytes in a bilayered living cellular construct used in wound healing. Wound Repair Regen. 2014;22(2):246–55.

18. Colley HE, Hearnden V, Jones A V, Weinreb PH, Violette SM, Macneil S, et al. Development of tissue-engineered models of oral dysplasia and early invasive oral squamous cell carcinoma. Br J Cancer. 2011;105(10):1582–92.

19. Ghahary A, Ghaffari A. Role of keratinocyte-fibroblast cross-talk in development of hypertrophic scar. Wound Repair Regen. 2007;15(SUPPL. 1).

20. Yadev NP, Murdoch C, Saville SP, Thornhill MH. Evaluation of tissue engineered models of the oral mucosa to investigate oral candidiasis. Microb Pathog. 2011;50(6):278–85.

21. Torras N, García-Díaz M, Fernández-Majada V, Martínez E. Mimicking Epithelial Tissues in Three-Dimensional Cell Culture Models. Front Bioeng Biotechnol. 2018;6(DEC):1–7.

22. Moharamzadeh K, Colley H, Murdoch C, Hearnden V, Chai WL, Brook IM, et al. Tissue-engineered Oral Mucosa. J Dent Res. 2012;91(7):642–50.

23. Bierbaumer L, Schwarze UY, Gruber R. Cell culture models of oral mucosal barriers : A review with a focus on applications , culture conditions and barrier properties. Tissue Barriers. 2018;6(3):1–42.

24. Sanchez-Quevedo MC, Alaminos M, Capitan LM, Moreu G, Garzon I, Crespo P V, et al. Histological and histochemical evaluation of human oral mucosa constructs developed by tissue engineering. Histol Histopathol. 2007;22(6):631–40.

25. Golinski PA, Gröger S, Herrmann JM, Bernd A, Meyle J, Groger S, et al.

Oral mucosa model based on a collagen-elastin matrix. J Periodontal Res. 2011;46(6):704–11.

26. Debels H, Hamdi M, Abberton K, Morrison W. Dermal matrices and bioengineered skin substitutes: a critical review of current options. Plast Reconstr surgery Glob open. 2015;3(1):63–72.

27. Bucchieri F, Fucarino A, Marino Gammazza A, Pitruzzella A, Marciano V, Paderni C, et al. Medium-term culture of normal human oral mucosa: a novel three-dimensional model to study the effectiveness of drugs administration. Curr Pharm Des. 2012;18(34):5421–30.

28. Bulysheva AA, Bowlin GL, Klingelhutz AJ, Yeudall WA. Low-temperature electrospun silk scaffold for in vitro mucosal modeling. J Biomed Mater Res Part A. 2012;100(3):757–67.

29. Moutsopoulos NM, Konkel JE. Tissue-Specific Immunity at the Oral Mucosal Barrier. Trends Immunol. 2018;39(4):276–87.

30. Langdon A, Crook N, Dantas G. The effects of antibiotics on the microbiome throughout development and alternative approaches for therapeutic modulation. Genome Med. 2016;8(1):1–16.

31. Graves DT, Corrêa JD, Silva TA. The Oral Microbiota Is Modified by Systemic Diseases. J Dent Res. 2019;98(2):148–56.

32. Rafiei M, Kiani F, Sayehmiri F, Sayehmiri K, Sheikhi A, Azodi MZ. Study of Porphyromonas gingivalis in periodontal diseases: A systematic review and meta-analysis. Med J Islam Repub Iran. 2017;31(1):355–62.

33. Pereira-Cenci T, Del Bel Cury AA, Crielaard W, Ten Cate JM. Development of Candida-associated denture stomatitis: new insights. J Appl oral Sci. 2008;16(2):86–94.

34. Williams DW, Kuriyama T, Silva S, Malic S, Lewis MAO. Candida biofilms and oral candidosis: Treatment and prevention. Periodontol 2000. 2011;55(1):250–65.

35. Cavalcanti YW, Morse DJ, da Silva WJ, Del-Bel-Cury AA, Wei X, Wilson M, et al. Virulence and pathogenicity of Candida albicans is enhanced in biofilms containing oral bacteria. Biofouling. 2015;31(1):27–38.

36. Baena-Monroy T, Moreno-Maldonado V, Franco-Martinez F, Aldape-Barrios B, Quindos G, Sanchez-Vargas LO. Candida albicans, Staphylococcus aureus and Streptococcus mutans colonization in patients wearing dental prosthesis. Oral Med Pathol. 2005;10:27–39.

37. Chopde N, Jawale B, Pharande A, Chaudhari L, Hiremath V, Redasani R. Microbial colonization and their relation with potential cofactors in patients with denture stomatitis. J Contemp Dent Pract. 2012;13(4):456–9.

38. Naik AV, Pai RC. A study of factors contributing to denture stomatitis in a North Indian community. Int J Dent. 2011;2011:1–4.

39. Gendreau L, Loewy ZG. Epidemiology and Etiology of Denture Stomatitis. J Prosthodont. 2011;20(4):251–60.

40. Gual-Vaqués P, Jané-Salas E, Egido-Moreno S, Ayuso-Montero R, Marí-Roig A, López-López J. Inflammatory papillary hyperplasia: A systematic review. Med Oral Patol Oral Cir Bucal. 2017;22(1):36–42.

41. Schlecht LM, Peters BM, Krom BP, Freiberg JA, Hansch GM, Filler SG, et al. Systemic Staphylococcus aureus infection mediated by Candida albicans hyphal invasion of mucosal tissue. Microbiol (United Kingdom). 2015;161(1):168–81.

42. Morse DJ, Wilson MJ, Wei X, Lewis MAO, Bradshaw DJ, Murdoch C, et al. Denture-associated biofilm infection in three-dimensional oral mucosal tissue models. J Med Microbiol. 2018;67(3):364–75.

43. Buchs R, Lehner B, Meuwly P, Schnyder B. Host-Pathogen Interaction Reconstituted in Three-Dimensional Cocultures of Mucosa and Candida albicans. Tissue Eng - Part C Methods. 2018;24(7):412–7.

44. Hau J. Animal models for human diseases: An overview. Source Book of Models for Biomedical Research. 2008. 3–8 p.

45. Zschaler J, Schlorke D, Arnhold J. Differences in innate immune response between man and mouse. Crit Rev Immunol. 2014;34(5):433–54.

46. Kim J, Amar S. Periodontal disease and systemic conditions: a bidirectional relationship. 2006;94(1):10–21.

47. Winning L, Linden GJ. Periodontitis and systemic disease. Nat Publ Gr. 2015;2:1–4.

48. Shepherd J, Douglas I, Rimmer S, Swanson L, MacNeil S. Development of three-dimensional tissue-engineered models of bacterial infected human skin wounds. Tissue Eng Part C Methods. 2009;15(3):475–84.

49. Hogk I, Kaufmann M, Finkelmeier D, Rupp S, Burger-Kentischer A. An In Vitro HSV-1 Reactivation Model Containing Quiescently Infected PC12 Cells . Biores Open Access. 2013;2(4):250–7.

50. Bouabe H, Okkenhaug K. Virus-Host Interactions. Bailer SM, Lieber D, editors. Methods Mol Biol. 2013;1064:239–51.

51. Dabija-Wolter G, Sapkota D, Cimpan MR, Neppelberg E, Bakken V, Costea DE. Limited in-depth invasion of Fusobacterium nucleatum into in vitro reconstructed human gingiva. Arch Oral Biol. 2012;57(4):344–51.

52. De Ryck T, Grootaert C, Jaspaert L, Kerckhof FM, Van Gele M, De Schrijver J, et al. Development of an oral mucosa model to study host-microbiome interactions during wound healing. Appl Microbiol Biotechnol. 2014;98(15):6831–46.

53. Chaudhari AA, Joshi S, Vig K, Sahu R, Dixit S, Baganizi R, et al. A three-dimensional human skin model to evaluate the inhibition of Staphylococcus aureus by antimicrobial peptide-functionalized silver carbon nanotubes. J Biomater Appl. 2019;33(7):924–34.

54. Reddersen K, Wiegand C, Elsner P, Hipler U-C. Three-dimensional human skin model infected with Staphylococcus aureus as a tool for evaluation of bioactivity and biocompatibility of antiseptics. Int J Antimicrob Agents. 2019;54(3):283–91.

55. Ren X, van der Mei HC, Ren Y, Busscher HJ. Keratinocytes protect soft-tissue integration of dental implant materials against bacterial challenges in a 3D-tissue infection model. Acta Biomater. 2019;96:237–46.

56. Bugueno IM, Batool F, Keller L, Kuchler-Bopp S, Benkirane-Jessel N, Huck O. Porphyromonas gingivalis bypasses epithelial barrier and modulates fibroblastic inflammatory response in an in vitro 3D spheroid model. Sci Rep. 2018;8(1):1–13.

57. Dongari-Bagtzoglou A, Kashleva H. Development of a novel three-dimensional in vitro model of oral Candida infection. Microb Pathog. 2006;40(6):271–8.

58. Silva S, Henriques M, Oliveira R, Azeredo J, Malic S, Hooper SJ, et al. Characterization of Candida parapsilosis infection of an in vitro reconstituted human oral epithelium. Eur J Oral Sci. 2009;117(6):669–75.

59. Xiong X, Wu T, He S. Physical forces make rete ridges in oral mucosa. Med Hypotheses. 2013;81:883–6.

60. Kimball JR, Nittayananta W, Klausner M, Chung WO, Dale BA. Antimicrobial Barrier of an in vitro Oral Epithelial Model. Arch Oral Biol. 2006;51(9):775–83.

61. Sivard P, Dezutter-Dambuyant C, Kanitakis J, Mosnier JF, Hamzeh H,

Bechetoille N, et al. In vitro reconstructed mucosa-integrating Langerhans' cells. Exp Dermatol. 2003;12(4):346–55.

62. Linde N, Gutschalk CM, Hoffmann C, Yilmaz D, Mueller MM. Integrating macrophages into organotypic co-cultures: A 3D in vitro model to study tumor-associated macrophages. PLoS One. 2012;7(7).

63. Bechetoille N, Vachon H, Gaydon A, Boher A, Fontaine T, Mueller CG, et al. Letter to the Editor A new organotypic model containing dermal-type macrophages. 2011;20:1035–7.

64. Belair DG, Abbott BD. Engineering epithelial-stromal interactions in vitro for toxicology assessment. Toxicology. 2017;382(1):93–107.

65. Régnier M, Patwardhan A, Scheynius A, Schmidt R. Reconstructed human epidermis composed of keratinocytes, melanocytes and Langerhans cells. Med Biol Eng Comput. 1998;36(6):821–4.

66. Régnier M, Staquet MJ, Schmitt D, Schmidt R. Integration of Langerhans cells into a pigmented reconstructed human epidermis. J Invest Dermatol. 1997;109(4):510–2.

67. Jung MH, Jung SM, Shin HS. Co-stimulation of HaCaT keratinization with mechanical stress and air-exposure using a novel 3D culture device. Sci Rep. 2016;6(May):1–7.

68. Maas-Szabowski N. Epidermal tissue regeneration and stromal interaction in HaCaT cells is initiated by TGF-. J Cell Sci. 2003;116(14):2937–48.

69. Colombo I, Sangiovanni E, Maggio R, Mattozzi C, Zava S, Corbett Y, et al. HaCaT Cells as a Reliable in Vitro Differentiation Model to Dissect the Inflammatory/Repair Response of Human Keratinocytes. Mediators Inflamm. 2017;2017.

70. Gursoy UK, Gursoy M, Könönen E, Sintim HO, Uitto VJ, Syrjänen S. Construction and characterization of a multilayered gingival keratinocyte culture model: the TURK-U model. Cytotechnology. 2016;68(6):2345–54.

71. Deyrieux AF, Wilson VG. In vitro culture conditions to study keratinocyte differentiation using the HaCaT cell line. Cytotechnology. 2007;54(2):77–83.

72. Dabija-Wolter G, Bakken V, Cimpan MR, Johannessen AC, Costea DE. In vitro reconstruction of human junctional and sulcular epithelium. J Oral Pathol Med Off Publ Int Assoc Oral Pathol Am Acad Oral Pathol. 2013;42(5):396–404.

73. Nolte SV, Xu W, Rennekampff HO, Rodemann HP. Diversity of fibroblasts - A review on implications for skin tissue engineering. Cells Tissues Organs. 2008;187(3):165–76.

74. Llames S, García-Pérez E, Meana Á, Larcher F, Del Río M. Feeder Layer Cell Actions and Applications. Tissue Eng - Part B Rev. 2015;21(4):345–53.

75. Tsuchiya S, Gota Y, Okumura H, Nakae S, Konno T, Tada K, et al. Induction of Maturation in Cultured Human Monocytic Leukemia Cells by a Phorbol Diester. Cancer Res. 1982;42(4):1530–6.

76. Tedesco S, De Majo F, Kim J, Trenti A, Trevisi L, Fadini GP, et al. Convenience versus Biological Significance: Are PMA-Differentiated THP-1 Cells a Reliable Substitute for Blood-Derived Macrophages When Studying in Vitro Polarization? Front Pharmacol. 2018;9(FEB):1–13.

77. Bosshart H, Heinzelmann M. THP-1 cells as a model for human monocytes. Ann Transl Med. 2016;4(21):438–438.

78. Tamai IA, Salehi TZ, Sharifzadeh A, Shokri H, Khosravi AR. Repetitive sequences based on genotyping of candida albicans isolates obtained from iranian patients with human immunodeficiency virus. Iran J Basic Med Sci. 2014;17(11):831–5.

79. Al-obidi WIA, Abaas ZK. Microbiological and Molecular study On Candida species Isolated From Catheterized urine specimen In Ramadi general Teaching Hospital. 2012;11(2):82–7.

80. Wang SS, Tang YL, Pang X, Zheng M, Tang YJ, Liang XH. The maintenance of an oral epithelial barrier. Life Sci. 2019;227:129–36.

81. Cruchley AT, Bergmeier LA. Structure and functions of the oral mucosa. Oral Mucosa Heal Dis A Concise Handb. 2018;1–18.

82. Adams D. Keratinization of the oral epithelium. Ann R Coll Surg Engl. 1976;58(5):351–8.

83. Deo PN, Deshmukh R. Pathophysiology of keratinization. J oral Maxillofac Pathol. 2018;22(1):86–91.

84. Moll R, Divo M, Langbein L. The human keratins: Biology and pathology. Histochem Cell Biol. 2008;129(6):705–33.

85. Nelson WG, Sun TT. The 50- and 58-kdalton keratin classes as molecular markers for stratified squamous epithelia: Cell culture studies. J Cell Biol. 1983;97(1):244–51.

86. Alam H, Sehgal L, Kundu ST, Dalal SN, Vaidya MM. Novel function of keratins 5 and 14 in proliferation and differentiation of stratified epithelial cells. Mol Biol Cell. 2011;22(21):4068–78.

87. Groeger S, Meyle J. Oral mucosal epithelial cells. Front Immunol. 2019;10(FEB):1–22.

88. Kinikoglu B, Damour O, Hasirci V. Tissue engineering of oral mucosa: a shared concept with skin. J Artif Organs. 2015;18(1):8–19.

89. Fuchs E. Keratin genes, epidermal differentiation and animal models for the study of human skin diseases. Biochem Soc Trans. 1991;19(4):1112–5.

90. Prost-Squarcioni C. Histologie de la peau et des follicules pileux. Medecine/Sciences. 2006;22(2):131–7.

91. Kim HS, Kim NH, Kim J, Cha IH. Inducing re-epithelialization in skin wound through cultured oral mucosal keratinocytes. J Korean Assoc Oral Maxillofac Surg. 2013;39(2):63.

92. Lee J, Shin D, Roh JL. Use of a pre-vascularised oral mucosal cell sheet for promoting cutaneous burn wound healing. Theranostics. 2018;8(20):5703–12.

93. Gursoy UK, Pöllänen M, Könönen E, Uitto V-J. A Novel Organotypic Dento-Epithelial Culture Model: Effect of Fusobacterium nucleatum Biofilm on B-Defensin-2, -3, and LL-37 Expression . J Periodontol. 2012;83(2):242–7.

94. Bainbridge P. Wound healing and the role of fibroblasts. J Wound Care. 2013;22(8):407–12.

95. Sriram G, Bigliardi PL, Bigliardi-Qi M. Fibroblast heterogeneity and its implications for engineering organotypic skin models in vitro. Eur J Cell Biol. 2015;94(11):483–512.

96. Phipps RP, Borrello MA, Blieden TM. Fibroblast heterogeneity in the periodontium and other tissues. J Periodontal Res. 1997;32(1):159–65.

97. Dabija-Wolter G, Sapkota D, Cimpan MR, Neppelberg E, Bakken V, Costea DE. Limited in-depth invasion of Fusobacterium nucleatum into in vitro reconstructed human gingiva. Arch Oral Biol. 2012;57(4):344–51.

98. Katakura Y, Alam S, Shirahata S. Immortalization by Gene transfection. Methods Cell Biol. 1998;57:69–91.

99. Mondello C, Chiodi I. Cellular immortalization and neoplastic transformation: Simultaneous, sequential or independent? Telomeres, telomerase or karyotypic variations? Cell Cycle. 2013;12(11):1804–5.

100. Wang Y, Chen S, Yan Z, Pei M. A prospect of cell immortalization combined with matrix microenvironmental optimization strategy for tissue engineering and regeneration. Cell Biosci. 2019;9(1):7.

101. Kaur G, Dufour JM. Cell lines: Valuable tools or useless artifacts. Spermatogenesis. 2012;2(1):1–5.

102. ATCC. ATCC hTERT immortalized Cell Culture Guide [Internet]. Cell culture guides. 2019. Available from: www.atcc.org

103. ATCC. ATCC Primary cell culture guide [Internet]. Cell culture guides. 2019. Available from: www.atcc.org

104. Bosman FT, Stamenkovic I. Functional structure and composition of the extracellular matrix. J Pathol. 2003;200(4):423–8.

105. Garcia-Gareta E, Ravindran N, Sharma V, Samizadeh S, Dye JF. A novel multiparameter in vitro model of three-dimensional cell ingress into scaffolds for dermal reconstruction to predict in vivo outcome. Biores Open Access. 2013;2(6):412–20.

106. LeBleu VS, MacDonald B, Kalluri R. Structure and function of basement membranes. Exp Biol Med. 2007;232(9):1121–9.

107. Smola H, Stark HJ, Thiekötter G, Mirancea N, Krieg T, Fusenig NE. Dynamics of basement membrane formation by keratinocyte-fibroblast interactions in organotypic skin culture. Exp Cell Res. 1998;239(2):399–410.

108. Medzhitov R, Janeway CA. Innate immunity: The virtues of a nonclonal system of recognition. Cell. 1997;91(3):295–8.

109. Chaturvedi A, Pierce SK. How location governs Toll like receptor signaling (NIH Public Access author manuscript). Allergy. 2009;10(6):621–8.

110. Netea MG, Brown GD, Kullberg BJ, Gow NAR. An integrated model of the recognition of Candida albicans by the innate immune system. Nat Rev Microbiol. 2008;6(1):67–78.

111. Pålsson-McDermott EM, O'Neill LAJ. Signal transduction by the lipopolysaccharide receptor, Toll-like receptor-4. Immunology. 2004;113(2):153–62.

112. Takeda K, Takeuchi O, Akira S. Recognition of lipopeptides by Toll-like receptors. J Endotoxin Res. 2002;8(6):459–63.

113. Schwandner R, Dziarski R, Wesche H, Rothe M, Kirschning CJ. Peptidoglycan- and lipoteichoic acid-induced cell activation is mediated by Toll-like receptor 2. J Biol Chem. 1999;274(25):17406–9.

114. Natsuka M, Uehara A, Yang S, Echigo S, Takada H. A polymer-type water-soluble peptidoglycan exhibited both Toll-like receptor 2- and NOD2-agonistic activities, resulting in synergistic activation of human monocytic cells. Innate Immun. 2008;14(5):298–308.

115. Takeuchi O, Hoshino K, Kawai T, Sanjo H, Takada H, Ogawa T, et al. Differential Roles of TLR2 and TLR4 in Recognition of Gram-Negative and Gram-Positive Bacterial Cell Wall Components. Immunity. 1999;11(4):443–51.

116. Hajjar AM, O'Mahony DS, Ozinsky A, Underhill DM, Aderem A, Klebanoff SJ, et al. Cutting Edge: Functional Interactions Between Toll-Like Receptor (TLR) 2 and TLR1 or TLR6 in Response to Phenol-Soluble Modulin. J Immunol. 2001;166(1):15–9.

117. Jones BW, Means TK, Heldwein KA, Keen MA, Hill PJ, Belisle JT, et al. Different Toll-like receptor agonists induce distinct macrophage responses. J Leukoc Biol. 2001;69(6):1036–44.

118. Hayashi F, Smith KD, Ozinsky A, Hawn TR, Yi EC, Goodlett DR, et al. The innate immune response to bacterial flagellin is mediated by Toll-like receptor 5. Nature. 2001;410(6832):1099–103.

119. Ashkar A, Rosenthal K. Toll-like Receptor 9, CpG DNA and Innate Immunity. Curr Mol Med. 2005;2(6):545–56.

120. Ozinsky A, Underhill DM, Fontenot JD, Hajjar AM, Smith KD, Wilson CB, et al. The repertoire for pattern recognition of pathogens by the innate immune system is defined by cooperation between Toll-like receptors. PNAS. 2000;97(25):13766–71.

121. Tada H, Nemoto E, Shimauchi H, Watanabe T, Mikami T, Matsumoto T, et al. Saccharomyces cerevisiae- and Candida albicans-derived mannan induced production of tumor necrosis factor alpha by human monocytes in a CD14- and Toll-like receptor 4-dependent manner. Microbiol Immunol. 2002;46(7):503–12.

122. Jouault T, Ibata-Ombetta S, Takeuchi O, Trinel P, Sacchetti P, Lefebvre P, et al. *Candida albicans* Phospholipomannan Is Sensed through Toll-Like Receptors. J Infect Dis. 2003;188(1):165–72.

123. Monari C, Pericolini E, Bistoni G, Casadevall A, Kozel TR, Vecchiarelli A. Cryptococcus neoformans Capsular Glucuronoxylomannan Induces Expression of Fas Ligand in Macrophages . J Immunol. 2005;174(6):3461–8.

124. Kim SJ, Kim HM. Dynamic lipopolysaccharide transfer cascade to TLR4/MD2 complex via LBP and CD14. BMB Rep. 2017;50(2):55–7.

125. Park BS, Song DH, Kim HM, Choi BS, Lee H, Lee JO. The structural basis of lipopolysaccharide recognition by the TLR4-MD-2 complex. Nature. 2009;458(7242):1191–5.

126. Goh FG, Midwood KS. Intrinsic danger: Activation of Toll-like receptors in rheumatoid arthritis. Rheumatology. 2012;51(1):7–23.

127. Morandini ACF, Chaves Souza PP, Ramos-Junior ES, Brozoski DT, Sipert CR, Souza Costa CA, et al. Toll-Like Receptor 2 Knockdown Modulates Interleukin (IL)-6 and IL-8 but not Stromal Derived Factor-1 (SDF-1/CXCL12) in Human Periodontal Ligament and Gingival Fibroblasts. J Periodontol. 2013;84(4):535–44.

128. Hirschfeld M, Ma Y, Weis JH, Stefanie N, Weis JJ, Receptor L, et al. Cutting Edge: Repurification of Lipopolysaccharide Eliminates Signaling Through Both Human and Murine Toll-Like Receptor 2. J Immunol. 2000;165(2):618–22.

129. Liu X, Yin S, Chen Y, Wu Y, Zheng W, Dong H, et al. LPS-induced proinflammatory cytokine expression in human airway epithelial cells and macrophages via NF-κB, STAT3 or AP-1 activation. Mol Med Rep. 2018;17(4):5484–91.

130. Jefferies CA. Regulating IRFs in IFN driven disease. Front Immunol. 2019;10(MAR):1–15.

131. Murdock JL, Núñez G. TLR4: The Winding Road to the Discovery of the LPS Receptor. 2016;197(7):2561–2.

132. Aulock S Von, Morath S, Hareng L, Knapp S, Kessel KPM Van, Strijp JAG Van. Lipoteichoic acid from Staphylococcus aureus is a potent stimulus for neutrophil recruitment. Immunobiology. 2003;422:413–22.

133. Dunn-Siegrist I, Tissières P, Drifte G, Bauer J, Moutel S, Pugin J. Toll-like Receptor Activation of Human Cells by Synthetic Triacylated Lipid A-like Molecules. J Biol Chem. 2012;287(20):16121–31.

134. Dammermann W, Wollenberg L, Bentzien F, Lohse A, Lüth S. Toll like receptor 2 agonists lipoteichoic acid and peptidoglycan are able to enhance

antigen specific IFNγ release in whole blood during recall antigen responses. J Immunol Methods. 2013;396(1–2):107–15.

135. Naderi B, Ko G, Voelcker V, Behrendt H, Ring J, Bauer S, et al. Various members of the Toll-like receptor family contribute to the innate immune response of human epidermal keratinocytes. 2005;531–41.

136. Cario E, Brown D, Mckee M, Lynch-devaney K, Gerken G, Podolsky DK. Commensal-Associated Molecular Patterns Induce Selective Toll-Like Receptor-Trafficking from Apical Membrane to Cytoplasmic Compartments in Polarized Intestinal Epithelium. 2002;160(1):165–73.

137. Köllisch G, Kalali BN, Voelcker V, Wallich R, Behrendt H, Ring J, et al. Various members of the Toll-like receptor family contribute to the innate immune response of human epidermal keratinocytes. Immunology. 2005;114(4):531–41.

138. Kawai K, Shimura H, Minagawa M, Ito A, Tomiyama K, Ito M. Expression of functional Toll-like receptor 2 on human epidermal keratinocytes. J Dermatol Sci. 2002;30(2002):185–94.

139. Olaru F, Jensen LE. Chemokine expression by human keratinocyte cell lines after activation of Toll-like receptors. Exp Dermatol. 2010;19(8):314–6.

140. Mempel M, Voelcker V, Köllisch G, Plank C, Rad R, Gerhard M, et al. Toll-Like Receptor Expression in Human Keratinocytes: Nuclear Factor κB Controlled Gene Activation by Staphylococcus aureus is Toll-Like Receptor 2 But Not Toll-Like Receptor 4 or Platelet Activating Factor Receptor Dependent. J Invest Dermatol. 2003;121(6):1389–96.

141. Pivarcsi A, Koreck A, Bodai L, Széll M, Szeg C, Belso N, et al. Differentiation-regulated expression of toll-like receptors 2 and 4 in HaCat keratinocytes. Arch Dermatol Res. 2004;296(3):120–4.

142. Takada. AU and H. Functional TLRs and NODs in Human Gingival Fibroblasts. Dent Res. 2007;86(3):247–54.

143. Tang L, Zhou X, Wang Q, Zhang L, Wang Y. Expression of TRAF6 and pro-inflammatory cytokines through activation of TLR2 , TLR4 , NOD1 , and NOD2 in human periodontal ligament fibroblasts. Arch Oral Biol. 2011;56(10):1064–72.

144. Hirao K, Yumoto H, Takahashi K, Mukai K, Nakanishi T, Matsuo T. Roles of TLR2, TLR4, NOD2, and NOD1 in Pulp Fibroblasts. J Dent Res. 2009;88(8):762–8.

145. Wang P, Oido-mori M, Fujii T, Kowashi Y, Kikuchi M, Suetsugu Y, et al. Heterogeneous Expression of Toll-like Receptor 4 and Downregulation of Toll-like Receptor 4 Expression on Human Gingival Fibroblasts by Porphyromonas gingivalis Lipopolysaccharide. 2001;867:863–7.

146. Mahanonda R, Sa-Ard-Iam N, Montreekachon P, Pimkhaokham A, Yongvanichit K, Fukuda MM, et al. IL-8 and IDO Expression by Human Gingival Fibroblasts via TLRs. J Immunol. 2007;178(2):1151–7.

147. Wang P, Ohura K, Fujii T, Oido-mori M, Kowashi Y, Kikuchi M, et al. DNA microarray analysis of human gingival fibroblasts from healthy and inflammatory gingival tissues. 2003;305(2003):970–3.

148. Tamai R, Sakuta T, Matsushita K, Torii M, Takeuchi O, Akira S, et al. Human Gingival CD14 ♀ Fibroblasts Primed with Gamma Interferon Increase Production of Interleukin-8 in Response to Lipopolysaccharide through Up-Regulation of Membrane CD14 and MyD88 mRNA Expression. 2002;70(3):1272–8.

149. Whiley R a, Cruchley AT, Gore C, Hagi-Pavli E. Candida albicans strain-dependent modulation of pro-inflammatory cytokine release by in vitro oral and vaginal mucosal models. Cytokine. 2012;57(1):89–97.

150. Jones SA, Hunter CA. IL-6 as a keystone cytokine in health and disease. Nat Immunol. 2015;16(5):448–57.

151. Castell JV, David M, Klapproth J, Heinrich PC, Andus T, Geiger T, et al. Interleukin-6 is the Major Regulator of Acute Phase Protein Synthesis in Rat and Man. In: Advances in Immunopharmacology. Elsevier; 1989. p. 191–201.

152. Yasukawa K, Hirano T, Watanabe Y, Muratani K, Matsuda T, Nakai S, et al. Structure and expression of human B cell stimulatory factor-2 (BSF-2/IL-6) gene. EMBO J. 1987;6(10):2939–45.

153. Woloski BM, Fuller GM. Identification and partial characterization of hepatocyte-stimulating factor from leukemia cell lines: comparison with interleukin 1. Proc Natl Acad Sci. 1984;82(5):1443–7.

154. Yoshizaki K, Nakagawa T, Fukunaga K, Tseng LT, Yamamura Y, Kishimoto T. Isolation and characterization of B cell differentiation factor (BCDF) secreted from a human B lymphoblastoid cell line. J Immunol. 1984;132(6):2948 LP – 2954.

155. Hirano T, Yasukawa K, Harada H, Taga T, Watanabe Y, Matsuda T, et al. Complementary DNA for a novel human interleukin (BSF-2) that induces B lymphocytes to produce immunoglobulin. Nature. 1986;324(6092):73–6.

156. Li B, Jones LL, Geiger TL. IL-6 Promotes T Cell Proliferation and Expansion under Inflammatory Conditions in Association with Low-Level RORγt Expression. J Immunol. 2018;201(10):2934 LP – 2946.

157. Klimpel GR. Soluble factor(s) from LPS-activated macrophages induce cytotoxic T cell differentiation from alloantigen-primed spleen cells. J Immunol. 1980;125(3):1243 LP – 1249.

158. Scheller J, Chalaris A, Schmidt-Arras D, Rose-John S. The pro- and anti-inflammatory properties of the cytokine interleukin-6. Biochim Biophys Acta - Mol Cell Res. 2011;1813(5):878–88.

159. Jones SA, Takeuchi T, Aletaha D, Smolen J, Choy EH, Mcinnes I. Interleukin 6 : The biology behind the therapy. Considerations Med. 2018;2:2–6.

160. Tanaka T, Narazaki M, Kishimoto T. Interleukin (IL-6) Immunotherapy. Perspect Biol. 2017;1–16.

161. Rose-John S. The Soluble Interleukin 6 Receptor: Advanced Therapeutic Options in Inflammation. Clin Pharmacol Ther. 2017;102(4):591–8.

162. Hoge J, Yan I, Jänner N, Schumacher V, Chalaris A, Steinmetz OM, et al. IL-6 Controls the Innate Immune Response against Listeria monocytogenes via Classical IL-6 Signaling . J Immunol. 2013;190(2):703–11.

163. Allard JB, Rincon M, Dienz O, Ciliberto G, Neveu WA, Wargo MJ, et al. IL-6 Is Required for Airway Mucus Production Induced by Inhaled Fungal Allergens. J Immunol. 2009;183(3):1732–8.

164. Smith KA, Maizels RM. IL-6 controls susceptibility to helminth infection by impeding Th2 responsiveness and altering the Treg phenotype in vivo. Eur J Immunol. 2014;44(1):150–61.

165. Puel A, Picard C, Lorrot M, Pons C, Chrabieh M, Lorenzo L, et al. Recurrent Staphylococcal Cellulitis and Subcutaneous Abscesses in a Child with Autoantibodies against IL-6. J Immunol. 2008;180(1):647–54.

166. Schett G. Physiological effects of modulating the interleukin-6 axis. Rheumatology. 2018;57(suppl_2):ii43–50.

167. Genovese MC, Rubbert-Roth A, Smolen JS, Kremer J, Khraishi M, Gómez-Reino J, et al. Longterm Safety and Efficacy of Tocilizumab in Patients with Rheumatoid Arthritis: A Cumulative Analysis of Up to 4.6 Years of Exposure. J Rheumatol. 2013;40(6):768 LP – 780.

168. Bauer J, Bauer TM, Kalb T, Taga T, Lengyel G, Hirano T, et al. Regulation of interleukin 6 receptor expression in human monocytes and monocyte-derived macrophages. Comparison with the expression in human hepatocytes. J Exp Med. 1989;170(5):1537–49.

169. Barnes TC, Anderson ME, Moots RJ. The Many Faces of Interleukin-6: The Role of IL-6 in Inflammation, Vasculopathy, and Fibrosis in Systemic Sclerosis. Int J Rheumatol. 2011;2011:1–6.

170. Russo RC, Garcia CC, Teixeira MM, Amaral FA. The CXCL8/IL-8 chemokine family and its receptors in inflammatory diseases. Expert Rev Clin Immunol. 2014;10(5):593–619.

171. Yoshimura T. Discovery of IL-8/CXCL8 (The Story from Frederick). Front Immunol. 2015;6(June):6–8.

172. Yoshimura T, Matsushima K, Oppenheim JJ, Leonard EJ. Neutrophil chemotactic factor produced by lipopolysaccharide (LPS)-stimulated human blood mononuclear leukocytes: partial characterization and separation from interleukin 1 (IL 1). J Immunol. 1987;139(3):788 LP – 793.

173. Yoshimura T, Matsushimat K, Tanakat S, Robinsont EA, Oppenheimt JJ, Leonard EJ. Purification of a human monocyte-derived neutrophil chemotactic factor that has peptide sequence similarity to other host defense cytokines. 1987;84(December):9233–7.

174. Larsen CG, Anderson A, Appella E, Oppenheim JJ, Matsushima K. The Neutrophil-Activating Protein (NAP-1) Is Also Chemotactic for T Lymphocytes. 1988;243(1986):64–7.

175. Bonecchi R, Facchetti F, Dusi S, Luini W, Lissandrini D, Simmelink M, et al. Induction of Functional IL-8 Receptors by IL-4 and IL-13 in Human Monocytes. J Immunol. 2000;164(7):3862–9.

176. Nilsson BG, Mikovits JA, Metcalfe DD, Taub DD. Mast Cell Migratory Response to Interleukin-8 Is Mediated Through Interaction With Chemokine Receptor CXCR2/Interleukin-8RB. Blood. 1999;93(9):2791–7.

177. Ochensberger B, Tassera L, Bifrare D, Rihs S, Clemens A. Regulation of cytokine expression and leukotriene formation in human basophils by growth factors , chemokines and chemotactic agonists. Eur J Immunol. 1999;29:11–22.

178. Thomas SY, Hou R, Boyson JE, Means TK, Hess C, Olson DP, et al. CD1d-Restricted NKT Cells Express a Chemokine Receptor Profile Indicative of Th1-Type Inflammatory Homing Cells. J Immunol. 2003;171(5):2571–80.

179. Nirodi CS, Devalaraja R, Nanney LB, Arrindell S, Russell S, Trupin J, et al. Chemokine and chemokine receptor expression in keloid and normal fibroblasts. Wound Repair Regen. 2000;8(5):371–82.

180. Kondo S, Yoneta A, Yazawa H, Kamada A, Jimbow K. Downregulation of CXCR-2 but not CXCR-1 expression by human keratinocytes by UVB. J Cell Physiol. 2000;182(3):366–70.

181. Botelho RJ, Grinstein S. Phagocytosis. Curr Biol. 2011;21(14):533–8.

182. Faurschou M, Borregaard N. Neutrophil granules and secretory vesicles in inflammation. Microbes Infect. 2003;5(14):1317–27.

183. Amulic B, Hayes G. Quick guide Neutrophil extracellular traps. CURBIO. 2004;21(9):R297–8.

184. Chan FK-M, Moriwaki KR, De and MJ. Immune Homeostasis. In: Encyclopedic Dictionary of Genetics, Genomics and Proteomics. Hoboken, NJ, USA: John Wiley & Sons, Inc.; 2004. p. 8–12.

185. Miyake Y, Yamasaki S. Sensing necrotic cells. Adv Exp Med Biol. 2012;738:144–52.

186. Roh JS, Sohn DH. Damage-associated molecular patterns in inflammatory diseases. Immune Netw. 2018;18(4):1–14.

187. Maeda A, Fadeel B. Mitochondria released by cells undergoing TNF-α-induced necroptosis act as danger signals. Cell Death Dis. 2014;5(7):e1312-9.

188. Agarwal S, Baran C, Piesco NP, Quintero JC, Langkamp HH, Johns L, et al. Synthesis of proinflammatory cytokines by human gingival fibroblasts in response to lipopolysaccharides and interleukin-1β. J Periodontal Res. 1995;30:382–9.

189. Byrne A, Reen DJ. Lipopolysaccharide Induces Rapid Production of IL-10 by Monocytes in the Presence of Apoptotic Neutrophils. J Immunol. 2002;168(4):1968–77.

190. Schulze C, Wetzel F, Kueper T, Malsen A, Muhr G, Jaspers S, et al. Stiffening of human skin fibroblasts with age. Biophys J. 2010;99(8):2434–42.

191. Brauer E, Lippens E, Klein O, Nebrich G, Schreivogel S, Korus G, et al. Collagen Fibrils Mechanically Contribute to Tissue Contraction in an In Vitro Wound Healing Scenario. Adv Sci. 2019;6(9).

192. Ando T, Mikawa K, Nishina K, Misumi T, Obara H. Hypocapnic alkalosis enhances oxidant-induced apoptosis of human alveolar epithelial type II cells. J Int Med Res. 2007;35(1):118–26.

193. Edye ME, Lopez-Castejon G, Allan SM, Brough D. Acidosis drives damage-associated molecular pattern (DAMP)-induced interleukin-1 secretion via a caspase-1-independent pathway. J Biol Chem. 2013;288(42):30485–94.

194. Ge Q, Moir LM, Black JL, Oliver BG, Burgess JK. TGFβ1 induces IL-6 and inhibits IL-8 release in human bronchial epithelial cells: The role of Smad2/3. J Cell Physiol. 2010;225(3):846–54.

195. Barthes J, Özçelik H, Hindié M, Ndreu-Halili A, Hasan A, Vrana NE. Cell Microenvironment Engineering and Monitoring for Tissue Engineering and Regenerative Medicine: The Recent Advances. Biomed Res Int. 2014;2014(i):1–18.

196. Almela T, Al-sahaf S, Brook IM, Khoshroo K, Fahimipour F, Tahriri M. 3D printed tissue engineered model for bone invasion of oral cancer. Tissue Cell. 2018;52(1):71–7.

197. Navarro FA, Mizuno S, Huertas JC, Glowacki J, Orgill DP. Perfusion of medium improves growth of human oral neomucosal tissue constructs. Wound Repair Regen Off Publ Wound Heal Soc [And] Eur Tissue Repair Soc. 2001;9(6):507–12.

198. Zhao Y, Ding C. Effects of Hydrocortisone on Regulating Inflammation, Hemodynamic Stability, and Preventing Shock in Severe Sepsis Patients. Med Sci Monit. 2018;24:3612–9.

199. Page-mccaw A, Ewald AJ, Werb Z. Matrix metalloproteinases and the regulation of tissue remodelling. Nat Rev Mol cell Biol. 2009;8(3):221–33.

200. Thirkettle S, Decock J, Arnold H, Pennington CJ, Jaworski DM, Edwards DR. Matrix metalloproteinase 8 (collagenase 2) induces the expression of interleukins 6 and 8 in breast cancer cells. J Biol Chem. 2013;288(23):16282–94.

201. Chaussain Miller C, Septier D, Bonnefoix M, Lecolle S, Lebreton-Decoster C, Coulomb B, et al. Human dermal and gingival fibroblasts in a three-dimensional culture: a comparative study on matrix remodeling. Clin Oral Investig. 2002;6(1):39–50.

202. Naruishi K, Nagata T. Biological effects of interleukin-6 on Gingival Fibroblasts: Cytokine regulation in periodontitis. J Cell Physiol. 2018;233(9):6393–400.

203. Sugawara T, Gallucci RM, Simeonova PP, Luster MI. Regulation and role of interleukin 6 in wounded human epithelial keratinocytes. Cytokine. 2001;15(6):328–36.

204. Hernández-Quintero M, Kuri-Harcuch W, González Robles A, Castro-Muñozledo F. Interleukin-6 promotes human epidermal keratinocyte proliferation and keratin cytoskeleton reorganization in culture. Cell Tissue Res. 2006;325(1):77–90.

205. Jiang WG, Sanders AJ, Ruge F, Harding KG. Influence of interleukin-8 (IL-8) and IL-8 receptors on the migration of human keratinocytes, the role of plc-γ and potential clinical implications. Exp Ther Med. 2012;3(2):231–6.

206. Spörri B, Müller KM, Wiesmann U, Bickel M. Soluble IL-6 receptor induces calcium flux and selectively modulates chemokine expression in human dermal fibroblasts. Int Immunol. 1999;11(7):1053–8.

207. Dunlevy JR, Couchman JR. Interleukin-8 induces motile behavior and loss of focal adhesions in primary fibroblasts. J Cell Sci. 1995;108(1):311–21.

208. Morandini ACF, Chaves Souza PP, Ramos-Junior ES, Brozoski DT, Sipert CR, Souza Costa CA, et al. Toll-Like Receptor 2 Knockdown Modulates Interleukin (IL)-6 and IL-8 but not Stromal Derived Factor-1 (SDF-1/CXCL12) in Human Periodontal Ligament and Gingival Fibroblasts. J Periodontol. 2013;84(4):535–44.

209. Sugawara Y, Uehara A, Fujimoto Y, Kusumoto S, Fukase K, Shibata K, et al. Toll-like Receptors, NOD1, and NOD2 in Oral Epithelial Cells. J Dent Res. 2006;85(6):524–9.

210. Fournier B, Philpott DJ. Recognition of Staphylococcus aureus by the Innate Immune System. 2005;18(3):521–40.

211. Ding P, Wang C, Darveau RP, Jin L. Porphyromonas gingivalis LPS stimulates the expression of LPS-binding protein in human oral keratinocytes in vitro. Innate Immun. 2013;19(1):66–75.

212. Mahanonda R, Sa-Ard-Iam N, Montreekachon P, Pimkhaokham A, Yongvanichit K, Fukuda MM, et al. IL-8 and IDO Expression by Human Gingival Fibroblasts via TLRs. J Immunol. 2007;178(2):1151–7.

213. Buskermolen JK, Reijnders CMA, Spiekstra SW, Steinberg T, Kleverlaan CJ, Feilzer AJ, et al. Development of a Full-Thickness Human Gingiva Equivalent. Tissue Eng. 2016;22(8):781–91.

214. Deshmane SL, Kremlev S, Amini S, Sawaya BE. Monocyte chemoattractant protein-1 (MCP-1): An overview. J Interf Cytokine Res.

2009;29(6):313–25.

215. Chomarat P, Banchereau J, Davoust J, Karolina Palucka A. IL-6 switches the differentiation of monocytes from dendritic cells to macrophages. Nat Immunol. 2000;1(6):510–4.

216. Chen L, Wang S, Wang Y, Zhang W, Ma K, Hu C, et al. IL-6 influences the polarization of macrophages and the formation and growth of colorectal tumor. Oncotarget. 2018;9(25):17443–54.

217. Garlanda C, Riva F, Bonavita E, Gentile S, Mantovani A. Decoys and regulatory “receptors” of the il-1/toll-like receptor superfamily. Front Immunol. 2013;4(JUL):1–13.

218. Veillette A, Latour S, Davidson D. Negative Regulation of Immunoreceptor Signaling. Annu Rev Immunol. 2002;20(1):669–707.

219. Mantovani A, Locati M, Vecchi A, Sozzani S, Allavena P. Decoy receptors: A strategy to regulate inflammatory cytokines and chemokines. Trends Immunol. 2001;22(6):328–36.

220. Moore KW, de Waal Malefyt R, Coffman RL, O’Garra A. Interleukin-10 and the Interleukin-10 Receptor. Annu Rev Immunol. 2001;19(1):683–765.

221. Radtke S, Wüller S, Yang XP, Lippok BE, Mütze B, Mais C, et al. Cross-regulation of cytokine signalling: Pro-inflammatory cytokines restrict IL-6 signalling through receptor internalisation and degradation. J Cell Sci. 2010;123(6):947–59.

222. Arend WP, Gabay C. Physiologic role of interleukin-1 receptor antagonist. Arthritis Res. 2000;2(4):245–8.

223. Calderone, R A, Fonzi, W A. Virulence Factors of Candida albicans. Trends Microbiol. 2001;9(7):327–35.

224. Agrawal A, Singh A, Verma R, Murari A. Oral candidiasis: An overview. J Oral Maxillofac Pathol. 2014;18(4):81.

225. Calderone RA, Clancy CJ. Candida and candidiasis. Washington, DC: ASM Press; 2012.

226. Naglik JR, Richardson JP, Moyes DL. Candida albicans Pathogenicity and Epithelial Immunity. PLoS Pathog. 2014;10(8):8–11.

227. Bishop CT, Blank F, Gardner PE. the Cell Wall Polysaccharides of Candida Albicans: Glucan, Mannan, and Chitin. Can J Chem. 1960;38(6):869–81.

228. Wagener J, Mailänder-Sanchez D, Schaller M. Immune responses to Candida albicans in models of in vitro reconstituted human oral epithelium. Methods Mol Biol. 2012;845:333–44.

229. Cohen-Kedar S, Baram L, Elad H, Brazowski E, Guzner-Gur H, Dotan I. Human intestinal epithelial cells respond to β-glucans via Dectin-1 and Syk. Eur J Immunol. 2014;44(12):3729–40.

230. Biondo C, Malara A, Costa A, Signorino G, Cardile F, Midiri A, et al. Recognition of fungal RNA by TLR7 has a nonredundant role in host defense against experimental candidiasis. Eur J Immunol. 2012;42(10):2632–43.

231. Miyazato A, Nakamura K, Yamamoto N, Mora-Montes HM, Tanaka M, Abe Y, et al. Toll-like receptor 9-dependent activation of myeloid dendritic cells by deoxynucleic acids from Candida albicans. Infect Immun. 2009;77(7):3056–64.

232. Netea MG, Van De Veerdonk F, Verschueren I, Van Der Meer JWM, Kullberg BJ. Role of TLR1 and TLR6 in the host defense against disseminated candidiasis. FEMS Immunol Med Microbiol. 2008;52(1):118–23.

233. Zheng N, Wang Y, Hu D, Yan L, Jiang Y. The role of pattern recognition receptors in the innate recognition of Candida albicans. 2015;6(4):347–61.

234. Gow NAR, Van De Veerdonk FL, Brown AJP, Netea MG. Candida albicans morphogenesis and host defence: Discriminating invasion from colonization. Nat Rev Microbiol. 2012;10(2):112–22.

235. Wertheim HFL, Melles DC, Vos MC, Leeuwen W Van, Belkum A Van, Verbrugh HA, et al. The role of nasal carriage in Staphylococcus aureus infections. 2005;5(December):751–62.

236. McCormack MG, Smith AJ, Akram AN, Jackson M, Robertson D, Edwards G. Staphylococcus aureus and the oral cavity: An overlooked source of carriage and infection? Am J Infect Control. 2015;43(1):35–7.

237. Foster TJ. Antibiotic resistance in Staphylococcus aureus. Current status and future prospects. FEMS Microbiol Rev. 2017;41(3):430–49.

238. Peters BM, Jabra-Rizk MA, Scheper MA, Leid JG, Costerton JW, Shirtliff ME. Microbial interactions and differential protein expression in Staphylococcus aureus -Candida albicans dual-species biofilms. FEMS Immunol Med Microbiol. 2010;59(3):493–503.

239. Pereira CA, Toledo BC, Santos CT, Pereira Costa ACB, Back-Brito GN,

Kaminagakura E, et al. Opportunistic microorganisms in individuals with lesions of denture stomatitis. Diagn Microbiol Infect Dis. 2013;76(4):419–24.

240. A.V.Newton. Denture sore mouth a possible etiology. Br Dent J. 1962;112:357–60.

241. Smith AJ, Brewer A, Kirkpatrick P, Jackson MS, Young J, Watson S, et al. Staphylococcal species in the oral cavity from patients in a regional burns unit. J Hosp Infect. 2003;55(3):184–9.

242. Sumi Y, Miura H, Sunakawa M, Michiwaki Y, Sakagami N. Colonization of denture plaque by respiratory pathogens in dependent elderly. Gerodontology. 2002;19(1):25–9.

243. Sumi Y, Kagami H, Ohtsuka Y, Kakinoki Y, Haruguchi Y, Miyamoto H. High correlation between the bacterial species in denture plaque and pharyngeal microflora. Gerodontology. 2003;20(2):84–7.

244. Harriott MM, Noverr MC. Candida albicans and Staphylococcus aureus form polymicrobial biofilms: Effects on antimicrobial resistance. Antimicrob Agents Chemother. 2009;53(9):3914–22.

245. Carlson E, Johnson G. Protection by Candida albicans of Staphylococcus aureus in the establishment of dual infection in mice. Infect Immun. 1985;50(3):655–9.

246. Carlson E. Synergistic effect of Candida albicans and Staphylococcus aureus on mouse mortality. Infect Immun. 1982;38(3):921–4.

247. Carlson E. Effect of strain of Staphylococcus aureus on synergism with Candida albicans resulting in mouse Effect of Strain of Staphylococcus aureus on Synergism with Candida albicans Resulting in Mouse Mortality and Morbidity. 1983;42(1):285–92.

248. Peters BM, Ovchinnikova ES, Krom BP, Schlecht LM, Zhou H, Hoyer LL, et al. Staphylococcus aureus adherence to Candida albicans hyphae is mediated by the hyphal adhesin Als3p. Microbiology. 2012;158(12):2975–86.

249. Klotz SA, Chasin BS, Powell B, Gaur NK, Lipke PN. Polymicrobial bloodstream infections involving Candida species: analysis of patients and review of the literature. Diagn Microbiol Infect Dis. 2007;59(4):401–6.

250. del Rio A, Cervera C, Moreno A, Moreillon P, Miró JM. Patients at Risk of Complications of Staphylococcus aureus Bloodstream Infection . Clin Infect Dis. 2009;48(s4):S246–53.

251. Bertolini M, Ranjan A, Thompson A, Diaz PI, Sobue T, Maas K, et al. Candida albicans induces mucosal bacterial dysbiosis that promotes invasive infection. PLoS Pathog. 2019;15(4):1–30.

252. Martins CA de P, Jorge CYK-I, Cardoso AO. Prevalence of Staphylococcus spp and Candida spp in the oral cavity. Brazilian J Microbiol. 2002;33(1):236–40.

253. Singh A, Verma R, Murari A, Agrawal A. Oral candidiasis: An overview. J Oral Maxillofac Pathol. 2014;18(5):81–5.

254. Majima T, Ito-Kuwa S, Nagatomi R, Nakamura K. Study of the oral carriage of Candida sp. in dental students and staff-Identification of Candida sp. and background survey. Oral Sci Int. 2014;11(1):30–4.

255. Norris HL, Friedman J, Chen Z, Puri S, Wilding G, Edgerton M. Salivary metals, age, and gender correlate with cultivable oral Candida carriage levels. J Oral Microbiol. 2018;10(1).

256. Lewis N, Parmar N, Hussain Z, Baker G, Green I, Howlett J, et al. Colonisation of dentures by Staphylococcus aureus and MRSA in out-patient and in-patient populations. Eur J Clin Microbiol Infect Dis. 2015;34(9):1823–6.

257. Al-Dossary OAE, Al-Shamahy HA. Oral Candida Albicans Colonization in Dental Prosthesis Patients and Individuals with Natural Teeth, Sana'a City, Yemen. Biomed J Sci Tech Res. 2018;11(2):8388–92.

258. Alrayyes SF, Alruwaili HM, Taher IA, Elrahawy KM, Almaeen AH, Ashekhi AO, et al. Oral Candidal carriage and associated risk indicators among adults in Sakaka, Saudi Arabia. BMC Oral Health. 2019;19(1):1–7.

259. Zomorodian K, Haghighi NN, Rajaee N, Pakshir K, Tarazooie B, Vojdani M, et al. Assessment of Candida species colonization and denture-related stomatitis in complete denture wearers. Med Mycol. 2011;49(2):208–11.

260. Abu-Elteen KH, Abu-Alteen RM. The prevalence of Candida albicans populations in the mouths of complete denture wearers. New Microbiol. 1998;21(1):41–8.

261. Blicharz L, Rudnicka L, Samochocki Z. Staphylococcus aureus: An underestimated factor in the pathogenesis of atopic dermatitis? Postep Dermatologii i Alergol. 2019;36(1):11–7.

262. Soong G, Martin FJ, Chun J, Cohen TS, Ahn DS, Prince A. Staphylococcus aureus protein A mediates invasion across airway epithelial cells through activation of RhoA GTPase signaling and proteolytic activity. J Biol Chem.

2011;286(41):35891–8.

263. Kwak YK, Vikström E, Magnusson KE, Vécsey-Semjén B, Colque-Navarro P, Möllby R. The Staphylococcus aureus alpha-toxin perturbs the barrier function in Caco-2 epithelial cell monolayers by altering junctional integrity. Infect Immun. 2012;80(5):1670–80.

264. Todd OA, Fidel PL, Harro JM, Hilliard JJ, Tkaczyk C, Sellman BR, et al. Candida albicans augments staphylococcus aureus virulence by engaging the staphylococcal agr quorum sensing system. MBio. 2019;10(3):1–16.

265. Dongari-Bagtzoglou A, Kashleva H. Development of a highly reproducible three-dimensional organotypic model of the oral mucosa. Nat Protoc. 2006;1(4):2012–8.

266. Nash EE, Peters BM, Palmer GE, Fidel PL, Noverr MC. Morphogenesis Is Not Required for Candida albicans - Staphylococcus aureus Intra-Abdominal Infection-Mediated Dissemination and Lethal Sepsis. 2014;82(8):3426–35.

267. Peters BM, Noverra MC. Candida albicans-staphylococcus aureus polymicrobial peritonitis modulates host innate immunity. Infect Immun. 2013;81(6):2178–89.

268. Zhang Y, Wang X, Li H, Ni C, Du Z, Yan F. Human oral microbiota and its modulation for oral health. Biomed Pharmacother. 2018;99:883–93.

269. Torabi M, Drahansky M, Paridah M., Moradbak A, Mohamed A., Owolabi F abdulwahab taiwo, et al. Physiology and Pathology of Innate Immune Response Against Pathogens. Physiology and pathology of immunology. Intech; 2016. 99–134 p.

270. Castro-Sanchez P, Martin-Villa JM, Castro-Sánchez P, Martín-Villa JM. Gut immune system and oral tolerance. Br J Nutr. 2013;109 Suppl(S2):S3-11.

271. Wu R-Q, Zhang D-F, Tu E, Chen Q-M, Chen W. The mucosal immune system in the oral cavity-an orchestra of T cell diversity. Int J Oral Sci. 2014;6(3):125–32.

272. Garside P, Mowat AMI, Khoruts A. Oral tolerance in disease. Gut. 1999;44(1):137–42.

273. Aliberti J. Immunity and Tolerance Induced by Intestinal Mucosal Dendritic Cells. Mediators Inflamm. 2016;2016:1–8.

274. S SB, L L. Intraepithelial Lynphocytes: To serve and Protect. Curr

Gasternterology. 2010;12(6):513–21.

275. Coillard A, Segura E. In vivo Differentiation of Human Monocytes. Front Immunol. 2019;10(August):1–7.

276. Merry R, Belfield L, McArdle P, McLennan A, Crean S, Foey A. Oral health and pathology: A macrophage account. Br J Oral Maxillofac Surg. 2012;50(1):2–7.

277. Barrett AW, Cruchley AT, Road GI. Oral mucosal langerhans' cells. 1996;7(l):36–58.

278. Miriam Merad, Manz MG, Karsunky H, Wagers A, Peters W, Charo I, et al. Langerhans cells renew in the skin throughout life under steady- state conditions. Clin Res Hepatol Gastroenterol. 2002;3(12):1135–41.

279. Ginhoux F, Tacke F, Angeli V, Bogunovic M, Loubeau M, Dai XM, et al. Langerhans cells arise from monocytes in vivo. Nat Immunol. 2006;7(3):265–73.

280. Mantovani A, Sica A, Sozzani S, Allavena P, Vecchi A, Locati M. The chemokine system in diverse forms of macrophage activation and polarization. Trends Immunol. 2004;25(12):677–86.

281. Shapouri-Moghaddam A, Mohammadian S, Vazini H, Taghadosi M, Esmaeili S-A, Mardani F, et al. Macrophage plasticity, polarization, and function in health and disease. J Cell Physiol. 2018;233(9):6425–40.

282. Koh TJ, DiPietro LA. Inflammation and wound healing: The role of the macrophage. Expert Rev Mol Med. 2011;23(13):1–12.

283. Underhill DM, Bassetti M, Rudensky A, Aderem A. Dynamic interactions of macrophages with T cells during antigen presentation. J Exp Med. 1999;190(12):1909–14.

284. Elhelu MA. The role of macrophages in immunology. J Natl Med Assoc. 1983;75(3):314–7.

285. Davies LC, Philip R. Tissue-resident macrophages : then and now. Immunology. 2015;144(1):541–8.

286. Nyga A, Neves J, Stamati K, Loizidou M, Emberton M, Cheema U. The next level of 3D tumour models: immunocompetence. Drug Discov Today. 2016;21(9):1421–8.

287. Gleissner CA, Shaked I, Little KM, Ley and K. CXCL4 induces a unique transcriptome in monocyte-derived macrophages. J Immunol.

2012;29(6):997–1003.

288. Waldo SW, Li Y, Buono C, Zhao B, Billings EM, Chang J, et al. Heterogeneity of human macrophages in culture and in atherosclerotic plaques. Am J Pathol. 2008;172(4):1112–26.

289. Martinez FO, Gordon S, Locati M, Mantovani A. Transcriptional Profiling of the Human Monocyte-to-Macrophage Differentiation and Polarization: New Molecules and Patterns of Gene Expression. J Immunol. 2006;177(10):7303–11.

290. Gonzalez-Mejia ME, Doseff AI. Regulation of monocytes and macrophages cell fate. Front Biosci - Landmark. 2009;14(3):2413–31.

291. Tsuchiya S, Yamaguchi Y, Kobayashi Y. Tsuchiya S, Yamabe M, Yamaguchi Y, et al. Establishment and characterization of a human acute monocytic leukemia cell line (THP-1). Int J Cancer. 1980; 26:171–176. DOI: 10.1002/ijc.2910260208. 1980;176:171–6.

292. Bain BJ. What is a promonocyte? Am J Hematol. 2013;88(10):919–919.

293. Lukic A, Larssen P, Fauland A, Samuelsson B, Wheelock CE, Gabrielsson S, et al. GM-CSF– and M-CSF–primed macrophages present similar resolving but distinct inflammatory lipid mediator signatures. FASEB J. 2017;31(10):4370–81.

294. Kang K, Bachu M, Park SH, Kang K, Bae S, Park-Min K-H, et al. IFN-γ selectively suppresses a subset of TLR4-activated genes and enhancers to potentiate macrophage activation. Nat Commun. 2019;10(1):3320.

295. Hao J, Hu Y, Li Y, Zhou Q, Lv X. Involvement of JNK signaling in IL4-induced M2 macrophage polarization. Exp Cell Res. 2017;357(2):155–62.

296. Martinez FO, Gordon S. The M1 and M2 paradigm of macrophage activation: Time for reassessment. F1000Prime Rep. 2014;6(March):1–13.

297. Liang S, Cai J, Li Y, Yang R. 1,25-Dihydroxy-Vitamin D3 induces macrophage polarization to M2 by upregulating T-cell Ig-mucin-3 expression. Mol Med Rep. 2019;49(5):3707–13.

298. Daigneault M, Preston JA, Marriott HM, Whyte MKB, Dockrell DH. The identification of markers of macrophage differentiation in PMA-stimulated THP-1 cells and monocyte-derived macrophages. PLoS One. 2010;5(1).

299. Schwende H, Fitzke E, Ambs P, Dieter P. Differences in the state of differentiation of THP-1 cells induced by phorbol ester and 1,25-dihydroxyvitamin D3. J Leukoc Biol. 1996;59(4):555–61.

300. Park EK, Jung HS, Yang HI, Yoo MC, Kim C, Kim KS. Optimized THP-1 differentiation is required for the detection of responses to weak stimuli. Inflamm Res. 2007;56(1):45–50.

301. Maeß MB, Wittig B, Cignarella A, Lorkowski S. Reduced PMA enhances the responsiveness of transfected THP-1 macrophages to polarizing stimuli. J Immunol Methods. 2014;402(1–2):76–81.

302. Villaggio B, Soldano S, Cutolo M. 1,25-dihydroxyvitamin D3 downregulates aromatase expression and inflammatory cytokines in human macrophages. Clin Exp Rheumatol. 2012;30:934–8.

303. Foey AD, Crean SJ. Macrophage Subset Sensitivity to Endotoxin Tolerisation by Porphyromonas gingivalis. PLoS One. 2013;8(7).

304. Habil N, Al-Murrani W, Beal J, Foey AD. Probiotic bacterial strains differentially modulate macrophage cytokine production in a strain-dependent and cell subset-specific manner. Benef Microbes. 2011;2(4):283–93.

305. Rőszer T. Understanding the Mysterious M2 Macrophage through Activation Markers and Effector Mechanisms. Mediators Inflamm. 2015;2015:1–16.

306. Murray PJ, Allen JE, Fisher EA, Lawrence T. Macrophage activation and polarization: nomenclature and experimental guidelines. Immunity. 2014;41(1):14–20.

307. Atri C, Guerfali FZ, Laouini D. Role of human macrophage polarization in inflammation during infectious diseases. Int J Mol Sci. 2018;19(6).

308. Lund ME, To J, O'Brien BA, Donnelly S. The choice of phorbol 12-myristate 13-acetate differentiation protocol influences the response of THP-1 macrophages to a pro-inflammatory stimulus. J Immunol Methods. 2016;430:64–70.

309. Sabroe I, Jones EC, Usher LR, Whyte MKB, Dower SK, Moira KB, et al. Toll-Like Receptor (TLR)2 and TLR4 in Human Peripheral Blood Granulocytes: A Critical Role for Monocytes in Leukocyte Lipopolysaccharide Responses. J Immunol. 2002;168(9):4701–10.

310. Liu Y, Wang Y, Yamakuchi M, Isowaki S, Nagata E, Kanmura Y, et al. Upregulation of toll-like receptor 2 gene expression in macrophage response to peptidoglycan and high concentration of lipopolysaccharide is involved in NK-κB activation. Infect Immun. 2001;69(5):2788–96.

311. Zhou Z, Ding M, Huang L, Gilkeson G, Lang R, Jiang W. Toll-like receptor-

mediated immune responses in intestinal macrophages; implications for mucosal immunity and autoimmune diseases. Physiol Behav. 2016;173:81–6.

312. Vaure C, Liu Y. A comparative review of toll-like receptor 4 expression and functionality in different animal species. Front Immunol. 2014;5(JUL):1–15.

313. Gallego C, Golenbock D, Gomez MA, Saravia NG. Toll-like receptors participate in macrophage activation and intracellular control of Leishmania (Viannia) panamensis. Infect Immun. 2011;79(7):2871–9.

314. Medler J, Wajant H. Tumor necrosis factor receptor-2 (TNFR2): an overview of an emerging drug target. Expert Opin Ther Targets. 2019;23(4):295–307.

315. Idriss HT, Naismith JH. TNFα and the TNF receptor superfamily: Structure-function relationship(s). Microsc Res Tech. 2000;50(3):184–95.

316. Atzeni F, Sarzi-Puttini P. Tumor Necrosis Factor. Brenner's Encycl Genet Second Ed. 2013;266(12):229–31.

317. Thornberry NA, Bull HG, Calaycay JR, CHapman KT, Howard AD, Tocci MJ. A novel heterodimeric cysteine protease is required for interleukin-1b processing in monocytes. Nature. 1992;359:710–3.

318. Netea MG, Simon A, van de Veerdonk F, Kullberg B-J, Van der Meer JWM, Joosten LAB. IL-1β Processing in Host Defense: Beyond the Inflammasomes. Manchester M, editor. PLoS Pathog. 2010;6(2):1–9.

319. Mizutani H, Black R, Kupper TS. Human keratinocytes produce but do not process pro-interleukin-1 (IL-1) beta different strategies of IL-1 production and processing in monocytes and keratinocytes. J Clin Invest. 1991;87(3):1066–71.

320. Dinarello CA. Interleukin-1 in the pathogenesis and treatment of inflammatory diseases. 2011;117(14):3720–33.

321. Dinarello CA. Overview of the IL-1 family in innate inflammation and acquired immunity. Immunol Rev. 2018;281(1):8–27.

322. Kurushima H, Ramprasad M, Kondratenko N, Foster DM, Quehenberger O, Steinberg D. Surface expression and rapid internalization of macrosialin (mouse CD68) on elicited mouse peritoneal macrophages. J Leukoc Biol. 2000;67(1):104–8.

323. Chistiakov DA, Killingsworth MC, Myasoedova VA, Orekhov AN, Bobryshev Y V. CD68/macrosialin: Not just a histochemical marker. Lab

Investig. 2017;97(1):4–13.

324. Dupasquier M, Stoitzner P, Wan H, Cerqueira D, Van Oudenaren A, Voerman JSA, et al. The dermal microenvironment induces the expression of the alternative activation marker CD301/mMGL in mononuclear phagocytes, independent of IL-4/IL-13 signaling. J Leukoc Biol. 2006;80(4):838–49.

325. Zizzo G, Hilliard BA, Monestier M, Cohen PL. Efficient clearance of early apoptotic cells by human macrophages requires “M2c” polarization and MerTK induction. Immunology. 2012;189(7):3508–20.

326. Barros MHM, Hauck F, Dreyer JH, Kempkes B, Niedobitek G. Macrophage polarisation: An immunohistochemical approach for identifying M1 and M2 macrophages. PLoS One. 2013;8(11):1–11.

327. Valerius NH, Stendahl OI, Hartwig JH, Stossel TP. Distribution of actin-binding protein and myosin in neutrophils during chemotaxis and phagocytosis. Adv Exp Med Biol. 1982;141(February):19–28.

328. Zaynagetdinov R, Sherrill TP, Kendall PL, Segal BH, Weller KP, Tighe RM, et al. Identification of Myeloid Cell Subsets in Murine Lungs Using Flow Cytometry. Am J Respir Cell Mol Biol. 2013;49(2):180–9.

329. McCullough KC, Basta S, Knötig S, Gerber H, Schaffner R, Kim YB, et al. Intermediate stages in monocyte-macrophage differentiation modulate phenotype and susceptibility to virus infection. Immunology. 1999;98(2):203–12.

330. Soldano S, Pizzorni C, Paolino S, Trombetta AC, Montagna P, Brizzolara R, et al. Correction: Alternatively Activated (M2) Macrophage Phenotype Is Inducible by Endothelin-1 in Cultured Human Macrophages. Zissel G, editor. PLoS One. 2017;12(3):e0175238.

331. Genin M, Clement F, Fattaccioli A, Raes M, Michiels C. M1 and M2 macrophages derived from THP-1 cells differentially modulate the response of cancer cells to etoposide. BMC Cancer. 2015;15(1):577.

332. Aldo PB, Craveiro V, Guller S, Mor G. Effect of culture conditions on the phenotype of THP-1 monocyte cell line. 2014;70(1):80–6.

333. Buchacher T, Ohradanova-Repic A, Stockinger H, Fischer MB, Weber V. M2 polarization of human macrophages favors survival of the intracellular pathogen chlamydia pneumoniae. PLoS One. 2015;10(11):1–16.

334. Denholm EM, Stankus GP. Changes in the expression of mcp-1 receptors on monocytic thp-1 cells following differentiation to macrophages with

phorbol myristate acetate. Cytokine. 1995;7(5):436–40.

335. Parkinson EK. Phospholipase C mimics the differential effects of phorbol-12-myristate-13-acetate on the colony formation and cornification of cultured normal and transformed human keratinocytes. Carcinogenesis. 1987;8(6):857–60.

336. Papp H, Czifra G, Lázár J, Gönczi M, Csernoch L, Kovács L, et al. Protein kinase C isozymes regulate proliferation and high cell density-mediated differentiation in HaCaT keratinocytes. Exp Dermatol. 2003;12(6):811–24.

337. Abedian Z, Fattahi S, Pourbagher R, Edrisi S, Mostafazadeh A. Sustained small and intermediate size proteins expression in phorbol 12-myristate 13-acetate/ionomycine prolonged stimulated human fibroblasts. Asian Pac J Trop Biomed. 2017;7(5):432–6.

338. Manggau M, Kim D-S, Ruwisch L, Vogler R, Schäfer-Korting M, Kleuser B, et al. 1α,25-Dihydroxyvitamin D3 Protects Human Keratinocytes from Apoptosis by the Formation of Sphingosine-1-Phosphate. J Invest Dermatol. 2001;117(5):1241–9.

339. Hill NT, Zhang J, Leonard MK, Lee M, Shamma HN, Kadakia M. 1α, 25-DihydroxyVitamin D3 and the Vitamin D receptor regulates ΔNp63α levels and keratinocyte proliferation. Cell Death Dis. 2015;6(6):1–11.

340. Greiling D, Thieroff-Ekerdt R. 1alpha,25-dihydroxyvitamin D3 rapidly inhibits fibroblast-induced collagen gel contraction. J Invest Dermatol. 1996;106(6):1236–41.

341. Dobak J, Grzybowski J, Liu FT, Landon B, Dobke M. 1,25-Dihydroxyvitamin D3 increases collagen production in dermal fibroblasts. J Dermatol Sci. 1994;8(1):18–24.

342. Italiani P, Boraschi D. From monocytes to M1/M2 macrophages: Phenotypical vs. functional differentiation. Front Immunol. 2014;5(OCT):1–22.

343. Bertani FR, Mozetic P, Fioramonti M, Iuliani M, Ribelli G, Pantano F, et al. Classification of M1/M2-polarized human macrophages by label-free hyperspectral reflectance confocal microscopy and multivariate analysis. Sci Rep. 2017;7(1):1–9.

344. Hulspas R, O'Gorman MRG, Wood BL, Gratama JW, Robert Sutherland D. Considerations for the control of background fluorescence in clinical flow cytometry. Cytom Part B - Clin Cytom. 2009;76(6):355–64.

345. O'Gorman MRG, Thomas J. Isotype controls - Time to let go? Commun

Clin Cytom. 1999;38(2):78–80.

346. Takashiba S, Dyke TEVAN, Amar S, Murayama Y, Soskolne AW, Shapira L. Differentiation of Monocytes to Macrophages Primes Cells for Lipopolysaccharide Stimulation via Accumulation of Cytoplasmic Nuclear Factor ?B. Infect Immun. 1999;67(11):5573–8.

347. Martin TR, Mongovin SM, Tobias PS, Mathison JC, Moriarty AM, Leturcq DJ, et al. The CD14 differentiation antigen mediates the development of endotoxin responsiveness during differentiation of mononuclear phagocytes. J Leukoc Biol. 1994;56(1):1–9.

348. Seeley JJ, Ghosh S. Molecular mechanisms of innate memory and tolerance to LPS. J Leukoc Biol. 2017;101(1):107–19.

349. El-Ghalbzouri A, Gibbs S, Lamme E, Van Blitterswijk CA. Cutaneous Biology - Effect of fibroblasts on epidermal regeneration. Br J Dermatol. 2002;147(2):230–43.

350. El Ghalbzouri A, Jonkman MF, Dijkman R, Ponec M. Basement membrane reconstruction in human skin equivalents is regulated by fibroblasts and/or exogenously activated keratinocytes. J Invest Dermatol. 2005;124(1):79–86.

351. Turabelidze A, Guo S, Chung AY, Chen L, Dai Y, Marucha PT, et al. Intrinsic Differences between Oral and Skin Keratinocytes. 2014;9(9):1–10.

352. Yu YRA, O'Koren EG, Hotten DF, Kan MJ, Kopin D, Nelson ER, et al. A protocol for the comprehensive flow cytometric analysis of immune cells in normal and inflamed murine non-lymphoid tissues. PLoS One. 2016;11(3):1–23.

353. Sadtler K, Elisseeff JH. Analyzing the scaffold immune microenvironment using flow cytometry: practices, methods and considerations for immune analysis of biomaterials. Biomater Sci. 2019;7(11):4472–81.

354. Vitiello M, D'Isanto M, Galdiero M, Raieta K, Tortora A, Rotondo P, et al. Interleukin-8 production by THP-1 cells stimulated by Salmonella enterica serovar Typhimurium porins is mediated by AP-1, NF-κB and MAPK pathways. Cytokine. 2004;27(1):15–24.

355. Chiu L, Bazin T, Truchetet ME, Schaeverbeke T, Delhaes L, Pradeu T. Protective microbiota: From localized to long-reaching co-immunity. Front Immunol. 2017;8(DEC):1–19.

Appendices

Appendix 1: Participant recruitment poster.

Appendix 2: Participant information leaflet

RESEARCH WITH PLYMOUTH UNIVERSITY

PLYMOUTH UNIVERSITY PENINSULA SCHOOLS OF MEDICINE & DENTISTRY

DTA Doctoral Training Alliance Applied Biosciences for Health

Participants Required

For A Scientific Study to look for specific micro-organisms in your mouth and identify links between certain microorganisms and soreness under dentures (Denture stomatitis).

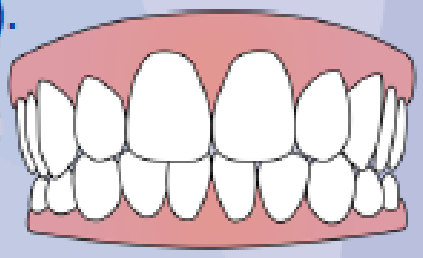

What do you need to do?

1) Read the reverse of this information leaflet.
2) Fill out a consent form and a personal details form.
3) Fill out a short questionnaire on lifestyle factors which may affect this study and allow your dentist to provide us with information about your denture, and oral health.
4) Have swabs taken from your mouth/and denture.

How long will it take?

6 minutes

Five minutes of paperwork plus one minute to take swabs.

Participation is voluntary, and will in no way affect the standard of treatment or care you receive.

PSMD-208291-SG-020 Version 1-20/06/2017

RESEARCH WITH PLYMOUTH UNIVERSITY

PLYMOUTH UNIVERSITY PENINSULA
SCHOOLS OF MEDICINE & DENTISTRY

DTA
Doctoral Training Alliance
Applied Biosciences for Health

Participants must:

Have removable upper dentures (Full or partial)*.

>50

Be over the age of 50.

Know if they have taken any antibiotics, antifungals or oral steroids in the past 3 months.

Be able to understand this information and consent for their self.

How will your data be used?

Personal data such as contact details will be kept only for admin purposes, and will remain separate from your questionnaire answers and laboratory findings (associated with only a participant number) so you remain anonymous. The swab samples and questionnaire answers will be grouped with others and used to look for links between particular microbes found in your mouth and the information you provide.

How will it benefit you?

The study will not directly benefit you, however it may in future help to further knowledge, and indicate potential treatment options for patients with denture stomatitis.

What if you change your mind?

If you want to withdraw from the study in future you may, by contacting us, or the practice from which you participated. Your sample and any associated information will be destroyed.

* 30 control patients who do not wear dentures are required

People with Denture Stomatitis are vital.

Questions? Email : denturestomatitisresearch@plymouth.ac.uk

Appendix 3: Denture-wearing participant information sheet

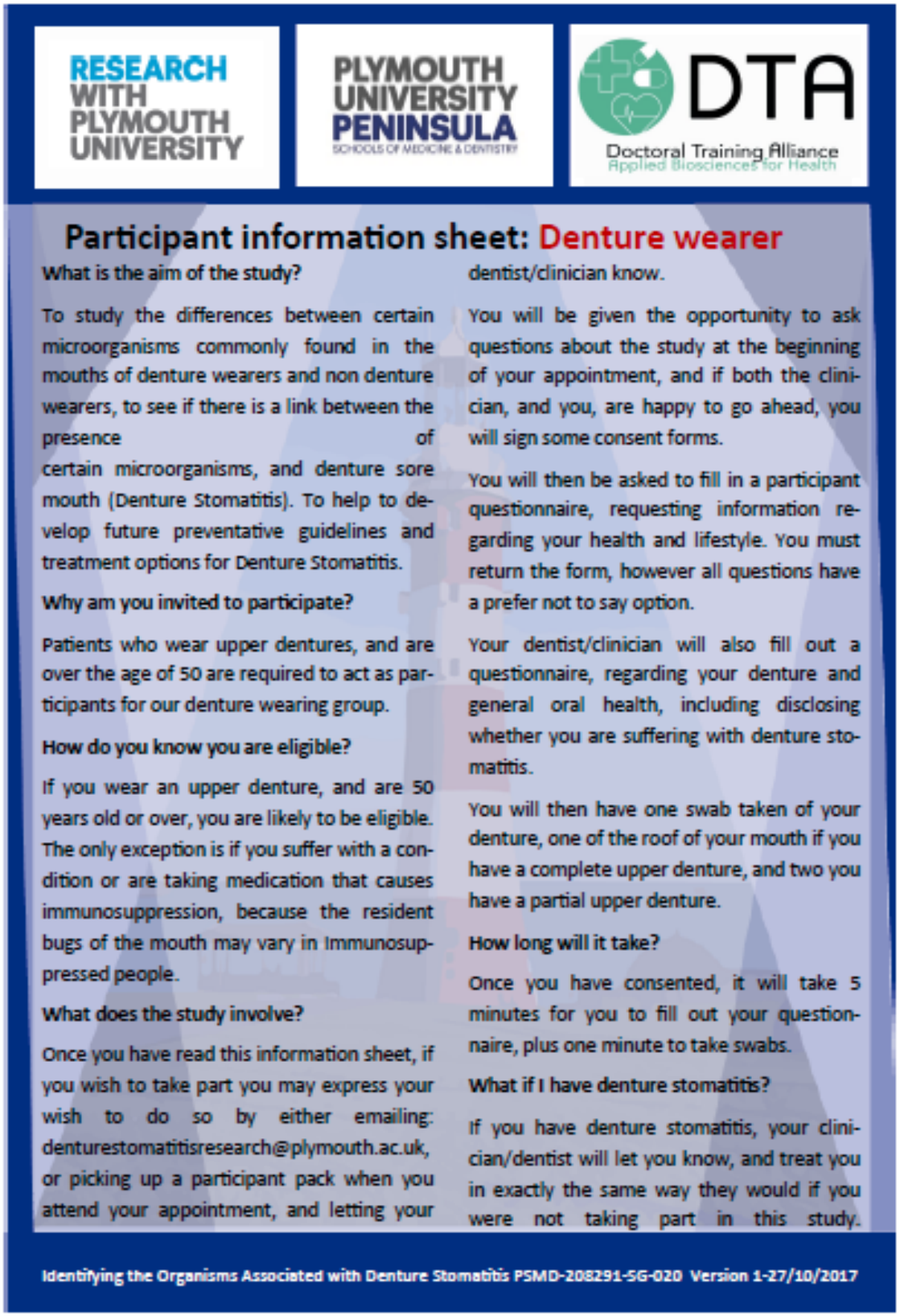

RESEARCH WITH PLYMOUTH UNIVERSITY

PLYMOUTH UNIVERSITY PENINSULA SCHOOLS OF MEDICINE & DENTISTRY

DTA Doctoral Training Alliance Applied Biosciences for Health

Participant information sheet: Denture wearer

What is the aim of the study?

To study the differences between certain microorganisms commonly found in the mouths of denture wearers and non denture wearers, to see if there is a link between the presence of certain microorganisms, and denture sore mouth (Denture Stomatitis). To help to develop future preventative guidelines and treatment options for Denture Stomatitis.

Why am you invited to participate?

Patients who wear upper dentures, and are over the age of 50 are required to act as participants for our denture wearing group.

How do you know you are eligible?

If you wear an upper denture, and are 50 years old or over, you are likely to be eligible. The only exception is if you suffer with a condition or are taking medication that causes immunosuppression, because the resident bugs of the mouth may vary in Immunosuppressed people.

What does the study involve?

Once you have read this information sheet, if you wish to take part you may express your wish to do so by either emailing: denturestomatitisresearch@plymouth.ac.uk, or picking up a participant pack when you attend your appointment, and letting your dentist/clinician know.

You will be given the opportunity to ask questions about the study at the beginning of your appointment, and if both the clinician, and you, are happy to go ahead, you will sign some consent forms.

You will then be asked to fill in a participant questionnaire, requesting information regarding your health and lifestyle. You must return the form, however all questions have a prefer not to say option.

Your dentist/clinician will also fill out a questionnaire, regarding your denture and general oral health, including disclosing whether you are suffering with denture stomatitis.

You will then have one swab taken of your denture, one of the roof of your mouth if you have a complete upper denture, and two you have a partial upper denture.

How long will it take?

Once you have consented, it will take 5 minutes for you to fill out your questionnaire, plus one minute to take swabs.

What if I have denture stomatitis?

If you have denture stomatitis, your clinician/dentist will let you know, and treat you in exactly the same way they would if you were not taking part in this study.

Identifying the Organisms Associated with Denture Stomatitis PSMD-208291-SG-020 Version 1-27/10/2017

RESEARCH WITH PLYMOUTH UNIVERSITY

PLYMOUTH UNIVERSITY PENINSULA SCHOOLS OF MEDICINE & DENTISTRY

DTA Doctoral Training Alliance Applied Biosciences for Health

Researchers will be notified by the clinician questionnaire that you do have denture stomatitis, so your samples and information can be added to the denture stomatitis group.

Will I get my results, and what will they say about me?

You will not get any individual results from the study, however the overall study report will be available at the reception of the participating clinic. We can also email or post it to you at your request. The study results will tell us nothing about your individual oral health that you wouldn't have already been notified about at your appointment.

How will you keep my data safe?

All data will be kept in a linked anonymised form, meaning your swabs and questionnaire answers will be identified with a number, not your personal details. It will be traceable to you via your consent form, solely for withdrawal purposes. All sensitive information provided will be kept in a confidential manner, and access will be limited to the research team.

What will my data be used for?

Swabs will be used to look for *Candia albicans* and Staphylococcus *aureus*, which are microorganisms thought to be associated with denture stomatitis. The microorganisms will be kept in order to study interactions between the microorganisms and mouth tissue, using advanced modelling techniques.

Questionnaire data will be used to look for correlations between health and lifestyle factors, and denture stomatitis presence.

What if I don't want to take part, or change my mind?

Participation in this study is voluntary and in no way will affect the standard of treatment or care you receive. You may choose to take part, or withdraw at any time. To withdraw, simply contact us at denturestomatitisresearch@plymouth.ac.uk, or notify your participating clinic. Your study information will be destroyed. It should be noted that any processed data which has already been published (anonymously) will be unable to be withdrawn.

What are the risks and benefits?

The study will not directly benefit you. However, as a denture wearer it may indirectly benefit you. This is because findings from the study are intended to influence better treatment options, and preventative guidelines for denture stomatitis in the long run.

No risk to your health is likely to occur from participation in this study.

Questions or complaints? Contact: denturestomatitisresearch@plymouth.ac.uk

Appendix 4: Non denture-wearing (control) participant information sheet

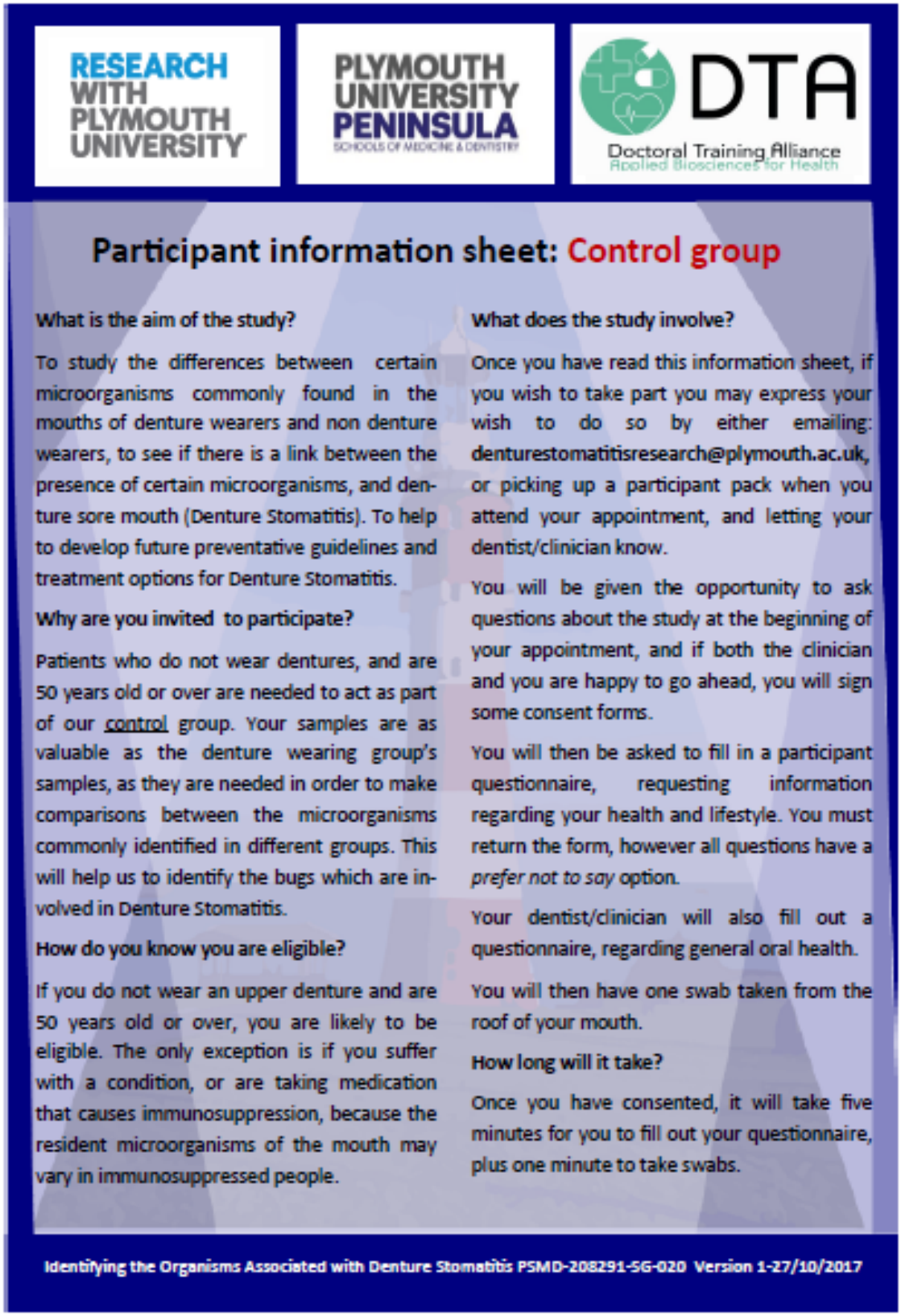

RESEARCH WITH PLYMOUTH UNIVERSITY

PLYMOUTH UNIVERSITY PENINSULA SCHOOLS OF MEDICINE & DENTISTRY

DTA Doctoral Training Alliance Applied Biosciences for Health

Participant information sheet: Control group

What is the aim of the study?

To study the differences between certain microorganisms commonly found in the mouths of denture wearers and non denture wearers, to see if there is a link between the presence of certain microorganisms, and denture sore mouth (Denture Stomatitis). To help to develop future preventative guidelines and treatment options for Denture Stomatitis.

Why are you invited to participate?

Patients who do not wear dentures, and are 50 years old or over are needed to act as part of our control group. Your samples are as valuable as the denture wearing group's samples, as they are needed in order to make comparisons between the microorganisms commonly identified in different groups. This will help us to identify the bugs which are involved in Denture Stomatitis.

How do you know you are eligible?

If you do not wear an upper denture and are 50 years old or over, you are likely to be eligible. The only exception is if you suffer with a condition, or are taking medication that causes immunosuppression, because the resident microorganisms of the mouth may vary in immunosuppressed people.

What does the study involve?

Once you have read this information sheet, if you wish to take part you may express your wish to do so by either emailing: denturestomatitisresearch@plymouth.ac.uk, or picking up a participant pack when you attend your appointment, and letting your dentist/clinician know.

You will be given the opportunity to ask questions about the study at the beginning of your appointment, and if both the clinician and you are happy to go ahead, you will sign some consent forms.

You will then be asked to fill in a participant questionnaire, requesting information regarding your health and lifestyle. You must return the form, however all questions have a *prefer not to say* option.

Your dentist/clinician will also fill out a questionnaire, regarding general oral health.

You will then have one swab taken from the roof of your mouth.

How long will it take?

Once you have consented, it will take five minutes for you to fill out your questionnaire, plus one minute to take swabs.

Identifying the Organisms Associated with Denture Stomatitis PSMD-208291-SG-020 Version 1-27/10/2017

RESEARCH WITH PLYMOUTH UNIVERSITY

PLYMOUTH UNIVERSITY PENINSULA SCHOOLS OF MEDICINE & DENTISTRY

DTA Doctoral Training Alliance Applied Biosciences for Health

Will you get your results, and what will they say about you?

You will not get any individual results from the study, however the overall study report will be available at the reception of the participating clinic. We can also email or post it to you at your request. The study results will tell us nothing about your individual oral health that you wouldn't have already been notified about at your appointment.

How will we keep your data safe?

All data will be kept in a linked anonymised form, meaning your swabs and questionnaire answers will be identified with a number, not your personal details. It will be traceable to you via your consent form, solely for withdrawal purposes. All sensitive information provided will be kept in a confidential manner, and access will be limited to the research team.

What will your data be used for?

Swabs will be used to look for *Candia albicans* and *Staphylococcus aureus*, which are microorganisms thought to be associated with denture stomatitis. The microorganisms will be kept in order to study interactions between them and mouth tissue using advanced modelling techniques.

Questionnaire data will be pooled and used to look for correlations between health and lifestyle factors, and denture stomatitis presence.

What if you don't want to take part, or change your mind?

Participation in this study is voluntary and in no way will affect the standard of treatment or care you receive. You may choose to take part, or withdraw at any time. To withdraw, simply contact us at : denturestomatitisresearch@plymouth.ac.uk, or notify your participating clinic. Your study information will be destroyed. It should be noted that any processed data which has already been published (anonymously) will be unable to be withdrawn.

What are the risks and benefits?

The study will not directly benefit you. However the study may indirectly benefit denture wearers in the future. This is because findings from the study are intended to influence better treatment options, and preventative guidelines for denture stomatitis in the long term.

No risk to your health is likely to occur from participation in this study.

Questions or complaints?

Email Contact:

denturestomatitisresearch@plymouth.ac.uk

Appendix 5: Frequently asked questions

RESEARCH WITH PLYMOUTH UNIVERSITY

PLYMOUTH UNIVERSITY PENINSULA SCHOOLS OF MEDICINE & DENTISTRY

DTA Doctoral Training Alliance Applied Biosciences for Health

Study FAQ Sheet

PSMD-208291-SG-020 Version 1-6/11/2017

What is a microorganism?

A microorganism is an organism which can usually only be seen with the use of a microscope, this includes: Bacteria, Fungi, Protozoa and Viruses.

What is denture stomatitis?

Denture stomatitis has several different names including denture sore mouth. It is a condition which is extremely common among denture wearers. It causes redness and soreness of the area under the denture, and the severity can range from a mild reddening with little to no discomfort, to pain, swelling and the formation of bumps called nodules.

How is denture stomatitis treated?

Denture stomatitis is often treated with antifungal medication and advisory preventative measures, such as removing the dentures overnight for cleaning.

What causes denture stomatitis?

Researchers do not believe that there is one direct cause of denture stomatitis, however it is thought that the presence of the yeast *Candida albicans* is strongly linked with its development when other factors are present such as: Improper denture cleansing, smoking, diet, some medical conditions, age, gender, and sometimes just the presence of the denture alone is thought to be enough to trigger the condition. Different denture materials, types and ages are also thought to have an influence on the development of the condition.

Why study denture stomatitis?

Firstly, the frequent occurrence of denture stomatitis within denture wearers is a cause for research in this area. Currently, the re-occurrence of this condition is common and therefore there is thought to be room for improvement with regards to treatment.

Another reason for this study is to look for the presence of a bacterium called *Staphylococcus aureus*. This bacterium, when found with the fungus *Candida albicans*, may be able to cause more severe infections elsewhere in the body. We therefore want to find out whether they are commonly found together, and if so, consider both of these microorganisms in future treatments, rather than just one.

Email: denturestomatitisresearch@plymouth.ac.uk

RESEARCH WITH PLYMOUTH UNIVERSITY

PLYMOUTH UNIVERSITY PENINSULA SCHOOLS OF MEDICINE & DENTISTRY

DTA Doctoral Training Alliance

Who will this study benefit?

This study will not directly benefit you, however it will help to add to the current knowledge surrounding the condition denture sore mouth. In turn, the findings from this study may influence the way in which this condition is managed and treated in future, which will benefit the majority of denture wearers at some point. The study will also benefit the scientific community by adding to the knowledge of how the microorganisms identified, interact in the mouth. Studying these microorganisms will allow a better understanding of denture stomatitis.

How will my swab samples be used?

Your samples will firstly be used to confirm whether or not the yeast *Candida albicans*, or the bacterium *Staphylococcus aureus*, was present in your mouth, or on your denture. This information will be used to look for a link between the presence of these microorganisms, and the presence of denture stomatitis.

Secondly your samples may be grown on artificial models of the of the mouth. This will allow us to model how the bacteria and fungi we find interact with the mouth, and study the disease process of denture stomatitis.

If you consent for us to keep your swab samples after the study is over, the microorganisms found within the samples may be used for other research purposes outside of this study in future; for example, to aid the discovery of novel antimicrobial peptides (alternative to antibiotics).

How will my questionnaire answers be used?

Your questionnaire answers will be used to look for links between each answer, and the clinician's questionnaire, as well as the data collected from your swabs. There will be a particular focus on whether there is a link between any of the questionnaire answers, and the presence of either microorganism, and the presence of denture stomatitis.

Will it hurt?

No, if you are suffering with denture sore mouth it might be a tiny bit uncomfortable, however no more than from wearing your denture.

Will it take long?

No, in total it will take you around five minutes to complete the questionnaire, and your dentist/dental nurse only around 1 minute to take swabs.

Why have I been invited?

You have been invited due to your age. We require patients aged 50 years and over to participate as a member of either our non denture wearing (control) group, or denture wearing and denture stomatitis groups.

Email: denturestomatitisresearch@plymouth.ac.uk

RESEARCH WITH PLYMOUTH UNIVERSITY | PLYMOUTH UNIVERSITY PENINSULA SCHOOLS OF MEDICINE & DENTISTRY | DTA Doctoral Training Alliance

Will it affect my treatment?

No, not at all. The rest of your appointment will go as planned, and no treatment will be altered whether you take part in the study or not.

Are there any other eligibility criteria?

Unfortunately patients which have immunosuppression will not be able to take part in this particular study. This is because the resident microorganisms in the mouth are often found to be altered in cases of immunosuppression, which would in turn affect the results of this study. Immunosuppression includes: diseases which lead to immunodeficiency such as HIV, patients undergoing cancer treatment, patients taking immunosuppressive medications, and patients with disorders and deficiencies of the immune system. If you are unsure whether you fall within any of these categories, please discuss this with your clinician.

How will my data be kept safe?

Any personal data such as your name and date of birth will only be present on the consent form, and not on any questionnaire sheets or swab samples. For out records these will be linked by a participant number, and will only be referred to should you wish to withdraw.

Questionnaire sheets will be kept separately to the consent forms, in a locked filing cabinet. Swabs will be kept in the freezer until processed, and some may be kept longer for future use. Any data generated from the swabs will be inputted onto a computer system alongside your participant number and questionnaire answers, but will NOT contain your personal details.

Who will have access to my personal data?

Aside from the NHS staff which have access to your personal data via your NHS records, the chief investigator and one other nominated member of the research team will have access to your personal data provided on the consent form. Reviewers may also wish to check all appropriate consent forms are present.

How do I withdraw?

In order to withdraw, all you need to do is contact **denturestomatitisresearch@plymouth.ac.uk** and provide your name and express your wish to withdraw. Once this email is received, your data will be destroyed. Alternatively, you may contact your participating clinic and ask to withdraw.

Am I going to get the results?

You will not be informed of your individual results. If you have denture stomatitis your clinician will discuss this with you. If you would like to receive a summary of the study results, please express this wish by email to: denturestomatitisresearch@plymouth.ac.uk. The study results will also be made available to you at the dental clinic/practice from which you took part.

What if I have more questions? Contact us at **denturestomatitisresearch@plymouth.ac.uk.**

Email: denturestomatitisresearch@plymouth.ac.uk

Appendix 6: Consent form

PSMD-208291-SG-020 Version 1- 21/10/2017

PLYMOUTH UNIVERSITY PENINSULA SCHOOLS OF MEDICINE & DENTISTRY — RESEARCH WITH PLYMOUTH UNIVERSITY

Participant Identification number:

(Add sticker here)

Participant Name:

DOB:

Participating Clinic:

Centre Number:

Study Number: 208291

CONSENT FORM

Title of Project: Identifying the organisms associated with Denture Stomatitis.

Name of Researcher: Samantha Gould

Please initial box

1. I confirm that I have read the information sheet dated 21/10/2017 (V1) for the above study. I have had the opportunity to consider the information, ask questions and have had these answered satisfactorily. ☐
2. I understand that my participation is voluntary and that I am free to withdraw at any time without giving any reason, without my medical care or legal rights being affected. ☐
3. I understand and accept that the information collected about me may be used to support other research in the future, and may be shared anonymously with other researchers. ☐
4. I agree to take part in the above study, including having swabs taken from my mouth and denture (if applicable), and I agree to my clinician providing information on my oral health. ☐

_____	_____	_____
Name of Participant	Date	Signature
_____	_____	_____
Name of Person taking consent	Date	Signature

Should you wish to withdraw or ask any further questions please contact denturestomatitisresearch@plymouth.ac.uk

When completed: 1 for participant; 1 for researcher site file; 1 (original) to be kept in notes.

Appendix 7: Participant questionnaire

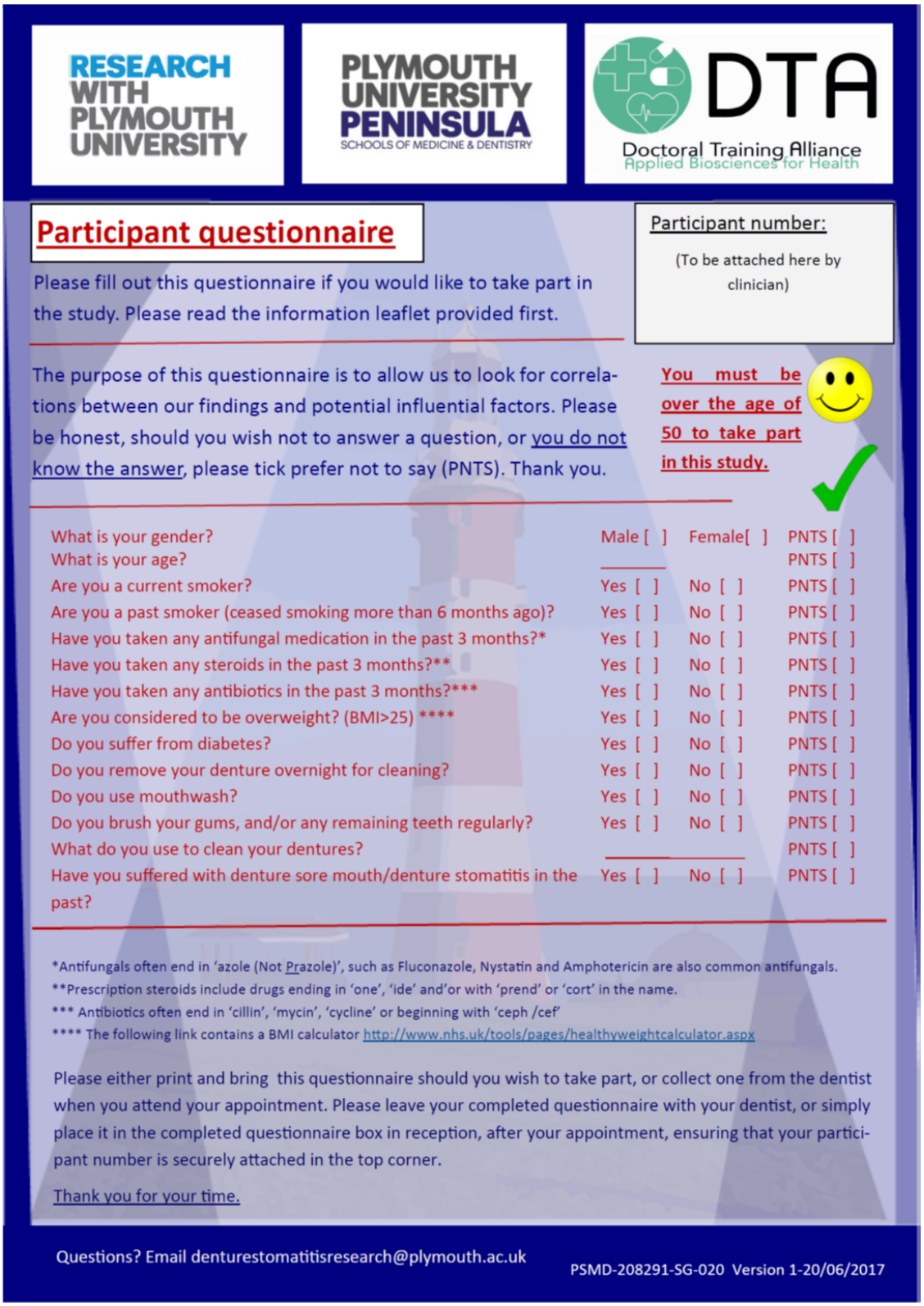

RESEARCH WITH PLYMOUTH UNIVERSITY

PLYMOUTH UNIVERSITY PENINSULA SCHOOLS OF MEDICINE & DENTISTRY

DTA Doctoral Training Alliance Applied Biosciences for Health

Participant questionnaire

Participant number:

(To be attached here by clinician)

Please fill out this questionnaire if you would like to take part in the study. Please read the information leaflet provided first.

The purpose of this questionnaire is to allow us to look for correlations between our findings and potential influential factors. Please be honest, should you wish not to answer a question, or you do not know the answer, please tick prefer not to say (PNTS). Thank you.

You must be over the age of 50 to take part in this study.

What is your gender?	Male [ ]	Female[ ]	PNTS [ ]
What is your age?	_____		PNTS [ ]
Are you a current smoker?	Yes [ ]	No [ ]	PNTS [ ]
Are you a past smoker (ceased smoking more than 6 months ago)?	Yes [ ]	No [ ]	PNTS [ ]
Have you taken any antifungal medication in the past 3 months?*	Yes [ ]	No [ ]	PNTS [ ]
Have you taken any steroids in the past 3 months?**	Yes [ ]	No [ ]	PNTS [ ]
Have you taken any antibiotics in the past 3 months?***	Yes [ ]	No [ ]	PNTS [ ]
Are you considered to be overweight? (BMI>25) ****	Yes [ ]	No [ ]	PNTS [ ]
Do you suffer from diabetes?	Yes [ ]	No [ ]	PNTS [ ]
Do you remove your denture overnight for cleaning?	Yes [ ]	No [ ]	PNTS [ ]
Do you use mouthwash?	Yes [ ]	No [ ]	PNTS [ ]
Do you brush your gums, and/or any remaining teeth regularly?	Yes [ ]	No [ ]	PNTS [ ]
What do you use to clean your dentures?	_____		PNTS [ ]
Have you suffered with denture sore mouth/denture stomatitis in the past?	Yes [ ]	No [ ]	PNTS [ ]

*Antifungals often end in 'azole (Not Prazole)', such as Fluconazole, Nystatin and Amphotericin are also common antifungals.
**Prescription steroids include drugs ending in 'one', 'ide' and'or with 'prend' or 'cort' in the name.
*** Antibiotics often end in 'cillin', 'mycin', 'cycline' or beginning with 'ceph /cef'
**** The following link contains a BMI calculator http://www.nhs.uk/tools/pages/healthyweightcalculator.aspx

Please either print and bring this questionnaire should you wish to take part, or collect one from the dentist when you attend your appointment. Please leave your completed questionnaire with your dentist, or simply place it in the completed questionnaire box in reception, after your appointment, ensuring that your participant number is securely attached in the top corner.

Thank you for your time.

Questions? Email denturestomatitisresearch@plymouth.ac.uk

PSMD-208291-SG-020 Version 1-20/06/2017

Appendix 8: Clinician questionnaire

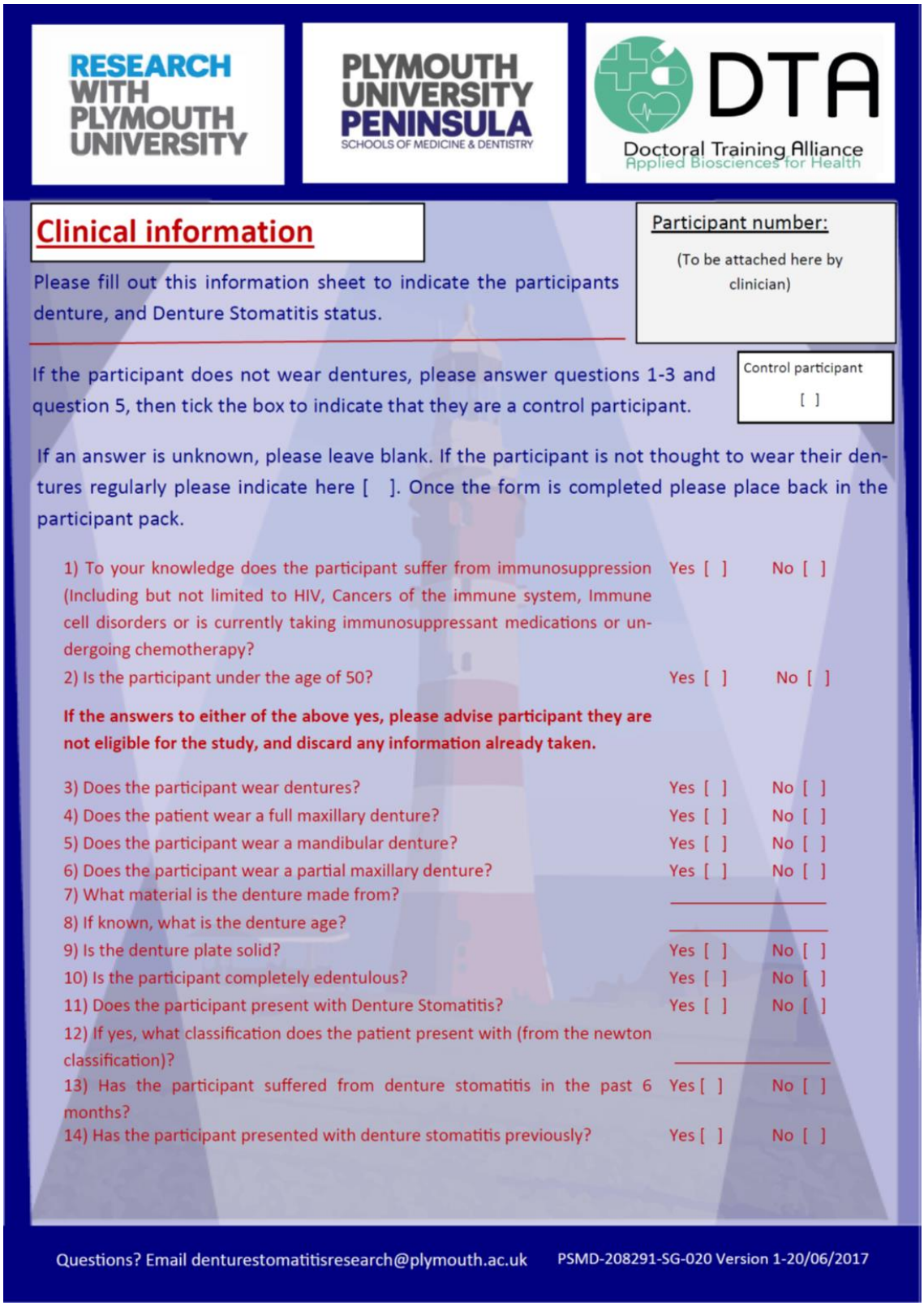

RESEARCH WITH PLYMOUTH UNIVERSITY

PLYMOUTH UNIVERSITY PENINSULA SCHOOLS OF MEDICINE & DENTISTRY

DTA Doctoral Training Alliance Applied Biosciences for Health

Clinical information

Participant number:

(To be attached here by clinician)

Please fill out this information sheet to indicate the participants denture, and Denture Stomatitis status.

If the participant does not wear dentures, please answer questions 1-3 and question 5, then tick the box to indicate that they are a control participant.

Control participant [ ]

If an answer is unknown, please leave blank. If the participant is not thought to wear their dentures regularly please indicate here [ ]. Once the form is completed please place back in the participant pack.

1) To your knowledge does the participant suffer from immunosuppression (Including but not limited to HIV, Cancers of the immune system, Immune cell disorders or is currently taking immunosuppressant medications or undergoing chemotherapy?	Yes [ ]	No [ ]
2) Is the participant under the age of 50?	Yes [ ]	No [ ]

If the answers to either of the above yes, please advise participant they are not eligible for the study, and discard any information already taken.

3) Does the participant wear dentures?	Yes [ ]	No [ ]
4) Does the patient wear a full maxillary denture?	Yes [ ]	No [ ]
5) Does the participant wear a mandibular denture?	Yes [ ]	No [ ]
6) Does the participant wear a partial maxillary denture?	Yes [ ]	No [ ]
7) What material is the denture made from?	_____	
8) If known, what is the denture age?	_____	
9) Is the denture plate solid?	Yes [ ]	No [ ]
10) Is the participant completely edentulous?	Yes [ ]	No [ ]
11) Does the participant present with Denture Stomatitis?	Yes [ ]	No [ ]
12) If yes, what classification does the patient present with (from the newton classification)?	_____	
13) Has the participant suffered from denture stomatitis in the past 6 months?	Yes [ ]	No [ ]
14) Has the participant presented with denture stomatitis previously?	Yes [ ]	No [ ]

Questions? Email denturestomatitisresearch@plymouth.ac.uk PSMD-208291-SG-020 Version 1-20/06/2017

Appendix 9: Clinician protocol